

A NUMERICAL MODEL FOR MORPHO-
LOGICAL COMPUTATIONS IN RIVERS
WITH NON-UNIFORM SEDIMENT

K.W. Olesen

R/1981/6/H

DELFT UNIVERSITY OF TECHNOLOGY
Department of Civil Engineering
Fluid Mechanics Group

UNIVERSITY OF TECHNOLOGY
Department of Civil Engineering
Laboratory of Fluid Mechanics
Stevinweg 4
DELFT-8 THE NETHERLANDS

A NUMERICAL MODEL FOR MORPHOLOGIC COMPUTATIONS

IN RIVERS WITH NON - UNIFORM SEDIMENT

Kim Wium Olesen

CONTENTS

<u>0. Introduction</u>	1
<u>1. Morphological models for rivers</u>	3
1.1. Model for uniform sediment	3
1.2. Model for non - uniform sediment	12
<u>2. Discussion on basic equations</u>	27
2.1. Alluvial roughness	27
2.2. Sediment transport formulas	46
2.3. Transport layer thickness	61
2.4. The variables P_{iz_0}	68
2.5. Interaction between the elements	69
2.6. Unsteady conditions	71
<u>3. Numerical modelling</u>	73
3.1. Numerical analysis	73
3.2. Numerical model for uniform sediment	97
3.3. Numerical model for non-uniform sediment	113
<u>4. Application of the model</u>	127
4.1. Filling in of dredged trench	127
4.2. Flume experiment with graded sediment	134
4.3. Sensitivity analysis	139
<u>5. Conclusions and suggestions for continuation</u>	149
<u>Appendix</u>	
A. Auxilary	151
B. Users guide	162
C. Documentation	175
D. List of numerical model for uniform sediment	205
E. Literature survey	209
F. References	215
List of main symbols	218

Preface:

The present report is part of the requirements for the Danish Degree of Master of Science.

The work has been carried out at the Delft University of Technology where I was granted a scholarship within the framework of a cultural exchange programme between the Netherlands and Denmark.

I wish to thank prof. M de Vries and F. Engelund who made my stay here possible.

The daily supervision has been performed by Jan Ribberink to whom I am indebted for good advice and guidance.

This thesis has been typed by Pia Umans.

Delft, June 1981.

Kim Wium Olesen.

0. Introduction.

During the recent years numerical models has become a tool for forecasting morphological changes in alluvial rivers due to natural cause or human interference. However these models have demonstrated serious shortcomings, when rivers with graded sediment which are close to the threshold of motions are considered. One of the main reasons is that changes of transport rate due to changes in grain size distribution are not taken into account (models for uniform sediment).

The aim of this study has been to develop a numerical model without this restriction; this has been done by taking more grain fractions into consideration. (Model for non - uniform or graded sediment).

This extension of the mathematical model for uniform sediment is described in chapter 1, where the basic equations of the model for uniform as well as for non - uniform sediment are derived. The main assumptions in the deductions are that the flow can be considered quasi - steady and that the sediment transport is a function of the local hydraulic conditions. The characteristic directions in the model for non - uniform sediment are derived, in case of two grain fractions, and will be briefly analysed.

In chapter 2 the basic equations will be discussed and some models for the component parts of the mathematical models will be suggested. Here also some of the general limitations for the morphological computation will be mentioned.

An extensive numerical analysis of some finite difference methods for a linear hyperbolic equation is given in chapter 3. A predictor - corrector method is preferred for the solution of the model for non - uniform sediment, and the method is tested on the model for uniform sediment in order to check the applicability to a non - linear hyperbolic system. Finally the predictor - corrector method will be applied to the model for non - uniform sediment after a schematization of the vertical grain size distribution is carried out. The computational results from the numerical model for non - uniform sediment will be compared with solutions obtained from the characteristic method.

In chapter 4 it will be attempted to verify the model by means of a flume experiment with graded sediment and a measurement from prototype. A sensitivity analysis, with respect to the influence of the grain size characteristics and the transport layer thickness on an armoring process, is carried out.

In chapter 5 the conclusions are summarized and suggestions for continuation are given.

1. MORPHOLOGICAL MODELS FOR RIVERS.

The mathematical models for forecasting morphological changes in alluvial rivers consist in principle of an equation of motion and continuity for each fraction as well as for the water.

Although the variation of the alluvial roughness can have an important influence when morphological computation has to be carried out, the bed roughness is supposed not to vary in time in the following inference of the mathematical models.

First a morphological model for uniform sediment will be deduced, mainly in order to get some insight in the complex morphological phenomena and to justify description of the water movement by the equations for quasi steady flow.

Next a model for non-uniform sediment will be inferred, and attention will be paid to the proper definition of some variables in the model. In case of two sediment fractions the characteristic directions and relations will be derived and the features with these having influence on a numerical solution of the morphological model will be discussed in broad outlines. For a profound discussion of the characteristic of the model for non-uniform sediment see Ribberink (1980).

1.1 Model for uniform sediment.

The model consists of an equation of motion and continuity for both the fluid and the sediment, i.e. there are four equations to relate the four dependent variables.

$u(x,t)$ time (turbulent fluctuation) and depth averaged
flow velocity
 $S(x,t)$ sediment transport
 $a(x,t)$ water depth
 $z(x,t)$ bed level

1.1.1. Equations for the water

The equation of motion is the one-dimensional form of the Navier-Stokes equation for hydrostatical pressure, known as the long wave equation.

$$\frac{\partial U}{\partial t} + U \frac{\partial U}{\partial x} + g \frac{\partial a}{\partial x} + g \frac{\partial Z}{\partial x} = R \quad (1.1.1)$$

where

x space coordinate, positive in flow direction

t time coordinate

g the gravitational constant

R a friction term, for instance expressed by the Chezy equation

$$R = - \frac{u^2}{C^2 a} \quad (1.1.2)$$

in which C is the Chezy roughness coefficient, in this deduction supposed not to vary in time.

The equation of continuity is the classical one for non-incompressively fluids which yields

$$\frac{\partial a}{\partial t} + a \frac{\partial U}{\partial x} + U \frac{\partial a}{\partial x} = 0 \quad (1.1.3)$$

1.1.2. Equations for sediment

The continuity equation for the sediment yields that a sediment transport gradient in the flow direction causes a local change of the bed level. The equation can easily be inferred from fig. 1.1.1, where an infinitesimal section of the bed is considered.

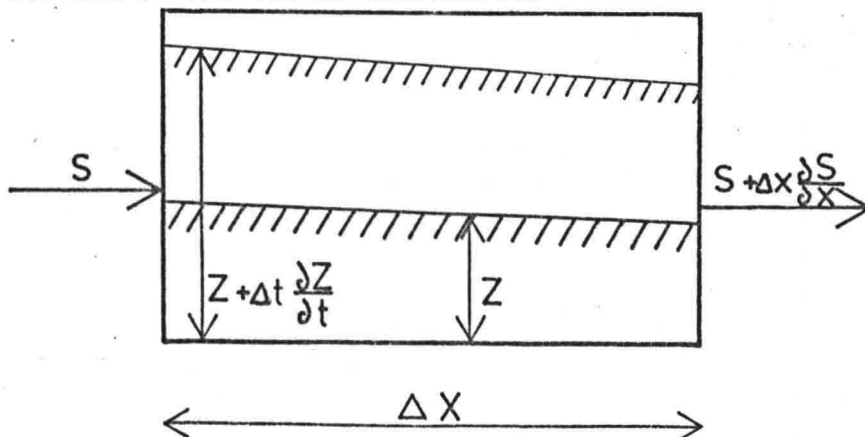


Fig. 1.1.1 Continuity equation for sediment

$$(S + \Delta x \frac{\partial S}{\partial x} - S) \Delta t + (Z + \Delta t \frac{\partial Z}{\partial t} - Z) \Delta x = 0$$

$$\frac{\partial S}{\partial x} + \frac{\partial Z}{\partial t} = 0 \quad (1.1.4)$$

where S is the sediment transport per unit width, included the pore volume.

The equation of motion for the sediment is the so called transport formula, from which there are existing several (see chapter 2). The different transport formulas are more or less explicit relating the amount of sediment in transport to the mean flow velocity of the fluid and other parameters

$$S = f(u, \dots) \quad (1.1.5)$$

1.1.3. Mathematical character

The characteristic directions of the set of partial differential equations can give information about the solution method and the boundary conditions that have to be applied

By combining eqs. (1.1.4) and (1.1.5) the transport can be eliminated as a variable

$$\frac{\partial Z}{\partial t} + f_u \frac{\partial U}{\partial t} = 0 \quad (1.1.6)$$

with $f_u = \frac{\partial f(U)}{\partial U}$

The total derivatives of the three remaining dependent variables yield

$$dU = \frac{\partial U}{\partial t} dt + \frac{\partial U}{\partial x} dx \quad (1.1.7a)$$

$$da = \frac{\partial a}{\partial t} dt + \frac{\partial a}{\partial x} dx \quad (1.1.7b)$$

$$dz = \frac{\partial Z}{\partial t} dt + \frac{\partial Z}{\partial x} dx \quad (1.1.7c)$$

The eqs. (1.1.1), (1.1.3), (1.1.6) and (1.1.7) now form a system of linear equations in the six partial derivatives, which in matrix form reads

$$\begin{pmatrix} 1 & u & 0 & g & 0 & g \\ 0 & a & 1 & u & 0 & 0 \\ 0 & f_u & 0 & 0 & 1 & 0 \\ 1 & c & 0 & 0 & 0 & 0 \\ 0 & 0 & 1 & c & 0 & 0 \\ 0 & 0 & 0 & 0 & 1 & c \end{pmatrix} \cdot \begin{pmatrix} \frac{\partial u}{\partial t} \\ \frac{\partial u}{\partial x} \\ \frac{\partial a}{\partial t} \\ \frac{\partial a}{\partial x} \\ \frac{\partial z}{\partial t} \\ \frac{\partial z}{\partial x} \end{pmatrix} = \begin{pmatrix} R \\ 0 \\ 0 \\ du/dt \\ da/dt \\ dz/dt \end{pmatrix} \quad (1.1.8)$$

in which $c = \frac{dx}{dt}$ is the characteristic direction.

As the characteristic directions are propagation velocities for disturbances in the variables, i.e. discontinuities in the derivatives, the set of equations has no solution along the characteristics. This means, according to Cramer's rule, that the characteristic directions can be found as the values for which the determinant is zero. This can be expressed in the cubic equation

$$\phi^3 - 2\phi^2 + (1 - F^{-2} - \psi F^{-2})\phi + \psi F^{-2} = 0 \quad (1.1.9)$$

in which the following dimensionless quantities are introduced

$$\phi = \frac{c}{u} \quad \text{relative celerity}$$

$$F = u/\sqrt{ga} \quad \text{Froude number}$$

$$\psi = f_u/a \quad \text{dimensionless transport concentration}$$

For realistical values of F and ψ de Vries (1976) found three real roots in eq. (1.1.9). The three roots ϕ_1, ϕ_2, ϕ_3 are depicted in fig. (1.1.2) as a function of F and for liner of equal values of ψ .

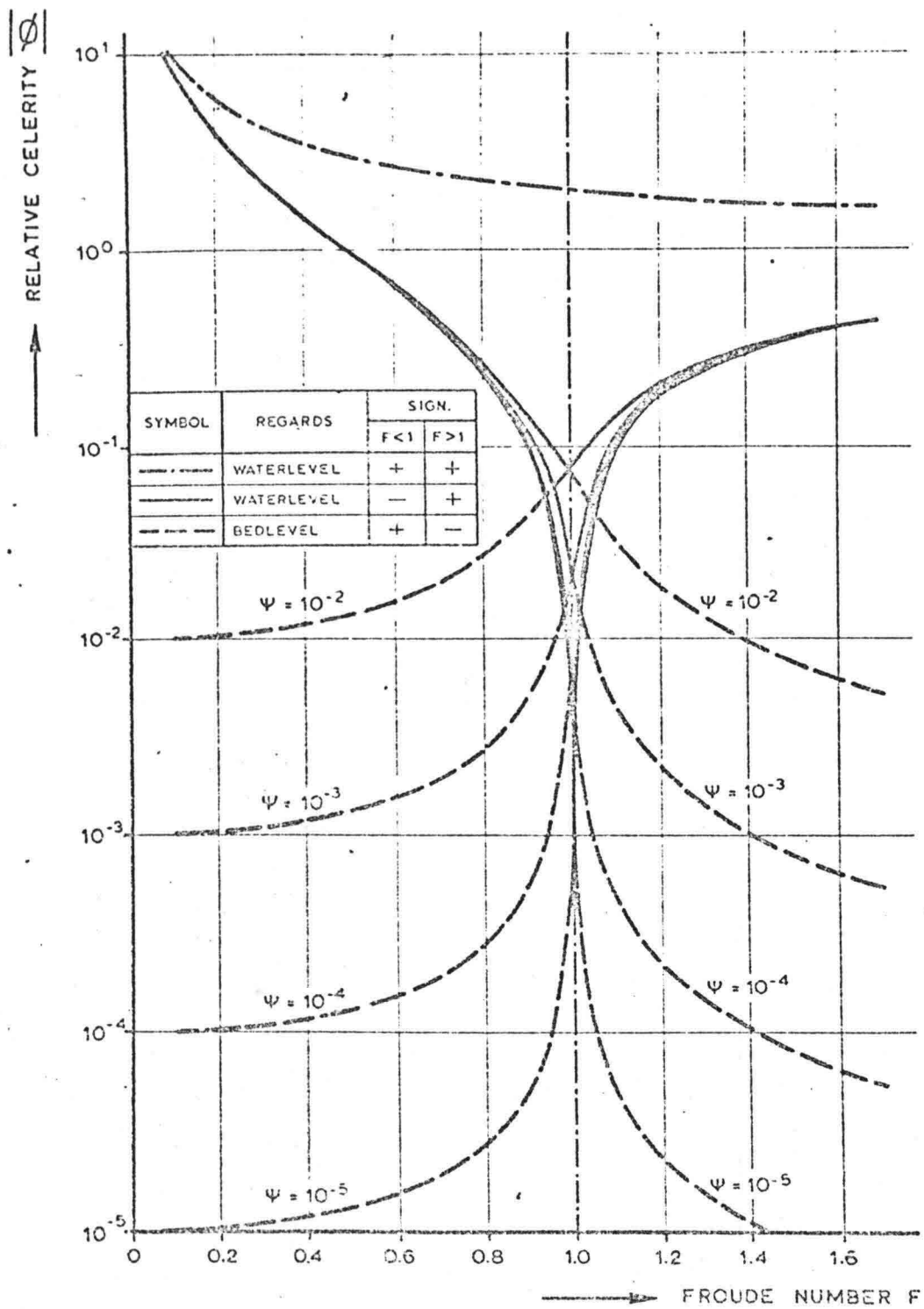


Fig. 1.1.2. Relative Celerities after de Vries (1976).

Interpretating the celerities as directions of information flow it is seen from fig. (1.1.2) that there have to be two upstream and one downstream boundary conditions as there are two positive characteristic directions and a negative one.

1.1.4. Discussion of celerities

Here the behaviour of the celerities will only be discussed in broad outlines, for profound information see de Vries (1976).

For a fixed bed the transport concentration is zero and eq. (1.1.9) can be reduced to

$$\phi^2 - 2\phi + 1 - F^{-2} = 0 \quad (1.1.10)$$

which gives the well known characteristic directions of the long wave equations

$$\phi_1 = 1 + F^{-1} \quad (1.1.11)$$

$$\phi_2 = 1 - F^{-1} \quad (1.1.12)$$

From fig. (1.1.2) it is seen that ϕ_1 is hardly affected by the mobility of the bed and for Froude numbers less than ± 0.6 nor ϕ_2 is affected. The product of the roots in eq. (1.1.9) have to be $-\psi F^{-2}$, from which the characteristic direction for the bed can be found in case of low Froude numbers

$$\phi_3 = \frac{-\psi F^{-2}}{(1 + F^{-1})(1 - F^{-1})} = \frac{\psi}{1 - F^2} \quad \text{for } F < \pm 0.6 \quad (1.1.13)$$

In case of supercritical flow it is again seen that ϕ_1 is not affected by the mobility of the bed ($F > \pm 1.4$) and eq. (1.1.13) is again valid as an approximation for the bed celerity. Notice that ϕ_3 now is negativ, which is in agreement with observations from nature, where antidunes are propagating against the flow direction.

For critical flow ($F = 1$) the celerities read

$$\phi_1 = 2 \quad \text{and} \quad -\phi_{2,3} = \pm \sqrt{\frac{1}{2}U} \quad (1.1.14)$$

In alluvial streams low Froude numbers are prevailing, and in this case

$$|\phi_{1,2}| \gg \phi_3 \quad \text{for} \quad F \ll 1 \quad (1.1.15)$$

Comparing the three characteristic directions it can be concluded

$|C_{1,2}| \rightarrow \infty$ or $dt \rightarrow 0$, thus the partial time derivatives in eqs. (1.1.7a) and (1.1.7b) can be neglected and therefore eqs. (1.1.1) and (1.1.3) can be approximated with the equations for quasi steady flow

$$U \frac{\partial U}{\partial x} + g \frac{\partial a}{\partial x} + g \frac{\partial Z}{\partial x} = R \quad (1.1.16)$$

$$U \frac{\partial a}{\partial x} + a \frac{\partial U}{\partial x} = \frac{\partial q}{\partial x} = 0 \quad (1.1.17)$$

where q is the discharge per unit width.

The physical interpretation of the neglecting of the time derivatives is that the flow is changing instantaneous to the new flow situation due to a change in the bed level.

The system of equations (1.1.4,5,16 and 17) is of a mixed hyperbolic-parabolic character, because there are two characteristic directions with infinite velocity and one with the velocity given by eq. (1.1.13).

1.1.5 Linearization of equations

Although the transport formula is strongly non-linear there can be obtained some insight in the nature of the process from a linearization of the equations.

The dependent variables are considered to consist of a constant part and a varying part; for the bed level for instance

$$z = z_0 + z' \quad z_0 \gg z' \quad (1.1.18)$$

where z_0 is the constant part and z' the varying part. The derivation of the linearized equation is given in appendix A1 and the result is:

$$\frac{\partial z'}{\partial t} - D \frac{\partial^2 z'}{\partial x^2} - \frac{D}{C} \frac{\partial^2 z'}{\partial x \partial t} = 0 \quad (1.1.19)$$

with $C = u_0 \frac{f_u(U_0)}{a_0(1-F^2)}$ (1.1.20)

and $D = U \frac{f_u(U_0)}{3I_p}$ (1.1.21)

in which $I_0 = \frac{U_0^2}{C^2 a_0}$ is the equilibrium bed slope.

The character of eq. (1.1.19) can be illustrated by inserting a periodical solution of the form

$$Z(x,t) = Z \exp(i k x + r t) \quad (1.1.22)$$

where k is the wave number which leads to

$$r - (ik) D - ik r \frac{D}{C} = 0$$

or

$$r = - D k \frac{1 + i \frac{D}{C} k}{1 + \frac{D^2}{C^2} k^2} \quad (1.1.23)$$

Combining eqs. (1.1.22) and (1.1.23) there occurs a solution similar to that of a convective diffusion equation, for an initial value $z(x,c) = Z \exp i k x$, with an effective diffusion coefficient D_e and an effective propagation velocity C_e given by

$$D_e = \frac{D}{1 + (k \frac{D}{C})^2} \quad (1.1.24)$$

$$C_e = \frac{C(k \frac{D}{C})^2}{1 + (k \frac{D}{C})^2} \quad (1.1.25)$$

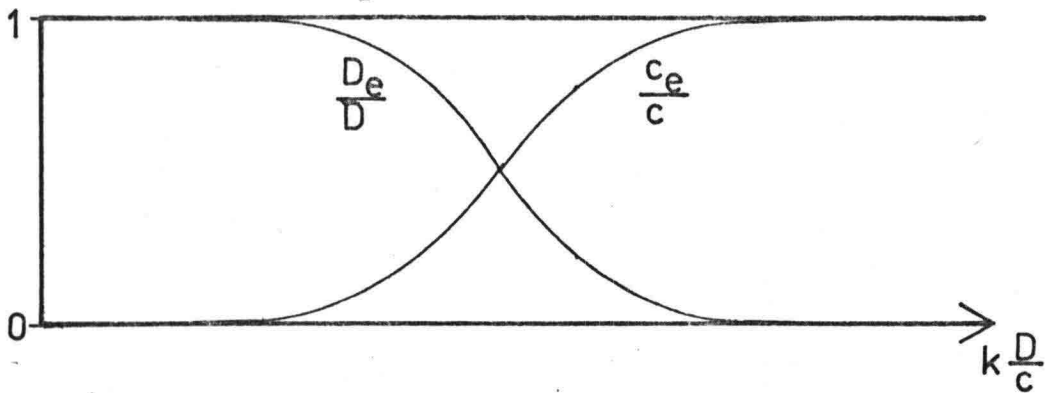


Fig. 1.1.3. Effective propagation velocity and diffusion coefficient for bed disturbances.

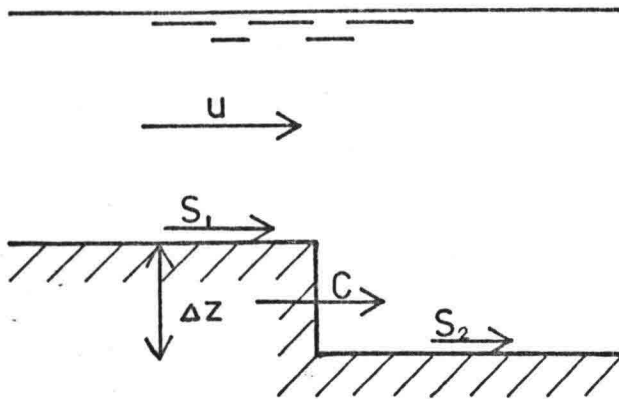
According to fig. 1.1.3 the linearized equation has a pure convective character for short waves (large k) and for long waves a diffusion character, but in most cases both features will have an influence. Further it is noticed that the character of the linearized equation depends on the parameter

$$k \frac{D}{c} = k \frac{a(1 - F^2)}{3L_0} \quad (1.1.26)$$

which is independent of the transport formula.

1.1.6. Non - linearity

The celerity is increasing strongly with the water velocity which will tend to deform waves: the tails will expand and the fronts compress. There will be formed a vertical front, a shock wave, and locally the differential equations will not be valid any longer, but the principles of conservation of mass and impuls are still valid. For conservation of mass for instance eq. (1.1.27) is valid.



$$C \cdot \Delta z = S_1 - S_2$$

Fig. 1.1.4. Locally continuity equation

$$C = \frac{\Delta S}{\Delta z} \quad (1.1.27)$$

1.2 Model for non-uniform sediment.

This model also consists of an equation of motion and an equation of continuity for each sediment fraction and for the fluid. In case of N fractions there are $2N + 2$ equations to relate the $2N + 2$ dependent variables

$u(x,t)$	flow velocity
$a(x,t)$	water depth
$z(x,t)$	bed level
$S_1 \dots S_N(x,t)$	sediment transport per fraction
$p_1 \dots p_{N-1}(x,t)$	probability of fraction i .

1.2.1. Equations for the water

The water movement is, as for the model for uniform sediment, described by the equations for quasi steady flow. By combining the equation of motion and continuity the water depth gradient can be eliminated. From eq. (1.1.17)

$$\frac{\partial a}{\partial x} = -\frac{a}{u} \frac{\partial u}{\partial x} \quad (1.2.1)$$

which inserted in eq. (1.1.16) gives

$$G \frac{\partial u}{\partial x} + g \frac{\partial Z}{\partial x} = R \quad (1.2.2)$$

where $G = u - \frac{ga}{u} = u(1 - F^{-2})$

1.2.2. Equations for sediment

The equation of continuity for an arbitrary fraction i can in a conservative form be written as

$$\frac{\partial S_i}{\partial x} + \frac{\partial Z \bar{p}_i}{\partial t} = 0 \quad (1.2.3)$$

in which \bar{p}_i is an averaged probability of fraction i . See fig. 1.2.1.

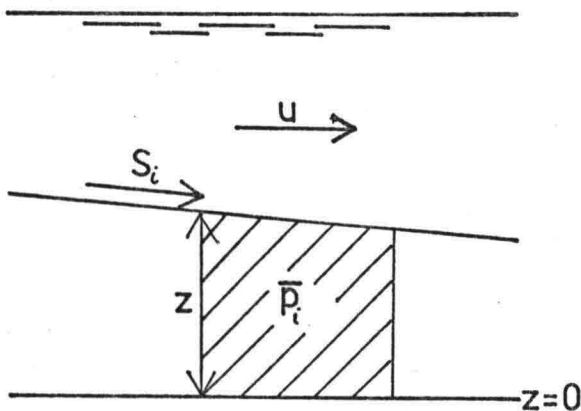


Fig. 1.2.1. Continuity equation for fraction i .

cant dune height

$$\left| \frac{\partial Z}{\partial t} \right| \ll \left| \frac{\partial z_*}{\partial t} \right| \quad (1.2.5)$$

The instantaneous bed level $z_*(x,t)$ is defined as the level below which no grainmovement occurs, and the time averaged bed level is defined as

$$Z(x,t) = \frac{1}{T} \int_0^T z_*(x,t) dt \quad (1.2.6)$$

where T is an averaging period which must be chosen so big that a representative fluctuation of the instantaneous bed level is taken into account, but so small that the averaged bed level can be considered not changed. The validity of the averaging process can be expressed in mathematical terms by eq. (1.2.5).

The z_0 level is defined as the minimum instantaneous bed level in the averaging period T , i.e. there is no grainmovement below the z_0 -level in the averaging period

$$z_0(x,t) = \min_T z_*(x,t) \quad (1.2.7)$$

The variation of the instantaneous bed level has a stocastical nature. In prototype and flume experiments deep throughs and high crests are infrequently observed. A probability density function for the instantaneous bed level will typically have the form sketched in fig. (1.2.3)

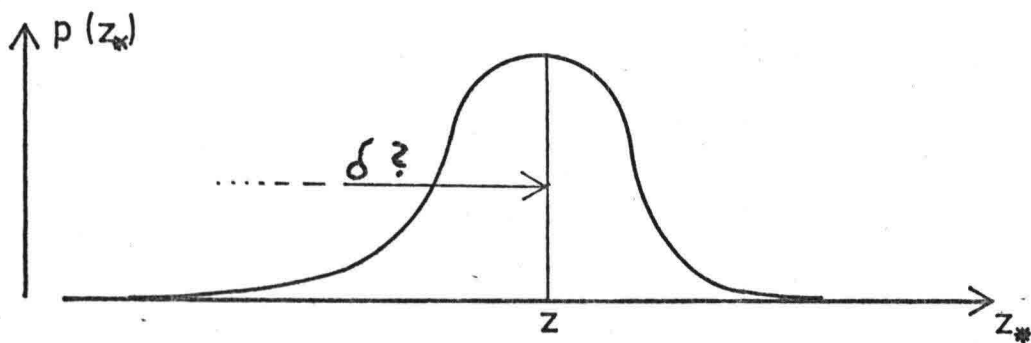


Fig. 1.2.3. Probability density function for the instantaneous bed level.

The sketch illustrates that there has to be chosen a large averaging period T to get a representative picture of the fluctuations in the instantaneous bed level, in which, in case of fast sedimentation or erosion, the time averaged bed level can change considerably, i.e. eq. (1.2.5) is not valid.

The stochastical fluctuation of the instantaneous bed level has as a consequence that the z_0 level, and with that the transport layer thickness, is poorly defined. It does not seem physically reasonable to relate the transport to the composition of the bed at the levels which are only very infrequently exposed for the flow. This feature leads to the necessity of choosing the z_0 level as the level for which for instance 95% of the instantaneous bed level is above, i.e. only take a certain part of the fluctuations into account.

The composition of the bed is given by the following quantities

$$p_i(x,t) = \frac{1}{T} \int_0^T \frac{1}{\delta} \int_{z_0}^{z_x} p_{i*}(x,t,z) dz dt \quad (1.2.8)$$

and

$$p_{i z_0}(x,t) = \frac{1}{Z_0} \int_0^{z_0} p_{i z_0 *}(x,t,z) dz \quad (1.2.9)$$

in which * indicates local value. It is necessary to know or to assume something about the composition of the z_0 level, in order not to have an indeterminable model. From fig. (1.2.2) an expression for the averaged probability in the continuity equation (1.2.3) can be found

$$\bar{p}_i Z = p_i \delta + p_{i z_0} Z_0 \quad (1.2.10)$$

which inserted in the continuity equation gives

$$\frac{\partial S_i}{\partial x} + \frac{\partial p_i \delta}{\partial t} + \frac{\partial p_{i z_0} Z_0}{\partial t} = 0 \quad (1.2.11)$$

1.2.3. Characteristics of the set of equations

The deriving of the characteristic directions and the characteristic relations gives information about the mathematical character of the set of equations and more insight in the physical process described by these. The mathematical character gives information about the solution method which has to be chosen, and the number and direction of the celerities determines the type and number of boundary conditions.

For the following the continuity equation for the sediment fractions (1.2.11) will be written in an alternative form (not conservative). Defining $\bar{p}_{i z_0}$ as the probability at the z_0 -level, i.e.

$$\bar{p}_{i z_0} = \frac{\partial p_{i z_0} Z_0}{\partial Z_0} \quad (1.2.12)$$

the continuity equation becomes

$$\frac{\partial S_i}{\partial x} + \delta \frac{\partial p_i}{\partial t} + p_i \frac{\partial \delta}{\partial t} + \bar{p}_{i z_0} \frac{\partial Z_0}{\partial t} = 0 \quad (1.2.13)$$

from which the variable z_0 can be eliminated with $z_0 = z - \delta$

$$\frac{\partial S_i}{\partial x} + \delta \frac{\partial p_i}{\partial t} + p_{i z_0} \frac{\partial Z}{\partial t} + p_i \frac{\partial \delta}{\partial t} = 0 \quad (1.2.14)$$

where $p_i = p_i - \bar{p}_{i z_0}$

In appendix A2 a quadratic equation for the two dimensionless celerities, in case of two fractions is derived for a time independent specific discharge and the transport layer thickness considered as a function of the local hydraulic parameters $\delta(a, u)$.

The characteristic directions can in this case be found as the roots of the quadratic equation

$$\phi^2 - \phi(A + B + D) + C = 0 \quad (1.2.15)$$

where

$$\Phi = \frac{c}{u} \quad \text{dimensionless celerity}$$

$$A = \frac{\bar{p}_1 z_0 f_1 p_1 - \bar{p}_2 z_0 f_2 p_1}{\delta U}$$

$$B = \frac{\psi_1 + \psi_2}{1 - F^2}$$

$$C = \frac{\psi_1 f_2 p_1 - \psi_2 f_1 p_1}{U \delta (1 - F^2)}$$

$$D = -P_1 \frac{f_1 p_1 + f_2 p_1}{\delta U} \frac{\frac{U}{a} \delta_u - \delta_a}{1 - F^2}$$

$$f_i p_i = \frac{\partial f_i}{\partial p_i}, \quad \delta_u = \frac{\partial \delta}{\partial U} \quad \text{etc.}$$

$$\psi_i = \frac{f_i u}{a} = \frac{1}{a} \frac{\partial f_i}{\partial u}$$

For a constant transport layer thickness Ribberink (1980) gives a very profound discussion of the behavior of the celerities. Here only the most important features for the present purpose will be resumed.

1.2.4. Relative size of the celerities

The difference in magnitude between the characteristic directions has a large influence on a choice of an efficient numerical method for the problem. With making some assumption the ratio between the celerities can be found.

In case of a constant transport layer thickness D in eq. (1.2.15) vanishes and the celerities are then given by

$$\begin{aligned} \Phi_{1,2} &= \frac{1}{2} \left\{ A + B \pm \sqrt{(A+B)^2 - 4C} \right\} = \\ &= \frac{1}{2} \left\{ A + B \pm \sqrt{(A+B)^2 - 4(C-AB)} \right\} \end{aligned} \quad (1.2.16)$$

and for $C - AB = 0$

$$\phi_1 = A$$

$$\phi_2 = B$$

(1.2.17)

The condition $C - AB = 0$ can be shown to be fulfilled for

$$(\bar{p}_{2z} \psi_1 - \bar{p}_{1z_0} \psi_2)(f_{1p_1} + f_{2p_1}) = 0$$

(1.2.18)

For a simple transport formula of the form

$$S_i = p_i f_i'(U)$$

(1.2.19)

in which $\frac{\partial f_i'}{\partial p_j} = 0$

eq. (1.2.18) can be written as

$$(\bar{p}_{2z_0} p_1 f_{1u}' - \bar{p}_{1z_0} p_2 f_{2u}')(f_1' - f_2') = 0$$

(1.2.20)

which is true in case of uniform sediment $f_1' = f_2'$ and for

$$\frac{\bar{p}_{1z_0} (1 - p_1)}{p_1 (1 - \bar{p}_{1z_0})} = \frac{f_{1u}'}{f_{2u}'}$$

(1.2.21)

As f_1' gives the transport of the finer fraction, it can, for realistic transport formulas, be concluded that $f_{1u}' / f_{2u}' > 1$, and eq. (1.2.21) can then be reduced to

$$p_{1z_0} > p_1$$

(1.2.22)

Locally the transport formula per fraction can be approximated to a simple power formula

$$S_i = p_i m_i U^n$$

(1.2.23)

where respectively m_i and n are not a function of p_i and u . Notice that eq. (1.2.23) is not in contradiction with eq. (1.2.19). Another way to write the transport of fraction i is

$$S_i = p_i \delta U_{gi} \quad (1.2.24)$$

where u_{gi} is the average velocity in the transport layer of the grain with the diameter d_i .

With these assumption the celerities are now given by

$$\phi_1 = A = \frac{\bar{p}_{1,z_0} U_{g1} + \bar{p}_{1,z_0} U_{g2}}{U} \quad (1.2.25)$$

$$\phi_2 = B = \frac{n\delta}{a} \frac{p_1 U_{g1} + p_2 U_{g2}}{U} \quad (1.2.26)$$

and it is seen

$$\text{for } \bar{p}_{1,z_0} \rightarrow 1 \quad \text{and } U_{g2} \rightarrow 0 \quad \frac{\phi_1}{\phi_2} \rightarrow 0$$

$$\text{for } p_1 \rightarrow 0 \quad \text{and } U_{g2} \rightarrow 0 \quad \frac{\phi_1}{\phi_2} \rightarrow \infty$$

Resuming the assumptions

δ constant

$$C - AB = 0 \quad \Rightarrow \quad \bar{p}_{1,z_0} > p_1$$

Transport locally app. with eq. (1.2.23)

$$n \frac{\delta}{a} \approx 1$$

it is seen that no unrealistic simplification or assumption is made, so it is concluded that the difference between the two celerities can have a considerable magnitude, a fact which has a large influence on the choice

of an efficient numerical method.

1.2.5. Mathematical character

The mathematical character of the set of partial differential equations forming the model for non-uniform sediment depends on the form of the characteristic directions. In case of respectively complex, real and equal or real and different characteristic directions the set of partial differential equations is elliptic, parabolic or hyperbolic.

In a hyperbolic problem the characteristic directions define an area of influence and an area of dependence (see fig. 1.2.4), so the here treated problem is a typical hyperbolic problem, but in some cases complex characteristic directions are found.

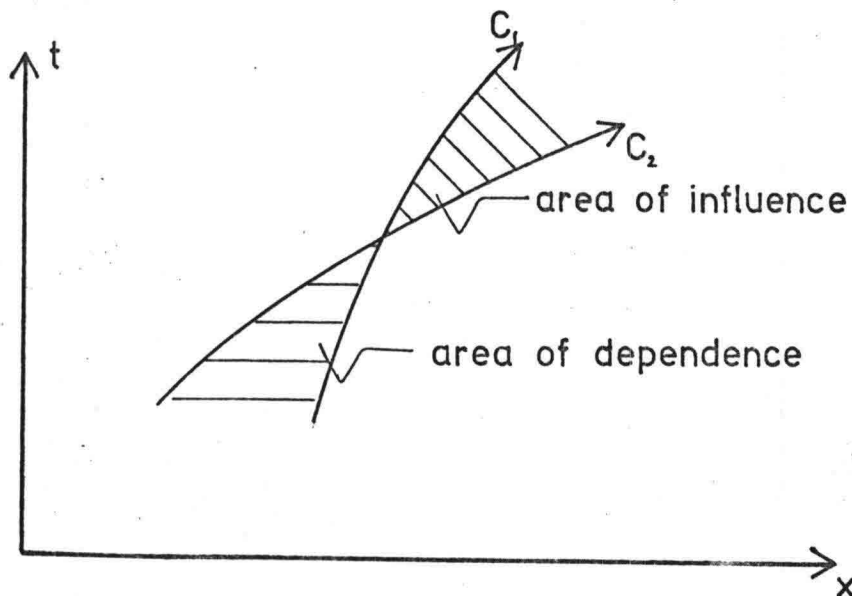


Figure 1.2.4. Hyperbolic problem in the x, t -plane

Again with the assumption that the transport layer thickness is constant, the form of the characteristic directions depends on the sign of the discriminant in eq. (1.2.16), and a necessary but not a sufficient condition for complex celerities is

$$C - AB > 0 \quad (1.2.27)$$

which, in case of a simple transport formula given by eq. (1.2.19), can be written as

$$(\bar{p}_{2z_0} p_1 f_{1u} - \bar{p}_{1z_0} p_2 f_{2u})(f_1' - f_2') < 0 \quad (1.2.28)$$

Recalling $d_1 < d_2$, thus $f_{1u}' > f_{2u}'$ and $f_1' > f_2'$, the equation can be reduced to

$$\frac{p_{1z_0} (1 - p_1)}{p_1 (1 - p_{1z_0})} > \frac{f_{1u}}{f_{2u}} > 1 \quad (1.2.29)$$

which is only valid for $p_{1z_0} > p_1$

1.2.6. Physical interpretation of elliptical character

Complex characteristic directions in a from nature hyperbolic system can have two causes: the model is describing a physical unstable situation or there is an error in the formulation of the model.

Physical instability

A mathematical indication of a physical instable situation can be that an infinitesimal disturbance in a variable is amplified. For the bed level this criterion for instability can be formulated as

$$\frac{\partial \sum S_i}{\partial z} < 0 \quad (1.2.30)$$

or for two fractions

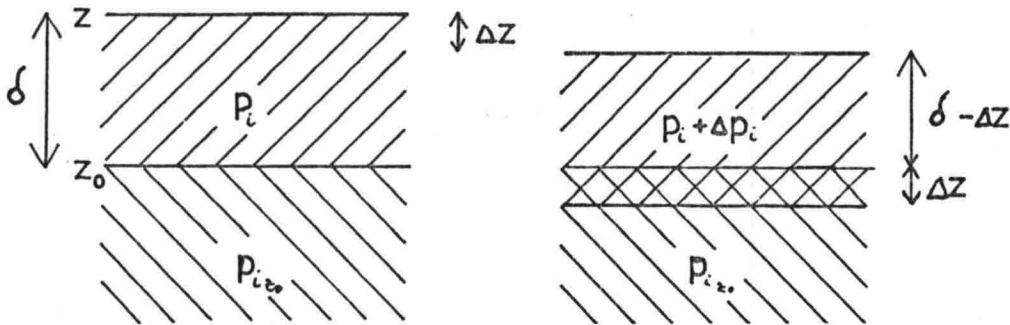
$$\left(\frac{\partial S_1}{\partial u} + \frac{\partial S_2}{\partial u} \right) \frac{\partial u}{\partial z} + \left(\frac{\partial S_1}{\partial p_1} + \frac{\partial S_2}{\partial p_1} \right) \frac{\partial p_1}{\partial z} < 0 \quad (1.2.31)$$

An expression for $\frac{\partial u}{\partial z}$ can be obtained from the local energy level $\frac{u}{2g} + a + z = \text{const.}$ Eliminating the water depth with help of the continuity equation for the water and differentiating with respect to the bed level z , the following expression occurs

$$\frac{u}{g} \frac{\partial u}{\partial z} - \frac{a}{u} \frac{\partial u}{\partial z} + 1 = 0$$

or
$$\frac{\partial u}{\partial z} = \frac{u}{a} \frac{1}{1 - F^2} \quad (1.2.31)$$

For a constant transport layer thickness $\frac{\partial p_i}{\partial z}$ can be deduced from fig. (1.2.5)



$$\Delta p_i = p_i - [(\delta - \Delta z) p_i + \Delta z \bar{p}_{i,z_0}] \frac{1}{\delta} \quad \text{for } \Delta z < 0$$

$$\Delta p_i = \Delta z \frac{p_i - \bar{p}_{i,z_0}}{\delta}$$

Figure 1.2.5. Change of composition for small disturbance in bed level.

$$\frac{\partial p_i}{\partial z} = \frac{p_i - p_{i,z_0}}{\delta} \quad (1.2.32)$$

Insert the obtained expressions for $\frac{\partial u}{\partial z}$ and $\frac{\partial p_i}{\partial z}$ in eq. (1.2.30) the criterion for instability now yields

$$B + A - A_p < 0 \quad (1.2.33)$$

where A and B are given in connection with eq. (1.2.15) and

$$A_p = \frac{p_2 f_1 p_1 - p_1 f_2 p_2}{\delta u}$$

For a realistic transport formula a necessary, but not a sufficient condition for the validity of eq. (1.2.33) is also that the transport layer is coarser than the underlying layer. For the Meyer - Peter and Muller transport formula it was found that when eq. (1.2.33) is fulfilled the celerities are always complex, but it was also found that it is not a sufficient criterion for elliptic character in the set of partial differential equations.

1.2.7. Error in the formulation of the model

A shortcoming in the model, which perhaps underlies the elliptic character, is that the model can not describe an exchange of sediment between the transport layer and the z_0 - layer independent of the change of the z_0 - level, i.e. sedimentation of coarse material and erosion of finer material at the same time, a process that especially is taking place when the transport layer is much coarser than the underlying layer. See fig. 1.2.6.

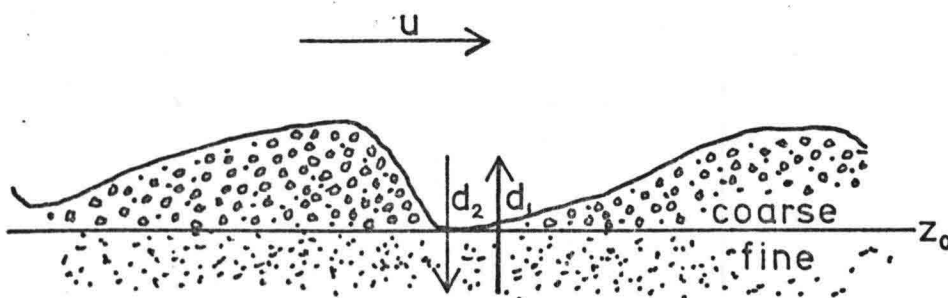


Figure 1.2.6. Exchange of sediment between transport layer and z_0 layer.

The feature can-not be described because the assumption that has to be made for the P_{iz_0} is based on the sign of $\frac{\partial z_0}{\partial t}$.

It can not be stated with certainty what the actual cause for the elliptic character in the set of partial differential equations is, but fortunately there are only problems close to initiation of motion, where it is especially interesting to use a model for non-uniform sediment, when there is chosen a very extreme combination of p_{iZ_0} and the transport layer thickness.

1.2.8. Characteristic relations

In case of real and unequal characteristic directions the set of partial differential equations is hyperbolic and can be solved by integration along the characteristics. The relations valid along the characteristics are a set of ordinary differential equations. Ribberink (1980) found, in case of a constant transport layer thickness, the characteristic relations

$$\frac{dp_i}{dt} (\phi - B) + \frac{dz}{dt} \frac{p_2 \psi_1 - p_1 \psi_2}{\delta(1 - F^2)} = \phi \frac{uR}{g} \frac{p_2 \psi_1 - p_1 \psi_2}{\delta(1 - F^2)} \quad (1.2.34)$$

valid along both the characteristics

Solving the model by numerical integration along the characteristics is very elaborate, and the method is hardly used for practical application. The principle of the characteristic method can be illustrated by fig. 1.2.7.

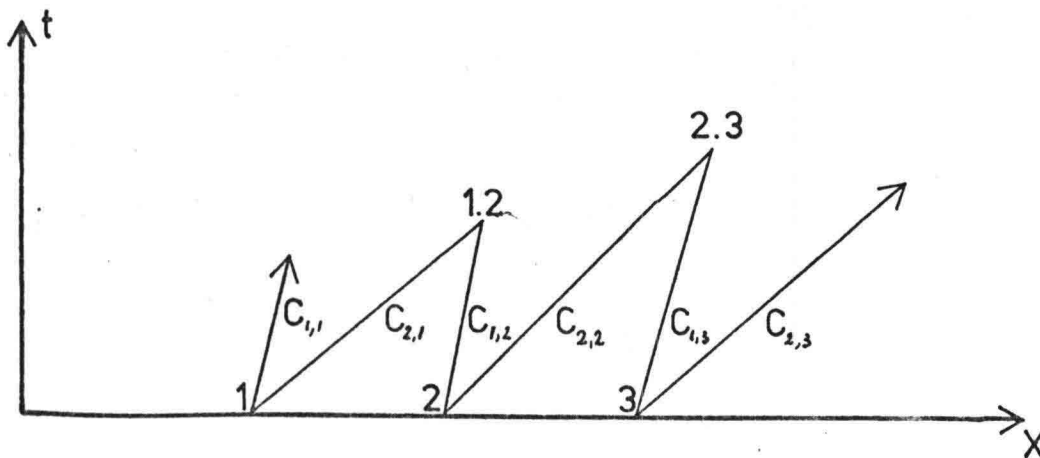


Figure 1.2.7. Solving with the characteristic method.

In point 1, 2 and 3 the bed level, composition etc. is known, and the characteristic directions and the characteristic relations in the three points can be calculated. Along the characteristic $c_{2,1}$ the characteristic relation will have the form

$$\alpha_{2,1} \frac{dp}{dt} + \beta_{2,1} \frac{dz}{dt} = \gamma_{2,1} \quad (1.2.35)$$

and along $c_{1,2}$

$$\alpha_{1,2} \frac{dp}{dt} + \beta_{1,2} \frac{dz}{dt} = \gamma_{1,2} \quad (1.2.36)$$

The space -and time coordinate for the new point, where the characteristics are intersecting, can be calculated from the characteristic directions and discretizing eqs. (1.2.35) and (1.2.36) the new bed level and the probability of fraction one can be found from solving two linear equations with two unknowns.

Because of the non-linear character of the system the new calculated points will be situated at different time levels and there have to be made linear interpolations between the old and new points in order to get the bed level at the same time level for a proper calculation of the flow velocity.

In some cases it is a good approximation to consider the water level as horizontal, i.e. neglect the friction and the convective terms in the equation of motion for the fluid (1.1.16), and the characteristic method becomes a little less unhandy because the right side of eqs. (1.2.35 and 36) vanish and the flow velocity is only dependent on the bed level, so linear interpolation is not necessary.

The advantage of the characteristic method is that there is found a very accurate mathematical solution for the set of partial differential equations.

2. DISCUSSION ON BASIC EQUATIONS

In the previous section the model was described in general mathematical terms, and in the following the component parts of the basic equations will be discussed.

First the roughness, a very important parameter in the model, will be treated. Roughness predictors based on global parameters and on the dune dimensions will be discussed. Further a procedure for correcting for the influence from the side walls on the bed shear stress will be treated.

Then three transport formulas for uniform sediment will be mentioned, they will be adapted for heterogeneous sediment and a model for the critical shear stress will be presented.

Both empirical and theoretical dune height predictors for estimating the transport layer thickness will be treated, and two methods will be compared with experimental data.

Finally the variable \bar{p}_{iz} , eq. (1.2.) will be discussed, and a brief description of the mutual interaction between the component parts of the model will be given together with some other general limits of the model.

2.1 Alluvial Roughness

An alluvial river is a river streaming in sediment deposited by the river itself, and the roughness of a river of that kind is referred to as alluvial roughness opposite to hydraulic resistance caused by for instance rocky protuberances, energy loss in river bends, diffusion between summer and winter bed etc.

The roughness can be expressed in several ways and in the following it will be done in terms of the Darcy - Weisbach coefficient and in terms of the Chézy coefficient, defined as

$$I = \frac{f}{8g} \frac{u^2}{a} \quad (2.1.1)$$

with f Darcy - Weisbach roughness coefficient

$$I = \frac{1}{c^2} \frac{u^2}{a} \quad (2.1.2)$$

with C Chézy roughness coefficient.

By combining eq. (2.1.1) and (2.1.2) a relation between the roughness coefficients appears

$$C = \sqrt{\frac{8g}{f}} \quad (2.1.3)$$

Under certain flow conditions bed forms will develop, which have a considerable influence on the alluvial roughness. It is convenient to divide the total alluvial resistance into a skin resistance and a form resistance. The skin resistance is caused by the friction between the fluid and the grains in the bed, and the form resistance is due to the expansion loss behind the tops of the bed forms. In terms of the Darcy - Weisbach coefficients it reads

$$f = f' + f'' \quad (2.1.4)$$

where f' D. - W. coefficient due to skin friction

f'' D. - W. coefficient due to bed forms.

2.1.1 Bed forms

As outlined before the bed forms have a large influence on the alluvial roughness, and the occurrence of these will be briefly discussed here.

For low flow velocities an alluvial channel has a flat bed and for increasingly velocity it will form ripples, dunes and again flat bed. In fig. 2.1.1 the different bed forms are depicted, and fig. 2.1.2 gives a qualitative idea of the bed forms influence on the roughness.

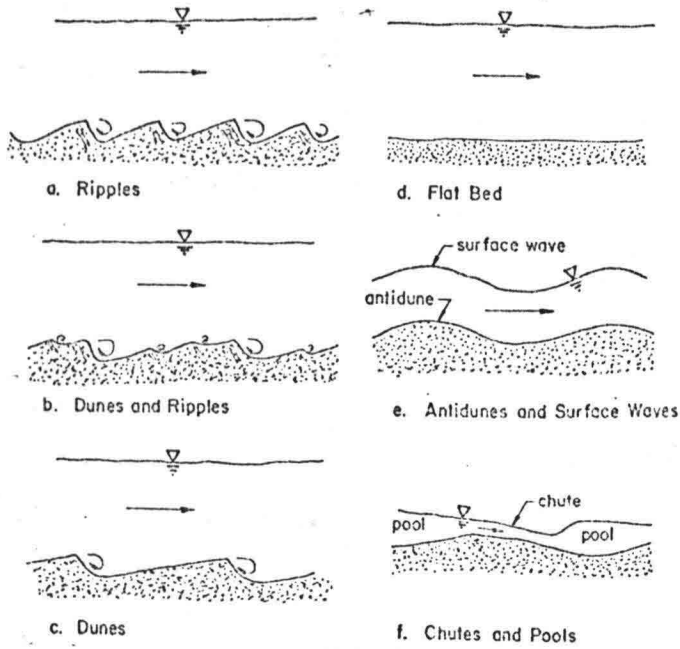


Figure 2.1.1. Bed forms [20]

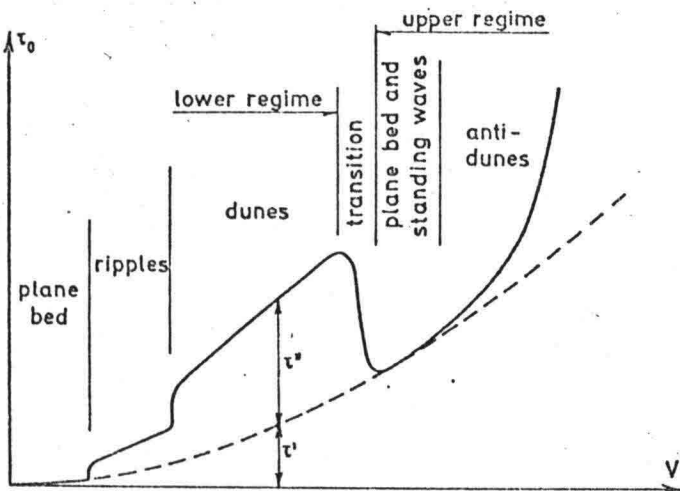


Figure 2.1.2 Shear stress - flow velocity graph for an alluvial channel

[10]

The presence of bed forms depends on hydrodynamic stability and the change between bed form types can therefore take place all most discontinuous. For instance is it observed that a small change in temperature, thus change in viscosity, can cause a change from a dune covered bed into flat bed / ripples and then influence the roughness considerable.

As the bed form has such a large influence on the hydraulic resistance it is convenient to discuss the flow over a dune fig. 2.1.3.

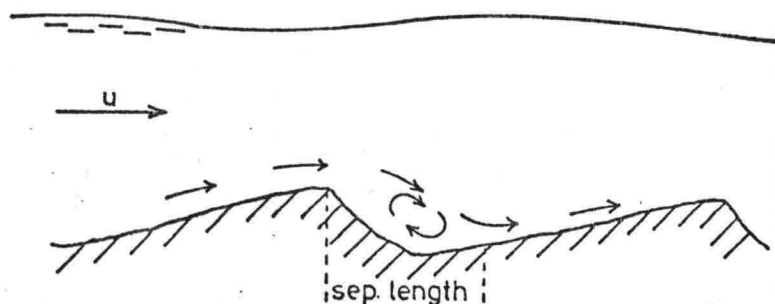


Figure 2.1.3. Sketch of flow over dune or ripple.

Immediately after the crest separation takes place and a zone of free turbulence is formed. After a certain length, the separation length, the flow is getting in contact with the bed again. In fig. 2.1.4 the pressure and shear stress distribution over a dune is depicted. The measurements are carried out by Raudkivi and the calculated values are obtained from a boundary layer model.

The resistance the dune is performing on the flow can now be found from fig. 2.1.4 by integrating the horizontal component parts of the pressure and the shear stress.

Although it is possible to calculate the roughness from the local dune dimensions, there has to be used empirical formulas for the roughness prediction based on the dune dimension because the expenses for these calculations still are large.

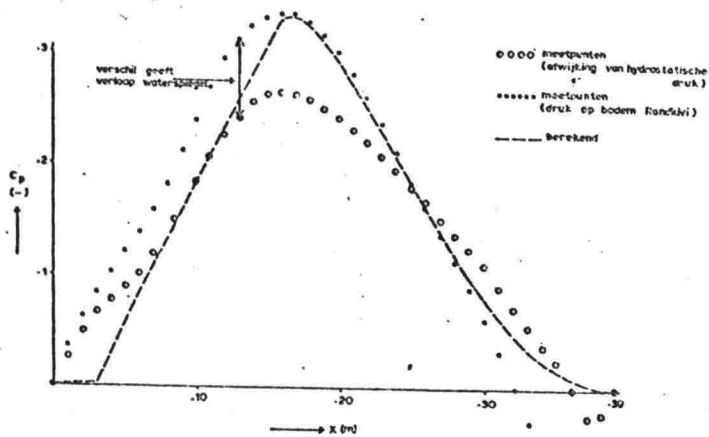
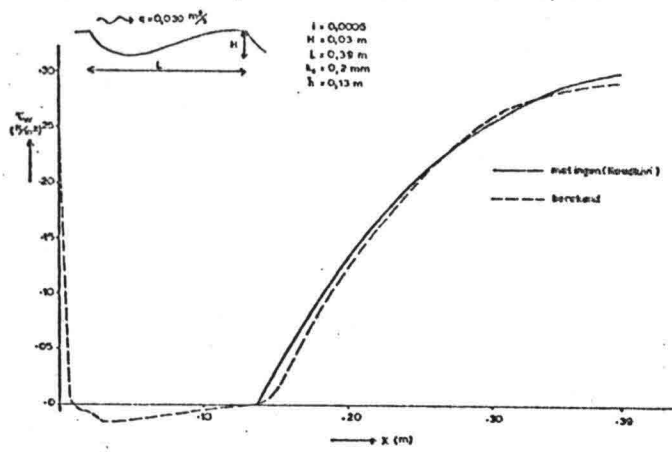


Figure 2.1.4. Shear stress and pressure distribution over a dune [13]

2.1.2. Roughness Predictors based on dune dimensions.

For the present purpose it seems attractive to use a roughness predictor based on the dimension of the dunes, because there any way has to be performed a dune height prediction for estimating the transport layer thickness.

A summary of the most important empirical relations are given in table 2.1.1.

Reference	Hydraulic Resistance	
	f	f''
Vanoni and Hwang (1967)		$f''^{-\frac{1}{2}} = 3.3 \log \frac{La}{H^2} - 2.3$
Fredsoe (1975)	$f = 1.88 \frac{H}{L}$	
Engelund (1978)		$f'' = 10^{\frac{H}{a} - 2.5 \frac{H}{aL}}$
Van Rijn (1980)	$f^{-\frac{1}{2}} = \frac{18}{\sqrt{8g}}$ $\log \frac{12a}{(0.75 \log \frac{H}{L} + 1.75)H}$	

where L dune length, H dune height and a water depth

Table 2.1.1. Empirical roughness predictors [13]

Comparing around 500 measurements from World Flume Data with the calculated roughness of the four methods in table 2.1.1 it was found that the Fredsoe method is predicting the roughness relatively bad compared with the three other methods which were rather reliable [13]. As a part of the same test the three methods predicting the roughness good for the World Flume Data were compared with proto-type measurements performed during a high water (the flood plains were inundated), in march 1979, in Pannerdensch Kanaal. The results of this test is depicted in figure 2.1.5.

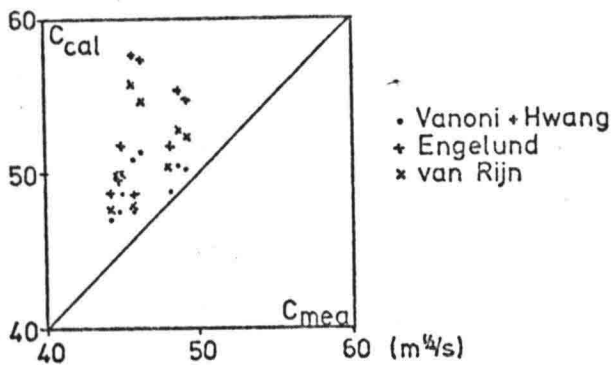


Figure 2.1.5. Measured and calculated Chézy roughness in Pannerdensch Kanaal.

The roughness predictors are all underestimating the roughness in the proto-type. The deviation between measured and calculated values, which were not found in the test with the flume data, is maybe caused by

- additional resistance in the proto-type: diffusion between stream branches, vegetation etc.
- unaccurate correction for the resistance of the flood plains
- using an average dune dimension instead of a dominant one.

From table 2.1.1 it is seen that the roughness coefficient is very sensitive to changes in the dune dimensions, which means that the dune dimension predictions have to be accurate in order to get a good estimation of the roughness, but there are no accurate dune dimension predictors available (see Chapter 2.3). Further more the measurements in the Pannerdensch Kanaal indicate that there has to be chosen dominant dune dimensions, which introduce more uncertainties in the roughness prediction based on the dune dimensions.

An other group of roughness predictors only uses the specific discharge (q) bed slope (I_0) and a characteristic grain diameter (d_c) in the bed.

2.1.3. Roughness predictors based on q , I_0 and d_c .

Several scientists have attempted to obtain a stage discharge relation for alluvial channels without taking the dune dimensions explicit into account. The obtained relations are either pure empirical or are based on

the dividing of the energy loss into two parts (eq. 2.1.4), where then the skin friction is found from a logarithmic boundary formula

$$\frac{U}{U_{fr}} = C_1 + C_2 \ln f(U_f, d_c) \quad (2.1.5)$$

where C_1 , C_2 are constants,

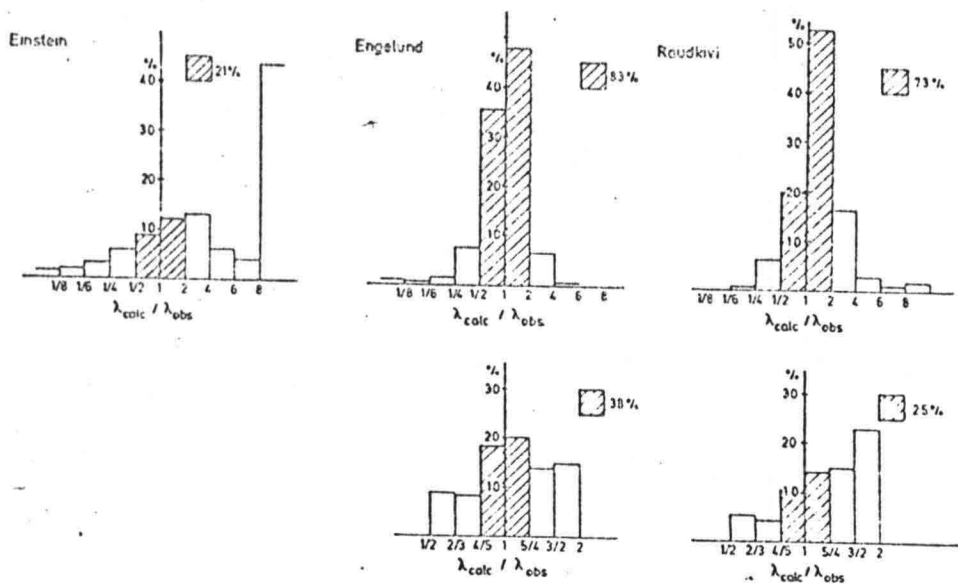
$$\text{and } U_{fr} = \sqrt{\frac{f}{8}} \cdot U \quad - \quad \text{the friction velocity}$$

and the form friction is determined more or less empirical.

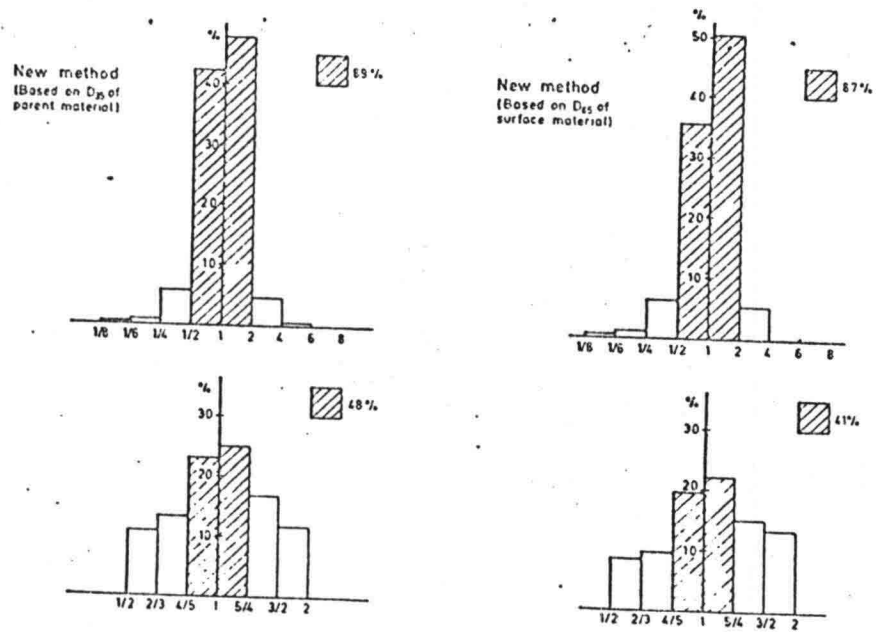
None of the roughness predictors are very reliable especially in the dune region where the largest applicability is found [20]. White et al (1980) has carried out a comparison of some of the best predictors of the measured and calculated roughness for a large number of flume experiments. In fig. 2.1.6 the result from this test is depicted where the "New Method" is the method from White et al (1980).

The relative accuracy of the Darcy - Weisbach coefficient is comparable with the accuracy for the bed slope. The new method is only predicting the roughness within a margin of error of 80% - 125% in 42% of the cases and an error on 25% in the bed slope has a large influence on the amount of sediment there have to be degraded or aggrated before equilibrium is reached.

However, as the roughness predictors based on the dune dimensions can not produce a reliable result because the lack of a trustworthy dune dimension predictor, a predictor based on the hydraulic parameters is preferred. According to figure 2.1.6 the "New Method" is the best, but it has the disadvantage that it is not explicit dividing the friction into a form and skin friction which is convenient for the transport formulas (see Chapter 2.2). The "New Method" is not significant better than the Engelund - method which has the advantage that it is applicable for



Distribution of discrepancy ratios (Einstein, Engelund, Raudkivi)



Distribution of discrepancy ratios (New method)

λ Darcy - Weisbach coefficient

Figure 2.1.6. Accuracy of roughness predictors [13]

all bed forms in the lower regime, so the Engelund method will be applied in the numerical model for morphological changes in rivers.

2.1.4. The Engelund Roughness Predictor

Engelund is applying the basic hypothesis (eq. 2.1.4), and states a similar relation for the shear stress, which in dimensionless form reads

$$\theta = \theta' + \theta'' \quad (2.1.6)$$

where θ total dimensionless shear stress

$$= \frac{\tau_o}{\rho g \Delta d} = \frac{Ia}{\Delta d} \quad (2.1.7)$$

Δ is the relative density of the sediment

θ' effective (skin) dimensionless shear stress

$$\theta' = \frac{Ia'}{\Delta d} \quad (2.1.8)$$

θ'' shear stress due to bed forms

in which a' can be interpreted as a boundary layer thickness, and can be obtained from a boundary layer formula

$$\frac{U}{U'_{fr}} = 6 + 2.5 \ln \frac{a'}{k_s} \quad (2.1.9)$$

with $U'_{fr} = \sqrt{\frac{\tau_o'}{\rho}} = \sqrt{ga'I} = \sqrt{g\Delta d \theta'}$

$$\frac{U}{\sqrt{g\Delta d \theta'}} = 6 + 2.5 \ln \frac{a \theta'}{k_s}$$

in which k_s is the Nikuradses grain roughness, experimentally estimated to $k_s = 2 \cdot d_{65} \approx 2 \cdot d_{50}$

To obtain an estimate for the expansion loss Engelund uses the Carnot formula

$$\Delta H'' = \alpha \frac{(U_c - U_t)}{2g} \quad (2.1.10)$$

where U_c and U_t are respectively the flow velocity over the crests and over the troughs of the dunes and α is the velocity distribution coefficient. For

$$U_c = \frac{q}{\alpha + \frac{1}{2}H} \quad \text{and} \quad U_t = \frac{q}{\alpha - \frac{1}{2}H} \quad (2.1.11)$$

an expression for the energy loss per unit length due to the expansion loss appears

$$I'' = \frac{\Delta H''}{L} = \frac{q}{L} \frac{1}{2g} \left(\frac{1}{\alpha + \frac{1}{2}H} - \frac{1}{\alpha - \frac{1}{2}H} \right)^2 \approx \alpha \frac{u^2}{2g} \frac{H^2}{La^2} \quad (2.1.12)$$

Recalling the definition of the Darcy - Weisbach coefficient (eq. 2.1.1) it is seen

$$f'' = 4\alpha \frac{H^2}{La} \quad (2.1.13)$$

Engelund now considers two streams with different slope (distorted vertical scale) and states that the principle of similarity is valid if the following conditions are fulfilled

$$\begin{aligned} \theta_1' &= \theta_2' && \text{dynamic similarity} \\ \frac{\theta_1''}{\theta_1} &= \frac{\theta_2''}{\theta_2} \end{aligned}$$

where 1 and 2 are referring respectively to stream one and two. Applying eq. (2.1.13) the second condition can be expressed in terms of the roughness coefficients with

$$\frac{f}{f} = \frac{f}{f} = \frac{f''}{f''} = \frac{\lambda_H}{\lambda_L} \quad (2.1.14)$$

in which λ_H and λ_L are the vertical and horizontal length scale.

With the hypothesis that alluvial streams tend to adjust their roughness according to the rules of similarity with distorted scale it can be shown that the total dimensionless shear stress is only a function of the effective dimensionless shear stress

$$\theta = \theta(\theta') \quad \text{or} \quad \theta' = \theta(\theta') \quad (2.1.15)$$

From extensive flume experiments (12) Engelund obtained an empirical relation for eq. (2.1.15) in the dune and ripple region

$$\theta' = 0.06 + 0.4\theta^2 \quad (2.1.16)$$

This empirical relation between the total dimensionless shear stress and the effective shear stress is depicted in figure 2.1.7 where the experimental results also are plotted

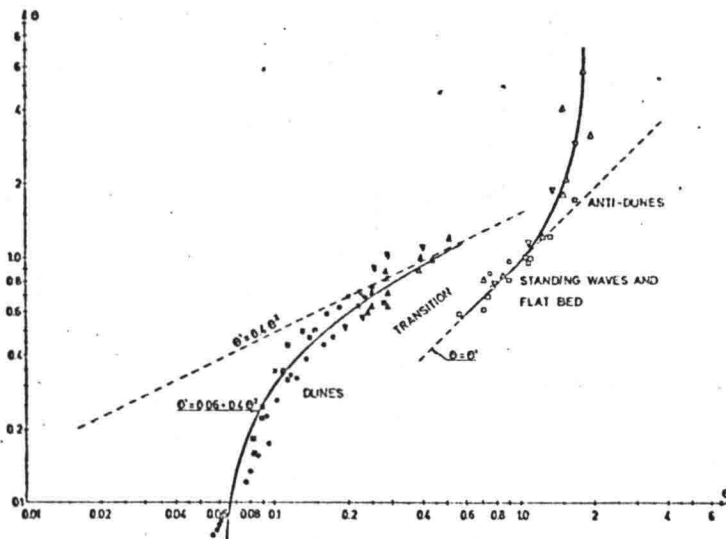


Figure 2.1.7. Relation between effective and totale dimensionless shear stress (8)

In case of plane bed and standing waves there is no expansion loss and eq. 2.1.15 becomes

$$\theta' = \theta \quad (2.1.17)$$

2.1.5. Application of the Engelund roughness predictor.

There has to be carried out some modifications of the method before it is applicable for a numerical model.

The relation, figure 2.1.7, is a two valued function, which is in agreement with observations from nature, where there is found discontinuous rating curves [20], but it is unacceptable in a computer programme. To avoid the two values problem the modification proposed by Challet and Cunge (1980) is applied, figure 2.1.8.

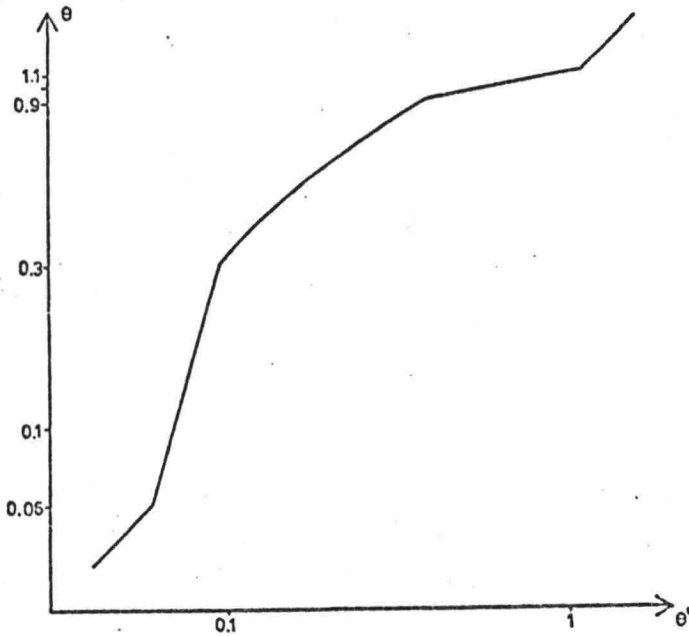


Figure 2.1.8. Modified $\theta' - \theta$ relation.

The modified relation now becomes

$\theta \leq 0.06$	$\theta' = \theta$	
$0.06 < \theta \leq 0.3$	$\theta' = 0.136 \theta^{0.292}$	
$0.3 < \theta < 0.9$	$\theta' = 0.06 + 0.4 \theta^2$	
$0.9 \leq \theta < 1.1$	$\theta' = 0.667 \theta^{5.24}$	(2.1.18)
$\theta \geq 1.1$	$\theta' = \theta$	

Equation (2.1.9) has to be solved iterative, but Engelund (1967) proposes an approximation so a solution can be found explicit

$$\frac{U}{\sqrt{U'_{fr}}} = 9.45 \left(\frac{a'}{k_s} \right)^{1/8} \quad (2.1.19)$$

which is approximating eq. (2.1.9) with a 5% margin of error in the interval

$$13 < \frac{a'}{k_s} < 1.5 \cdot 10^4$$

Equation (2.1.19) can be written in a alternative form

$$\frac{\theta'^6}{\theta} = \frac{2.5}{g^4 \Delta^4 9.45^8} \frac{u^8}{a d^3} \quad (2.1.20)$$

Combining eqs. (2.1.18) and (2.1.20) the shear stress, thus the roughness, can be found explicit, except in the dune region where an iteration has to be performed, for known flow velocity, slope or water depth.

2.1.6. Roughness coefficient in flumes with different roughnesses of bed and side walls.

For simulating sediment transport experiments in flumes, where the bed generally is much rougher than the side walls, it is important to know how the total shear force is distributed between the bed and side walls.

Two methods are available for this purpose, the Einstein and the Prandtl / v. Karman method. The principal assumptions in both methods are that the flow cross section can be divided into parts separated with shear-stress-less surfaces, thus the gravity force is only balanced by the shear stress along the walls and the bed (eq. 2.1.21), and that the roughness relations (Chézy, Darcy - Weisbach etc.) can be applied to each part of the cross section as well as to the whole.

$$\Sigma_b \cdot B + \Sigma_w \cdot 2 \cdot a = \rho g A I \quad (2.1.21)$$

2.1.7. The Einstein method.

Einstein assumed further that the mean velocity in all the cross section parts are the same.

Here the method will be derived for the Chézy roughness relation and for a case where the wetted perimeter can be divided into n parts each with constant Chézy roughness. The Chézy equation applied to the total cross section yields

$$U = C \sqrt{RI} \quad (2.1.22)$$

where R is the hydraulic radius, defined as the total area of the cross section divided by the wetted perimeter

$$R = \frac{A}{P} \quad (2.1.23)$$

The Chézy equation applied to each cross section part reads

$$U = C_i \sqrt{R_i I} \quad (2.1.24)$$

By combining eqs. 2.1.22 and 2.1.24 an expression for the hydraulic radius for the cross section parts appears

$$R_i = R \left(\frac{C}{C_i} \right)^2 \quad (2.1.25)$$

From the definition of the hydraulic radius and eq. 2.1.25

$$A = P \cdot R = \sum P_i R_i = R C^2 \sum \frac{P_i^2}{C_i^2} \quad (2.1.26)$$

from which the mean roughness coefficient can be found

$$C = \left[\frac{P}{\sum \frac{P_i^2}{C_i^2}} \right]^{\frac{1}{2}} \quad (2.1.27)$$

The roughness coefficient from the component parts of the cross section can be obtained from the Colebrook and White formula

$$C_i = 18 \log \frac{12 R_i}{k_i + 0.3 \delta_i} \quad (2.1.28)$$

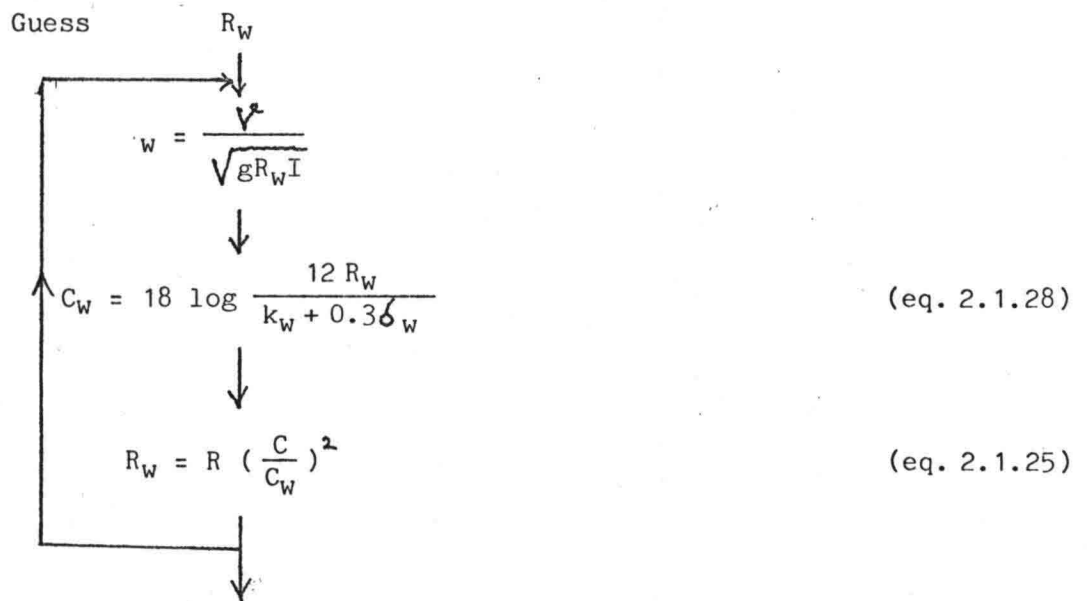
in which k_i Nikuradses roughness for section i ($k_w \approx 10^{-5}$ for concrete)

$$\delta_i = 11.6 \frac{\nu}{\sqrt{g R_i I}} \quad \text{viscous sublayer}$$

ν kinematic viscosity.

When flume experiments, carried out in a rectangular flume with different roughness at walls and bed, have to be interpreted the bed shear stress can be attained from the following trial and error procedure.

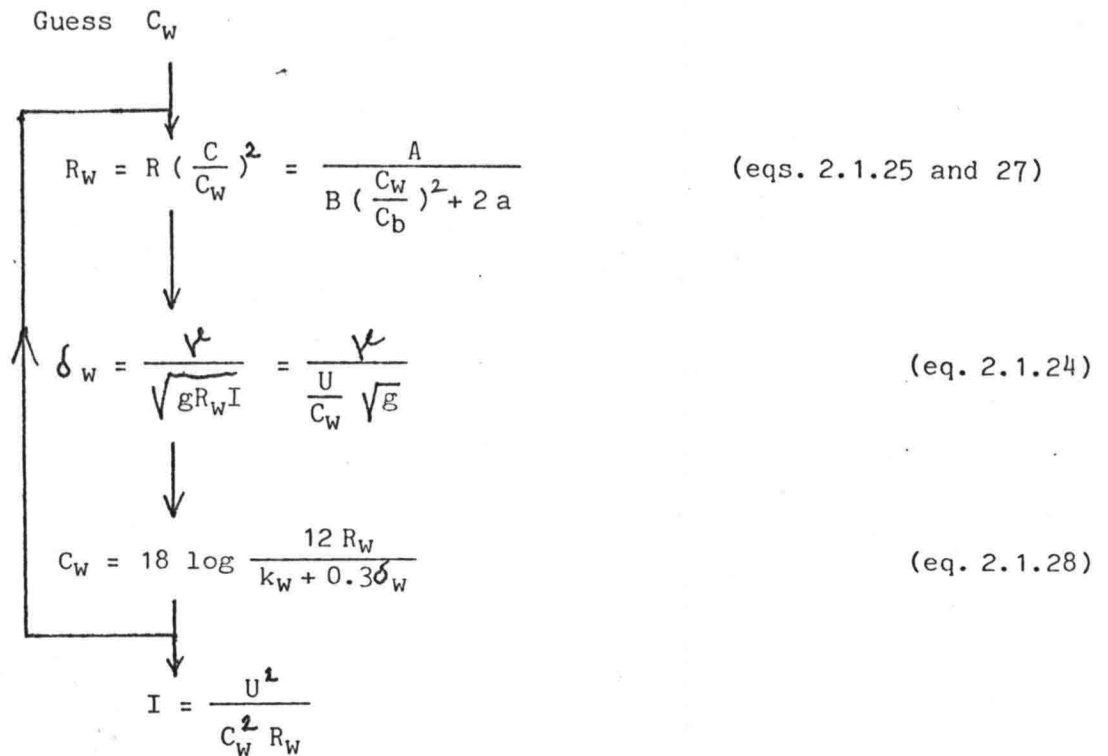
Given: a , u , I (thus also R and C)



$$\tau_b = \frac{1}{B} (\rho g I A - \rho g I R_w 2 a) \quad (eq. 2.1.21)$$

If a flume experiment is simulated the energy line gradient is unknown and the procedure is different

Given: C_b , U and $\tau_b = g I R_b = g \left(\frac{U}{C_b} \right)$



The method is convergating rather fast. For a good first guess 3 - 4 iterations is sufficient to approximate τ_b or I within a 1% margin of error.

2.1.8. Prandtl / von Karman method.

For this method it is not necessary to assume that the mean velocity is equal in all cross section parts. The basic assumption for this method is that the velocity in a point in the cross section part belonging to the wall or the bed, only depends on the roughness of respectivly the wall or the bed. The velocity profile is calculated with the Colebrook - White formula, and the surfaces separating the cross section parts is determind with equalizing the velocities.

The velocity profile formula in the transition zone between hydraulic rough and smooth for the walls yields

$$\frac{U_w}{U_{fw}} = \frac{1}{K} \ln \frac{30 y}{0.3 \delta_w + k_w} \quad (2.1.29)$$

and for the cross section part belonging to the bed

$$\frac{U_b}{U_{fb}} = \frac{1}{K} \ln \frac{30z}{0.3\delta_b + k_b} \quad (2.1.30)$$

in which

$$K \text{ von Karman constant } \frac{1}{K} = 2.45$$

δ_w, δ_b viscous sublayer thickness respectively at walls and bed

k_w, k_b Nikuradse's grain roughnesses

U_{fw}, U_{fb} friction velocities

y distance to wall

z distance to bed

Stating that the surface, which is dividing the cross section, is only slightly curved, Prandtl and von Karman approximate it to a straight line with a slope $\alpha = y_*/a$ where y_* is found from $U_w(y_*) = U_b(a)$. By integrating eqs. 2.1.29 and 2.1.30 the mean velocities in the cross section parts and the discharge are found as a function of R_w, R_b and k_b , which in combination with the principal assumption, i.e. eqs. 2.1.21, 22 and 24, gives a system from which the roughnesses of bed and walls can be obtained.

The method is also iterative, but complicated and very elaborate compared with the Einstein method.

2.1.9. Experimental verification.

Yassin (1953) carried out experiments in order to verify the Einstein method for the Darcy - Weisbach and the Strickler roughness relations. The experiments are performed for varying depth width ratios (0.05 - 1) in three cases:

1. Both bed and side walls smooth

2. Bed rough and side walls smooth
3. Both bed and side walls rough.

The results of the experiments are that the theoretical calculated and measured values are deviating with a maximum margin of error on 7%, worst for large depth width ratios. However, there is a scatter between the measured and calculated values on 3 - 4% even for small depth width ratios, so a good deal of the 7% deviation can probably be attributed to experimental inaccuracy.

In [6] the two methods, with the Chézy roughness relation, are compared with experimental results. From a number of experiments with a constant Nikuradses roughness for the walls $k_W = 0.4 \times 10^{-4}$, with and without bedforms and with different depth width ratios and discharges the bed and wall roughness are calculated from a known mean roughness coefficient.

The conclusion from the test was that the two methods can predict Chézy values for the walls that can differ considerable, but for moderate depth width ratios the influence from the walls on the bed roughness is very small: the maximum difference between the two calculated values for the bed roughness did not exceed 1% (depth width ratio ~ 0.5).

Consider the little difference in the quality of the methods it is not important which one is applied so the relative simple Einstein method is preferred, also because one often only has a crude estimate for the Nikuradses grain roughness for the walls.

2.2. Sediment transport formula.

The purpose of the transport formula is to relate the amount of sediment in transport to the local hydraulic parameters and to the bed composition. Before discussion of the different transport models in details it is convenient to give definitions of some concepts of the sediment transport.

2.2.1. Classification.

The bed material load is defined as the sediment in transport which is related to the local composition of the bed. The bed material load is divided into the bed load and the suspended load.

The bed load is the sediment in transport which is sliding, rolling or jumping over the bed.

The suspended load is the part of the bed material load which is moving without continuous contact with the bed. The concentration of the suspended load will decrease with the distance from the bed. The material is kept in suspension because the turbulent mixing of the flow will balance the fall velocity of the grains. Although suspended load can have a considerable influence on morphological processes in rivers no separate calculation of the suspended load will take place.

The wash load is very fine sediment carried over long distances in suspension. The wash load is not related to the local bed composition and can therefore not be predicted by a sediment transport formula. Fortunately the wash load has often a neglectable influence on morphological changes in alluvial streams.

2.2.2. Initiation of motion.

The forces working on a grain in the bed determining whether it moves or not. When the acting forces is exceeding the stabilising forces the grain start to move, figure 2.2.1.

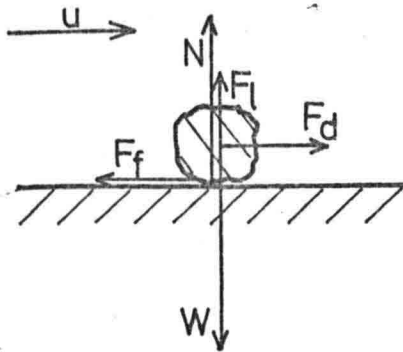


Figure 2.2.1. Forces working on a sediment grain on the treshhold of of movement.

Introducing the friction angle ϕ the treshhold of movement or the initia-
tion of motion is given by

$$F_d = F_f = N \cdot \tan \phi = (W - F_l) \tan \phi \quad (2.2.1)$$

However the treshhold of movement is only rarely attained from considerations about forces on a single grain. Usually the initiation of motion is related to the dimensionless shear stress and often assumed to be constant equal the Shields-value 0.06, but also critical dimensionless shear stress equal 0.03 is proposed.

2.2.3. Transport mechanism

In sedimentation engineering problems with dune or ripple covered bed is prevailing, and it is useful to discuss the transport mechanism in case of bed load for these bed forms.

On a part of the upstream side of the dunes the shear stress is moving the grain along the surface until they roll over the crest and become buried on the lee side until they again are exposed for the flow. Evidently grains are degraded on the upstream side and aggrated on the downstream side and consequently the dune will migrate downstream.

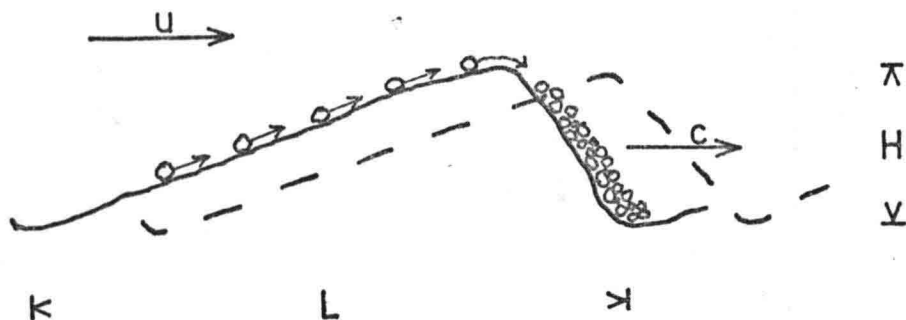


Figure 2.2.2. Bed load over dune covered bed.

With the assumption that the dunes are migrating with a constant velocity and without changing shape and expression for the local bed load at the dunes can be found

$$S_l = C_d y \quad (2.2.2)$$

where S_l local transport included pore
 C_d migration velocity of dune
 y level above plane through the troughs

In the following some models for the more overall sediment transport S will be described, i.e.

$$S = \frac{1}{T} \int_0^T \frac{1}{H} \int_0^H S_l dy dt \quad T \gg \frac{L}{C_d} \quad (2.2.3)$$

2.2.4. Sediment transport formulas for uniform sediment.

Several scientists have attempted to obtain a unique relation between the effective shear stress and the sediment in transport, i.e.

$$S = f(\theta') = f(U, C, d, \dots) \quad (2.2.4)$$

Figure 2.2.3 gives an impression of the large number of available sediment formulas and the large scatter between the sediment discharge pre-

dicted by these. Note that the scale is logarithmic, comparing for instance the Shields and the Meyer - Peter and Müller formula it is seen that for low discharge the ratio between the predicted values is around 100!

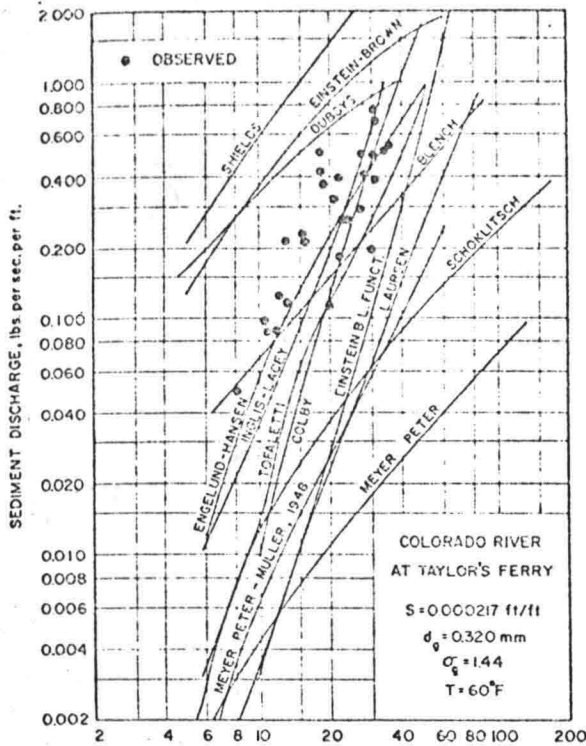


Figure 2.2.3. Transport formulas, after (20)

Regarding the large number of transport models it has been necessary to restrict the number of transport relations taken into consideration. Two typical bed load formulas and one bed material load formula are selected because of their simplicity and practical applicability.

Before presentation of the formulas it is convenient to define two dimensionless parameters.

Dimensionless transport rate

$$\Phi = \frac{q_T}{\sqrt{\Delta g d^3}}$$

(2.2.5)

where q_T = the totale transport in volume of material (excluded pore)
per unite time and width

$q_T = S(1-\epsilon)$ ϵ the pore volume

d = a characteristic grain diameter

Ripple factor

$$\mu = \frac{\theta'}{\theta}$$

which for the Chézy roughness relation reads

$$\mu = \left(\frac{C}{C_g}\right)^2 \quad (2.2.6)$$

where C_g is the Chézy coefficient for the grains which can be obtained from the White - Colebrook formula or a logarithmic resistance formula from the hydraulic rough zone. Large confusion is prevailing regarding the choice of a Nikuradses grain roughness for these formulas.

Meyer - Peter and Müller

In the dimensionless notation the Meyer - Peter and Müller transport formula reads

$$\Phi = 8(\mu\theta - \Theta_c)^{3/2} \quad (2.2.7)$$

in which the characteristic grain diameter is d_m and Θ_c is an empirical constant, which according to Meyer - Peter and Müller must not be interpreted as the critical shear stress.

$$\Theta_c = 0.047$$

Meyer - Peter and Müller suggest that the C_g is calculated from a boundary layer equation from the rough zone with $k_s = d_{90}$, and they found that the formula were fitting their experimental data better if the ripple factor was calculated as

$$\mu = \left(\frac{C}{C_g} \right)^{3/2}$$

The formula has the typical form of a bed load formula with a threshold value. The formula only holds good for small transport rates of coarse material. The formula is often applied for the lower part of the river Rhine with acceptable results [15], which however may have something to do with the fact, that the ripple factor often is used to calibrate the formula.

Engelund - Fredsoe

The transport model developed by Engeland and Fredsoe (1976) is also a typical bed load formula

$$\Phi = 5 \left[1 + \left(\frac{0.267}{\theta' - \theta_c} \right)^4 \right]^{-1/4} (\sqrt{\theta'} - 0.7\sqrt{\theta_c}) \quad (2.2.8)$$

The authors suggest a characteristic diameter equal d_{50} .

The formula is so new that no information about results from practical application is available. The formula is based on a description of physical processes and the model is modified from experimental data ([11] and others).

Engelund - Hansen

The Engelund - Hansen formula [10] is a total transport formula based on a principle of similarity from which is found that the dimensionless transport rate is only a function of the dimensionless effective shear stress and the roughness. In the derivation of the model the Engeland - Hansen relation between the total and effective shear stress (eq. 2.1.16) is applied so the transport rate appears as a function of the total shear stress

$$\Phi = 0.05 \frac{C^2}{g} \theta^{2.5} \quad \text{for } \theta > \theta_c \quad (2.2.9)$$

The characteristic diameter is according to Engeland and Hansen equal to the geometrical mean diameter (d_{50}).

The formula is based on a large number of flume experiments and has therefore a large applicability, but the formula is not very reliable close to initiation of motion. The transport formula has been successfully applied to Dutch rivers when sediment in transport both in suspension and as bed load are present.

A quantitative comparison of the three formulas is given in figure 2.2.4 with the assumptions

$$C = 35 \text{ m}^{\frac{1}{2}}/\text{s}$$

$$\theta' = 0.06 + 0.4 \theta^2$$

$$\theta_c = 0.06 \text{ for Engeland - Fredsoé}$$

$$\sigma_g = 1 \text{ thus } d_m = d_{50}$$

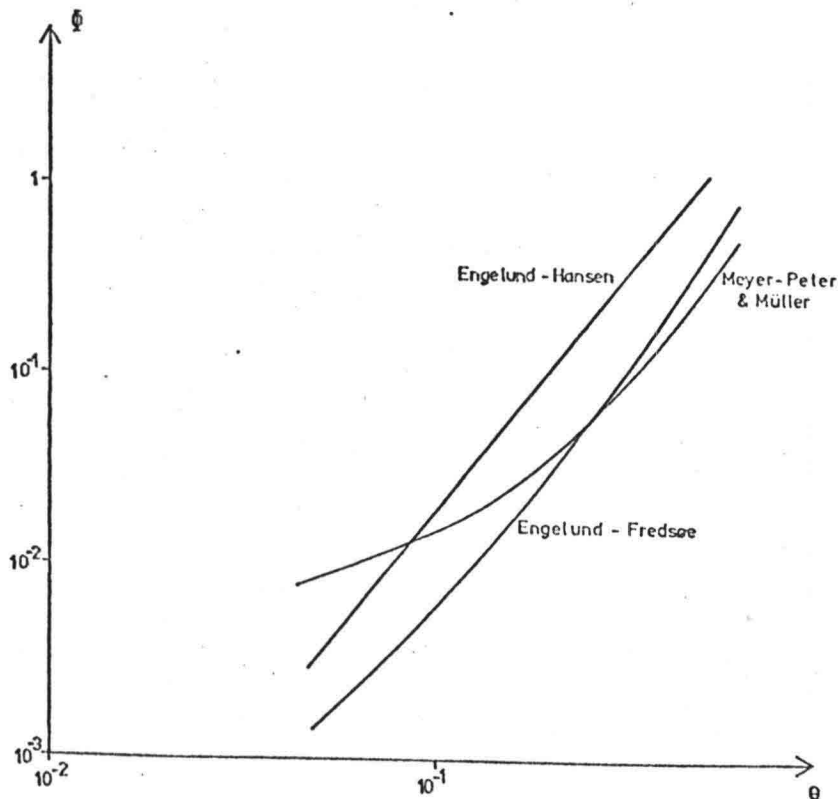


Figure 2.2.4. Transport rate as a function of the total dimensionless shear stress.

2.2.5. Transport formula for non-uniform sediment.

Only few transport formulas for non uniform sediment are available, and most of them modified versions of models for uniform sediment. The most general form of a formula for non-uniform sediment reads

$$S_i = f_i (U, p \dots p_{N-1}, d \dots d_N, C) \quad (2.2.10)$$

The transport formulas per sediment fraction that will be discussed here are adaptations of the already mentioned formulas for uniform sediment. It is assumed that the formulas are valid for each fraction, using the total or effective shear stress made dimensionless with the characteristic diameter of fraction i instead of with the mean diameter

$$\theta_i = \frac{\tau}{\rho g \Delta d_i} = \theta \frac{d_{50}}{d_i} \quad (2.2.11)$$

The difference in the amount of sediment available for transport is taken into account by multiplying with the probability of fraction i in the transport layer. Further there is the possibility to normalize the transport of each fraction, so the sum of the transport is equal to the total transport predicted by the transport formula for uniform sediment using the characteristic diameter of the whole mixture.

In the non-dimensionless form the Meyer-Peter and Müller transport formula per fraction without normalization reads

$$S_i = p_i \frac{8}{1-\xi} \sqrt{g\Delta} \left(\mu \frac{U^2}{C^2 \Delta} - \theta_{c,d_i} \right)^{3/2} \quad (2.2.12)$$

which shows that the composition of the sediment in transport is finer than the sediment in the transport layer. This selective transport especially takes place for low flow velocities, where the shear stress for the courser grain is of the same order of magnitude as the critical shear stress. For the same reason it is understood that the predicted amount of sediment in transport close to initiation of motion is very sensitive to the choice of a critical value, and to describe sorting processes it is very important to have the proper value for the critical shear stress.

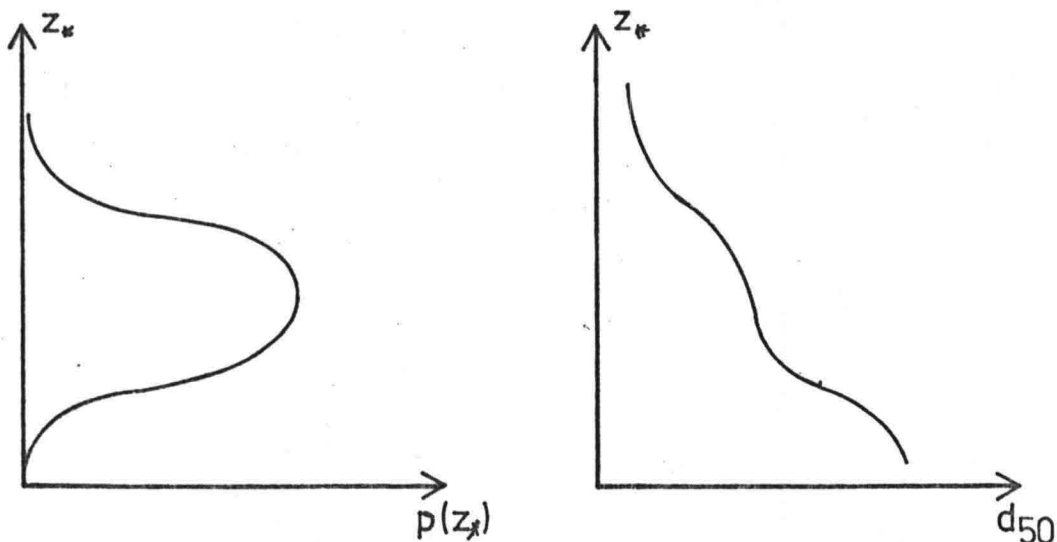
The transport of fraction i can be written in an alternative way

$$S_i = p_i \delta U_{gi} \quad (2.2.13)$$

where U_{gi} is the mean velocity of grain size i in the transport layer. As a consequence of the selective transport the mean velocity of finer grains must be larger than the velocity of coarser ones

$$U_{gi} > U_{gi+1} \quad (2.2.14)$$

As migrating dunes are not considerably deformed the coarser grain must have a larger averaged rest period between being in transport than the finer. Consequently the coarser grains must dominate in the infrequently occurring deep troughs in the bed, a feature that is recognized in flume experiments, figure 2.2.5.



where $p(z_*)$ is the probability of a certain instantaneous bed level z_*

Figure 2.2.5. Vertical gradient in mean diameter in transport layer.

The vertical sorting in the transport layer may be an explanation for the fact, that dunes are overtaken and disappearing. After a deep trough

in the bed there will, at the following dune, be relative much coarse sediment in transport which will tend to slow down the migration of the dune.

Due to the poorly defined transport layer and the vertical sorting in the dunes, experimental measured transport layer composition has to be interpreted with caution. If for instance samples are taken at the surface of the bed along the channel, samples taken in the troughs must be weighted higher than the transport taken at the crests. A similar procedure have to be made when deep samples are taken, and in this case also a problem about how deep to take the samples occurs.

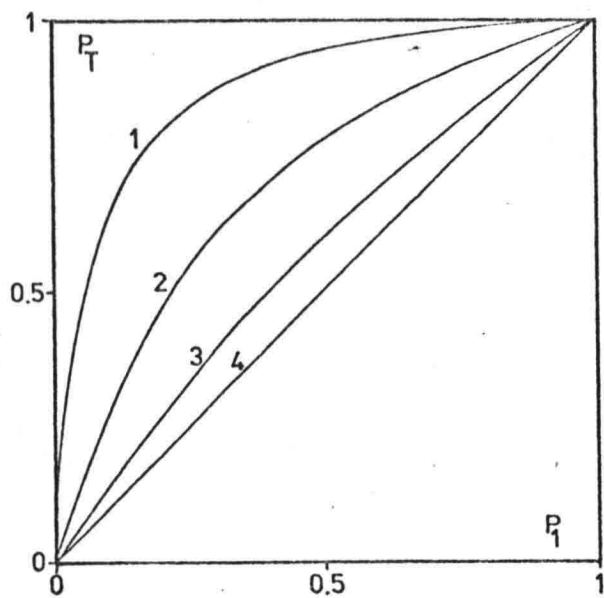
The selective transport is illustrated in figure 2.2.6 in case of two fractions $\frac{d_2}{d_1} = 1.5$. The probability of the sediment in transport of fraction one $p_T = S_1 / (S_1 + S_2)$ is depicted versus the probability of fraction one in the transport layer for equal values of the dimensionless shear stress for fraction two. Notice that the selective transport for the Engelund-Hansen formula is independent of the shear stress, due to the absence of a critical value, which does not seem very reasonable close to initiation of motion, but the formula is also known not to be reliable in this area. The two bed load formulas give for small shear stresses transport that is much finer than the sediment in the bed.

From flume experiments with graded sediments, and even very low transport rates, it is found that the sediment in transport is only slightly finer than the sediment in the bed, but selection of the grains is taking place otherwise armouring would not occur.

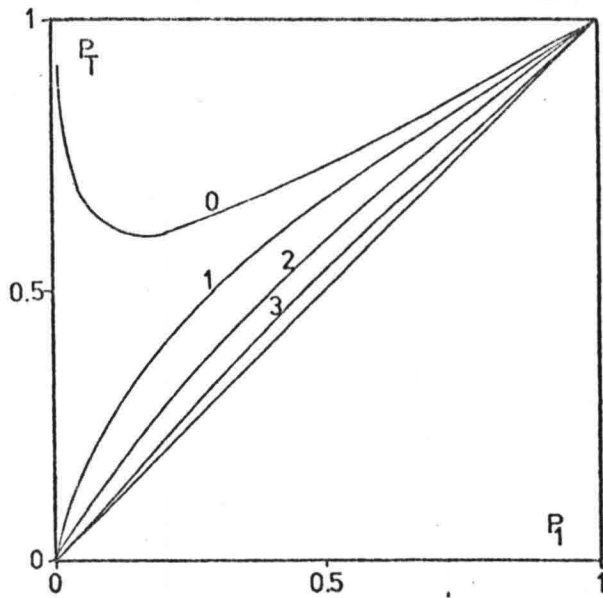
Pantelopulos (1957) carried out some experiments with non-uniform sediment, and he calculated, with a transport formula, what the critical shear stress should be for resulting in the measured transport of each fraction, figure 2.2.7

The critical shear stress is almost constant, thus in the dimensionless form $\Theta_{c1} = \text{constant} / d_1$, which inserted in the Meyer-Peter and Müller formula (eq. 2.2.12) gives a transport where the dependency of the grain diameter vanishes!

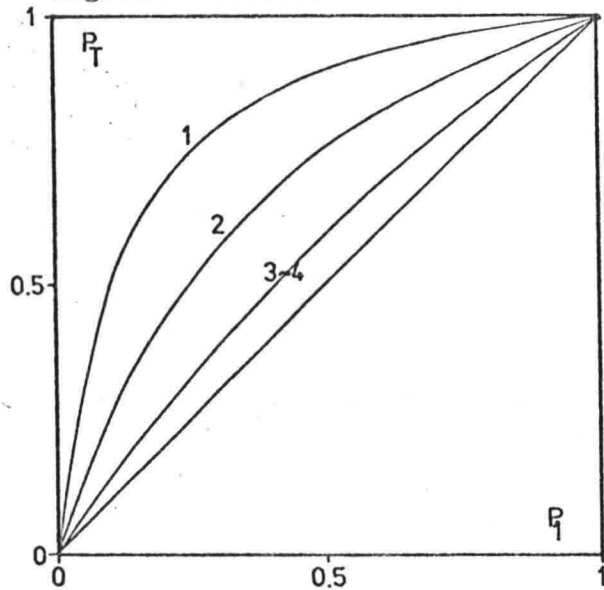
Meyer - Peter and Müller



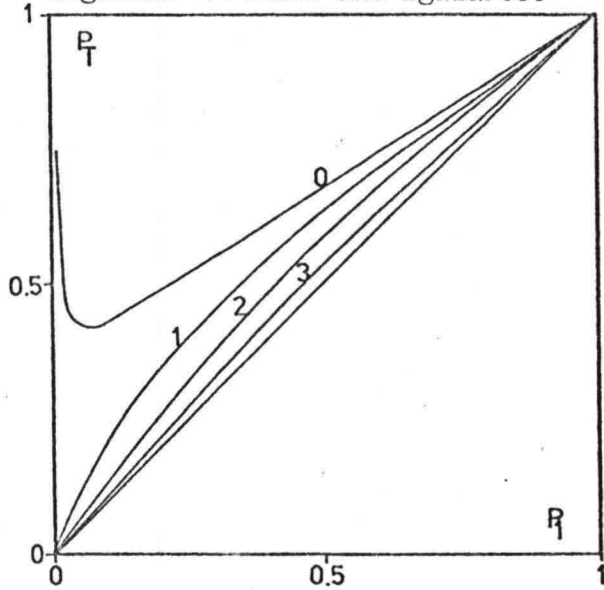
Meyer - Peter and Müller and Egazaroff



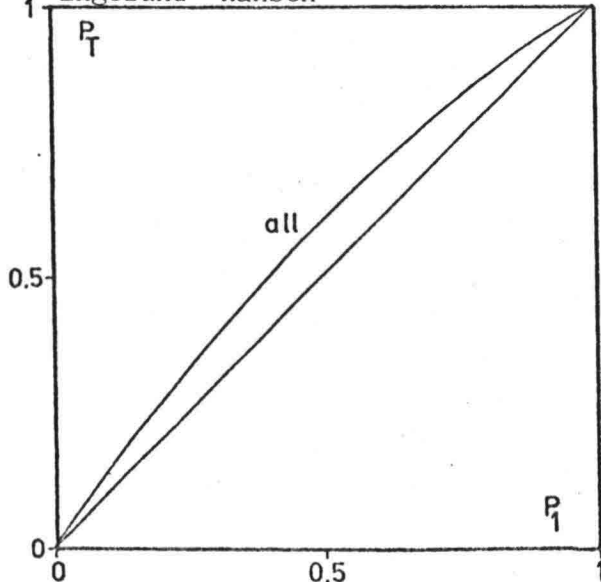
Engelund - Fredsoe



Engelund - Fredsoe and Egazaroff



Engelund - Hansen



- 0. $\theta = 0.047$
- 1. $\theta = 0.050$
- 2. $\theta = 0.0588$
- 3. $\theta = 0.0940$
- 4. $\theta = \infty$

Figure 2.2.6. Selective transport

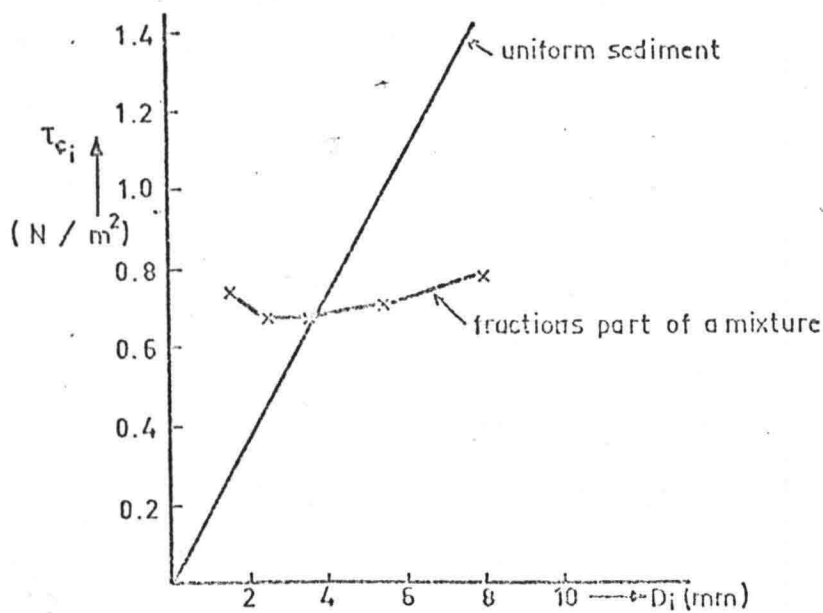


Figure 2.2.7. Critical shear stress in mixture [15]

The only little difference in the compositions may be explained by variation in the critical shear stress. Day (1980) found from flume experiments that same sized particles required a larger shear force to begin movement in coarser mixtures than in finer ones.

2.2.6. Critical shear stress in a mixture.

The observed variation of the critical shear stress in a mixture compared with the uniform case is caused by differences in the drag and friction forces on the grains figure 2.2.1.

The friction angle for a grain may depend on the ratio between the grain diameter and the mean grain diameter in the bed. It seems reasonable to assume that the friction angle, and thus the dimensionless shear stress, will be smaller for a grain larger than the mean diameter and the other way around, figure 2.2.8

From physical considerations Egiazaroff (1957) and (1965) finds an expression for the dimensionless critical shear stress of a spherical grain,

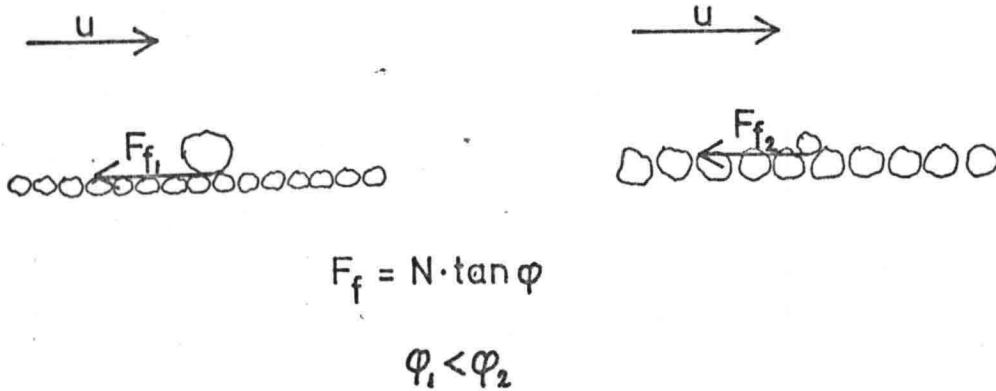


Figure 2.2.8. Variation of static friction angle.

which is a part of a mixture. Neglecting the lift force eq. 2.2.1 becomes for a spherical grain

$$\frac{\pi d^2}{4} C_d \frac{1}{2} \rho U_0^2 = \left(\frac{\pi d^3}{6} g \Delta \rho \right) \tan \varphi \quad (2.2.15)$$

where U_0 is a velocity close to the grain. Assuming complete turbulence (the drag coefficient $C_d = 0.4$) and a logarithmic velocity profile Egiazaroff finds, for uniform sediment, with putting the critical shear stress equal to the Shields value, the point of application of the drag force on the particle $Z = 0.63 d$. Now assuming that the velocity profile is determined by the mean grain diameter (Nikuradses grain roughness) and that the point of application is the same for a grain in a mixture $Z_i = 0.63 d_i$, he derives an expression for the critical shear stress.

$$\theta_{ci} = \frac{0.1}{\left(\log 19 \frac{d_i}{d_m} \right)^2} \quad (2.2.16)$$

The assumption complete turbulence means that the grain diameter is larger than the viscous sublayer thickness, which might not be a very good approximation for small grain sizes.

In the article from (1957) Egiazaroff correctly finds an expression for the threshold of movement depending on the friction angle, and in the second (1965) he is referring to the first article, but now coming up with an expression without the friction angle ($\tan \varphi = 1$), and then he

is obtaining eq. 2.2.16. However, Egiazaroff's theory gives a qualitative correct variation of the dimensionless critical shear stress: increased, compared with the uniform case, for diameters smaller than the mean diameter and decreased for larger grains.

In figure 2.2.6 the selective transport is illustrated for Egiazaroff's theory applied to the Meyer - Peter and Müller and the Engeland - Fredsoe formulas. Eq. 2.2.16 is multiplied by a factor (0.77) so it, in case of uniform sediment, yields the same critical shear stress as the one proposed by Meyer - Peter and Müller. The theory gives a picture of the composition of the sediment in transport, which qualitative is in much better agreement with experimental results. The extreme values in the graphs ($\Theta_2 = 0.047$) is because eq. 2.2.6 is approaching the effective shear stress, i.e. $S_2 \rightarrow 0$ "faster" than $S_1 \rightarrow 0$ for $p_1 \rightarrow 0$. The last feature also seems to be qualitative in agreement with experimental results. Day (1980) found from experiments that the Shield characteristics were changing very sudden.

Ashida and Michire (1973) carried out a few experiments in order to verify Egiazaroff's theory and they found good agreement between measured and calculated values, except for small diameters ($d_1 / d_m < 0.4$) [15].

2.2.8. Conclusion

The transport formulas must be applied with caution because they are of more or less empirical nature, and therefore only applicable for the range of grainsize, gradation, flow velocity etc. in which they are verified.

The Egiazaroff's theory is based on very simplified considerations. The trend the theory shows in the selection of grains can be expected to be even more pronounced because of the neglecting of the variation of the friction angle.

The theory is poorly verified because it is difficult to measure the critical shear stress directly. It is often done by calculating the critical

value with a transport formula from measured shear stresses, and composition which brings uncertainties into the estimation of the critical shear stress.

For large shear stresses it does not make sense to use the Meyer - Peter and Müller formula for non - uniform sediment because no selection of the grains takes place.

2.3. Transport layer thickness.

The transport layer thickness is an important parameter in the model for non-uniform sediment. The thickness has influence on the speed of changes in the composition, which can be seen from the characteristic directions eq. (1.2.15) where the transport layer thickness appears in the denominator. thus decreasing speed of changes for increasing transport layer thickness.

Existing dune height predictors can be used, if the transport layer thickness is interpreted as the half of the mean dune height. Here two theoretical and three empirical dune height predictors will be discussed.

2.3.1. Theoretical models.

The development of bed forms depend on hydrodynamic stability, and theoretical formulas for the dune dimensions deduced from a stability approach are available, but they do not give reliable results [13].

Suzuki (1976) obtains an explicit formula for the transport layer thickness from considerations about the celerities in case of two fractions. It was shown that A and B (eq. 1.2.21) are exact approximations for the two celerities in case of uniform sediment ($d_1 = d_2$). Interpreting the celerities as propagation velocities of changes in the bedlevel and composition it seems physical reasonable to assume that the two celerities are equal for $d_1 = d_2$.

For simple transport formulas eq. (1.2.19) the celerities read

$$C_1 = A = \frac{P_2 z_0 f_1' + P_1 z_0 f_2'}{\delta U} \xrightarrow{d_1 \rightarrow d_2} \frac{S}{\delta U} \quad (2.3.1)$$

$$\text{and } C_2 = B = \frac{\psi_1 + \psi_2}{1 - F} \xrightarrow{d_1 \rightarrow d_2} \frac{\psi}{1 - F^2} \quad (2.3.2)$$

From $A = B$ an expression for the transport layer thickness occurs

$$\delta = \frac{S}{U\psi} (1 - F^2) \quad (2.3.3)$$

or for the dune height depth ratio

$$\frac{H}{a} = \frac{S}{q\gamma} (1 - F^2) \quad (2.3.4)$$

If the celerity in the model for uniform sediment (eq. 1.1.13) is interpreted as the mean grain velocity U_g in the transport layer the same equation for the transport layer thickness appears, as

$$S = U_g \delta \quad (2.3.5)$$

and
$$C = U_g = \frac{\gamma}{1 - F^2} \quad (2.3.6)$$

Fredsoe (1979) approaches the problem from a hydrodynamic point of view. For bed load alone the local transport at a dune is given by eq. 2.2.2, and the migration velocity of the dune can be obtained from the dune height and the transport at the crest

$$C_d = \frac{S_{top}}{H} \quad (2.3.7)$$

where C_d is the migration velocity of the dune and S_{top} is the transport at the top of the dune. Combining eqs. 2.2.2 and 2.3.7 gives

$$S_l = S_{top} \frac{y}{H} \quad (2.3.8)$$

where y is the distance above a plane through the troughs. From measurements it is found that the roughness is constant close to the crest, so the local variation in the bed shear stress is given by

$$\theta_l = \theta_{top} \frac{U_l^2}{U_{top}^2} \quad (2.3.9)$$

Neglecting the contraction of the water level over the crest, i.e.

$F = 0$, eq. 2.3.9 becomes

$$\theta_l = \theta_{top} \left(1 - \frac{H}{a}\right)^2 / \left(1 - \frac{\gamma}{a}\right)^2 \quad (2.3.10)$$

The transport is only dependent on the local effective shear stress because only bed load is considered

$$\frac{dS}{dx} = \frac{\partial S_t}{\partial \theta_t} \frac{\partial \theta_t}{\partial x} = \frac{\partial S_t}{\partial \theta} \frac{2\theta_{top}}{1 - \frac{H}{2a}} \frac{\partial(\frac{H}{a})}{\partial x} \quad (2.3.11)$$

with $(1 - \frac{H}{a})^2 \cdot (1 - \frac{H}{a})^{-3} \approx (1 - \frac{H}{2a})$

Differentiating eq. 2.3.8 and combining with eq. 2.3.11 the dune height predictor appears

$$\frac{H}{a} / (1 - \frac{H}{2a}) = \left[\frac{S}{2\theta \frac{dS}{d\theta}} \right]_{top} \quad (2.3.11)$$

As $2\theta \frac{dS}{d\theta} = 2\theta \frac{\partial S}{\partial U} \frac{\partial U}{\partial \theta} = U \frac{\partial S}{\partial U}$ equation 2.3.11 can be

written like

$$\frac{H}{a} / (1 - \frac{H}{2a}) = \left[\frac{S}{U \gamma} \right]_{top} \quad (2.3.12)$$

The absence of the dependency of the Froude number, due to the neglecting of the contraction of the flow over the crests, does not introduce any large error, because the formula is any way only valid for bed load, where the Froude number is normally very small.

The method is for most transport formulas very unhandy to work with because the shear stress at the top of the dune is depending on the dune height, and the method is therefore iterative.

The two theoretical methods need to be combined with a transport formula. For the Meyer - Peter and Müller formula (eq. 2.2.7) a handy expression occur as

$$\frac{S}{2\theta \frac{\partial S}{\partial \theta}} = \frac{1}{3} \left(1 - \frac{\theta_c}{\theta} \right) \quad (2.3.13)$$

The Suzuki method with eq. 2.3.13 now becomes

$$\frac{H}{a} = \frac{2}{3} \left(1 - \frac{\theta_c}{\theta}\right) (1 - F^2) \quad (2.3.14)$$

and the Fredsoé method

$$\frac{H}{a} / \left(1 - \frac{H}{2a}\right) = \frac{1}{3} \left(1 - \frac{\theta_c}{\theta_{top}}\right) = \frac{1}{3} \left(1 - \left(\frac{1 - \frac{H}{a}}{1 - \frac{H}{2a}}\right)^2 \frac{\theta_c}{\theta}\right) \quad (2.3.15)$$

2.3.2. Empirical relations.

Several empirical relations are available and the most important are resumed in table 2.3.1.

Yalin (1964)	$\frac{H}{a} = \frac{1}{6} \left(1 - \frac{\theta_c}{\theta}\right)$
Allan (1968)	$\frac{H}{a} = 0.086 a^{0.19}$
Gill (1971)	$\frac{H}{a} = \frac{\beta}{\alpha} (1 - F^2) \left(1 - \frac{\theta_c}{\theta}\right)$

α = shape factor, $\frac{1}{6} < \beta < \frac{1}{3}$

Table 2.3.1. Empirical dune height predictors [13]

The Allen method is independent at the shear stress and is not giving flat bed when there is no transport, so this formula is not applicable close to initiation of motion. Yalin and Gill suggest relations with same dependence of the shear stress as the two theoretical with the Meyer - Peter and Müller formula do. The Yalin method is indicating a maximum dune height on 1/6 of the water depth, which is not in agreement with observations. The Gill method is some kind of modification of eq. 2.3.14 and no general rules for choosing the coefficients are available.

The conclusion is that the empirical formulas can not be expected to give a qualitative better result than the theoretical ones, and these has the advantage that different transport formulas can be applied.

2.3.3. Comparison of theoretical models.

In figure 2.3.1 the dune height depth ratio predicted by the two theoretical methods are depicted against the effective shear stress ($\Theta_c = 0.06$ for the Engeland - Fredsoe and $\Theta_c = 0.047$ for the Meyer - Peter and Müller method). The general trend shows that the Suzuki method is predicting higher dunes than the Fredsoe method, independent of which transport formula there is applied. Further the figure illustrates that it is very important to have a accurate estimate for the critical shear stress, when dune height prediction has to be performed for low shear stresses.

In figure 2.3.2 the method is compared with results from flume experiments, carried out at Fort Collins [11], where bed load was prevailing. The effective shear stress is calculated with a boundary layer formula (eq. 2.1.9). The general trend is here that both methods are overestimating lower dunes and under estimating high ones.

The very systematical deviation between the calculated and measured values may be used to make empirical modification of the methods. For instance for dune height depth ratios less than 0.4 the Fredsoe method, with the Meyer - Peter and Müller transport formula applied, gives an empirical relation

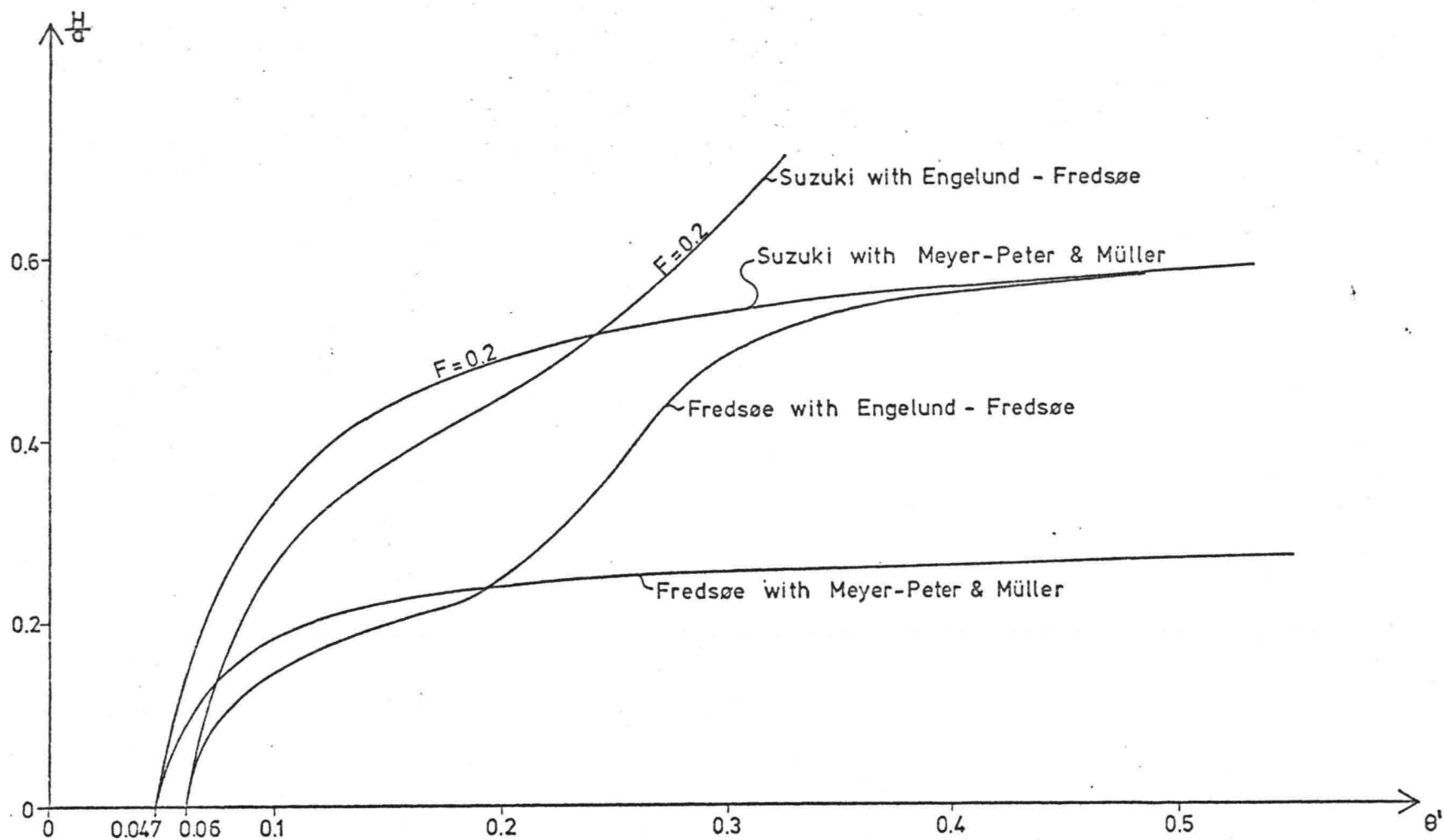
$$\left(\frac{H}{a}\right)_{\text{meas}} = 2.18 \left(\frac{H}{a}\right)_{\text{cal}}^{1.49} \quad (2.3.16)$$

with a correlation coefficient 0.83. However, this relation is only based on 11 measurements, and no independent experimental results has been compared with eq. 2.3.16 for verification.

As mentioned is the transport layer thickness equal half a significant dune height. This proper dune height can be estimated experimentally in two ways:

66

Figure 2.3.1. Dune height predictors.



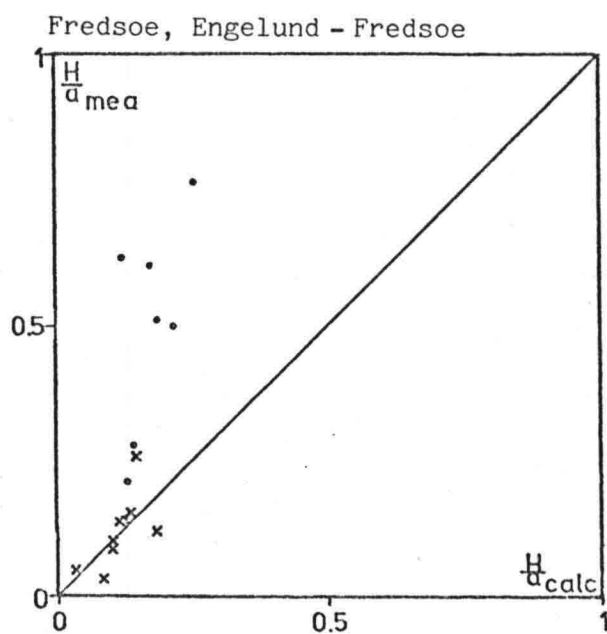
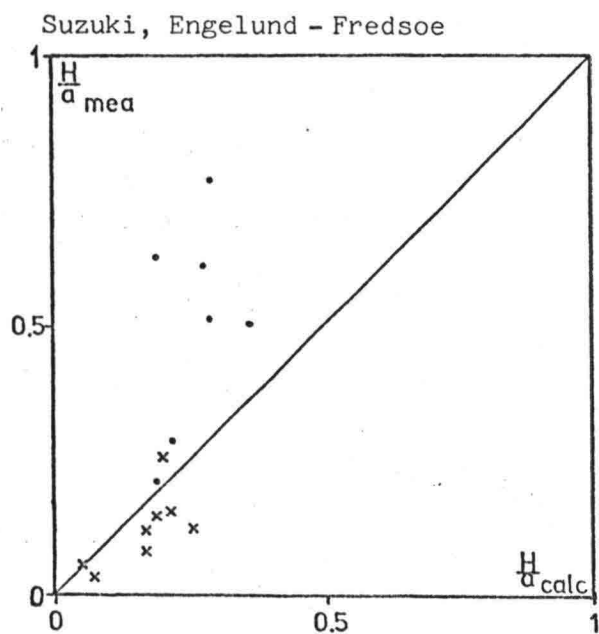
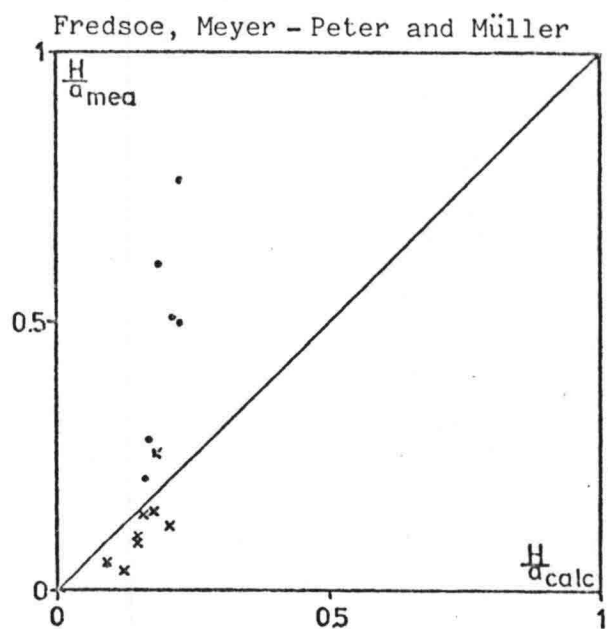
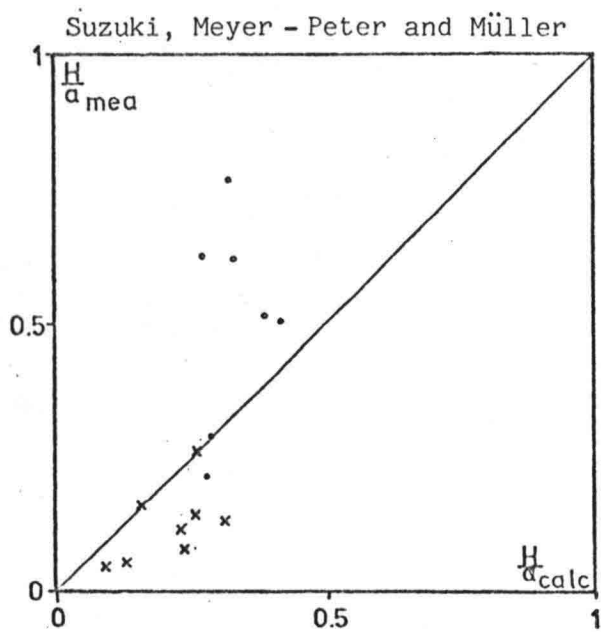


Figure 2.3.2. Comparison with flume experiments.

From measurements in unsteady experiments, and numerical simulation of the experiment with different transport layer thicknesses until the right one is found. This method however demands a reliable transport formula. With help of tracers, i.e. earmarked grains, in steady experiments. The tracers is feed into the flume at the upstream end, and the time of arrival at the downstream end is registrated. The mean grain velocity can now be calculated, and the transport layer thickness can be obtained from eq. 2.3.5. The grain velocity will have a large dispersion, and the mean velocity will therefore be poorly defined.

Considering the uncertainty in the definition of the transport layer and the scatter in the calculated dune height, no preference based on reliability can be made for a transport layer thickness predictor. On account of simplicity the Suzuki method must be preferred.

2.4. The variables \bar{p}_{iz_0}

In order to have a determinable model it is necessary to assume something or have knowledge about the variables \bar{p}_{iz_0} eq.(1.2.12)

In case of $\frac{\partial z_0}{\partial t} < 0$ (erosion for a constant transport layer thickness) $\bar{p}_{iz_0} \cdot \Delta z_0$ is the amount of sediment of fraction i there is picked up from the z_0 -layer into the transport layer. For sedimentation $\bar{p}_{iz_0} \cdot \Delta z_0$ is the amount of sediment leaving the trasport layer into the z_0 - layer, figure 2.4.1.

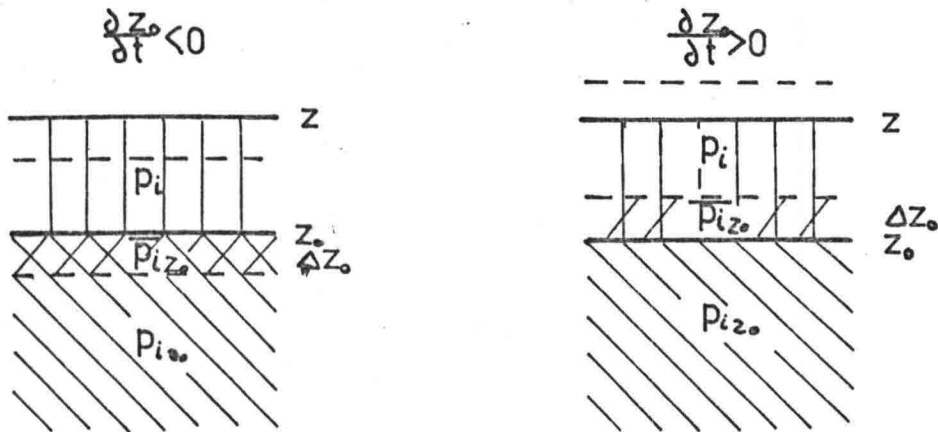


Figure 2.4.1. Composition at z_0 - level: \bar{p}_{iz_0} .

In case of erosion it is evident that the vertical distribution in the composition of the z_0 -layer has to be known, and the composition at z_0 -level can during an erosion process for instance be approximated by

$$\bar{p}_{i z_0} = \frac{1}{2} \left\{ \bar{p}_{i z} * (Z_0) + \bar{p}_{i z} * (Z_0 - \Delta Z_0) \right\} \quad (2.4.1)$$

where * indicates local value.

In case of sedimentation a problem occurs because the flow is mixing the sediment in the transport layer, and no quantitative knowledge about the vertical distribution in the transport layer is available. It was shown in Chapter 2.2 that there is a vertical gradient in the composition of the transport layer (figure 2.2.5) but how much coarser the sediment in the bottom of the transport layer is, compared with the averaged composition, is not known, so as a doubtful approximation

$$\bar{p}_{i z_0} = \bar{p}_i \quad \text{for } \frac{dz_0}{dt} > 0 \quad (2.4.2)$$

or during a sedimentation process

$$\bar{p}_{i z} = \frac{1}{2} \left\{ p_i(t) + p_i(t + \Delta t) \right\} \quad (2.4.3)$$

The stringent division between a displacement of the z_0 -level in positive and negative direction is necessary for lack of a better approach, but it is not physical correct, as coarser grains can leave the transport layer into the z_0 -layer, when at the same time finer particles are picked up, figure 1.2.6. To remedy this problem the model for non uniform sediment should be extended with an equation of motion and continuity in vertical direction describing this exchange!

2.5. Interaction between the elements.

The different component parts of the model for non-uniform sediment described in the previous are in mutual interaction.

The dune height has a large influence on the total roughness and which part of the total shear stress that is due to the skin friction, see

for instance table 2.1.1. Further on the bed composition has influence on the roughness (eq. 2.1.9). The dune height effects the speed of composition changes (eq. 1.1.15). Both the roughness and the composition effects the sediment transport (eq. 2.2.10) and at last the sediment transport has influence on the dune height (eq. 2.3.4). This mutual interaction is illustrated in figure 2.5.1.

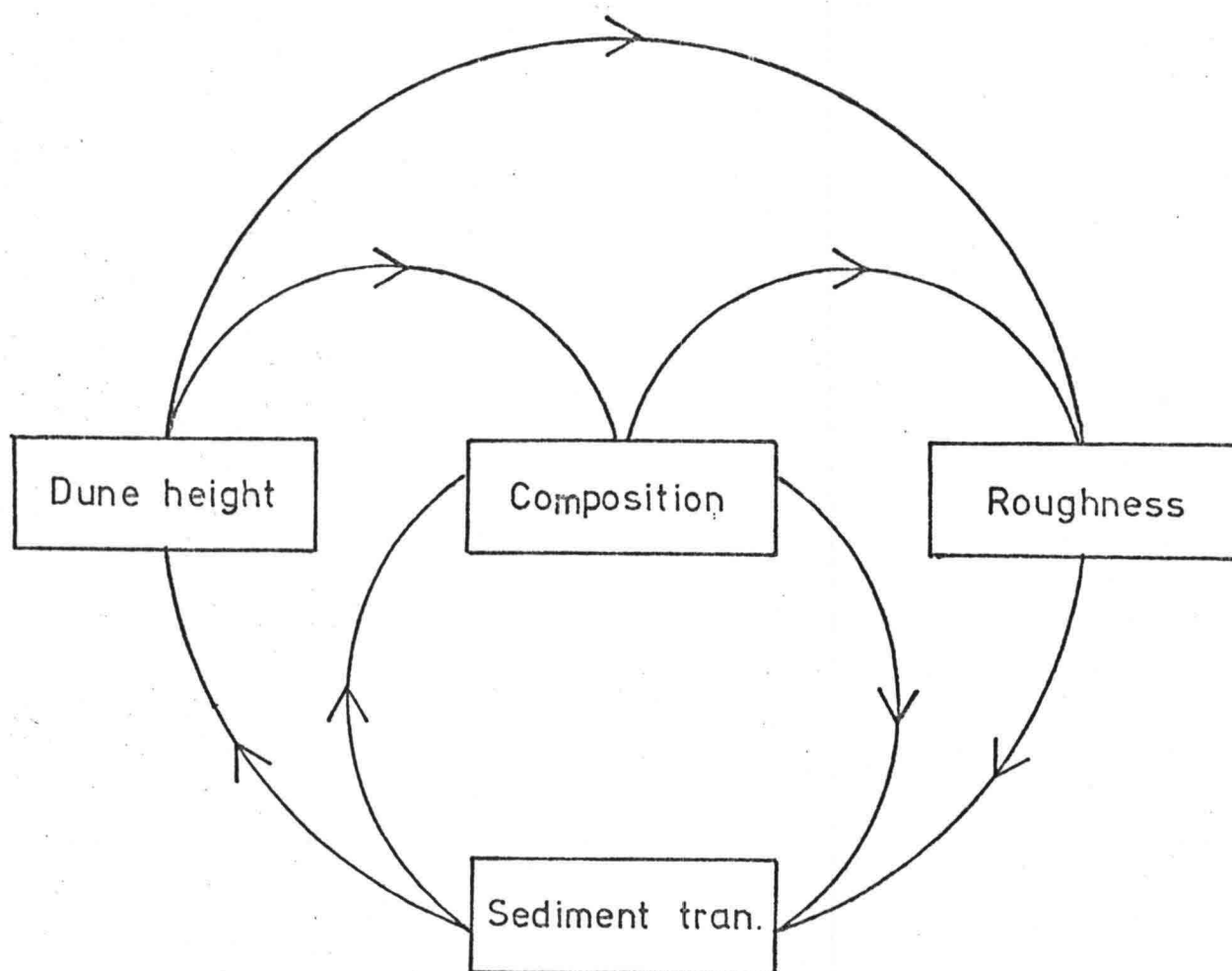


Figure 2.5.1. Mutual interaction.

If an error or unaccuracy is introduced in one of the elements, it will influence the accuracy of all the system. Especially the roughness is a very sensitive parameters in the system, because it determines the bed slope, and thus how much sediment that must be degraded or aggrated before equilibrium is reached.

Considering the mutual interaction the computational results must be interpreted with caution, because the component parts, although they are a part of a consistent system, are estimated from different approaches.

2.2.6. Unsteady Conditions.

The transport formulas and the roughness predictors are more or less empirical and based on results from steady experiments, and they should therefore be applied for unsteady cases with caution.

Here again the roughness is the questionable element. As the transport rate in relative low the change of the dune dimensions due to a change in the hydraulic conditions must take a considerable time. This phenomenon has been a subject for research at the Hydraulic Laboratory de Voorst and in figure 2.5.2 a result from this study is reproduced. The graphs shows a discharge wave and the development in the Chézy - coefficient and the dune dimensions.

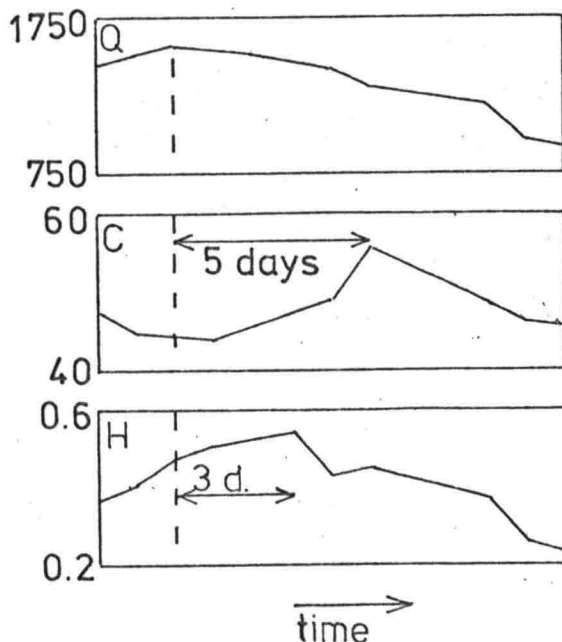


Figure 2.5.2. Measurements from Pannerdensch Kanaal during a flood [13]

A river will as good as never be in equilibrium due to the continuous changing discharge, and therefore only processes with a large time scale,

so the oscillation will be leveled, can be predicted by this model.

3. NUMERICAL MODELLING

In the morphological model for non-uniform sediment choices have to be made for a transport formula, a transport layer thickness, a roughness predictor, significant sediment properties, initial and boundary conditions, which all introduce sources of uncertainty. In order to obtain some insight in the complex physical process it has to be required that the numerical errors are not dominant, i.e. numerical errors have to be an order of magnitude smaller than errors from physical sources.

In excess of the above mentioned accuracy demands it is required, that it is not elaborate to change the transport formula, the formula for the transport layer thickness and to use different boundary conditions. Further more the calculation work has to be reasonable small.

First an extensive numerical analysis of some of the available numerical solution methods will be carried out and a method will be chosen.

The back-water calculation will be described, and the chosen method will be applied to the morphological model for uniform sediment in order to see whether the method behaves according to expectations.

Then the numerical method will be applied to the model for non-uniform sediment after a schematization of the vertical grain size distribution is carried out. The numerical model for non-uniform sediment will be described, and the limitations of the model will be mentioned. Finally some results from the numerical model will be compared with calculations carried out with the characteristic method.

3.1. Numerical analysis.

In principle there are two different methods available for numerical solution of a set of partial differential equations: the finite difference and the finite elements method.

The major force of a finite elements method is that it is not necessary to use a constant space step, so the grid can be refined in areas where

large changes are expected. In the present case where a propagating wave has to be described, this advantage is not important, and as the finite elements methods are more elaborate to work with than most finite difference methods, the following analysis will only be based on finite difference methods.

The model for non-uniform sediment can in principle be written like

$$\frac{\partial \underline{V}}{\partial t} + \underline{A} \frac{\partial \underline{V}}{\partial X} = \underline{F} \quad (3.1.1)$$

where \underline{V} and \underline{F} are vector and \underline{A} is a matrix. The set of partial differential equations is (in most cases) of hyperbolic character and the Eigenvalues in \underline{A} will therefore be real and positive, thus eq. 3.1.1 can be transformed into

$$\frac{\partial \underline{W}}{\partial t} + \underline{D} \frac{\partial \underline{W}}{\partial X} = \underline{G} \quad (3.1.2)$$

where \underline{W} and \underline{G} are vector and \underline{D} a diagonal matrix, i.e. the model for non-uniform sediment can be transformed into a number of non-linear hyperbolic equations.

The tools for numerical analysis of non-linear system are poorly developed, so the analysis will be based on a simple linear wave

$$\frac{\partial Z}{\partial t} + C \frac{\partial Z}{\partial X} = 0 \quad (3.1.3)$$

where C is constant.

Because of this simplification the analysis only gives a rough estimate for the expected accuracy, and therefore a sensitivity analysis has to be performed in order to get some insight into the reliability of the numerical model results.

3.1.1. Finite difference methods.

In order to get a numerical solution the set of equations has to be discretized in some way. This is done by giving a function a finite number of

function - values in a grid. In this case it has to be a two dimensional (space - time) grid.

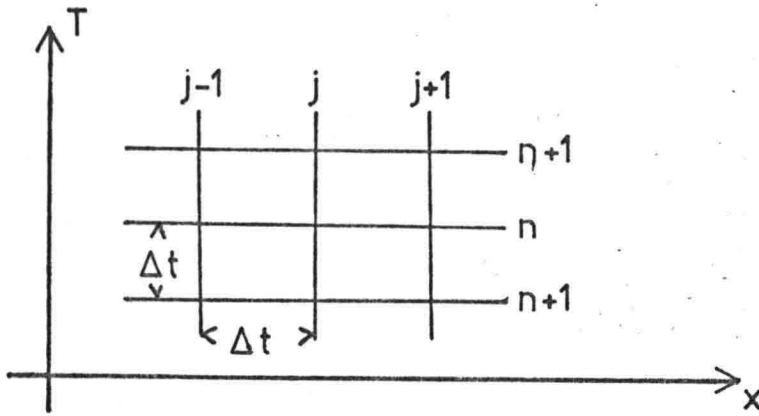


Figure 3.1.1. Definition sketch. Two dimensional grid.

The derivatives can be represented in several ways, i.e. there can be interpolated in different ways between the grid points. For instance

$$\left(\frac{\partial Z}{\partial X}\right)_{x = x.j} = \frac{Z_j - Z_{j-1}}{\Delta X} \quad (\text{backward difference})$$

$$= \frac{Z_{j+1} - Z_j}{\Delta X} \quad (\text{forward difference})$$

$$= \frac{Z_{j+1} - Z_{j-1}}{2\Delta X} \quad (\text{central difference})$$

Applying the differences to the space and time derivatives in eq. 3.1.3, among other, the following difference equations appears.

Modified Lax scheme

$$\frac{Z_j^{n+1} - Z_j^n}{\Delta t} + \frac{Z_{j+1}^n - Z_{j-1}^n}{2\Delta X} - \alpha \frac{Z_{j+1}^n - Z_j^n + Z_j^n - Z_{j-1}^n}{2\Delta t} = 0 \quad (3.1.4)$$

Upstream (Lelequier) scheme

$$\left. \begin{array}{l} \text{---} \\ \text{---} \end{array} \right\} \frac{z_j^{n+1} - z_j^n}{\Delta x} + c \frac{z_j^n - z_{j-1}^n}{\Delta t} = 0 \quad (3.1.5)$$

Crank - Nicholson scheme

$$\left. \begin{array}{l} \text{---} \\ \text{---} \end{array} \right\} \begin{array}{l} \theta \\ (1-\theta) \end{array} \frac{z_j^{n+1} - z_j^n}{\Delta x} + c \left\{ \theta \frac{z_{j+1}^{n+1} - z_{j-1}^{n+1}}{2\Delta x} + (1-\theta) \frac{z_{j+1}^n - z_{j-1}^n}{2\Delta x} \right\} = 0 \quad (3.1.6)$$

Four points scheme

$$\left. \begin{array}{l} \square \\ \square \end{array} \right\} \begin{array}{l} \theta \\ (1-\theta) \end{array} \frac{1}{2} \left\{ \frac{z_{j+1}^{n+1} - z_{j+1}^n}{\Delta t} + \frac{z_j^{n+1} - z_j^n}{\Delta t} + c \left[\theta \frac{z_{j+1}^{n+1} - z_j^{n+1}}{\Delta x} + \frac{z_{j+1}^n - z_j^n}{\Delta x} \right] \right\} = 0 \quad (3.1.7)$$

The two first mentioned schemes are explicit, because they lead to one new value at time level n+1 from known values at time level n. The Crank - Nicholson and four points schemes are coupling the values at level n+1 in a set of equation, which has to be solved together with the boundary conditions. The schemes are therefore called implicit schemes. Another possibility is to use the predictor - corrector method, i.e. use an explicit in the first iteration and an implicit in the following

In order to make a qualified choice of a finite difference method it is necessary to make an estimate of their characteristics.

Vreugdenhil (1979) shows the steps in a numerical solution of a problem, and the errors introduced at these steps. (see figure 3.1.2).

3.1.2. Consistency and truncation error.

The difference equation is an approximation to the differential equation. The magnitude of the error which is introduced by this approximation,

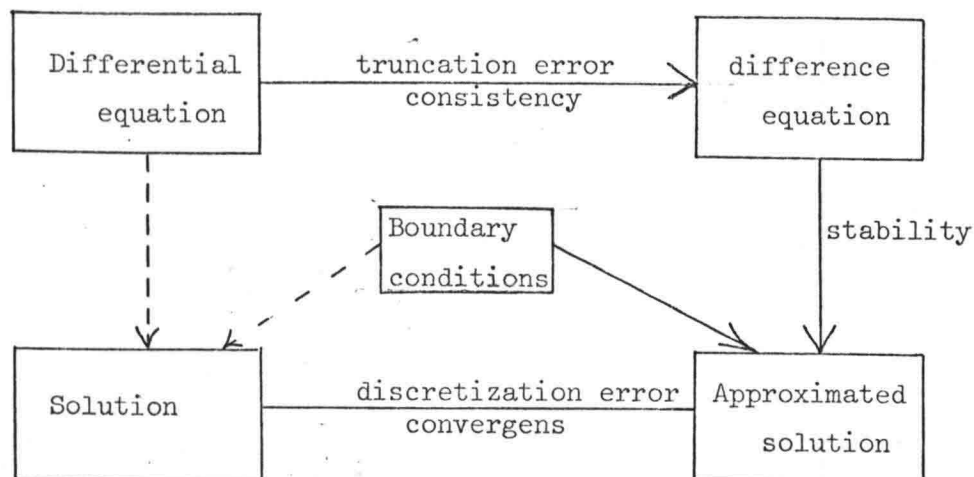


Figure 3.1.2. Numerical properties [21]

called the truncation error, can be estimated by applying a Taylor series for the difference equation.

For the Crank - Nicholson scheme (eq. 3.1.6), the Taylor series applied to the differences leads to

$$\frac{z_j^{n+1} - z_j^n}{\Delta t} = \frac{\partial z}{\partial t} + \frac{1}{2} \Delta t \frac{\partial^2 z}{\partial t^2} + \frac{1}{6} \Delta t^2 \frac{\partial^3 z}{\partial t^3} + \dots \quad (3.1.8)$$

$$\frac{z_{j+1}^n - z_{j-1}^n}{2\Delta x} = \frac{\partial z}{\partial x} + \frac{1}{6} \Delta x^2 \frac{\partial^3 z}{\partial x^3} + \dots \quad (3.1.9)$$

By combining eqs. 3.1.8 and 9 with last term in eq. 3.1.6.

$$\begin{aligned} \frac{z_{j+1}^{n+1} - z_{j-1}^{n+1}}{2\Delta x} &= \frac{\partial z}{\partial x} + \frac{1}{6} \Delta x^2 \frac{\partial^2 z}{\partial x^2} + \frac{\Delta t}{2\Delta x} \left[\left(\frac{\partial z}{\partial t} + \frac{1}{2} \Delta t \frac{\partial^2 z}{\partial x^2} + \dots \right)_{j+1} \right. \\ &\quad \left. - \left(\frac{\partial z}{\partial t} + \frac{1}{2} \Delta t \frac{\partial^2 z}{\partial x^2} + \dots \right)_{j-1} \right] \\ &= \frac{\partial z}{\partial x} + \frac{1}{6} \Delta x \frac{\partial^2 z}{\partial x^2} + \Delta t \frac{\partial^2 z}{\partial x \partial t} + \frac{1}{2} \Delta t^2 \frac{\partial^3 z}{\partial x^2 \partial t} + \dots \quad (3.1.10) \end{aligned}$$

The time derivatives in the Taylor series can be transformed into space derivatives. By differentiating eq. 3.1.3 with t

$$\frac{\partial^2 Z}{\partial t^2} = - \frac{\partial}{\partial t} \left(c \frac{\partial Z}{\partial X} \right) = -c \frac{\partial}{\partial X} \left(\frac{\partial Z}{\partial t} \right) = -c \frac{\partial}{\partial X} \left(-c \frac{\partial Z}{\partial X} \right)$$

or general

$$\frac{\partial^m Z}{\partial t^m} = (-c)^m \frac{\partial^m Z}{\partial X^m} \quad (3.1.11)$$

Summating the Taylor series for the differences and apply eq. 3.1.11 the "Modified Equation" for the Crank - Nicholson scheme occurs

$$\frac{\partial Z}{\partial t} + c \frac{\partial Z}{\partial X} - \frac{1}{2} \frac{\Delta X^2}{\Delta t} \sigma^2 (2\theta - 1) \frac{\partial^2 Z}{\partial X^2} - \frac{1}{6} \frac{\Delta X^3}{\Delta t} \sigma (\sigma^2 - 3\theta\sigma - 1) \frac{\partial^3 Z}{\partial X^3} + \dots = 0$$

(3.1.12)

in which $\sigma = c \frac{t}{x}$ is the Courant number. For fixed Courant number (space and time step ratio) and $\theta \neq \frac{1}{2}$ the truncation error decrease linear with Δx , and the scheme is said to be of first order. For $\theta = \frac{1}{2}$ the scheme is of second order. When the truncation error $\rightarrow 0$ for Δx and $\Delta t \rightarrow 0$ the scheme is consistent.

In appendix A3 the modified equation for the predictor (Modified Lax, $\alpha = 0$) - corrector (Crank - Nicholson) is derived. There the modified equation is also derived for the Upstream scheme as predictor and the Four points scheme as corrector, although this implicit scheme does not seem so attractive for a predictor - corrector method because of the two time differences.

The modified equation for the difference schemes can be written in the general form

$$\frac{\partial Z}{\partial t} + c \frac{\partial Z}{\partial X} - \frac{1}{2} \frac{\Delta X^2}{\Delta t} \lambda_2 \frac{\partial^2 Z}{\partial X^2} - \frac{1}{6} \frac{\Delta X^3}{\Delta t} \lambda_3 \frac{\partial^3 Z}{\partial X^3} = 0 \quad (3.1.13)$$

where the higher order terms are neglected. The expressions for λ_2 and

λ_3 for the mentioned schemes are given in table 3.1.1 and depicted as a function of the Courant number in figure 3.1.3 and 3.1.4.

Method	λ_2	λ_3
eq. 3.1.4		
Lax, =1	$1 - \sigma^2$	$2\sigma(1 - \sigma^2)$
Modified Lax, $=\sigma^2 + \beta$	β	$-\sigma(1 - \sigma^2 - 3\beta)$
Lax-Wendroff, =	0	$-\sigma(1 - \sigma^3)$

Upstream	$\sigma(1 - \sigma)$	$-\sigma(\sigma - 1)(2\sigma - 1)$
4 points	$(2\theta - 1)\sigma^2$	$\frac{1}{2}\sigma - (2 - 6\theta + 6\theta^2)$
Crank-Nicholson (C-N)	$(2\theta - 1)\sigma^2$	$\sigma(\sigma^2 - 3\theta\sigma^2 - 1)$
Pre(Lax, =0) - Co(C-N)	$(2\theta - 1)\sigma^2$	$-\sigma(1 - \sigma^2)$
Pre(Upstr.) - Co(4 p.)	$(4\theta - 1)\sigma^2 - \sigma$	$-\sigma(1 - \sigma^4)$

Table 3.1.1. Truncation error. Partially after Vreugdenhil (1981)

If the third order term is neglected in the modified equation, it is a convective diffusion equation, which explains why this sometimes is called a pseudo - viscosity approach.

From figure 3.1.3 it is seen that the implicit schemes and the predictor (Lax) - corrector (Crank - Nicholson) method are rather good concerning numerical diffusion. These schemes have as the Modified - Lax the advantage that the amount of numerical diffusion can be regulated with respectively θ and β . Further it is seen that the Lax scheme has extreme much damping for small Courant number. The predictor (Upstream) - corrector (Four points) has a negative diffusion coefficient for low Courant number, which will cause exponential growing solutions, and the method

will be left out of consideration because of this unstable character. (In the following there will be referred to the predictor (Lax, $\alpha = 0$) - corrector (Crank - Nicholson) method as the predictor - corrector method or short PC.)

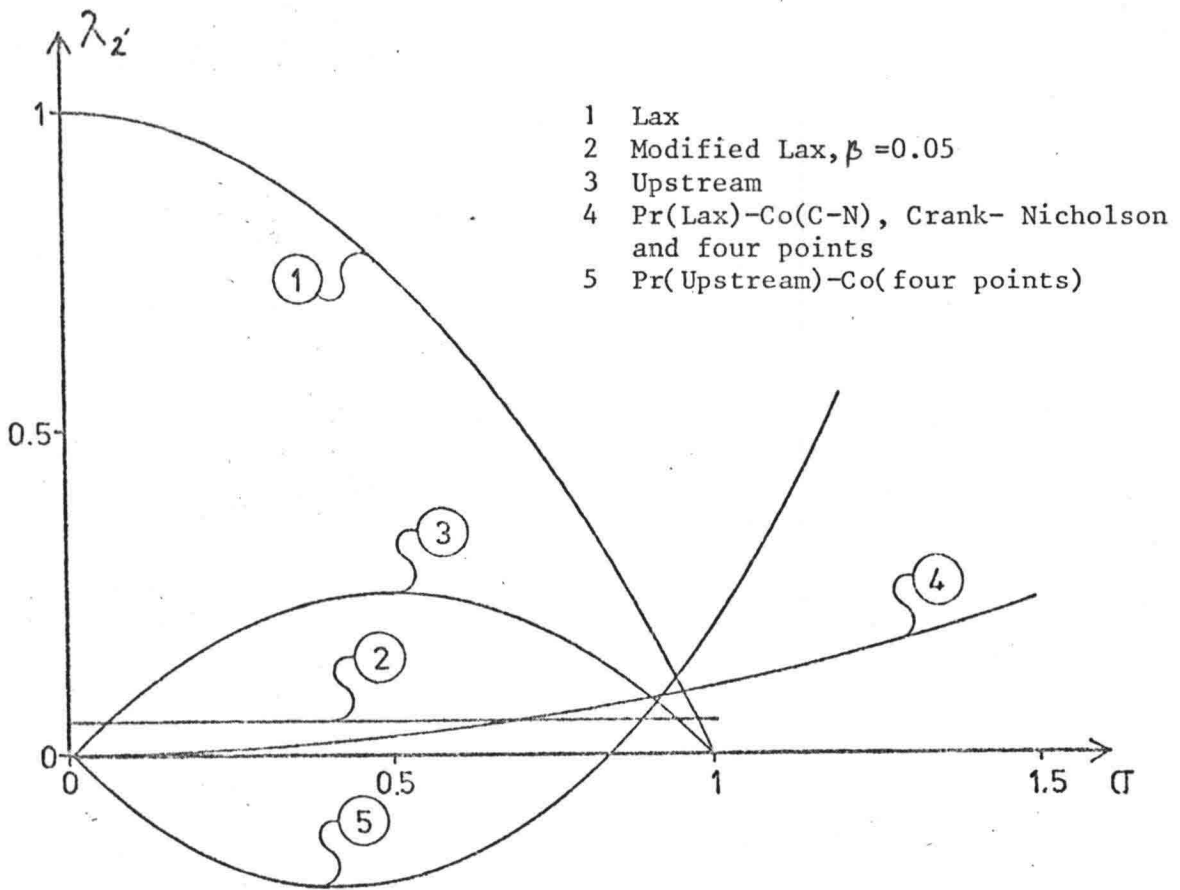


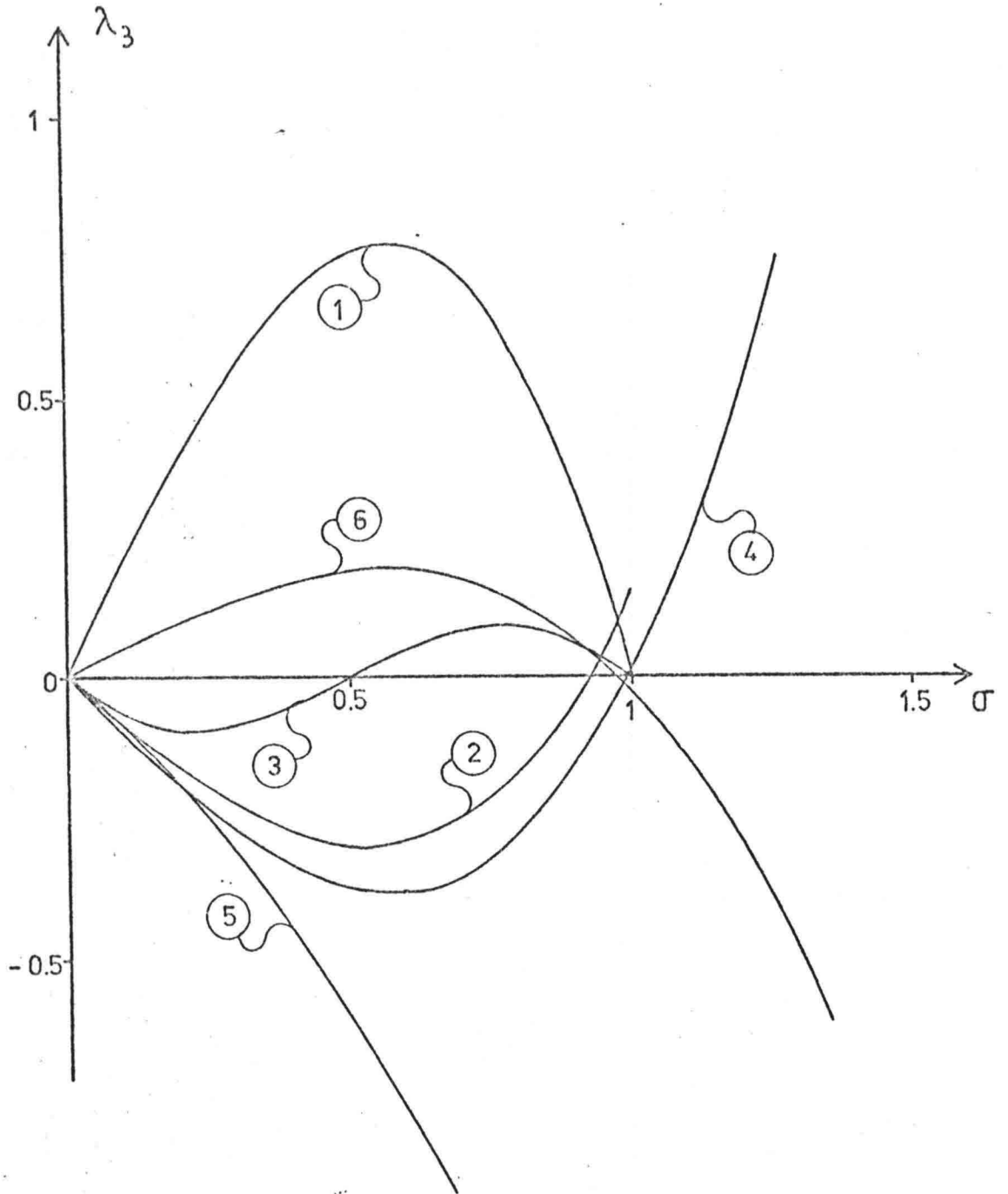
Fig. 3.1.3. Truncation error - λ_2

The third derivative is known to propagate secondary waves, which can be illustrated with the following. In a general form the modified equation can be written as

$$\frac{\partial Z}{\partial t} + C \frac{\partial Z}{\partial X} - D_{\text{num}} \frac{\partial^2 Z}{\partial X^2} - C_{\text{num}} \frac{\partial^3 Z}{\partial X^3} = 0 \quad (3.1.14)$$

Applying a periodical solution of the form

$$Z(x,t) = Z^i e^{i(kx - rt)} \quad (3.1.15)$$



- 1 Lax
- 2 Modified Lax, $\beta = 0.05$
- 3 Upstream
- 4 Four points
- 5 Crank-Nicholson
- 6 Lax-Wendroff, Pr-Co methods
and four points

Fig. 3.1.4. Truncation error - λ_3

where k is the wave number, the following expression appears

$$r = D_{\text{num}} k^2 + ik (C + C_{\text{num}} k^2) \quad (3.1.16)$$

Inserted in eq. 3.1.15 this leads to

$$Z(x,t) = Z' \exp(-D_{\text{num}} k^2 t) \exp ik \{x - (C_{\text{num}} k^2 + C)t\} \quad (3.1.17)$$

Comparing with the corresponding solution for the simple linear wave (eq. 3.1.3)

$$Z(x,t) = Z' \exp ik (x - ct) \quad (3.1.18)$$

it is seen that the solution is differing especially for short waves (big k). Secondary waves will propagate up - or down - stream depending on the sign of λ_3 , but fortunately eq. 3.1.17 provides most damping for these small wave lengths.

From figure 3.1.4 it is seen that the schemes without central space differences are giving rather little propagation of secondary waves, especially the upstream scheme. Further it is noticed that the predictor - corrector method has a better characteristic than the fully implicit scheme (Crank - Nicholson).

3.1.3. Stability.

Although the difference scheme is consistent the result might not be reasonable. There can occur explosively growing oscillations in the calculations. Figure 3.1.5 gives a physical explanation for these instabilities.

In figure 3.1.5 a the point $(j, n+1)$ is not situated in the area of influence from the point $(j-1, n)$ it is calculated, unlike in figure 3.1.5 b where the new point is seen to get sufficient information. This is called the Courant - Frederichs - Levy criterion for stability in explicit schemes.

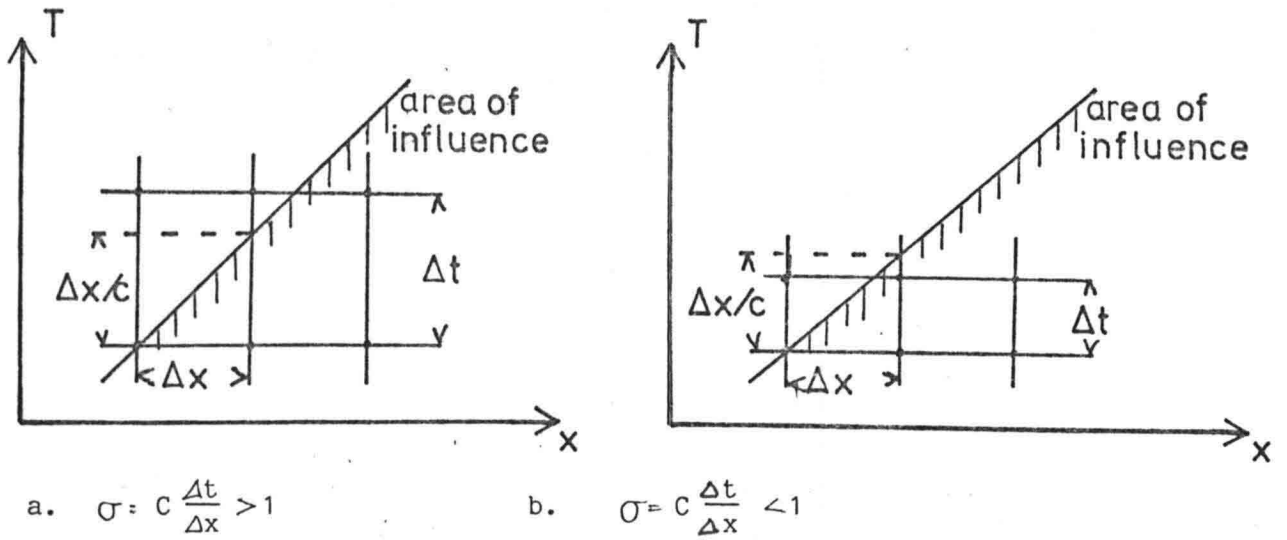


Figure 3.1.5. CFL criterion for stability for explicit schemes.

$$\sigma = c \frac{\Delta t}{\Delta x} < 1 \quad (3.1.19)$$

The CFL - criterion is a necessary but not a sufficient condition for stability for explicit schemes.

The criterion does not apply to implicit schemes because the area of influence is taken into account at the same time (figure 3.1.6). This is one of the major forces of this kind of schemes.

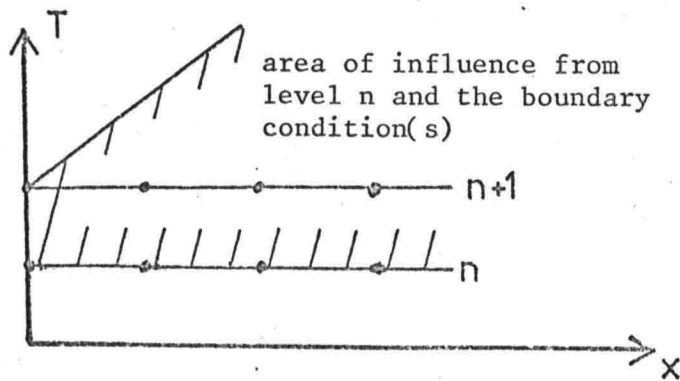


Figure 3.1.6. Area of influence for implicit schemes.

From table 3.1.1 a (not sufficient) stability criterion for the implicit schemes and the predictor - corrector method can be seen. The numerical diffusion coefficient (λ_2) has to be positive, otherwise it would lead to an exponential growing solution. The criterion yields

$$\theta > 0.5$$

(3.1.20)

3.1.4. Discretization error and convergence

The discretization error is often more dominant than the truncation error, but it is infortunatly difficult to say anything exact about the magnitude of it. The method is said to be convergent if the discretization error $\rightarrow 0$ for Δx and $\Delta t \rightarrow 0$.

As a consequence of the equivalence theorem it can be stated that the discretization error is of the same order (in space and time step) as the truncation error if the method is stable. The theorem yields (Abbot, 1979):

"Given a properly posed initial value problem and a finite difference approximation to it that satisfies the consistency condition, stability is the necessary and sufficient condition for convergence."

The order of the method does not have to tell much about the actual magnitude of the error, which also depends on the coefficients, for the truncation error the λ_1 and λ_2 -coefficients. Another way to estimate the accuracy of a numerical method is treated below.

3.1.5. Accuracy on wave propagation

The simple linear wave (eq. 3.1.3) with a initial value

$$Z(x,0) = Z' \exp i k x \quad (3.1.21)$$

in which $k = \frac{2\pi}{L}$ is the wave number and L the wave length, has a analytical solution given by eq. 3.1.18. If a finite difference scheme is applied to the simple linear wave and the initial value the numerical solution will after one wave period differ from the analytical one as outlined in figure 3.1.7.

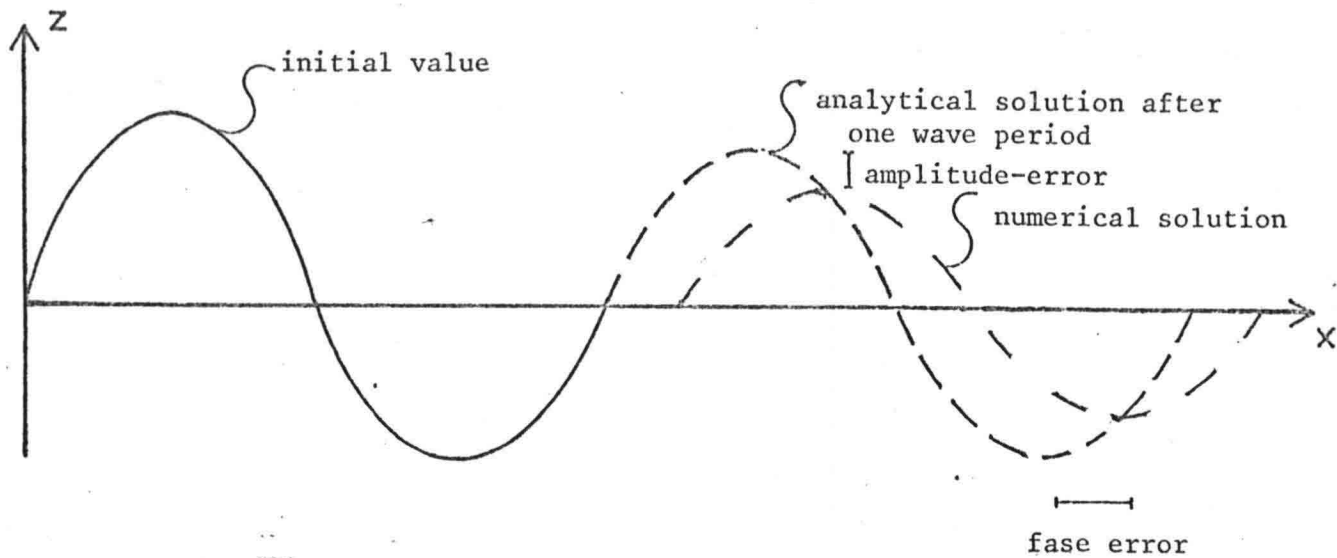


Figure 3.1.7. Numerical and analytical solution after one wave periode.

In order to say something quantitatively about the magnitude of the amplitude and fase error after one wave periode, it is presupposed that the numerical solution has the form

$$z_j^n = z' \rho^m \exp i k j \Delta x \quad (3.1.22)$$

where ρ is a complex propagation factor, defined as

$$\rho = z_j^{n+1} / z_j^n \quad (3.1.23)$$

i.e. it is assumed that also the numerical solution is sinusiodal.

The method can easily be extended to an arbitrary initial value, with instead considera single component of the Fourier - series for the solution

$$z_j^n = \sum \rho_k^n z_k' \exp (i j k \Delta x) \quad (3.1.24)$$

The number of steps in one wave periode $T = \frac{L}{c}$ is

$$n_t = \frac{T}{\Delta t} = \frac{2\pi}{\sigma \xi} \quad (3.1.25)$$

in which $\xi = k \Delta x$.

After one wave periode the numerical solution is given by

$$z_j^{n_t} = z' \rho^{n_t} \exp (i j \xi) \quad (3.1.26)$$

and the relative amplitude and phase is now determined by the following expressions

Damping factor per wave period

$$d = \frac{z' |\rho|^{n_t}}{z'} = |\rho|^{n_t} \quad (3.1.27)$$

Relative propagation velocity

$$c_r = \frac{n_t \arg(\rho)}{-2\pi} = -(\sigma \xi)^{-1} \arg(\rho) \quad (3.1.28)$$

In appendix A4 the complex propagation factor, the damping factor and the relative propagation velocity are derived for the predictor - corrector method. The complex propagation factor is found to be:

$$N = 1 + \sum_{l=1}^N (-i)^l \theta^{l-1} \sin^l \xi \sigma^l \quad (3.1.29)$$

where N is the number of iterations in the predictor - corrector method.

A stability requirement is that no periodic component of the Fourier series for the numerical solution must grow in time, which is known as the von Neumann stability criterion

$$|\rho| < 1 \quad \text{for all } \xi \quad (3.1.30)$$

It can be shown that the criterion is most critical for $\sin \xi = 1$ and the criterion then becomes for the predictor - corrector method with 2 iterations (PC 2)

$$\sigma^2 < \frac{2\theta - 1}{\theta^2} \quad (\text{and } \theta > \frac{1}{2}) \quad (3.1.31)$$

and for PC 3

$$\sigma^2 < \frac{1 + \sqrt{1 + 4(2\theta - 1)}}{2\theta^2} \quad (\text{and } \theta > \frac{1}{2}) \quad (3.1.32)$$

The predictor - corrector method with 3 iterations can be shown to have a larger area of stability (σ, θ) than any other number of iteration. The areas of stability for the predictor - corrector method are depicted in figure 3.1.8.

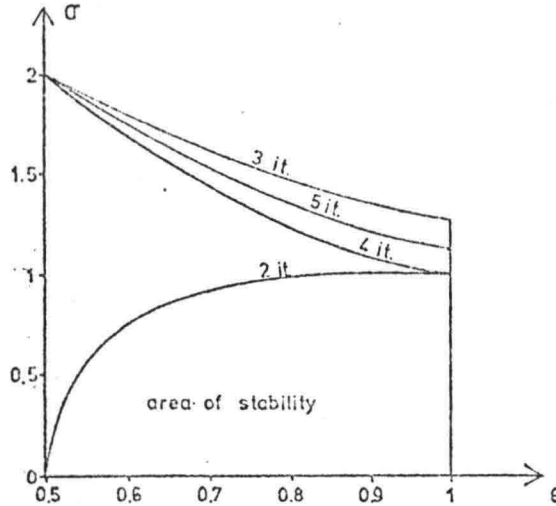


Figure 3.1.8. Area of stability for predictor - corrector method.

In table 3.1.2 the complex propagation factor, the damping factor, the relative propagation velocity and the stability criterion are resumed for the various difference schemes.

The required number of points per wave length to obtain a certain accuracy can be found as follows

$$|1 - d| \leq \epsilon \quad (3.1.33)$$

and similar for the relative propagation velocity. The principle can be illustrated with the damping factor for the Crank - Nicholson scheme, PC etc.

$$|1 - \{1 - (2\theta - 1)\pi\sigma\xi\}| \leq \epsilon \quad \text{for } \xi \ll \pi \quad (3.1.34)$$

which is only valid for large wave lengths because only the first component of the Taylor - series is applied: $\sin\{\alpha\xi\}$

The number of points per wave length n_x is given by

$$n_x = \frac{L}{\Delta x} = \frac{2\pi}{\xi} \quad (3.1.35)$$

Scheme	Eq.	ρ	Stability	d ($n_x \gg 2$)	c_r ($n_x \gg 2$)
Modified Lax	3.1.4	$1 - \alpha + \alpha \cos \xi - i \sigma \sin \xi$	$\sigma < \alpha < 1$	$1 - \frac{\pi \xi}{\sigma} (\alpha - \sigma)$	$1 + \frac{1}{6} \xi^2 (3\alpha - 2\sigma^2 - 1)$
Upstream	3.1.5	$1 - \sigma + \sigma \cos \xi - i \sigma \sin \xi$	$\sigma < 1$	$1 - \pi \sigma (1 - \sigma)$	$1 + \frac{1}{6} \xi^2 (3 - 2 - 1)$
Crank-nicholson	3.1.6	$\frac{1 - (1 - \theta) i \sigma \sin \xi}{1 + \theta i \sigma \sin \xi}$	$\theta \geq \frac{1}{2}$	$1 - (2\theta - 1) \sigma^2$	$1 - \frac{1}{6} \xi^2 (1 + 2\sigma^2 (1 - 3\theta + 3\theta^2))$
Four points	3.1.7	$\frac{1 - (1 - \theta) 2i \sigma \tan \frac{1}{2} \xi}{1 + 2i \theta \sigma \tan \frac{1}{2} \xi}$	$\theta \geq \frac{1}{2}$	$1 - (2\theta - 1) \sigma^2$	$1 + \frac{1}{12} \xi^2 (1 - 4\sigma^2 (1 - 3\theta + 3\theta^2))$
Predictor-Cor.	3.1.4+6	$1 + \sum_{k=1}^k (-i)^k \theta^{k-1} \sigma^{k-1} \sin^k \xi$			
2 iterations		$1 - \theta \sigma^2 \sin^2 \xi - i \sigma \sin \xi$	fig. 3.1.8	$1 - (2\theta - 1) \pi \sigma \xi$	$1 - \frac{1}{6} \xi^2 (1 + 2\sigma^2 (1 - \frac{1}{2} \theta))$
3 iterations		$1 - \theta \sigma^2 \sin^2 \xi - i (\sigma \sin \xi - \theta^2 \sigma^3 \sin^3 \xi)$		$1 - (2\theta - 1) \pi \sigma \xi$	$1 - \frac{1}{6} \xi^2 (1 + 2\sigma^2 (1 - 3\theta + 3\theta^2))$

Table 3.1.2. Simple wave propagation accuracy. Partially after Vreugdenhil (1979).

which inserted in eq. 3.1.34 gives the desired relation

$$n_x \geq \frac{(2\theta - 1)}{\varepsilon} \pi^2 \sigma \quad \text{for } n_x \gg 2 \quad (3.1.36)$$

For the mentioned schemes the approximated number of points per wave length for $|1 - d| = \frac{1}{2}\%$ is given in 3.1.9 and $|1 - C_p| = \frac{1}{2}\%$ in figure 3.1.10.

The upstream and the Lax schemes are very bad concerning the amplitude accuracy for Courant number not equal unity, which makes them inapplicable for the present problem, because there are more celerities in the set of equations, and furthermore the celerities are difficult to calculate for more than two fractions. For the same reason the Lax-Wendroff cannot be applied because the weight (α in eq. 3.1.4) has to be calculated from the Courant number at each step.

From figure 3.1.10 it is seen that no scheme is remarkable better than the others, still the four points scheme is giving the best propagation velocity accuracy for moderate Courant number.

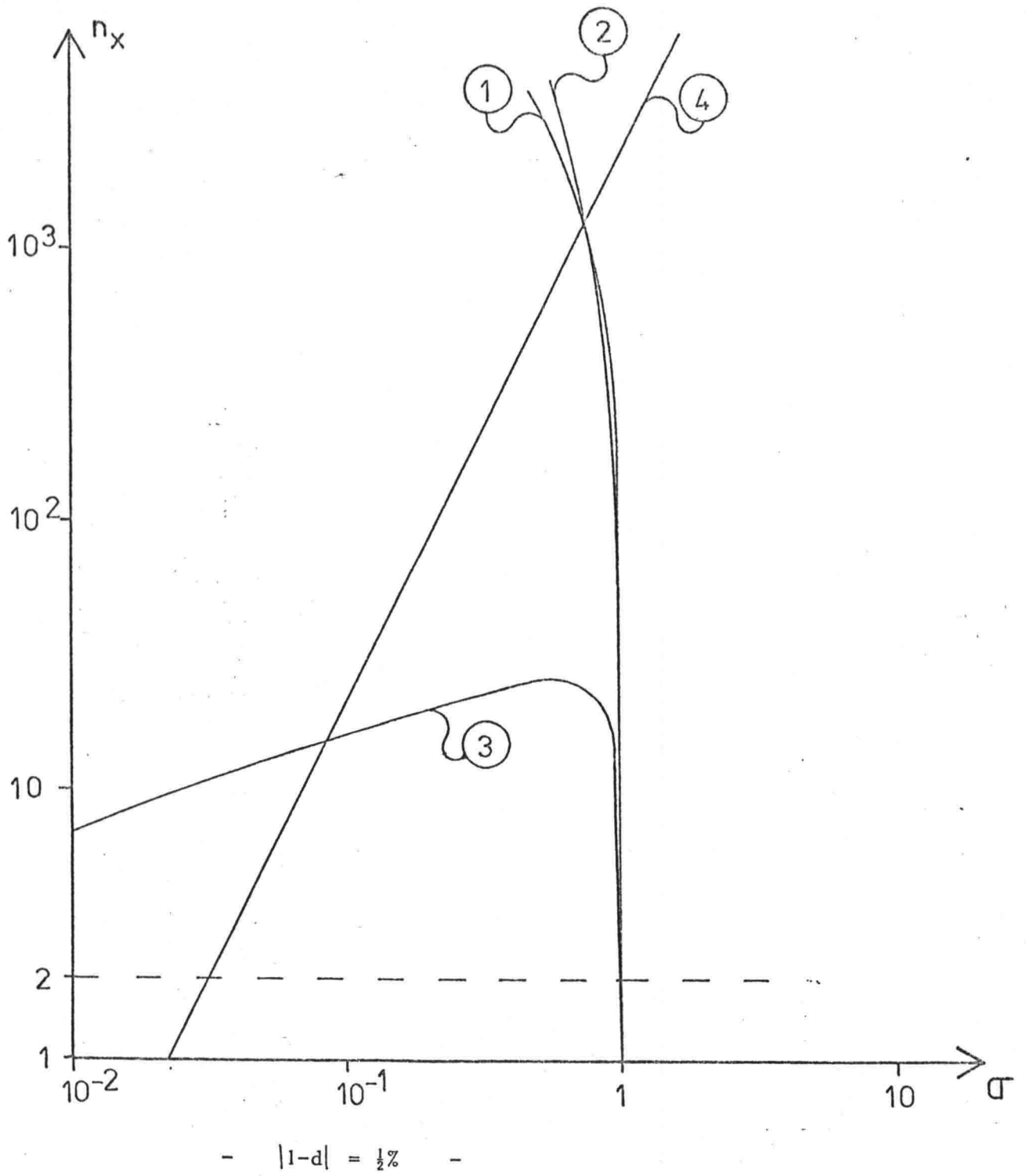
The stability limit in Courant number for the predictor-corrector method with 3 iterations does not make this method significant less applicable than the implicit schemes, because these schemes are becoming very inaccurate for large Courant numbers, which will result in an accuracy limit in Courant number for the implicit schemes.

3.1.6. Numerical and physical diffusion.

For long waves the linearized equation for the model for uniform sediment (eq. 1.1.19) has character of a diffusion equation with a diffusion coefficient D_{ph} given by eq. 1.1.21.

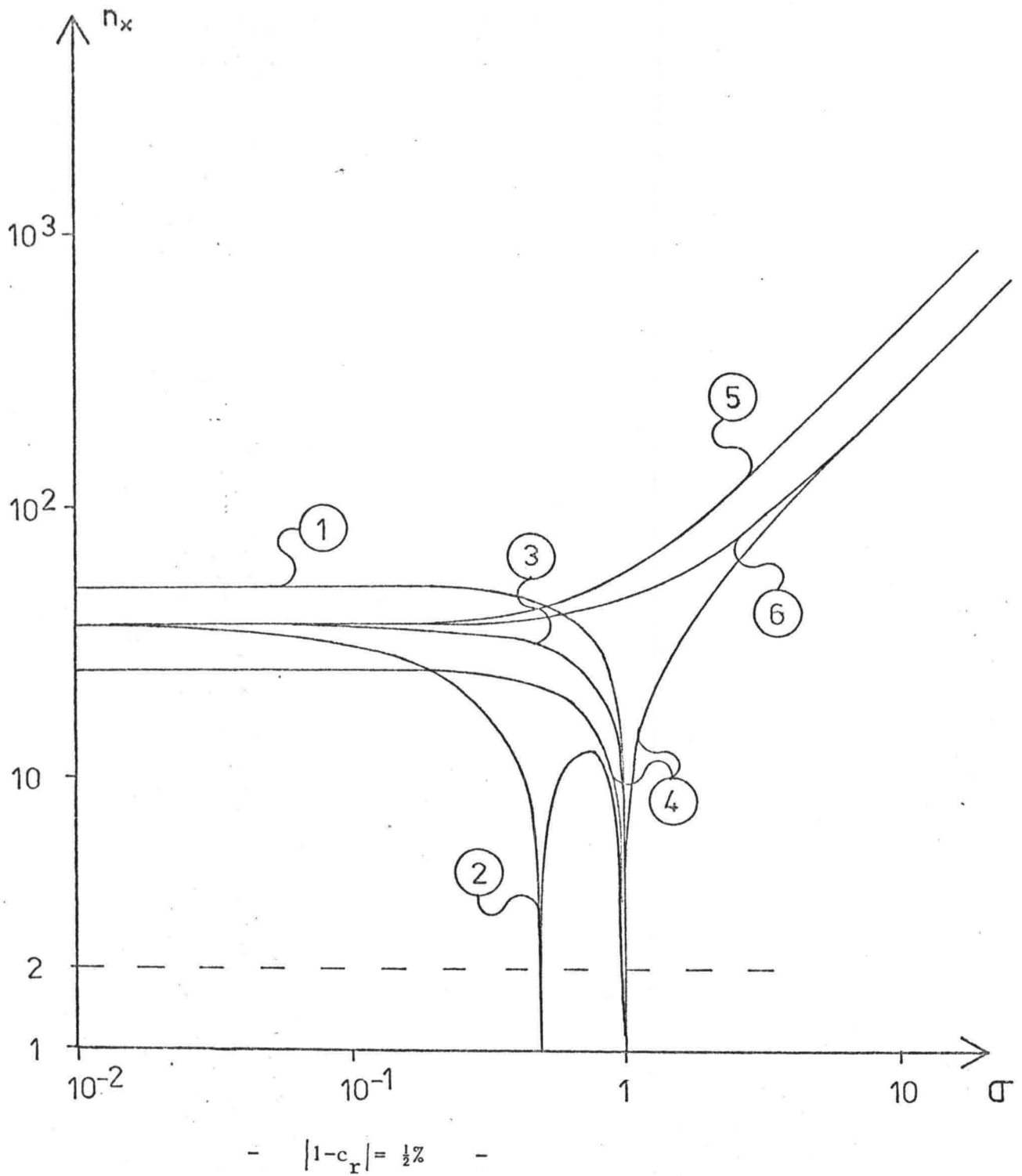
The presence of the numerical diffusion leads to an additional accuracy criterion, which yields that the numerical diffusion must be much smaller than the physical

$$D_{num} = \frac{\Delta x^2}{2\Delta t} \lambda_2 \ll D_{ph} \quad (3.1.37)$$



- 1 Lax
- 2 Upstream
- 3 Lax-Wendroff
- 4 4 points, C-N and PC $\theta=0.55$

Fig. 3.1.9. Damping factor.



- 1 Lax
- 2 Upstream
- 3 Lax-Wendroff
- 4 4 points, $\theta=0.55$
- 5 PC2, $\theta=0.55$
- 6 PC3 and C-N, $\theta=0.55$

Fig. 3.1.10. Relative propagation velocity.

From numerical solution of diffusion problems it is known that oscillations can be expected for too large space steps, which can be illustrated with the following.

Consider a stationary diffusion equation with a constant diffusion-coefficient D and propagation velocity C

$$C \frac{\partial Z}{\partial x} - D \frac{\partial^2 Z}{\partial x^2} = 0 \quad (3.1.38)$$

with the boundary conditions $Z(0) = 0$ and $Z(L) = 1$ eq. 3.1.38 has the analytical solution

$$Z(x) = \frac{\exp\left(\frac{Cx}{D}\right) - 1}{\exp\left(\frac{CL}{D}\right) - 1} \quad (3.1.39)$$

Therefore it does not seem forefetched to presuppose a numerical solution of the form

$$Z_j = r^j \quad (3.1.40)$$

from a finite difference scheme

$$C \frac{Z_{j+1} - Z_{j-1}}{2\Delta x} - D \frac{Z_{j+1} - 2Z_j + Z_{j-1}}{\Delta x^2} = 0$$

Inserting eq. 3.1.40 in the difference scheme and divide by Z_{j-1} a quadratic equation for r appears

$$\frac{C}{2x} (r^2 - 1) - \frac{D}{x} (r^2 - 2r + 1) = 0 \quad (3.1.41)$$

with the roots

$$r_1 = 1 \quad \text{and} \quad r_2 = \frac{2 + P_{\Delta x}}{2 - P_{\Delta x}} \quad (3.1.41)$$

in which $P_{\Delta x} = \frac{C\Delta x}{D}$ is the cell Peclet number.

The numerical solution will now be

$$Z_j = A r_1^j + B r_2^j = A + B \left(\frac{2 + P_{\Delta x}}{2 - P_{\Delta x}} \right)^j \quad (3.1.43)$$

where A and B can be found from the boundary conditions. For $P_{\Delta x} > 2$ r_2 becomes negative and the numerical solution will be oscillating. Thus a restriction for the space step

$$P_{\Delta x} = \frac{C\Delta x}{D} < 2 \quad (3.1.44)$$

The criterion can be expected to apply to the order of magnitude of the physical diffusion coefficient.

3.1.7. Non-linear phenomena.

The analysis in the previous has been based on a linear wave, but it is a well known fact that the morphological models are strongly non-linear. Consequently waves tend to deform and shocks will occur, i.e. the characteristics are intersecting.

If one of the difference schemes is applied to a non-linear wave of the form

$$\frac{\partial Z}{\partial t} + Z^p \frac{\partial Z}{\partial x} = 0 \quad (3.1.45)$$

there will occur product-terms like $(z_j^n)^p \cdot z_j^n$, $(z_j^n)^p \cdot z_{j-1}^n$ etc. Considering a component of the Fourier-series for the solution (eq. 3.1.24) it is seen that the product-terms are generating waves with a higher wave number

$$(z_j^n)^p z_j^n \approx (\exp ijk \Delta x)^p \exp ijk \Delta x = \exp ij(1+p)k \Delta x \quad (3.1.46)$$

i.e. there are generated harmonics with wave number $(p+1)k$. The phenomena is resulting in short wave oscillation around the shock front.

The secondary waves makes it desirable to have a scheme which causes damping of waves with higher wave numbers and hardly influencing longer waves. A scheme with this quality is called a dissipate scheme. The lowest number of points per wave length is two, and recalling eq. 3.1.35 it is seen $\xi = \pi$ for $n_x = 2$. From table 3.1.2 it is seen that all the schemes except the four point schemes has $\rho = 1$ for $n_x = 2$, thus they are not dissipate.

A graph for $|\rho|$ as a function of n_x is called a amplitude portait, and in figure 3.1.11 this relation is depicted for the predictor - corrector method with 3 iterations.

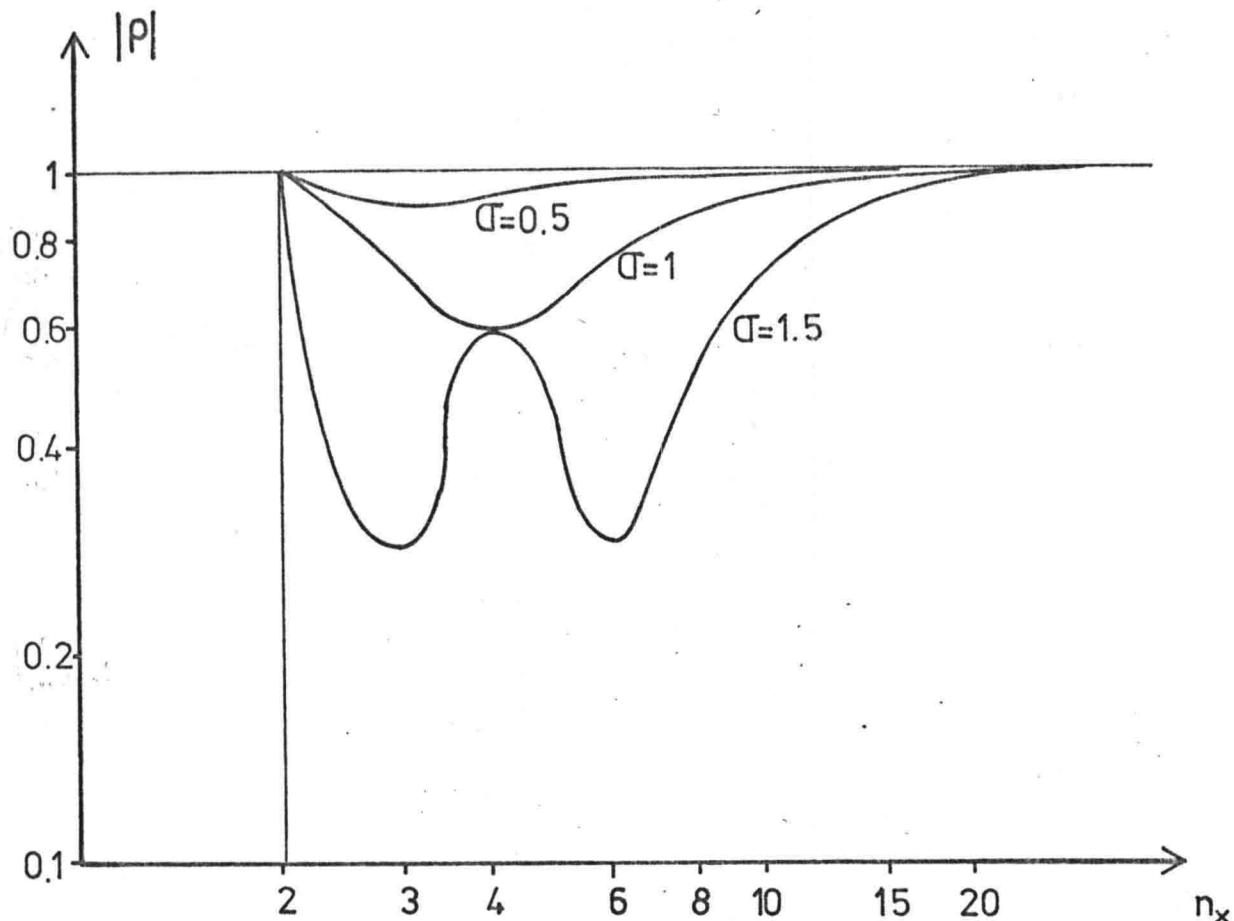


Figure 3.1.11. Amplitude protrait for PC 3 with $\sigma = 0.70$.

The space derivative in eq. 3.1.45 can be written in the conservative form

$$z^p \frac{\partial z}{\partial x} = \frac{1}{p+1} \frac{\partial z^{p+1}}{\partial x} \quad (3.1.47)$$

A backward difference applied to both the left and right side in eq. 3.1.47, and integrated over the thotal length gives

$$\sum_{j=1}^J (z_j)^p (z_j - z_{j-1}) \cong \frac{1}{1+p} \sum_{j=1}^J (z_j)^{p+1} - (z_{j-1})^{p+1} =$$

$$\frac{1}{p+1} \left\{ (z_J)^{p+1} - (z_0)^{p+1} \right\} \quad (3.1.48)$$

If the derivative is written in the conservative form the integrated value only depends on the values at the boundaries, and the over all mass balance is insured.

The scheme also has to be in conservative form, which is not the case for the Modified Lax and the Lax-Wendroff in the form they have mentioned in here, but they can very easily be written in a conservative form.

The error that is introduced in the mass balance, when the equations or schemes are applied in a non-conservative form, can have a considerable magnitude, when the variables locally are varying much, i.e. when there is formed a shock.

3.1.8. Conclusion and preference.

A choice has to be made for an efficient finite difference method with the following points in mind: programme flexibility, numerical diffusion, secondary waves, accuracy, stability and representation of shocks. In table 3.1.3 the different methods quality with respect to these points are resumed.

Method	Flexibility	Diffusion	Sec. waves	Accuracy	Stability	Dissipate	Remarks
Lax	+	-	-	-	-	-	
Modified Lax	+	+	o	-	-	-	Not applicable because more celerities
Lax-Wendroff	+	o	o	-	-	-	
Upstream	+	o	+	-	-	-	
Four points	-	+	+	+	+	+	
Crank-Nicholson	-	+	-	+	+	-	
Predictor-corrector	+	+	o	+	o	-	

Table 3.1.3.

The implicit scheme has the important disadvantage that a system of non-linear equations has to be solved at every time step, which makes it necessary to form the Jacobi-Matrix for the Newton iteration process. It will then be very elaborate to change for instance a transport formula: to calculate the derivatives of the transport formula with respect to the

variables and to place it at the right place in the Jacobi - Matrix. The derivatives can also be calculated numerical but the computational work will be very large. Further more the iteration itself can be expected to cost a lot in calculation time.

It is desired to have some numerical diffusion in the scheme because of the secondary waves, but at the same time it must be much smaller than the physical diffusion. This criterion excludes the Lax scheme and makes the schemes where the amount of damping can be regulated applicable.

For the accuracy it can be recalled that the amplitude accuracy is very bad for the explicit schemes except for Courant number close to unity, and with more celerities in the problem inaccurate solutions can be expected.

The implicit schemes has the advantage that they are stable for larger Courant number, but as the accuracy decreases for increasing Courant number, this force is only of major force when the wave lengths are very long, i.e. there are many points per wave length.

It is also desirable to have a dissipate scheme in order to avoid oscillation of undamped short waves.

From a purely numerical point of view (accuracy etc.) the four point scheme is seen to have the best characteristics, but considering the loss of flexibility in the computational model the predictor - corrector method is chosen. This method is also among the better.

The predictor - corrector method with three iterations requires more grid points than the four points scheme in order to obtain the same accuracy (figure 3.1.10), but the calculation time costing Newton iteration is avoided, so the predictor - corrector method is expected to be just as efficient as the four points scheme. Concerning secondary waves the predictor - corrector method is slightly worse than the four points scheme (figure 3.1.4), but this is not expected to be critical because the damping can be varied.

Thus the predictor - corrector method will be applied to the numerical model, with the possibility to vary the number of iterations. At the downstream boundary the predictor (upstream) - corrector (four points) will be applied.

As mentioned, this analysis is based on simplified assumptions and therefore only giving a rough guide-line for the qualities of the methods. A numerical model for uniform sediment is developed in order to see whether the predictor - corrector method is working according to expectations.

3.2. Numerical model for uniform sediment.

The numerical analysis in the previous was based on a linear wave, but because the morphological model for non - uniform sediment is strongly non - linear, a simple numerical model for uniform sediment is developed in order to see whether the predictor - corrector method can reproduce a non linear system.

The influence from the numerical parameters will be evaluated, but before discussion of the results of this test, some attention must be paid to the application of the numerical method to the morphological model.

The model for uniform sediment consists in principle of two coupled partial differential equations (eqs. 1.1.6 and 1.2.2), and the computational model will involve numerical solution of the differential equations for the back - water curve on each step in the predictor - corrector iteration. The flow in the calculation is illustrated in figure 3.2.1.

In appendix D a list and a short description of the programme for the computational model for uniform sediment can be found.

The reliability of the computational results of course depends on the accuracy of the flow velocity calculation, so it is necessary to discuss the back - water calculation.

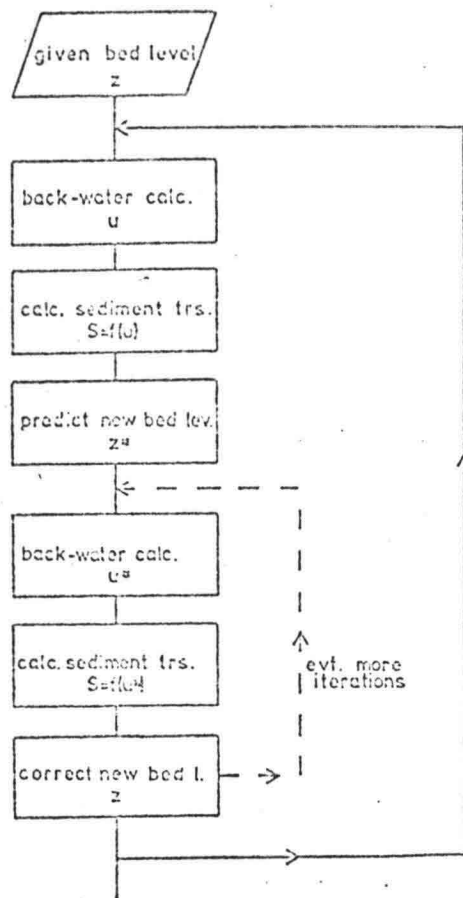


Figure 3.2.1. Flow chart in numerical model for uniform sediment.

3.2.1. Back - water calculation.

The flow velocity is, for a given bed level and for Froude number less than one, calculated from the differential equation

$$G \frac{\partial U}{\partial x} + g \frac{\partial Z}{\partial x} = R \quad (3.2.1)$$

where $G = U(1 - F^{-2}) = U - \frac{qg}{U}$

and $R = -g \frac{U^2}{C^2 a} = -g \frac{U^3}{C^2 q}$

with the boundary conditions: specific discharge (q) and downstream waterlevel (H).

The back - water calculation was not expected to be critical concerning accuracy and stability. Therefore a simple iterative finite difference method is applied. In the first iteration the flow velocity is treated explicit

$$U_j^* = U_{j-1} - \left[g(Z_j - Z_{j-1}) + R(U_{j-1}, C_{j-\frac{1}{2}}) \Delta x \right] / G(U_{j-1}) \quad (3.2.2)$$

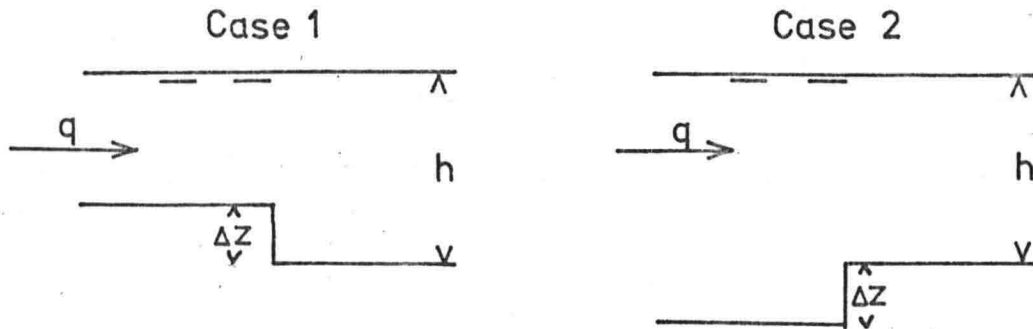
and implicit in the following iteration steps

$$U_j = U_{j-1} - \left[g(Z_j - Z_{j-1}) + R(U_{j-\frac{1}{2}}^*, C_{j-\frac{1}{2}}) \cdot \Delta x \right] / G(U_{j-\frac{1}{2}}^*) \quad (3.2.3)$$

where * indicates predicted value and $C_{j-\frac{1}{2}} = \frac{C_{j-1} + C_j}{2}$ and

$$U_{j-\frac{1}{2}}^* = \frac{U_{j-1} + U_j^*}{2}$$

No numerical analysis is carried out for this numerical method, but a convergence test is performed for vertical steps in the bed level, which are expected to be the most critical cases.



H = 0.20 m

$\Delta Z = 0.03$ m

I 0.04

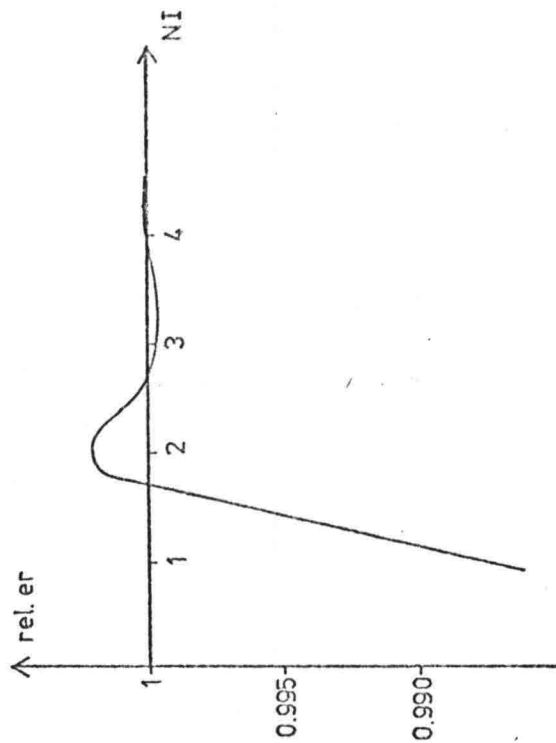
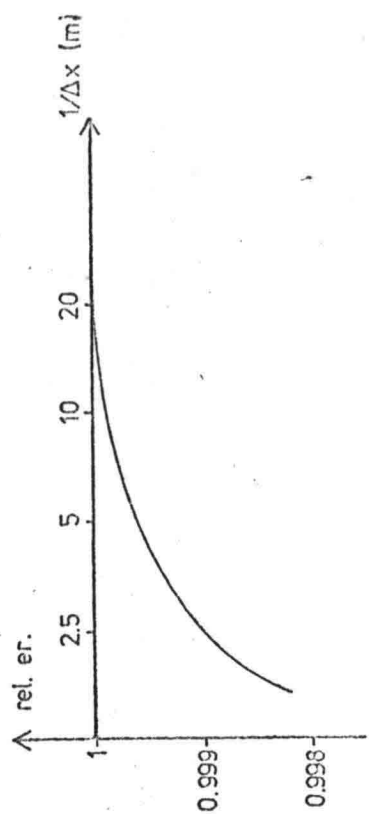
q = 0.10 m /s

C = 30 m^{1/2}/s

Figure 3.2.2. Test Cases.

The numerical parameters that can influence the accuracy are the number of iterations (NI) and the space step (Δx). The accuracy is estimated from comparing the flow velocity in the grid point immediately upstream for the step in the bed level. This velocity is a function of the number of iterations and the space step: $U(\Delta x, NI)$.

Case 2



Case 1

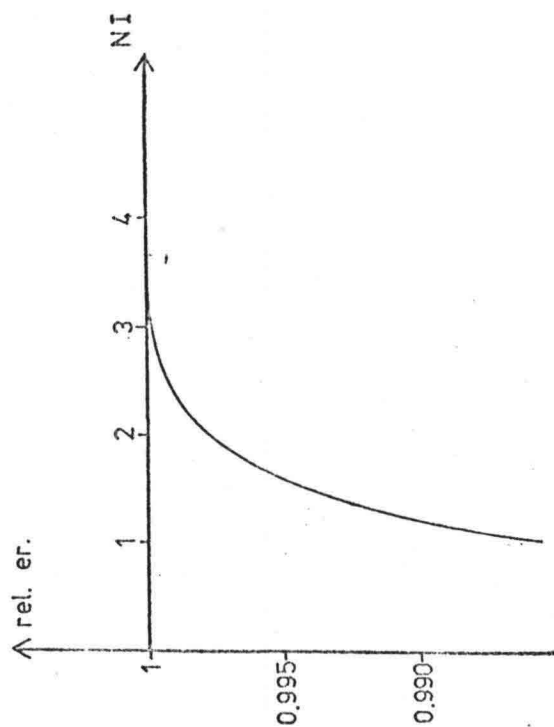
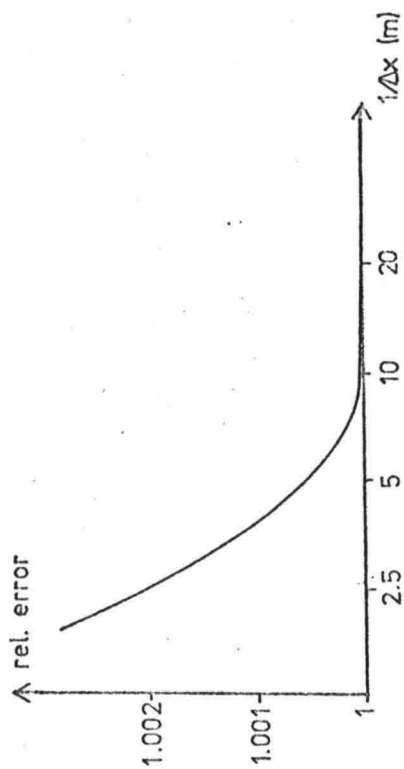


Fig. 3.2.3. Accuracy of back-water calculation.

The results from the test is depicted in figure 3.2.3. In the upper part of the figure an impression of the discretization error can be obtained: $U(\Delta x, NI \rightarrow \infty) / U(\Delta x \rightarrow 0, NI \rightarrow \infty)$ is depicted versus $\frac{1}{\Delta x}$. In the lower part the speed of convergence of the iteration is sketched: $U(\Delta x = 0.20 \text{ m}, NI) / U(\Delta x = 0.20 \text{ m}, NI \rightarrow \infty)$. Note that the vertical scale is different in the graphs.

During the same test it was found that the accuracy indeed was worse in the sketched cases, than when the steps in the bed are spread over more grid points. The trend outlined in figure 3.2.3 were also found to be the same. In the cases where are changes in flow velocities on $\pm 15\%$, which is of the order of magnitude, as expected in morphological computations, so it does not seem farfetched to generalize from the test cases.

It is then concluded that the discretization and "convergence" errors tend to neutralize each other in case of a sedimentation wave. This is also the case for an erosion wave when an even number of iterations is chosen. Further it is noticed that the space step does not have such a large influence on the accuracy as the number of iterations has.

The flow velocity is already after two iterations approximated within an margin of error on 2% , and for three iterations the accuracy is so good that inaccuracy in computational results must be attributed to inaccuracy in the predictor - corrector method.

3.2.2. Test of predictor - corrector method.

The test is carried out in case of a propagating sedimentation wave and in case of an erosion wave, both with a normal back-water calculation and with horizontal water level. When the flow velocity is calculated with horizontal water level the numerical results are compared with the solution obtained from the characteristic method. Finally the filling-in of a dredged trench will be calculated with the numerical model with the predictor - corrector method and compared with a computation carried out with the Modified Lax scheme. In all cases the transport is calculated with the Engelund - Hansen formula. The initial and boundary conditions for the examples are resumed in table 3.2.1.

Example	Initial situation		Boundary conditions			Flow vel. calc.
	I	C m /s	q m	a _{t=0}	S	
1 a	10 ⁻³	30	0.118	0.25	2E-5	back-water
1 b	0	-	-	-	-	horizontal
2	0	-	-	-	3E-6	-
3	10 ⁻⁴	40	4.7	5.00	bed lev. fixed	back-water

Table 3.2.1. Examples for sensitivity analysis.

The examples are computed with different combinations of the numerical parameters. In table 3.2.2 the numerical parameters are given together with the numerical properties discussed in chapter 3.1.

The computational results are given in figure 3.2.4 to 3.2.10. In the overview plots the bed level is indicated with "Z" and the water level with "H". The flow velocity is not recalculated after last correction of the bed level, so the flow velocity (U) water depth (A) and sediment transport (S) belongs to the bed level (Z) at the previous iteration step. When calculation is performed with horizontal water level the Froude number is zero, because the convective term in the equation of motion for the water is neglected. The celerity is in the programme computed from eq. 1.1.3, 4, 5 with Froude number calculated from the local flow velocity and depth, so the Courant number (COU) in the output must in case of horizontal water level be multiplied by $(1 - \frac{u^2}{ga})$.

re fig. 3.24 The influence from the weight Θ can be seen. For $\Theta = 0.50$ the numerical diffusion coefficient is equal zero, but the absolute value of the complex propagation factor provides a little damping. The method is not dissipate and secondary waves with 2 points per wave length were expected, but there is only harmonics with $n_x = 4$. The explanation herefore is maybe that the harmonics

Figure	x (m)	t (s)	θ	No. it.	σ	$\frac{m^2/\alpha \times 10^{-6}}{D_{\text{num}}}$	$\lambda, \frac{\Delta x^3}{\Delta t}$	$ P $ $n_x=4$	$\frac{m^2/\alpha \times 10^{-6}}{D_{\text{phys}}}$	$\times 10^{-3}$ $P_{\Delta x}$	Ex.
3.2.3.a	0.2	300	0.7	3	0.84	18.8	-1.10	0.75	2.02	5.53	1 a
3.2.3.b	-	-	0.6	-	-	9.41	-	0.85	-	-	-
3.2.3.c	-	-	0.5	-	-	0	-	0.95	-	-	-
3.2.4.a	0.2	600	0.7	3	1.68	37.6	6.80	1.17	2.02	5.53	1 a
3.2.4.b	-	300	-	-	0.84	18.8	-1.10	0.75	-	-	-
3.2.4.c	-	150	-	-	0.42	9.41	-3.07	0.96	-	-	-
3.2.5.a	0.2	300	0.7	3	0.84	18.8	-1.10	0.75	2.02	5.53	1 a
3.2.5.b	0.4	-	-	-	0.42	-	-12.3	0.96	-	10.06	-
3.2.5.c	0.6	-	-	-	0.28	-	-31.0	0.98	-	16.59	-
3.2.6.a	0.2	600	0.7	3	1.43	27.4	3.32	0.43	?	?	1 b
3.2.6.b	-	300	-	-	0.71	13.4	-1.56	0.84	-	-	-
3.2.7.a	0.2	300	0.7	3	0.71	13.4	-1.56	0.84	?	?	1 b
3.2.7.b	-	-	-	2	-	-	-	0.92	-	-	-
3.2.8	0.2	600	0.7	3	0.51	3.51	-0.84	0.93	?	?	2
3.2.9	5.0	3600	0.8	3	0.90	1690	-990	0.56	2×10^3	0.29	3

Table 3.2.2. Numerical parameters for sensitivity analysis.

TIME = 12000.0 SECONDS						SCALE = 272.962 (4/M)	
X(M)	Z(M)	A(M)	U(M/S)	COU-N	S(M ² /S)		
0.0	0.0527	0.2110	0.5593	0.8361	0.200E-04	#	Z
0.20	0.0523	0.2111	0.5590	0.8332	0.199E-04	#	Z
0.40	0.0519	0.2112	0.5587	0.8308	0.199E-04	#	Z
0.60	0.0515	0.2112	0.5587	0.8305	0.199E-04	#	Z
0.80	0.0511	0.2113	0.5584	0.8272	0.199E-04	#	Z
1.00	0.0506	0.2115	0.5579	0.8273	0.197E-04	#	Z
1.20	0.0504	0.2114	0.5581	0.8245	0.198E-04	#	Z
1.40	0.0500	0.2115	0.5580	0.8236	0.197E-04	#	Z
1.60	0.0493	0.2119	0.5547	0.8116	0.195E-04	#	Z
1.80	0.0491	0.2118	0.5571	0.8154	0.194E-04	#	Z
2.00	0.0490	0.2113	0.5584	0.8278	0.198E-04	#	Z
2.20	0.0480	0.2124	0.5556	0.8006	0.193E-04	#	Z
2.40	0.0474	0.2129	0.5543	0.7982	0.191E-04	#	Z
2.60	0.0484	0.2107	0.5600	0.8431	0.201E-04	#	Z
2.80	0.0473	0.2119	0.5547	0.8130	0.195E-04	#	Z
3.00	0.0449	0.2158	0.5469	0.7227	0.179E-04	#	Z
3.20	0.0409	0.2099	0.5423	0.5556	0.205E-04	#	Z
3.40	0.0494	0.2068	0.5707	0.9543	0.221E-04	#	Z
3.60	0.0353	0.2230	0.5271	0.5697	0.149E-04	#	Z
3.80	0.0199	0.2419	0.4879	0.3476	0.101E-04	#	Z
4.00	0.0137	0.2483	0.4753	0.2948	0.835E-05	#	Z
4.20	0.0121	0.2497	0.4726	0.2843	0.840E-05	#	Z
4.40	0.0116	0.2500	0.4721	0.2823	0.855E-05	#	Z
4.60	0.0114	0.2500	0.4720	0.2819	0.854E-05	#	Z
4.80	0.0112	0.2500	0.4719	0.2818	0.854E-05	#	Z
5.00	0.0110	0.2500	0.4719	0.2818	0.854E-05	#	Z
5.20	0.0108	0.2500	0.4719	0.2818	0.854E-05	#	Z
5.40	0.0106	0.2500	0.4720	0.2819	0.854E-05	#	Z
5.60	0.0104	0.2500	0.4720	0.2819	0.854E-05	#	Z
5.80	0.0102	0.2500	0.4720	0.2819	0.854E-05	#	Z
6.00	0.0100	0.2500	0.4720	0.2819	0.854E-05	#	Z

$\theta=0.70$

TIME = 12000.0 SECONDS						SCALE = 272.962 (4/M)	
X(M)	Z(M)	A(M)	U(M/S)	COU-N	S(M ² /S)		
0.0	0.0527	0.2111	0.5591	0.8339	0.199E-04	#	Z
0.20	0.0523	0.2111	0.5589	0.8324	0.199E-04	#	Z
0.40	0.0521	0.2107	0.5594	0.8376	0.200E-04	#	Z
0.60	0.0515	0.2112	0.5586	0.8286	0.199E-04	#	Z
0.80	0.0509	0.2118	0.5572	0.8162	0.196E-04	#	Z
1.00	0.0508	0.2113	0.5585	0.8283	0.198E-04	#	Z
1.20	0.0507	0.2109	0.5585	0.8386	0.200E-04	#	Z
1.40	0.0495	0.2121	0.5563	0.8076	0.194E-04	#	Z
1.60	0.0490	0.2125	0.5553	0.7979	0.193E-04	#	Z
1.80	0.0500	0.2106	0.5603	0.8457	0.201E-04	#	Z
2.00	0.0491	0.2111	0.5589	0.8327	0.197E-04	#	Z
2.20	0.0466	0.2143	0.5506	0.7547	0.185E-04	#	Z
2.40	0.0478	0.2126	0.5551	0.7962	0.192E-04	#	Z
2.60	0.0502	0.2094	0.5664	0.9077	0.213E-04	#	Z
2.80	0.0458	0.2133	0.5532	0.7781	0.187E-04	#	Z
3.00	0.0415	0.2198	0.5369	0.6413	0.163E-04	#	Z
3.20	0.0487	0.2104	0.5607	0.8517	0.203E-04	#	Z
3.40	0.0521	0.2037	0.5794	1.0543	0.236E-04	#	Z
3.60	0.0367	0.2221	0.5314	0.5999	0.155E-04	#	Z
3.80	0.0198	0.2420	0.4876	0.3463	0.101E-04	#	Z
4.00	0.0135	0.2435	0.4749	0.2931	0.891E-05	#	Z
4.20	0.0120	0.2498	0.4724	0.2837	0.899E-05	#	Z
4.40	0.0116	0.2500	0.4720	0.2821	0.895E-05	#	Z
4.60	0.0114	0.2500	0.4720	0.2819	0.894E-05	#	Z
4.80	0.0112	0.2500	0.4719	0.2818	0.894E-05	#	Z
5.00	0.0110	0.2500	0.4719	0.2818	0.894E-05	#	Z
5.20	0.0108	0.2500	0.4719	0.2818	0.894E-05	#	Z
5.40	0.0106	0.2500	0.4720	0.2819	0.894E-05	#	Z
5.60	0.0104	0.2500	0.4720	0.2819	0.894E-05	#	Z
5.80	0.0102	0.2500	0.4720	0.2819	0.894E-05	#	Z
6.00	0.0100	0.2500	0.4720	0.2819	0.894E-05	#	Z

$\theta=0.60$

TIME = 12000.0 SECONDS						SCALE = 272.963 (4/M)	
X(M)	Z(M)	A(M)	U(M/S)	COU-N	S(M ² /S)		
0.0	0.0527	0.2113	0.5586	0.8291	0.198E-04	#	Z
0.20	0.0538	0.2094	0.5636	0.8788	0.207E-04	#	Z
0.40	0.0523	0.2107	0.5601	0.8445	0.201E-04	#	Z
0.60	0.0489	0.2140	0.5493	0.7439	0.183E-04	#	Z
0.80	0.0509	0.2124	0.5557	0.8015	0.193E-04	#	Z
1.00	0.0545	0.2067	0.5710	0.9574	0.221E-04	#	Z
1.20	0.0504	0.2111	0.5590	0.8330	0.199E-04	#	Z
1.40	0.0447	0.2185	0.5400	0.6658	0.168E-04	#	Z
1.60	0.0493	0.2128	0.5545	0.7905	0.191E-04	#	Z
1.80	0.0548	0.2044	0.5772	1.0286	0.234E-04	#	Z
2.00	0.0476	0.2126	0.5550	0.7953	0.192E-04	#	Z
2.20	0.0399	0.2228	0.5297	0.5880	0.152E-04	#	Z
2.40	0.0476	0.2136	0.5526	0.7727	0.188E-04	#	Z
2.60	0.0552	0.2022	0.5837	1.1071	0.247E-04	#	Z
2.80	0.0446	0.2142	0.5508	0.7565	0.185E-04	#	Z
3.00	0.0330	0.2291	0.5150	0.4907	0.132E-04	#	Z
3.20	0.0421	0.2192	0.5384	0.6532	0.165E-04	#	Z
3.40	0.0558	0.1999	0.5903	1.1927	0.261E-04	#	Z
3.60	0.0454	0.2113	0.5585	0.8288	0.198E-04	#	Z
3.80	0.0237	0.2375	0.4968	0.3900	0.110E-04	#	Z
4.00	0.0141	0.2478	0.4762	0.2982	0.893E-05	#	Z
4.20	0.0121	0.2497	0.4726	0.2842	0.866E-05	#	Z
4.40	0.0116	0.2500	0.4720	0.2821	0.855E-05	#	Z
4.60	0.0114	0.2500	0.4720	0.2819	0.854E-05	#	Z
4.80	0.0112	0.2500	0.4719	0.2818	0.854E-05	#	Z
5.00	0.0110	0.2500	0.4719	0.2818	0.854E-05	#	Z
5.20	0.0108	0.2500	0.4719	0.2818	0.854E-05	#	Z
5.40	0.0106	0.2500	0.4720	0.2819	0.854E-05	#	Z
5.60	0.0104	0.2500	0.4720	0.2819	0.854E-05	#	Z
5.80	0.0102	0.2500	0.4720	0.2819	0.854E-05	#	Z
6.00	0.0100	0.2500	0.4720	0.2819	0.854E-05	#	Z

$\theta=0.50$

Fig. 3.2.4. Influence from θ .

with three to six points per wave length is damped so much (see figure 3.1.11) that, when waves with $n_x = 2$ are generated according to eq. 3.1.46, there is hardly any amplitude any longer. This would mean, that if there is started with a shock in the initial conditions, harmonics with $n_x = 2$ will be found (see figure 3.2.10).

re fig. 3.2.5 Influence from time step. The Courant number and so the numerical diffusion coefficient increases for increasing time step. For Courant number greater than one the propagation velocity of secondary waves becomes positive and secondary waves downstream of the front were expected, but due to the large diffusion coefficient they seem to have a wave length which causes immediately damping. The calculation carried out with $\Delta T = 600$ has $\sigma = 1.68$ and $\theta = 0.70$ which is not in the area of stability (figure 3.1.8). For Courant number around 0.50 there is very little damping and the λ_3 -coefficient has a maximum (figure 3.1.4) so it can be recommended to increase the time step.

re fig. 3.2.6 Influence from space step. The numerical diffusion coefficient is independent of the space step, but the propagation velocity for the secondary waves increase strongly with increasing space step.

re fig. 3.2.7 Calculation with horizontal water level compared with solution from the characteristic method (eq. 1.1.27). Both calculations seem to be very accurate, but $\Delta T = 600$ s must be preferred because there are less secondary waves. Comparing with figure 3.2.4 the influence from the bed friction on the damping can be seen.

re fig. 3.2.8 Three iterations in the predictor - corrector method does not only have the advantage that the stability area is larger (figure 3.1.8), than when only two iterations are performed, but it is also providing much more damping of small wave lengths. The numerical diffusion coefficient is the same in both cases, but the absolute value of the complex propagation factor is smaller for three iterations than for two.

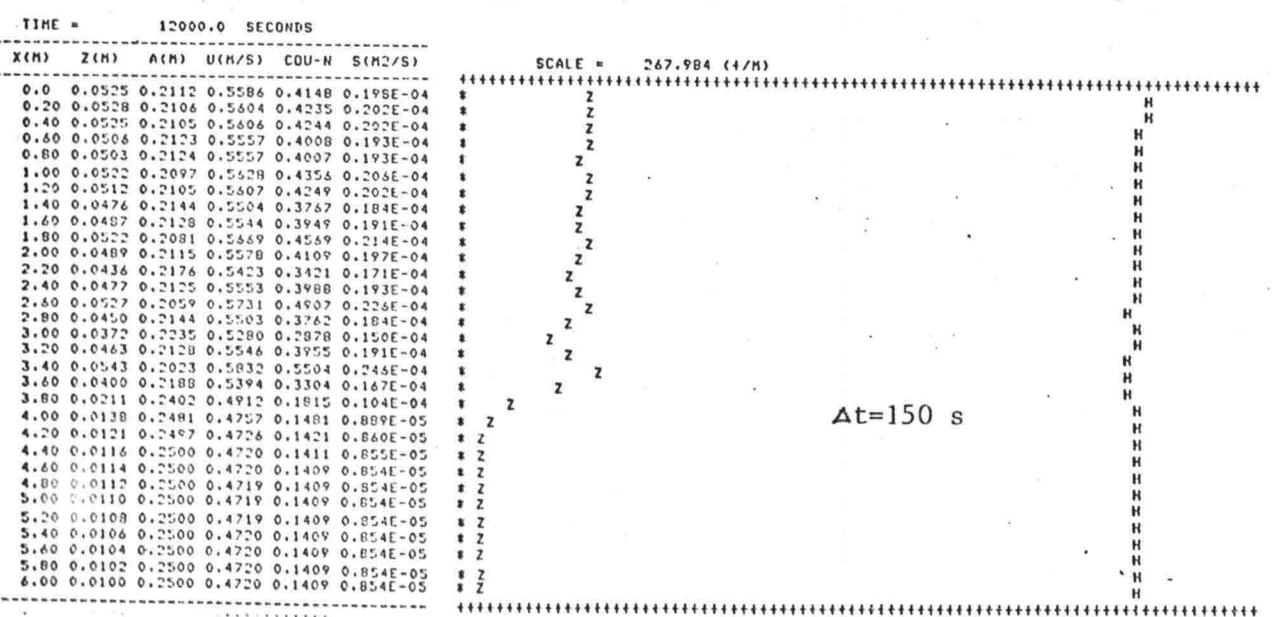
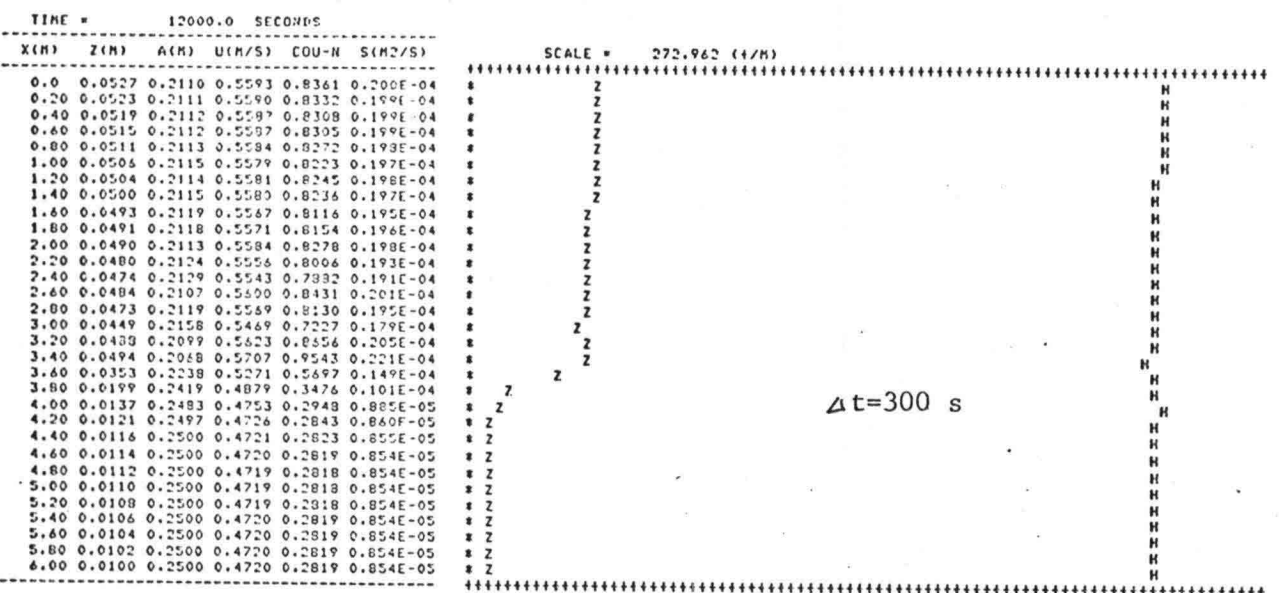
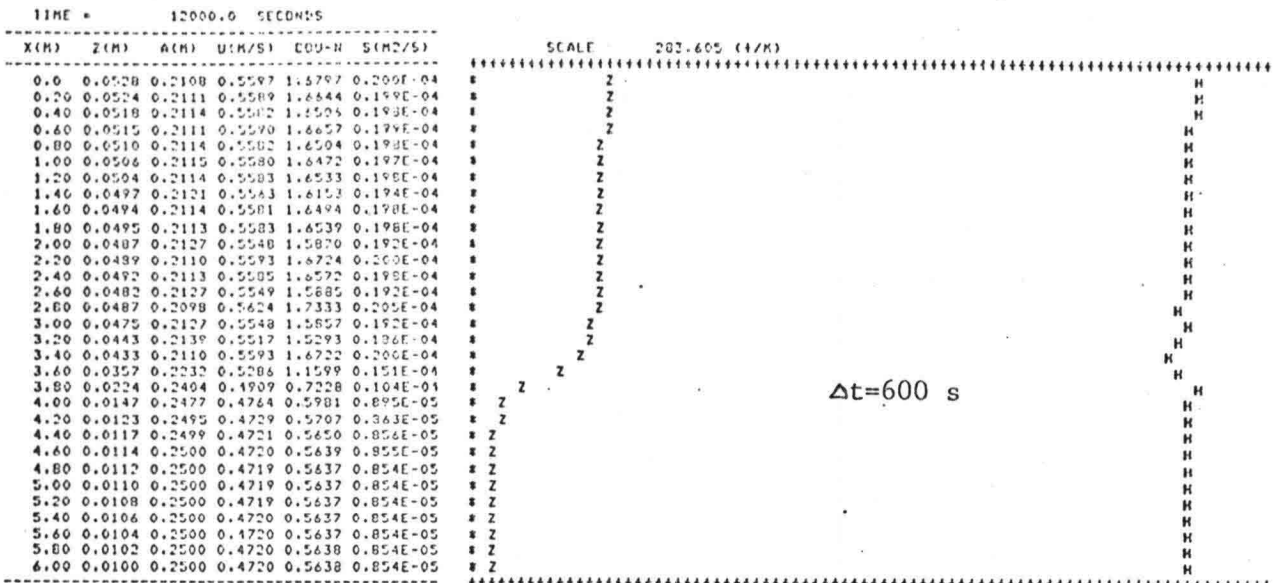


Fig. 3.2.5. Influence from timestep.

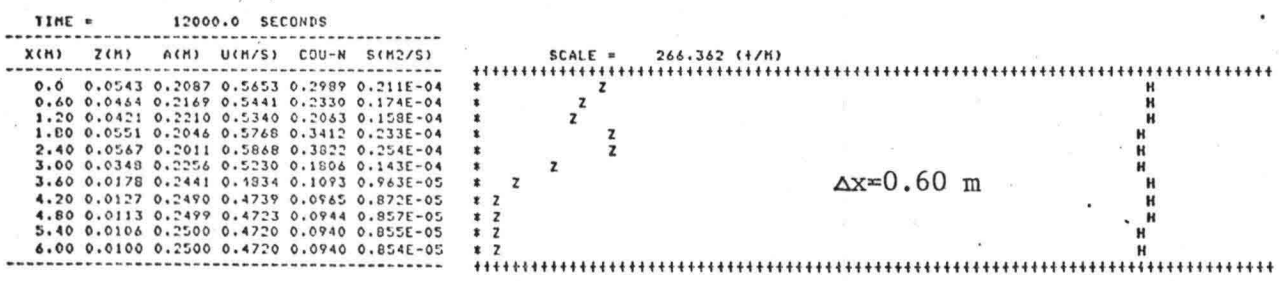
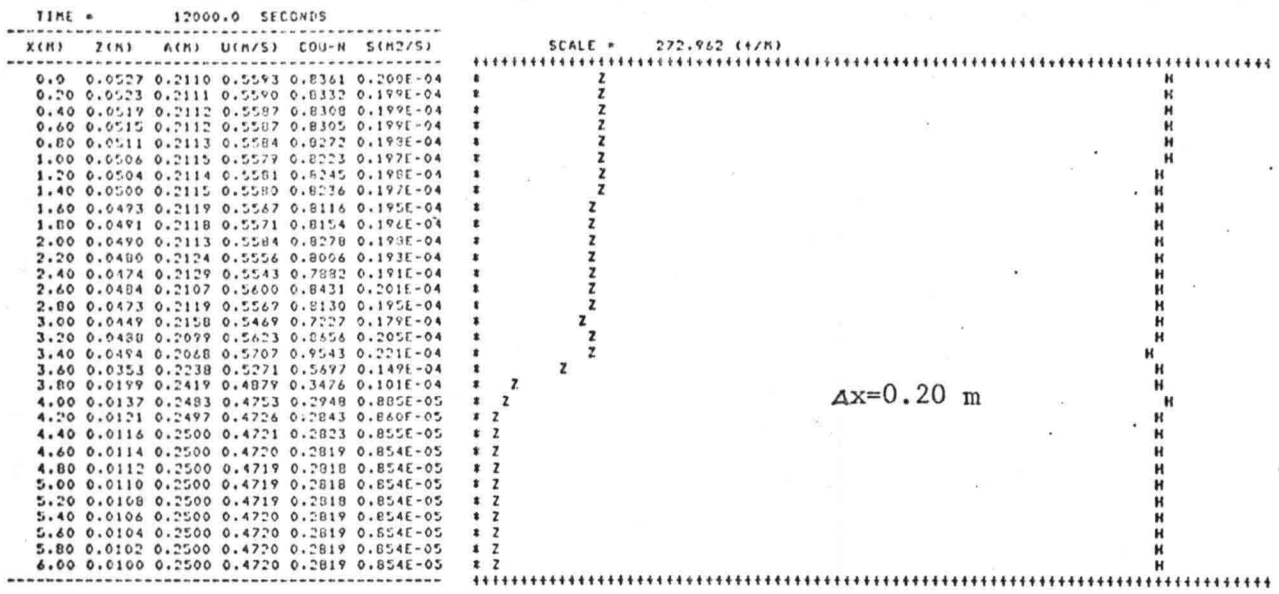


Fig. 3.2.5. Influence from space step.

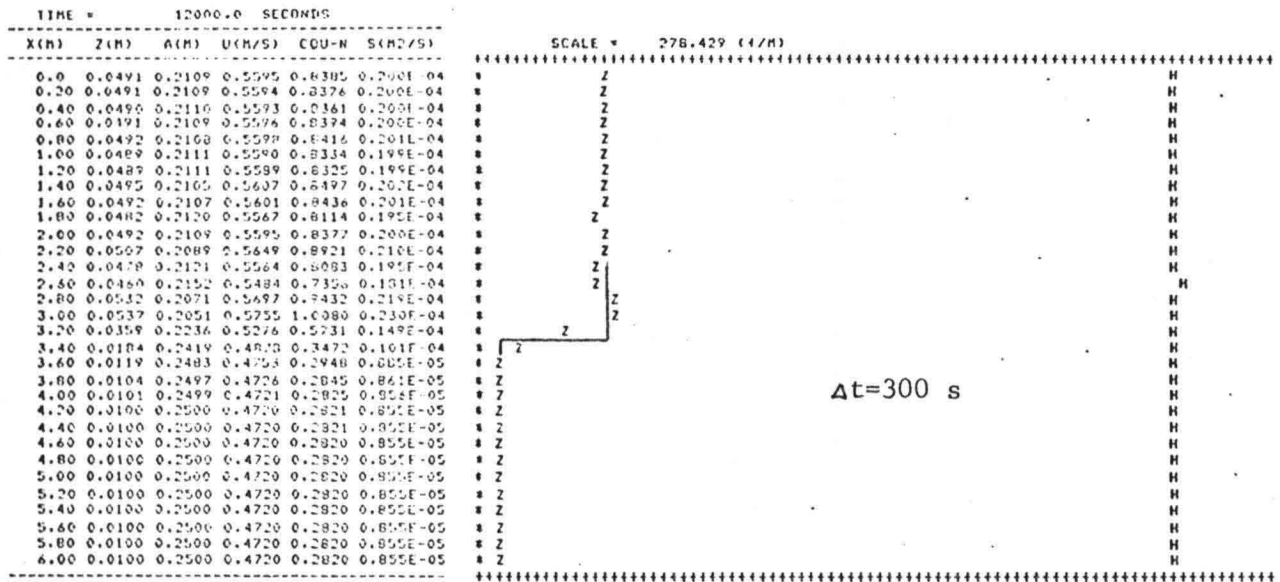
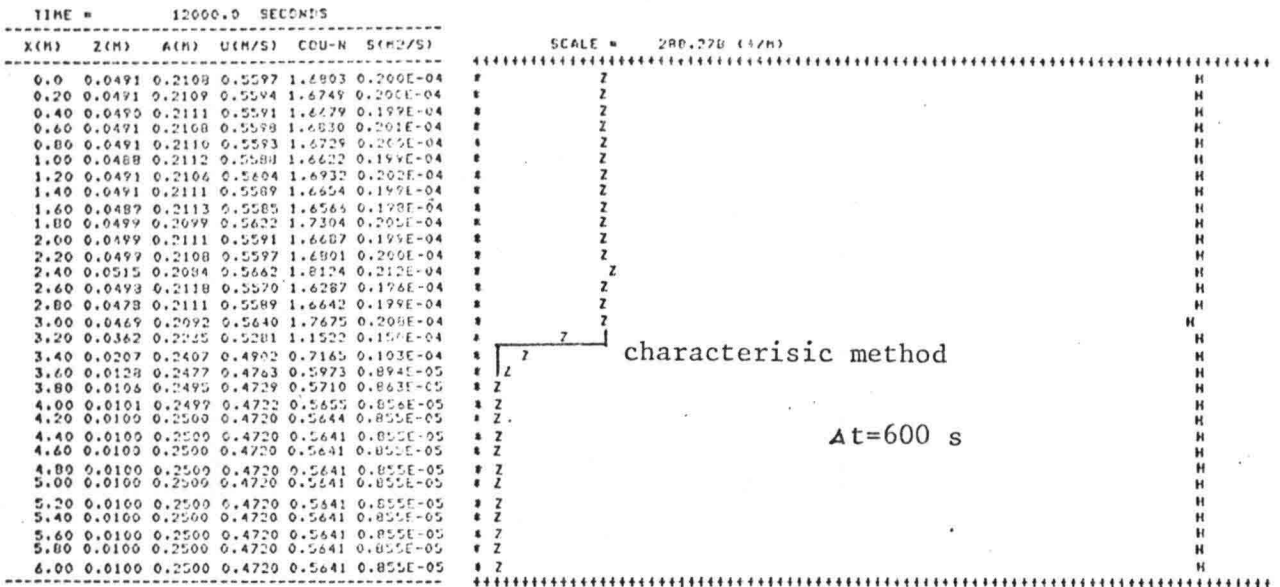


Fig. 3.2.7. Comparison with characteristic method.

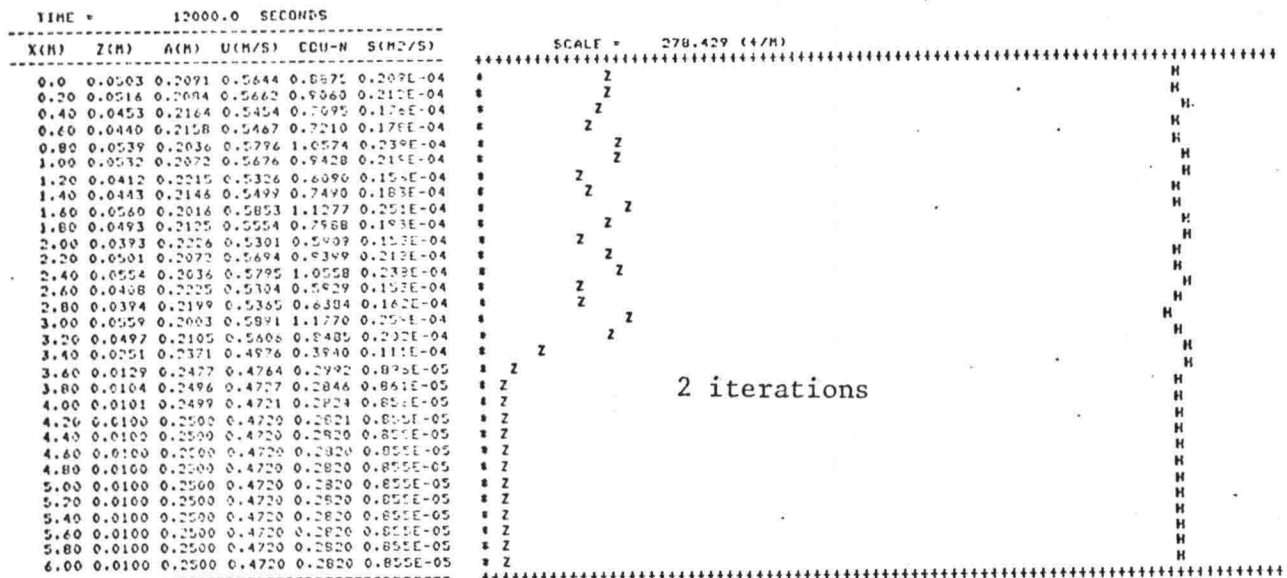
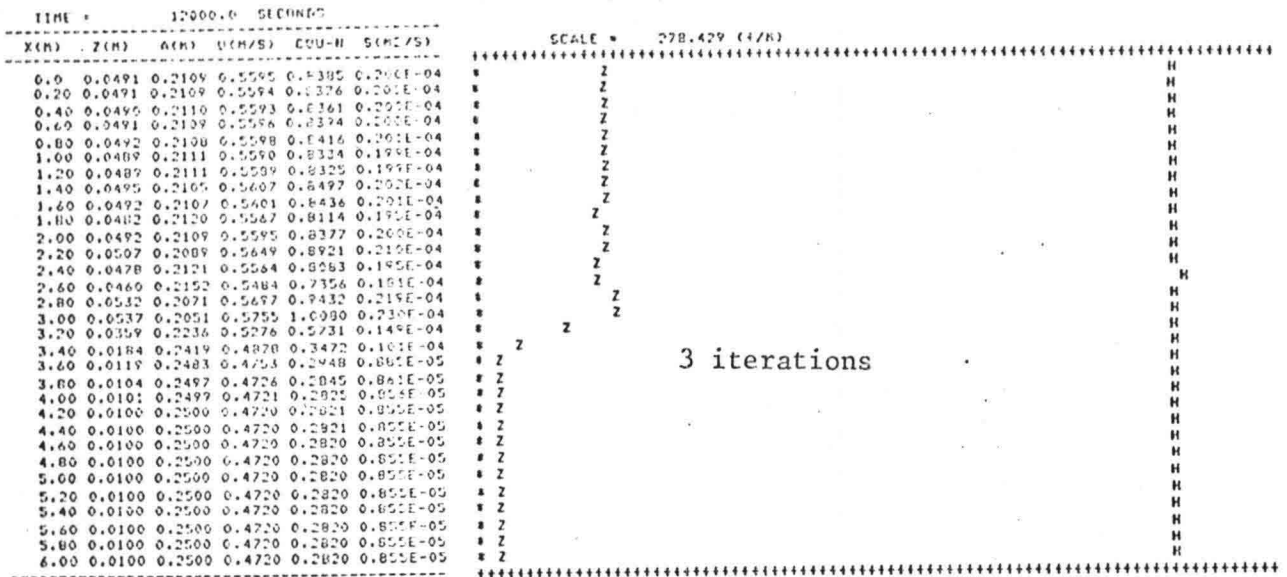


Fig. 3.28. Influence from number of iterations.

re fig. For an expanding wave there are hardly generated secondary waves,
3.2.9 further more they are propagating upstream out of the region. The deviation between the numerical solution and the one from the characteristic method is because there cannot be any sharp corners in the numerical solution, due to the numerical diffusion.

re fig. Filling - in of dredged trench. In the comparison between the mo-
3.2.10 dified Lax scheme and the predictor - corrector method the same time and space step are applied and in both cases the upstream boundary condition is a fixed bed level.

The calculation carried out with the modified Lax scheme is provided with much more numerical diffusion than the one with the predictor - corrector method although there is chosen a very large θ . Therefore is the solution with the predictor - corrector in a mathematical sense the best, but, as outlined in the figure, there are secondary waves with a very large amplitude.

The fixing of the upstream bed level may act like a reflection point for the secondary waves which not only would explain the large amplitude but also that the fluctuations are more irregular than in the other Test cases.

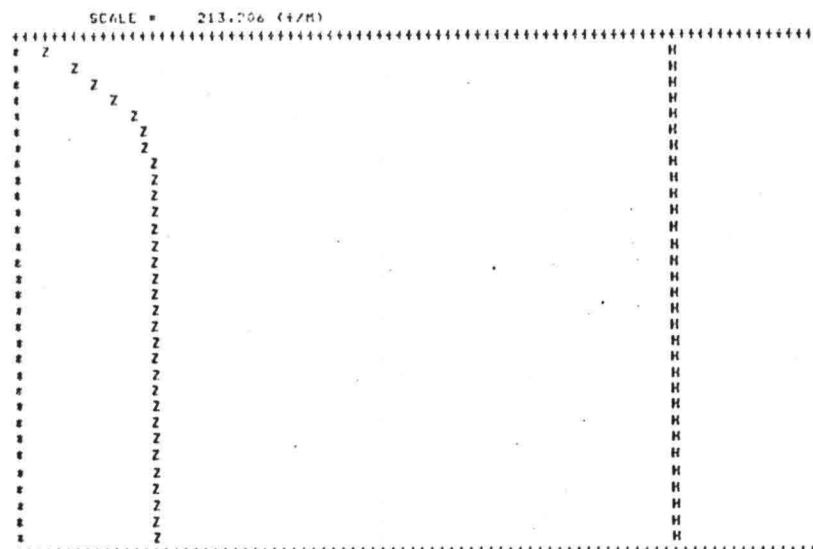
The modified Lax scheme is applied in a conservative form, but there is a trend that the trench is propagated further in the calculation with the predictor - corrector method. This may be caused by the secondary waves in the bed level which causes a fluctuation in the water level and thus influences the calculated transport at the upstream boundary.

In this case secondary waves with two points per wave length are found, which may be caused by the reflection point, but the reason could also be that these are started with a shock in the initial situation (see re figure 3.2.4)

The accuracy is, anyway for a sedimentation wave, not decreasing so much for increasing Courant number as expected according to

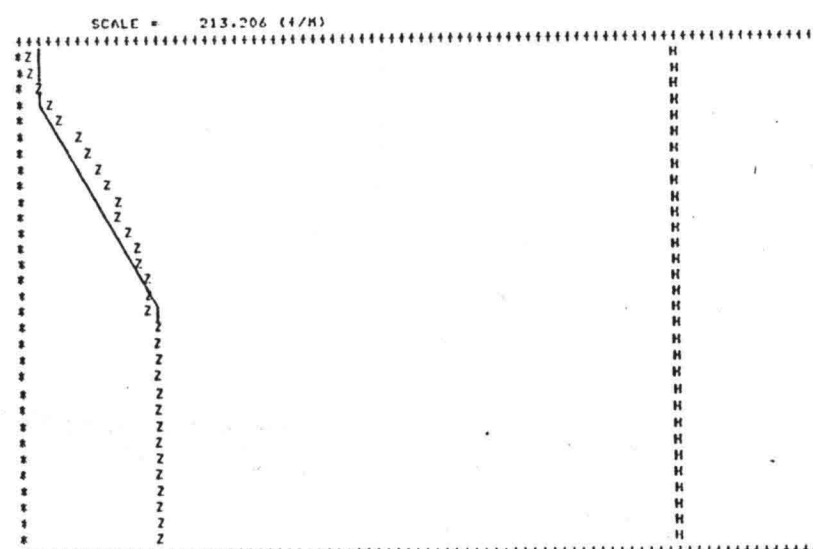
TIME = 6000.0 SECONDS

X(M)	Z(M)	A(M)	U(M/S)	COU-N	S(M2/S)
0.0	0.0104	0.3016	0.3912	0.1753	0.334E-05
0.20	0.0324	0.2976	0.3102	0.1351	0.424E-05
0.40	0.0443	0.2757	0.4269	0.3040	0.524E-05
0.60	0.0533	0.2667	0.4424	0.3757	0.616E-05
0.80	0.0597	0.2603	0.4533	0.4374	0.699E-05
1.00	0.0641	0.2550	0.4619	0.4865	0.760E-05
1.20	0.0669	0.2531	0.4661	0.5214	0.803E-05
1.40	0.0685	0.2515	0.4692	0.5432	0.829E-05
1.60	0.0693	0.2506	0.4708	0.5549	0.844E-05
1.80	0.0697	0.2503	0.4715	0.5605	0.850E-05
2.00	0.0699	0.2501	0.4718	0.5628	0.853E-05
2.20	0.0700	0.2500	0.4719	0.5637	0.854E-05
2.40	0.0700	0.2500	0.4720	0.5640	0.855E-05
2.60	0.0700	0.2500	0.4720	0.5640	0.855E-05
2.80	0.0700	0.2500	0.4720	0.5641	0.855E-05
3.00	0.0700	0.2500	0.4720	0.5641	0.855E-05
3.20	0.0700	0.2500	0.4720	0.5641	0.855E-05
3.40	0.0700	0.2500	0.4720	0.5641	0.855E-05
3.60	0.0700	0.2500	0.4720	0.5641	0.855E-05
3.80	0.0700	0.2500	0.4720	0.5641	0.855E-05
4.00	0.0700	0.2500	0.4720	0.5641	0.855E-05
4.20	0.0700	0.2500	0.4720	0.5641	0.855E-05
4.40	0.0700	0.2500	0.4720	0.5641	0.855E-05
4.60	0.0700	0.2500	0.4720	0.5641	0.855E-05
4.80	0.0700	0.2500	0.4720	0.5641	0.855E-05
5.00	0.0700	0.2500	0.4720	0.5641	0.855E-05
5.20	0.0700	0.2500	0.4720	0.5641	0.855E-05
5.40	0.0700	0.2500	0.4720	0.5641	0.855E-05
5.60	0.0700	0.2500	0.4720	0.5641	0.855E-05
5.80	0.0700	0.2500	0.4720	0.5641	0.855E-05
6.00	0.0700	0.2500	0.4720	0.5641	0.855E-05



TIME = 18600.0 SECONDS

X(M)	Z(M)	A(M)	U(M/S)	COU-N	S(M2/S)
0.0	0.0105	0.3095	0.3813	0.1497	0.294E-05
0.20	0.0096	0.3104	0.3801	0.1468	0.289E-05
0.40	0.0124	0.3076	0.3836	0.1554	0.303E-05
0.60	0.0130	0.3020	0.3907	0.1738	0.332E-05
0.80	0.0243	0.2957	0.3991	0.1983	0.369E-05
1.00	0.0306	0.2894	0.4077	0.2262	0.411E-05
1.20	0.0363	0.2837	0.4159	0.2559	0.454E-05
1.40	0.0414	0.2786	0.4235	0.2865	0.497E-05
1.60	0.0460	0.2740	0.4306	0.3175	0.540E-05
1.80	0.0500	0.2700	0.4371	0.3484	0.582E-05
2.00	0.0536	0.2664	0.4430	0.3788	0.622E-05
2.20	0.0568	0.2632	0.4483	0.4083	0.661E-05
2.40	0.0596	0.2604	0.4531	0.4365	0.697E-05
2.60	0.0620	0.2580	0.4574	0.4627	0.730E-05
2.80	0.0640	0.2560	0.4610	0.4864	0.760E-05
3.00	0.0657	0.2543	0.4641	0.5070	0.785E-05
3.20	0.0671	0.2529	0.4665	0.5240	0.806E-05
3.40	0.0681	0.2519	0.4684	0.5374	0.823E-05
3.60	0.0688	0.2512	0.4697	0.5473	0.834E-05
3.80	0.0693	0.2507	0.4707	0.5541	0.843E-05
4.00	0.0696	0.2504	0.4713	0.5585	0.848E-05
4.20	0.0698	0.2502	0.4716	0.5611	0.851E-05
4.40	0.0699	0.2501	0.4718	0.5626	0.853E-05
4.60	0.0699	0.2501	0.4719	0.5634	0.854E-05
4.80	0.0700	0.2500	0.4720	0.5637	0.854E-05
5.00	0.0700	0.2500	0.4720	0.5639	0.855E-05
5.20	0.0700	0.2500	0.4720	0.5640	0.855E-05
5.40	0.0700	0.2500	0.4720	0.5640	0.855E-05
5.60	0.0700	0.2500	0.4720	0.5641	0.855E-05
5.80	0.0700	0.2500	0.4720	0.5641	0.855E-05
6.00	0.0700	0.2500	0.4720	0.5641	0.855E-05



TIME = 26400.0 SECONDS

X(M)	Z(M)	A(M)	U(M/S)	COU-N	S(M2/S)
0.0	0.0123	0.3077	0.3834	0.1549	0.302E-05
0.20	0.0109	0.3091	0.3818	0.1509	0.296E-05
0.40	0.0093	0.3107	0.3796	0.1462	0.288E-05
0.60	0.0100	0.3100	0.3807	0.1483	0.292E-05
0.80	0.0132	0.3068	0.3846	0.1578	0.307E-05
1.00	0.0176	0.3024	0.3902	0.1726	0.330E-05
1.20	0.0224	0.2976	0.3966	0.1906	0.358E-05
1.40	0.0272	0.2928	0.4030	0.2106	0.388E-05
1.60	0.0317	0.2883	0.4093	0.2318	0.419E-05
1.80	0.0359	0.2841	0.4153	0.2537	0.451E-05
2.00	0.0397	0.2803	0.4210	0.2761	0.483E-05
2.20	0.0433	0.2767	0.4264	0.2987	0.514E-05
2.40	0.0465	0.2735	0.4315	0.3215	0.545E-05
2.60	0.0495	0.2705	0.4362	0.3442	0.576E-05
2.80	0.0522	0.2678	0.4407	0.3668	0.606E-05
3.00	0.0547	0.2653	0.4449	0.3891	0.636E-05
3.20	0.0571	0.2629	0.4488	0.4109	0.664E-05
3.40	0.0592	0.2608	0.4524	0.4321	0.691E-05
3.60	0.0611	0.2589	0.4557	0.4525	0.717E-05
3.80	0.0628	0.2572	0.4588	0.4718	0.741E-05
4.00	0.0643	0.2557	0.4615	0.4896	0.764E-05
4.20	0.0656	0.2544	0.4639	0.5058	0.784E-05
4.40	0.0667	0.2533	0.4659	0.5199	0.801E-05
4.60	0.0677	0.2523	0.4676	0.5319	0.816E-05
4.80	0.0684	0.2516	0.4689	0.5415	0.827E-05
5.00	0.0689	0.2511	0.4700	0.5489	0.836E-05
5.20	0.0693	0.2507	0.4707	0.5544	0.843E-05
5.40	0.0696	0.2504	0.4712	0.5581	0.848E-05
5.60	0.0698	0.2502	0.4715	0.5606	0.851E-05
5.80	0.0699	0.2501	0.4717	0.5621	0.852E-05
6.00	0.0699	0.2501	0.4719	0.5630	0.853E-05

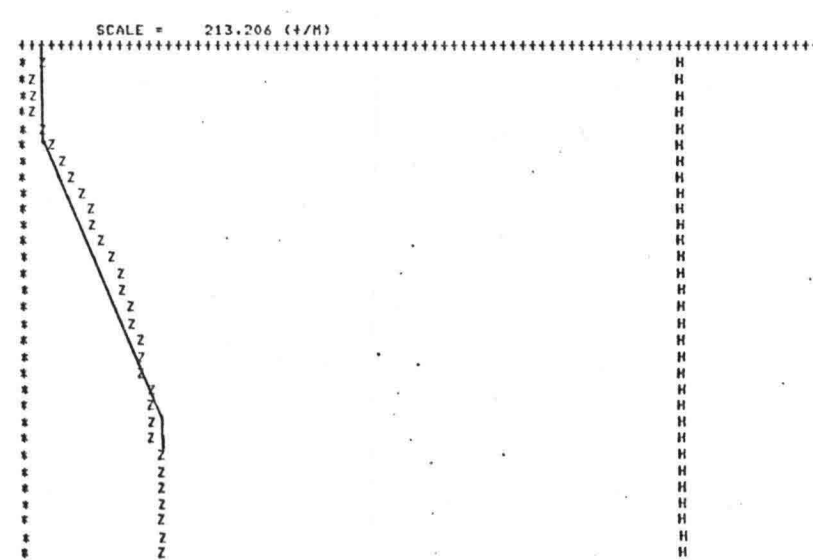


Fig. 3.2.9. Comparison with characteristic method.

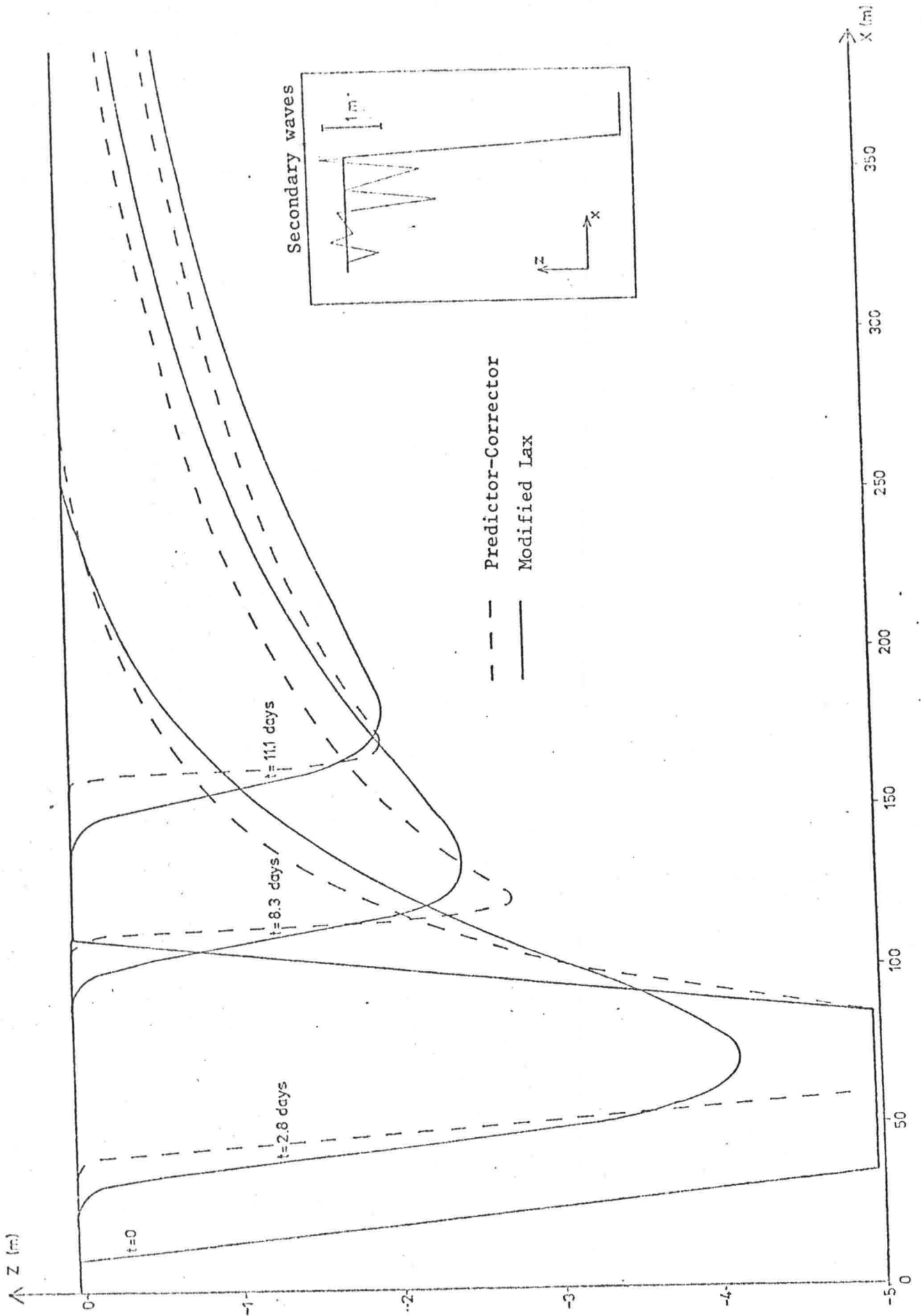


Fig. 3.2.10. Comparison with Modified Lax.
Filling-in of a dredged trench.

figure 3.1.9 and 3.1.10. The presence of physical diffusion in the model for uniform sediment does not seem to cause any problems (eqs. 3.1.37 and 44).

In a problem with more celerities, as in the model for non-uniform sediment, it can be expected that the stability criterion applies to the largest celerity, when a smaller celerity maybe can cause secondary waves. It is then desirable to have a numerical method where the secondary waves could be suppressed without having to calculate with Courant number close to or exceeding unity. The four points scheme has this quality, but the little flexibility and the expected increased calculation time for a fully implicit scheme justify the application of the predictor-corrector method to the model for non-uniform sediment. Besides the secondary waves only influence the accuracy considerable if the upstream boundary condition is a fixed bed level.

3.3. Numerical model for non-uniform sediment.

Before applying the predictor-corrector method to the model for non-uniform sediment a simplification of the model will be carried out and the model will be modified in order to be able to simulate flume experiments where sand feeding by elevator takes place.

3.3.1. Schematization of vertical grain distribution.

The vertical composition in the z_0 - layer will be schematized for simplification of the model.

When the infrequently deep throughs in the bed (which are not considered as a part of the transport layer) are occurring the finer material will be washed out. The vertical grain distribution will therefore typical have the form outlined in figure 3.3.1.

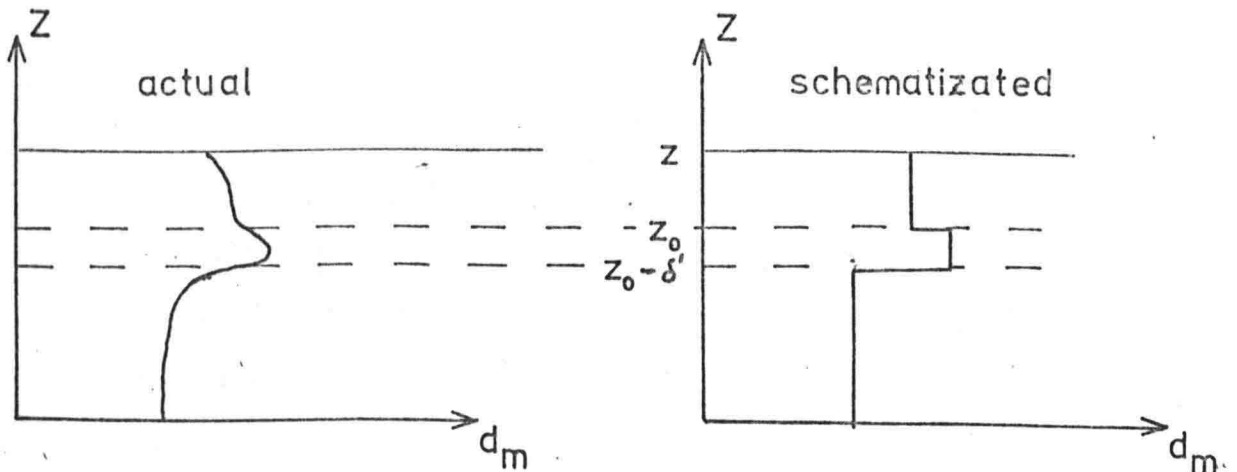


Figure 3.3.1. Vertical grain size distribution.

In case of erosion the composition at the Z_0 - level is in the schematized form given by (Z is here vertical coordinate)

$$\bar{p}_{iZ}(Z) = \begin{cases} p_{iZ_0} & \text{for } Z \geq Z_0 \\ p_{iZ_0} + \Delta p_i & \text{for } Z - \delta' < Z < Z_0 \\ p_{iZ_0} & \text{for } Z \leq Z_0 - \delta' \end{cases} \quad (3.3.1)$$

where p_{iZ_0} is the depth averaged composition of the Z_0 - layer. p_{iZ_0} is a function of time and Δp_i constant.

The placing of the coarse layer (δ') is fixed in the initial condition, and when ever the Z_0 - level is eroding in this layer the composition is given by $p_{iZ_0} + \Delta p_i$. Consequently the coarse layer can only be applied in case of pure erosion. If for instance first erosion takes place until below $Z_0 - \delta'$ and here after sedimentation to above this level then the coarse layer will be regenerated.

In case of sedimentation the material leaving the transport layer is considered to be uniform mixed over the Z_0 layer in the schematization there is applied to the model. The consequence of this is that the model cannot treat first sedimentation and then erosion correctly. However if the reference level is chosen close to the Z_0 - level the composition of the Z_0 - layer will be much influenced by the sedimentated material, and the model can be used to show a trend.

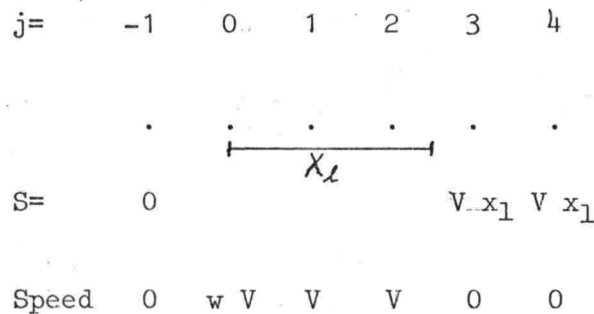
3.3.2. Sand elevator.

It has been considered important that the numerical model is able to simulate flume experiments where sand feeding is taking place by elevator. This is equivalent by adding a source term in the continuity equation per fraction and setting the sandinput at the upstream boundary equal zero.

$$\frac{\partial S_i}{\partial X} + \frac{\partial Z p_i}{\partial t} = V \cdot p_{i z_0} \quad \text{for } X < X_1 \quad (3.3.2)$$

where V is the sand elevator velocity and X_1 is the length of the elevator.

When the numerical method is applied to the sand elevator in a equilibrium situation it is necessary to weight the velocity of the first grid point. This is because the upstream sand input in the computational model is applied outside the region ($X = -\Delta X$), in order to inable the application of the Crank - Nicholson scheme in the first point as well. The weight of the velocity in the first grid point in a equilibrium situation can be obtained from figure 3.2.2.



$$\frac{S_4 - S_2}{2 \cdot x} = 0 \quad S_2 = S_4$$

$$\frac{S_3 - S_1}{2 \cdot x} = V \quad S_1 = V(x_1 - 2 \cdot x)$$

$$\frac{S_1 - S_{-1}}{2 \cdot x} = w \cdot V \quad S_1 = V \cdot w \cdot 2 \cdot x$$

Figure 3.2.2. Weight of sand elevator velocity.

$$w = V \frac{x_1 - 2 \cdot x}{2 \cdot x}$$

The length of the sand elevator is small compared with the length of the flume, so when the sand elevator is used one is forced to apply a very small space step, which increases the calculation time considerably. However the influence from the sand elevator on the wave lengths in bed level and composition is a local phenomena, so there can first be calculated a short time with the sand elevator, and then start a new calculation with normal sand input as boundary condition and applying a larger time and space step.

3.3.3. The structure in the programme.

A couple of different flows in the programme are possible, and the one that is expected to be most efficient is chosen (see flow chart p 181).

For a given transport layer composition and bed level at time level n the back-water calculation is carried out and the transport per fraction is calculated. As outlined in chapter 2.4 is it necessary to know whether there is a positive or negative displacement of the Z_0 -level, so the new bed level is predicted by summing the transport per fraction and use the equation of continuity from the model for uniform sediment.

Hereafter the composition at time level $n+1$ could be predicted by help of the continuity equation for each fraction, but as this procedure costs much calculation time, it was decided first to calculate the predicted transport at time level $n+1$ with predicted flow velocity and the composition at time level n , and then go on with a traditional predictor-corrector iterations.

The roughness predictions takes place in connection with the transport calculation because it is most convenient. The consequence of this is that the flow velocity is calculated with the roughness from the previous iteration step and the transport with the new roughness. This lagging does not introduce any serious error because the roughness only changes a little during one iteration step. Further more the lagging seems to be in agreement with the trend outlined in figure 2.5.2.

In appendix B a users guide for the numerical model can be found and in appendix C a short programme documentation.

3.3.4. Sensitivity analysis.

Four examples are calculated with the numerical model for different combinations of the numerical parameters, and the computational results are compared with solution obtained from the characteristic method.

The transport is calculated with the Meyer - Peter and Müller formula (ripple factor $\mu = 0.5$), two fractions and horizontal water level. The initial and boundary conditions for the examples are resumed in table 3.3.1.

The principle of the calculation with the characteristic method is described in chapter 1.2. From each point two celerities are issued. Where the celerities from the foot and from the top of the steps in bed level and composition are intersecting a temporary equilibrium develops.

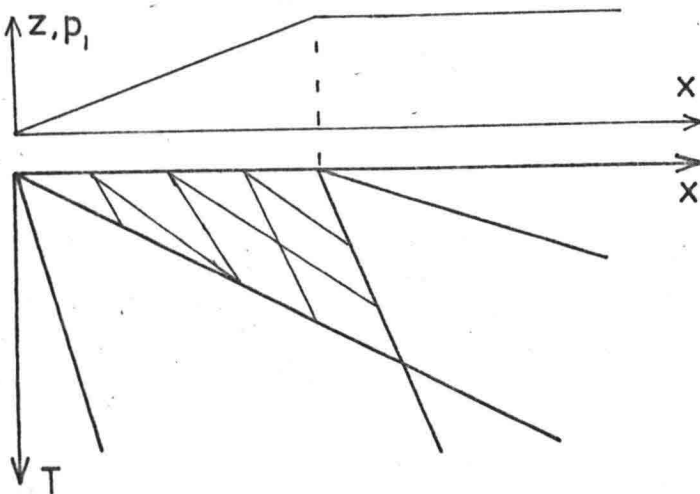

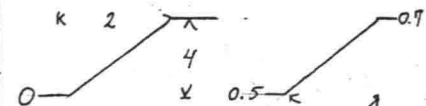
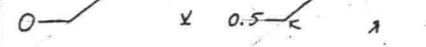
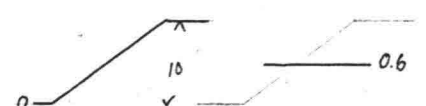
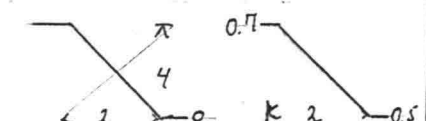


Figure 3.3.3. Temporary equilibrium.

The examples are in the characteristic method calculated with a increased number of points at the wave in the initial condition, until the converged solution is found. In example 1 and 2 the two celerities are

8/17

Example	Initial condition 	ϕ (m)	q (m ² /s)	h (m)	Celerities (m/h)	
					c _{max}	c _{min}
1		0.01	0.1376	0.40	1.65	0.06
2		0.20	same	same	0.38	0.004
3		0.10	0.25	0.50	3.20	0.30
4		0.10	0.1376	0.40	0.50	0.025

$C=30 \text{ m}^{\frac{1}{2}}/\text{s}$

$d_1=0.4 \text{ mm}$

$d_2=1.0 \text{ mm (1.2 mm in Ex 3)}$

Table 3.3.1. Test cases

calculated with Froude number calculated from the local water depth and flow velocity, although the Froude number is equal zero due to the horizontal water level. This gives a trend, that the processes are going faster, and conservation of mass cannot be expected, when the solution is compared with the results from the numerical model.

In example 1 and 2 the calculation with the characteristic method is carried out with $\bar{p}_{iZ_0} = p_i$ in order to reduce the number of variables. This is not physical correct in case of erosion. The procedure in the numerical model there is computing the composition is brought in agreement with $\bar{p}_{iZ_0} = p_i$.

In the calculation performed with the numerical model the upstream boundary condition is the equilibrium transport of each fraction. The results from the sensitivity analysis are depicted in the figures 3.3.4 to 3.3.9.

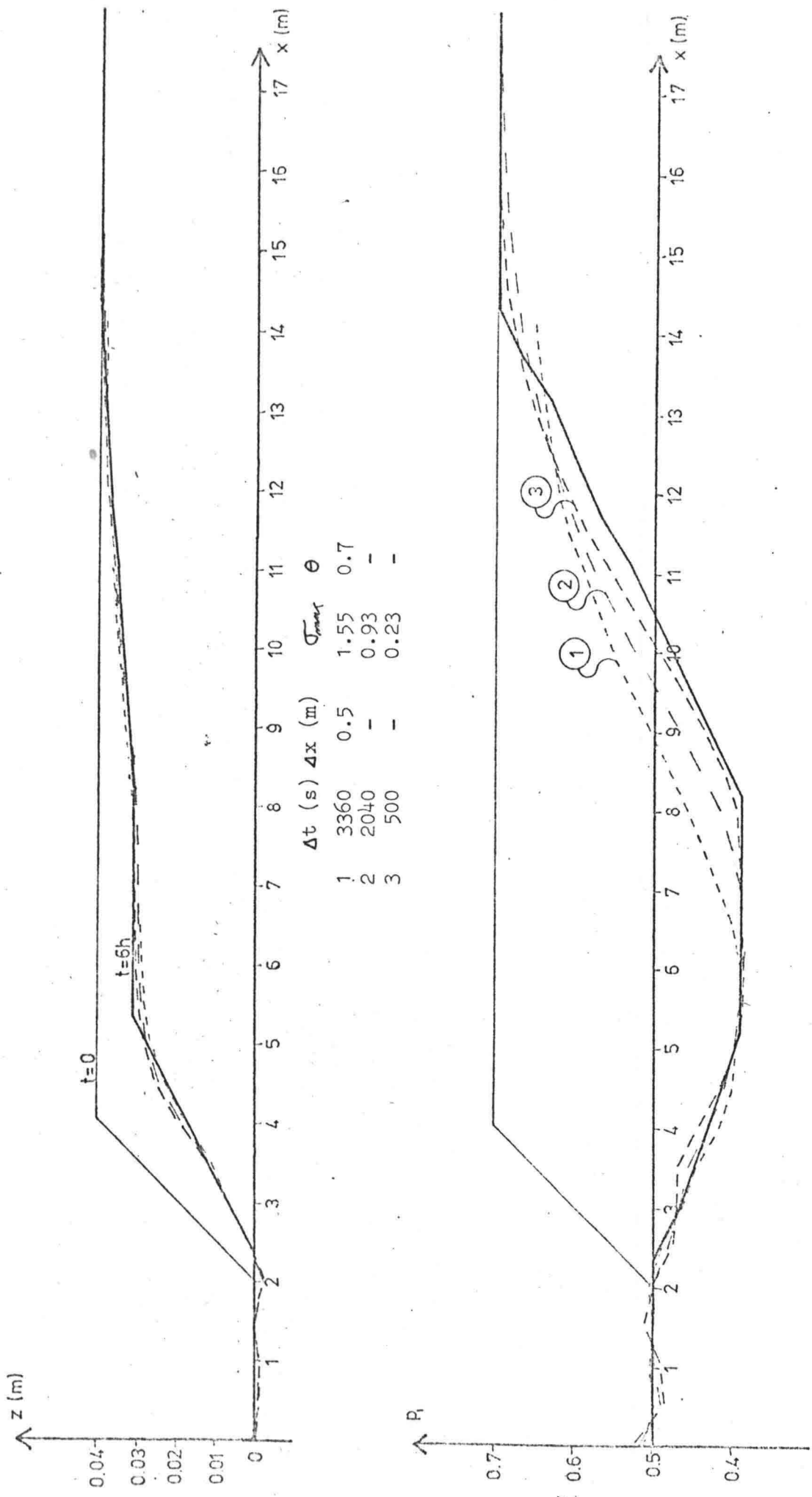
EX 1.

re fig. Here a very pronounced change in composition takes place, due to
3.3.4 the small transport layer thickness. Recall that total agreement between the results from the two calculation methods is not expected. The secondary waves upstream of the front are suppressed very good with $\Theta = 0.70$, but it provides much numerical diffusion especially for large time steps, which is the reason for the big difference in the computed results.

EX 2.

re fig. The same parameters is used as in EX 1 except the transport layer
3.3.5 thickness. The difference in the processes must not only be attributed to the transport layer thickness, because with $\bar{p}_{iZ_0} = p_i$ also the vertical grain distribution in the Z_0 - layer is different. In this example the changes especially take place in the bed level. The process is going much slower, because the transport layer thickness appears in the denominator in the celerities.

The calculation carried out with $\sigma_{\max} = 0.66$ and $\bar{\sigma}_{\max} = 1.32$ gives almost the same result, a completely different trend as in the computations for example 1, so it seems to cause the model less trouble to compute large changes in bed level than in com-

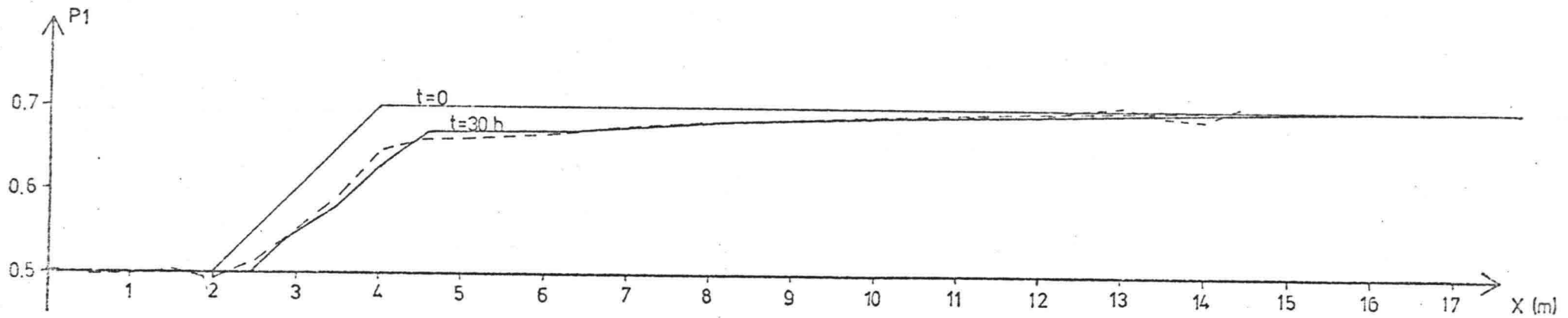
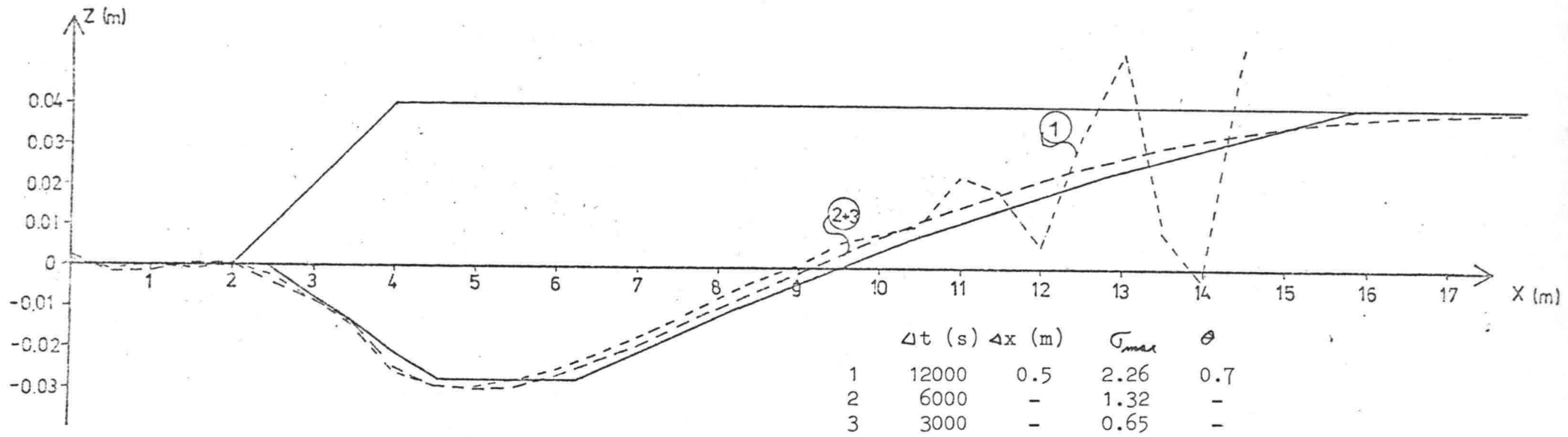


	Δt (s)	Δx (m)	σ_{max}	θ
1	3360	0.5	1.55	0.7
2	2040	-	0.93	-
3	500	-	0.23	-

Fig.3.3.4. Example 1

Fig. 3.3.5. Example 2

121



position. For $\Theta = 0.7$ the stability criterion yields according to the numerical analysis $\sigma < 1.50$, but the model can almost compute with $\sigma_{\max} = 2.65$.

re fig. Ex. 2. Here is the same trend as in the numerical model for uni-
3.3.6 form sediment: for increasing space step trouble with secondary waves occurs.

Comparing the two figures for example 2 it is seen, that it is more efficient to decrease the space step than the time step. In figure 3.3.6 no benefit in accuracy was won when the time step is halved (curve 1 and 2) but here a little accuracy is won by halving the space step (curve 3 and 4).

re fig. Ex. 3. Here both pronounced changes in bed level and composition
3.3.7 takes place and the accuracy is very good even for relative large space steps and Courant numbers. Both the calculated and composition behaves according to expectations: hardly any secondary waves for the small space step, and the amount of numerical diffusion is the same for equal time steps.

re fig. Ex. 4. A shock front. The expected influence from the numerical
3.3.8 diffusion coefficient is found in the reproduction of the shock front, but there is surprisingly little secondary waves. For $\sigma = \frac{1}{2}$ the propagation velocity for secondary waves should be at maximum (figure 3.1.4) and very little numerical damping is present.

Infinite accurate calculations can be carried out by decreasing the time and space steps. A very little Θ can be permitted because of the absence of secondary waves (λ_0 is equal zero for $\sigma = 1$, but there is more celerities in the problem).

re fig. Ex. 4. The propagating of the wave is compared with eq. 1.1.27,
3.3.9 and this seem to be accurate as well. Notice that the temporarily equilibrium is not expanding, because the differential equations do not apply after the shock is formed.

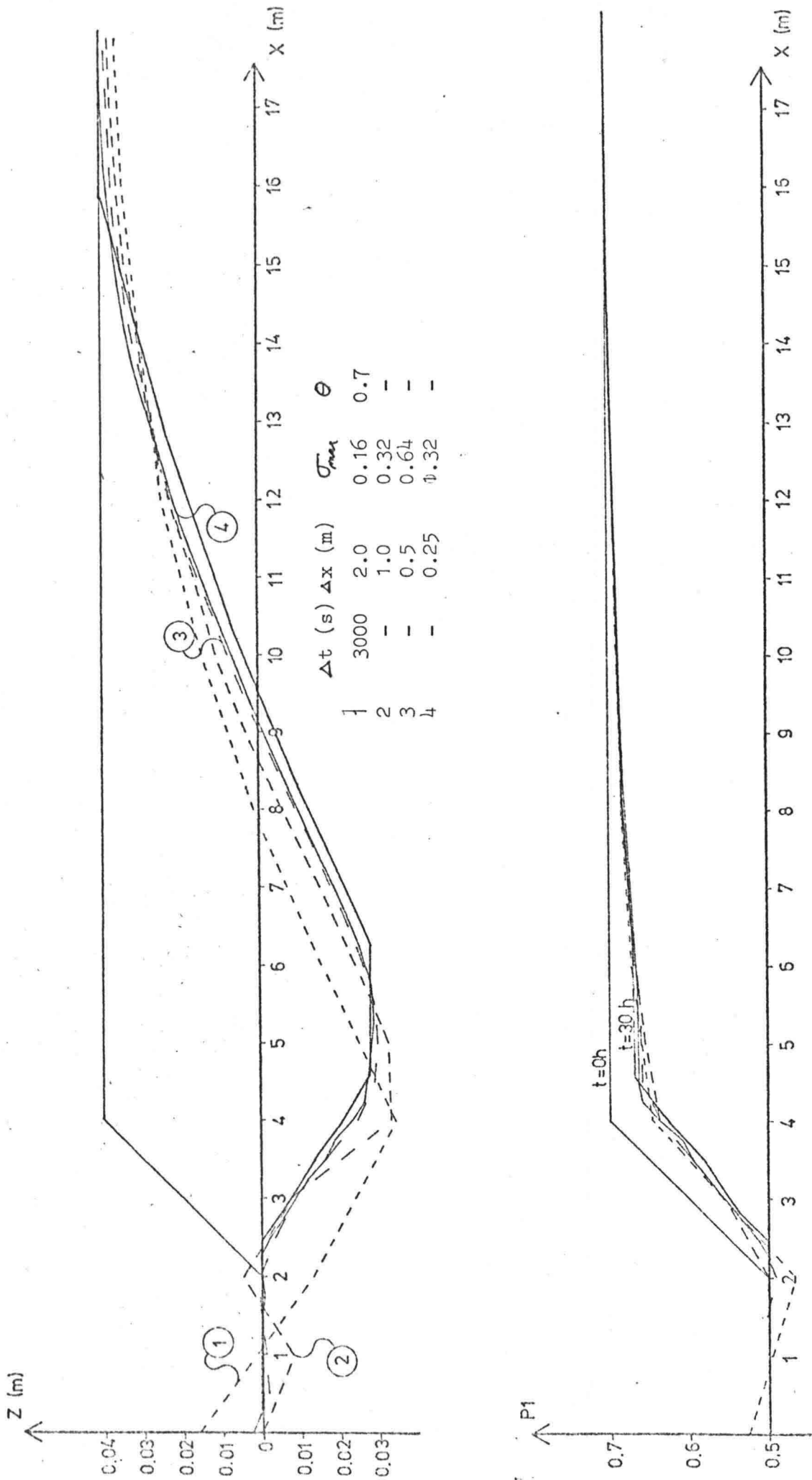


Fig.3.3.6. Example 2

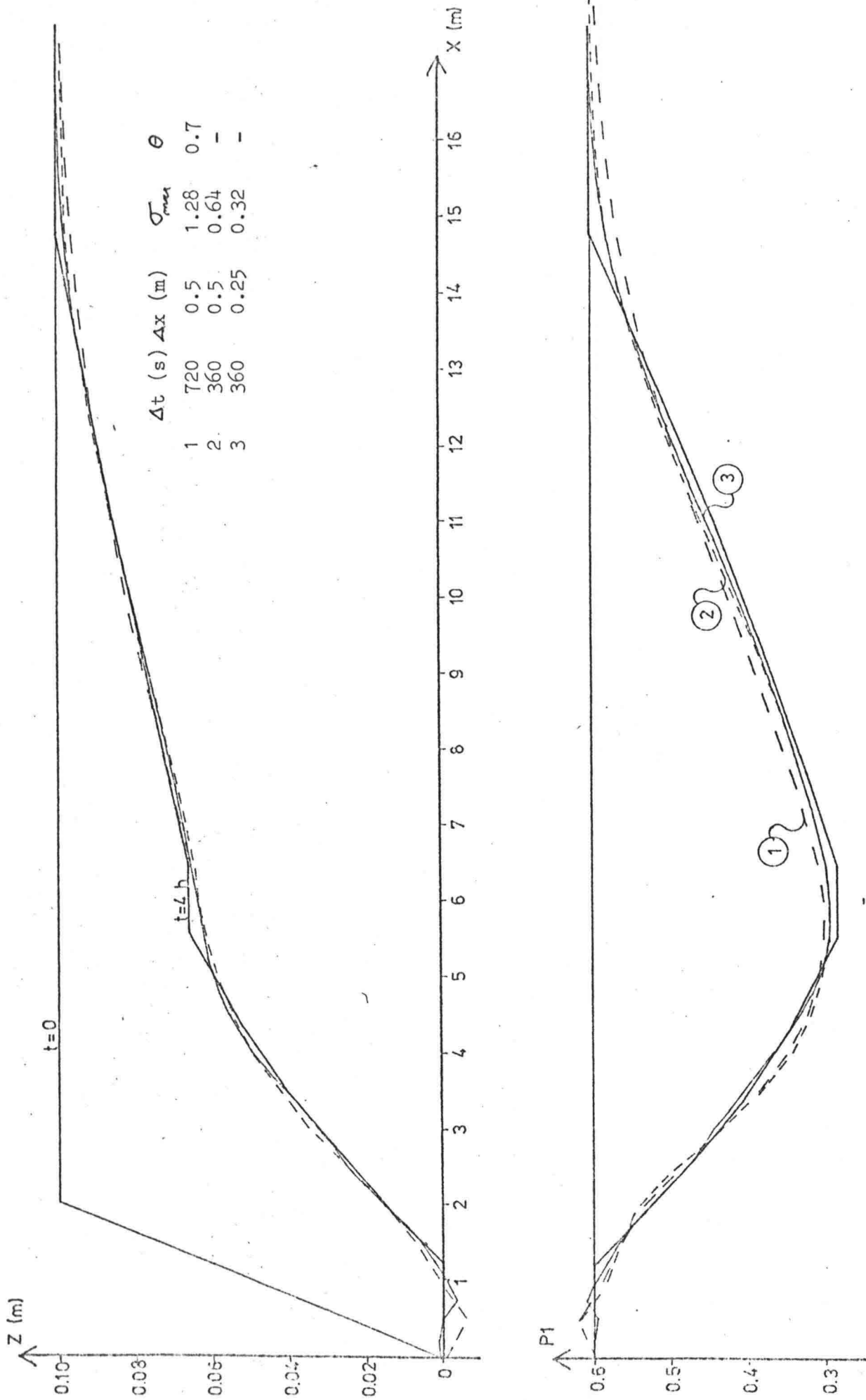
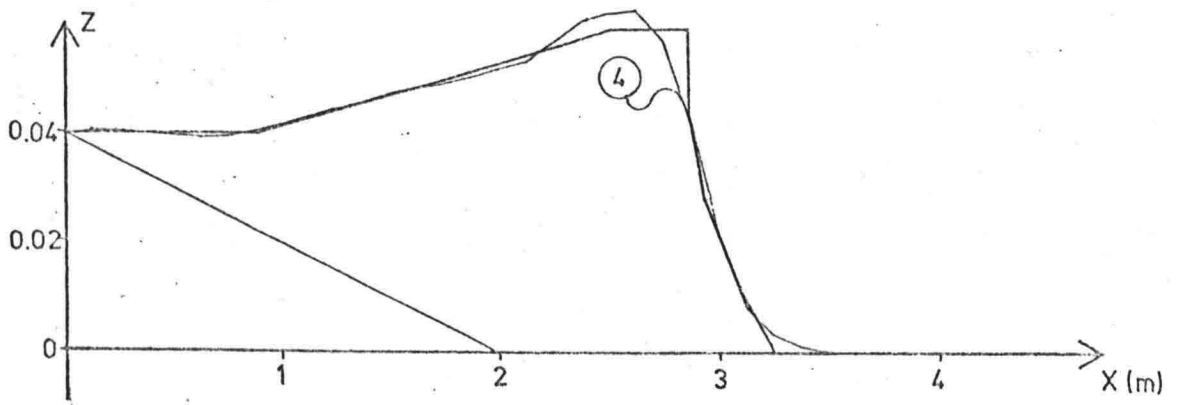
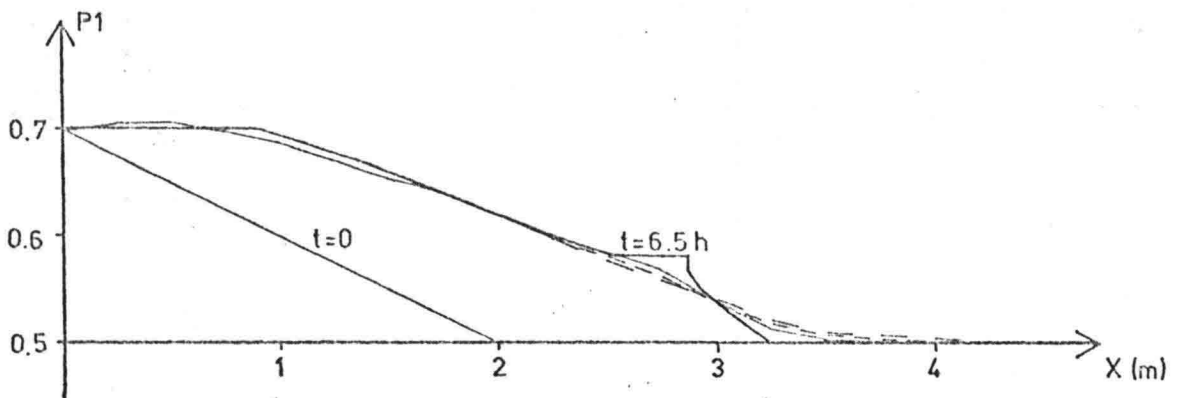
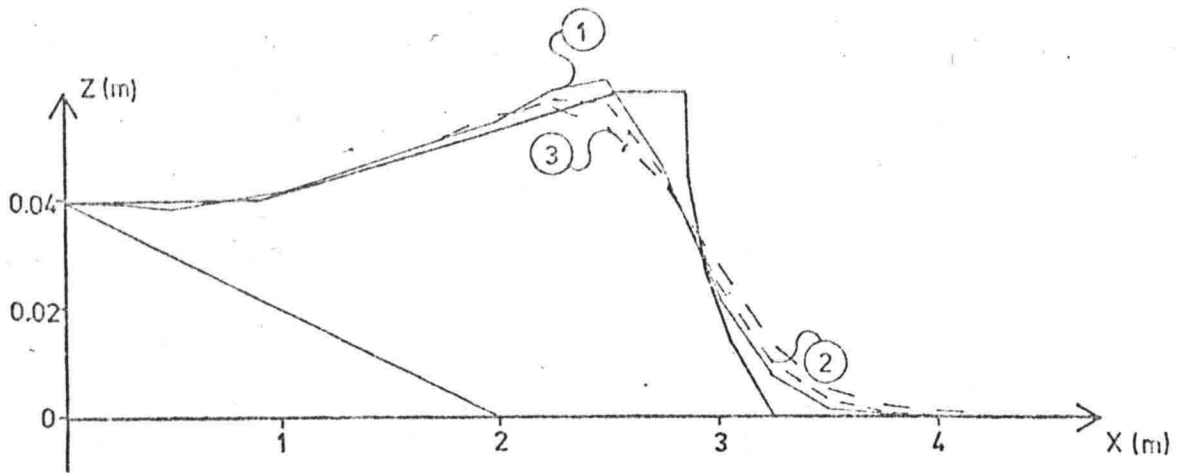


Fig.3.3.7. Example 3



	Δt (s)	Δx (m)	σ_{max}	θ
1	2600	0.25	1.45	0.7
2	1800	-	1.00	-
3	900	-	0.50	-
4	-	0.125	1.00	0.525

Fig 3.3.8. Example 4

3.3.5. Conclusion.

The predictor - corrector method is able to produce accurate results, although more calculation effort than expected has to be contributed. Luckily the secondary waves do not seem to cause so much trouble as first assumed.

It is concluded that the reliability of the computational results are not influenced by numerical errors, if the model is used with caution, i.e. the accuracy is tested by applying different space and time steps. The numerical model can therefore be used to study the model for non-uniform sediment as uncertainties in the computational result can be attributed to inaccuracy in the model or in the component parts of it.

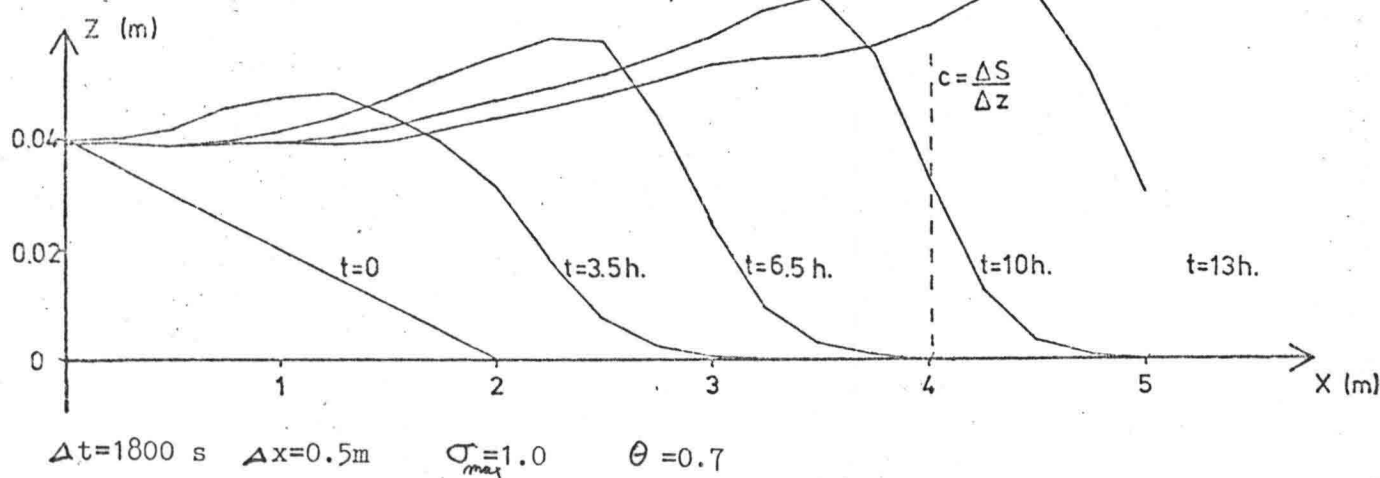


Fig 3.3.9. Example 4

4. APPLICATION OF THE MODEL.

The numerical model is a powerful means to forecast morphological changes in alluvial rivers, if the computational results are interpreted with caution. Measurements have to be carried out in order to verify and to calibrate the model and the consequence of varying the parameters in the model must be investigated by means of a sensitivity analysis in order to get some insight into the reliability of the computational results.

It will be attempted to verify the model with two examples: one measurement from prototype and one flume experiment. The examples are unfortunately not typical cases where a model for non-uniform sediment has its largest applicability, because the shear stresses in the examples are so large that only very little selective transport takes place, but it were the only examples available.

In the first example the filling-in of a dredged trench in the river IJssel will be simulated. This process has been the subject for extensive measurement and the initial and boundary conditions are therefore very reliable. The second example is a simulation of a flume experiment, but here only superficial information has been available.

In cases where it is especially interesting to calculate with a model for non-uniform sediment no experimental results or measurements from prototype were available. A sensitivity analysis, with attention to the transport layer thickness and the grain size characteristics, is carried out for an example concerning an imaginary river, where the upstream sediment supply is cut off. This is a case similar to what occurs downstream of a dam, when all the sediment is trapped in the reservoir.

4.1. Filling-in of a dredged trench [27]

In the framework of the River Research Group of the joint hydraulic research programme T.O.W. (Toegepast Onderzoek Waterstaat) a research project was carried out with the aim (among other things) to study dune migrations and migration velocity and in order to verify a numerical model for uniform sediment.

As a part of the project a trench was dredged during April 1980 in the river IJssel close to Deventer, the Netherlands. In figure 4.1.1 the dimensions of the trench are illustrated.

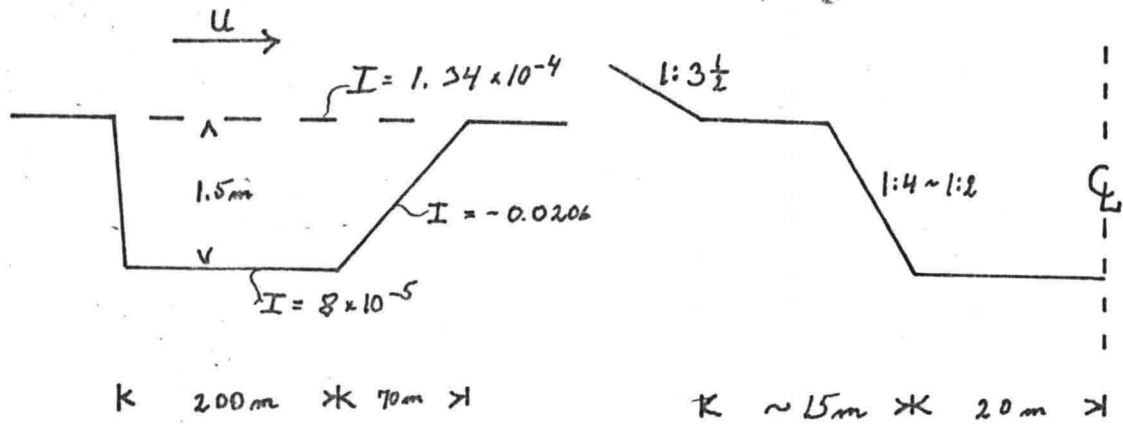


Figure 4.1.1. Dimensions of trench.

4.1.1. Field measurements

Extensive measurements were carried out of the sediment transport (suspended and bed load), the water level, the discharge and the bed profile were regulated during the filling in of the trench. In figure 4.1.2 the extent of the study reach is depicted, with indications of where the measurements were performed.

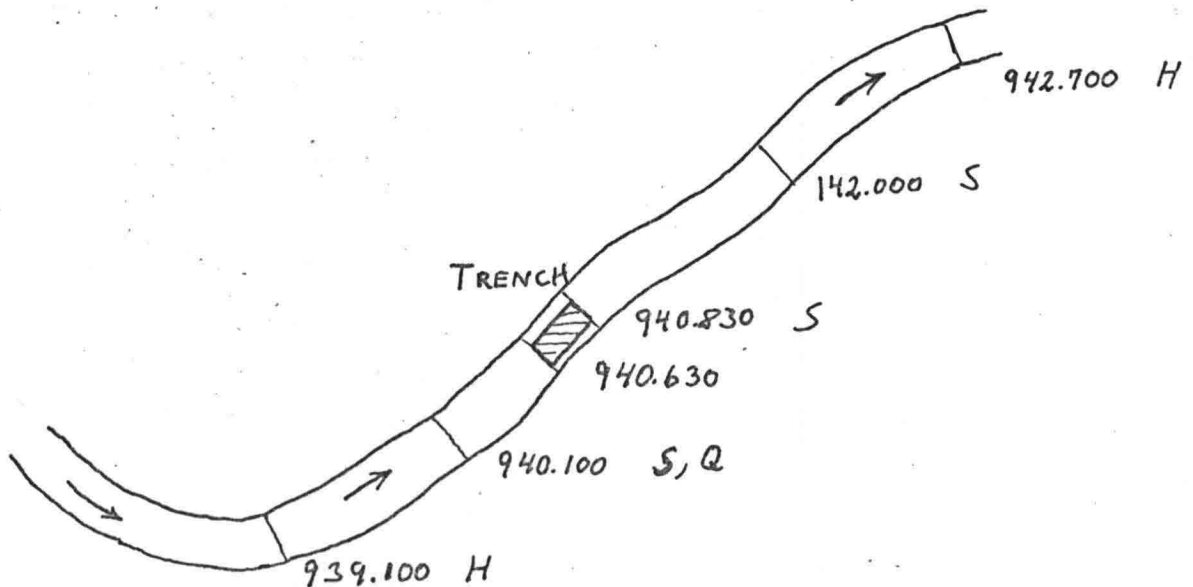


Figure 4.1.2. Extent of study reach.

Bed profile

The recording of the bed profile shows a maximum dune height on ± 1.5 m with an averaged value ± 0.4 m. The averaged dune length is 40 m and the migration velocity about 4 m/day, thus an averaged dune will travel it's own length in 10 days. Consequently the transport layer thickness does not depend on the average dune height as much as the actual dune height, and the transport layer thickness is therefore chosen as 0,75 m (15% of water depth) in the simulations.

Discharge

The discharge is measured in km. 940.100 during two periods of each three weeks in order to obtain the local discharge from the water level (rating curve). Several velocity profiles are measured and integrated over the width. The discharge is divided into two parts, one belonging to the cross-section part with movable bed and the other belonging to the part with fixed bed. This division is a procedure which introduces some uncertainty in the estimation of the specific discharge. The variation of the specific discharge is very well approximated by the hydrograph which is depicted in figure 4.1.3.

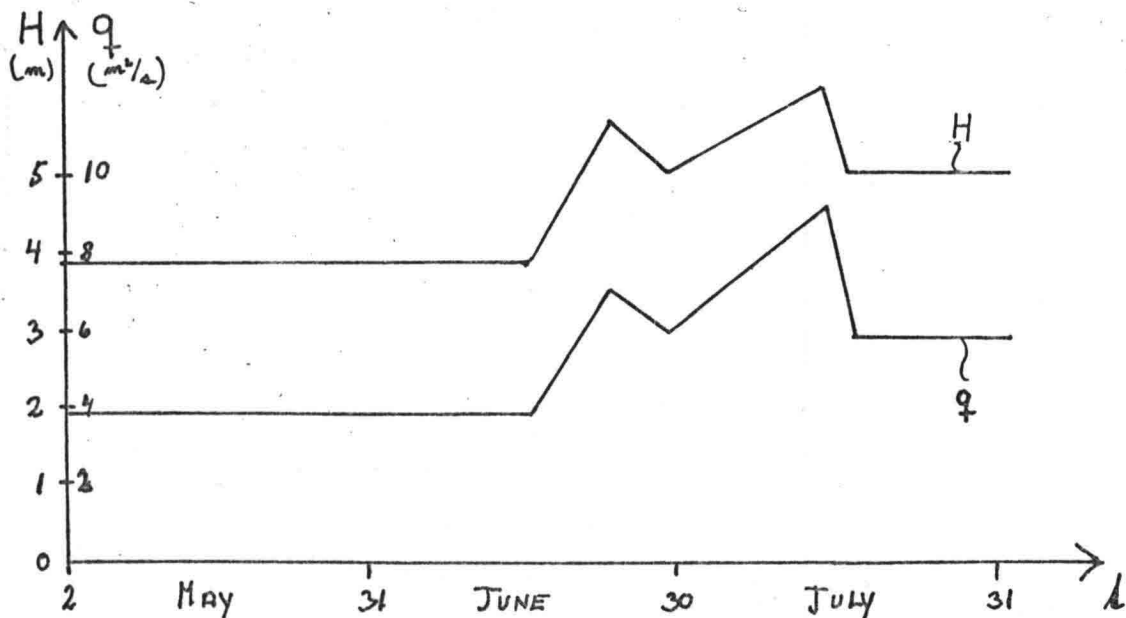


Figure 4.1.3. Boundary conditions for computations.

Water level

The water level is recorded continuously at km 939.100 and 942.700. During the period with constant discharge the difference in water level is approximately $\Delta h = 0.280$ m, thus a energy line gradient $I = 7.8 \times 10^{-5}$ which indicates a Chezy - roughness $C = 39 \text{ m}^{\frac{1}{2}} / \text{s}$. During the flood period $\Delta h = 0.270$ m which gives $C = 40 \text{ m}^{\frac{1}{2}} / \text{s}$, so the variation in roughness can be neglected.

The downstream water level is measured so far from the trench that it has been desirable to perform a back - water calculation in order to reduce the reach in the calculation. The back - water calculation is carried out with $C = 40 \text{ m}^{\frac{1}{2}} / \text{s}$ and the downstream boundary is hereafter at km. 941.200, were no significant changes in bed level is expected. A schematized variation of the water level is given in figure 4.1.3.

Sediment transport

The bed load is measured with a BTMA - sampler and the suspended load with a DF. During the period with constant discharge the total transport was approximately $S = 0.25 \times 10^{-4} \text{ m}^2 / \text{s}$ (large dispersion) from which around 15% was transported in suspension. As bed load is so dominating it is still possible to use bed - load transport formulas.

Bed Composition

Bed samples were taken regularly, but only the samples from before the dredged of the trench are evaluated, so no information about the vertical grain size distribution and the time dependent changes in composition is available. The geometrical mean diameter is estimated to $d_{50} = 0.6$ mm and the grain size distribution is well approximated to a log. - norm. distribution with $\sigma_g = 1.7$. These grain size characteristics are used in the computation as initial values of the transport and the Z₀ - layer composition.

4.1.2. The computational results

The computations are in all cases carried out with 3 predictor - corrector iterations, three iteration in the back - water calculation, $\theta = 0.70$ and a space step $\Delta x = 10$ m. The time step was $\Delta t = 3$ days, except in the calculations with the Engelund - Hansen formula during the period with the flood wave where stability problem forced to apply $\Delta t = 1.5$ days.

It was expected that the Engelund - Hansen formula would give the best result because both bed and suspended load was present. In figure 4.1.4 the predicted bed level and relative change in diameter in the transport layer ('rel d' = $d_{50} / 0.6$ mm) calculated with the Engelund - Hansen formula in a normalized form with 1 and 3 fraction is depicted.

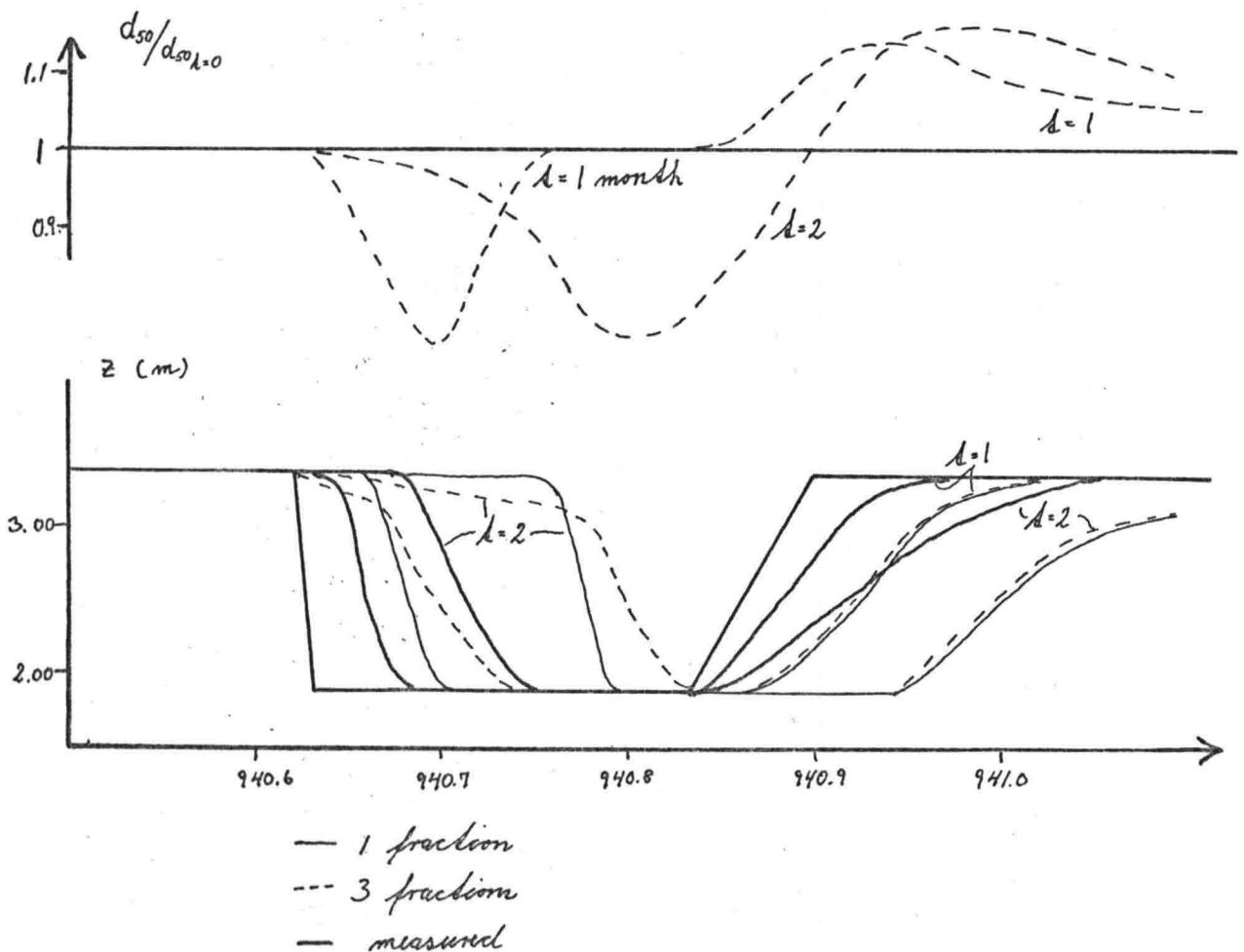


Figure 4.1.4. Calculation with Engelund - Hansen formula.

The trend is, independent of the number of fractions, that the formula gives far too much transport. The calculation with 3 fractions shows a more gradual sedimentation front because the sedimentated material has approximately the same composition as the sediment in transport (recall that the selective transport is independent of the shear stress, figure 2.2.6). Thus the sedimentated material is finer than the original bed material, and the transport - capacity is therefore larger. The opposite is the case for the erosion wave.

In figure 4.1.5 results from computations with the Meyer - Peter and Müller and the Engelund - Fredsoe bed load formulas are depicted.

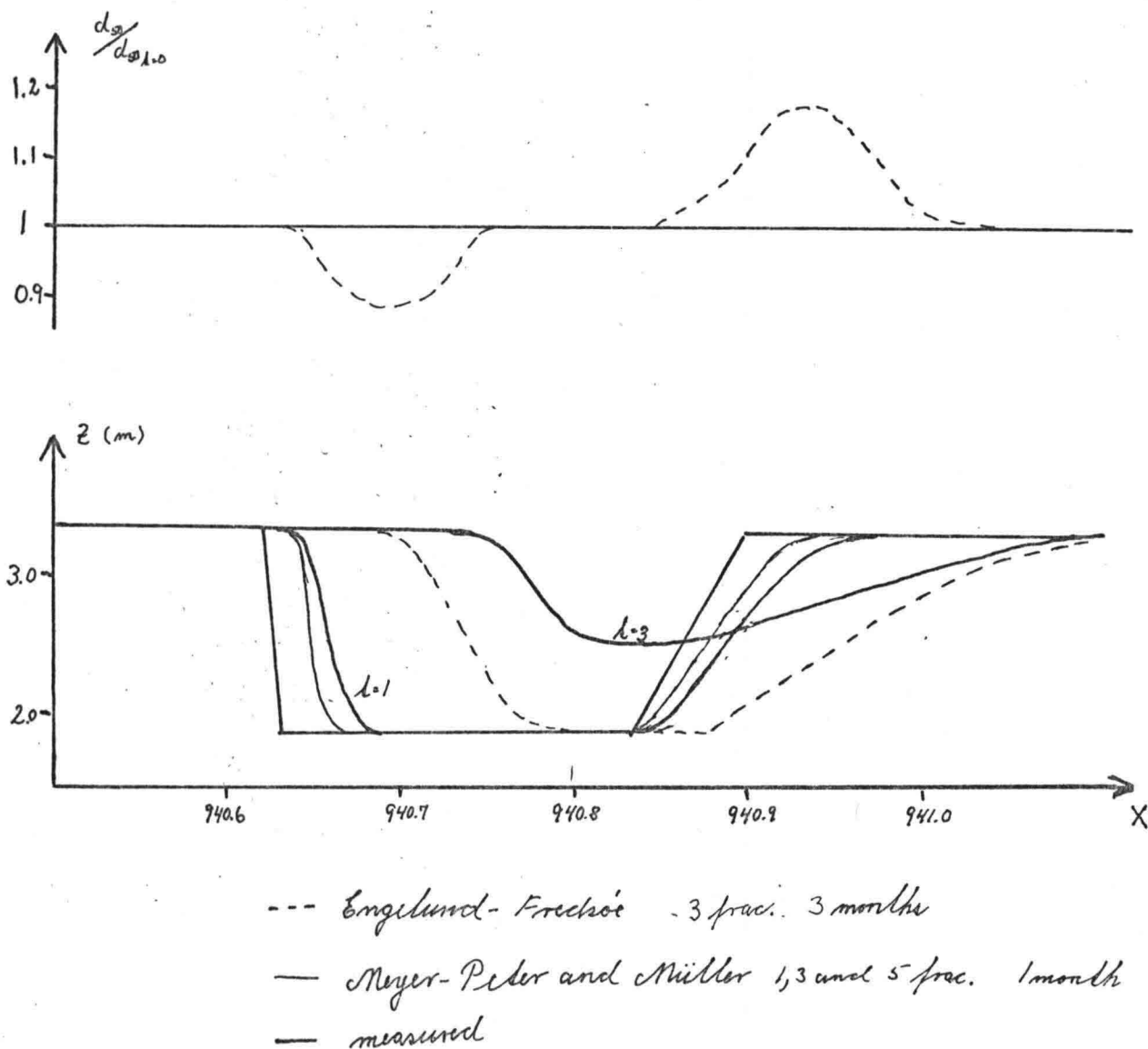


Figure 4.1.5. Calculations with bed - load formulas.

The calculation with these bed load formulas gives too little transport. The calculations with the Meyer - Peter and Müller formula with 1,3 and 5 fractions do not exhibit any noticeable difference in bed level, although the coarsest grain is immobile in the calculations with 3 and 5 fraction during the period with low discharge. The reason herefore is that the bed composition is only changed slightly.

The roughness predictor is applied in the calculation with the Engelund - Fredsoe transport formula. During the period with low discharge there is predicted a Chézy - coefficient $C = 77 \text{ m}^{\frac{1}{2}}/\text{s}$, thus the roughness is serious under estimated. The roughness prediction is performed in one of the areas where the modification of the method is applied. If the relation between the effective and total shear stress from the dune region (eq. 2.1.16) was used in stead of the modification it would have resulted in a roughness coefficient $C = 59 \text{ m}^{\frac{1}{2}}/\text{s}$. During the flood the roughness is calculated to $C = 40 \text{ m}^{\frac{1}{2}}/\text{s}$ which is in excellent agreement with the observed roughness coefficient.

The general trend in these examples is that the number of fractions in the calculations does not influence the computed bed level, and a model for uniform sediment would suite just as well. Only necessary information about bed composition changes could justify a calculation with the model for non - uniform sediment in preference of a model for uniform sediment.

A computation with a calibrated Meyer - Peter and Müller formula in a model for uniform sediment is performed as a part of the research project. This calculation did predict the position of the trench very well in the two first months, but then the agreement stops. The reason is maybe that there is supplied much sediment from the sides due to contraction of the flow during the period with the increased flow velocities (see figure 4.1.6)

4.1.3. Discussion

In the present case the gradation of the sediment has been too small or the shear stress too large to justify the application of the model for non - uniform sediment. Further more the calculations were carried out without considering the variation of the critical shear stress due to the

gradation (Egiazaroff's theory), which has resulted in an exaggeration of the changes in composition.

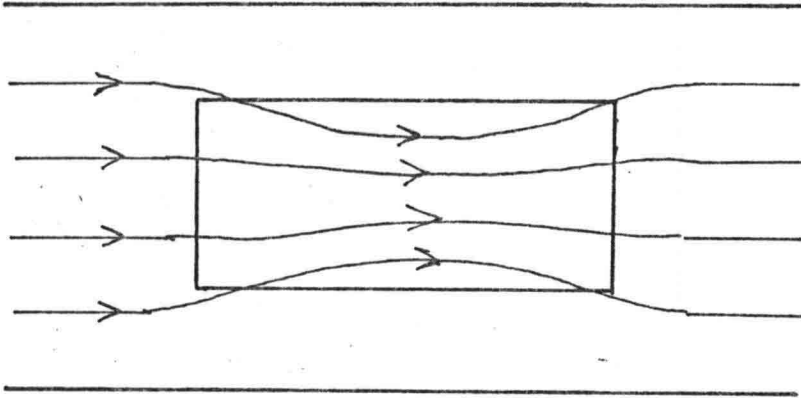


Figure 4.1.6. Contraction of flow.

The relative bad prediction of the bed level must entirely be attributed to the unreliability of the transport formulas, because the change of the bed composition has a negligible influence.

The roughness predictor did underestimate the roughness in case of low flow conditions, a trend which is amplified by the modification which has been applied to the roughness predictor. The bad prediction of the roughness is maybe because the bed and flow are not in equilibrium in the initial condition, i.e. bed form and slope belong to another flow situation.

4.2. Flume experiment with graded sediment

In 1972 Agostino carried out a series of experiments with graded sediment in a 30 m long and 0,5 m wide flume at the Laboratory of Fluid Mechanics Delft University of Technology.

The information which is used for the simulation of the experiment is obtained from disorderly notes Agostino made about the experiments. This has introduced some uncertainties in the boundary conditions which have been applied in the computations. There was no information about how the

bed composition is measured, but measurements from the equilibrium situations exhibit a large dispersion, which indicates that the bed samples are taken in a single point and not averaged over a dune.

The experiments were carried out with a mixture of two grain sizes with geometrical mean diameter respectively 1.00 mm and 1.75 mm. The initial condition for the here concerned experiment was the equilibrium situation from the previous experiment he had made. The downstream boundary conditions in that experiment was a water level $h = 0.28$ m above reference level, which resulted in a equilibrium water depth $a = 0.139$ m for the specific discharge $q = 0.09$ m²/s. The bed slope was $I = 0.0029$ which indicates a mean roughness coefficient $C_m = 40$ m^{1/2}/s. The sediment was supplied by a 1 m long sand elevator with the speed 0.86×10^{-5} m/s. The composition in the sand elevator were 60% fine and 40% coarse sediment, which resulted in 58.8% of the fine grains in the transport layer. The boundary conditions for the present experiment were (apparently) a raise of the downstream water level ($h = 0.30$ m) and a change of the composition in the sand elevator into 40% of the finer fraction.

4.2.1. The Computations

In order to apply a transport formula it is necessary to obtain the bed roughness coefficient, which has been done from the Einstein side-walls correction procedure (see chapter 2.1). The water temperature was around 20 C ($\nu = 1.01 \times 10^{-6}$ m²/s) and the Nikuradses grain roughness for the side-walls (concrete) has been estimated to $k_s = 1 \times 10^{-5}$ m. The calculated bed roughness coefficient $C_b = 33.2$ m^{1/2}/s has been kept constant during the computations.

It was considered important that the transport formula was giving the correct transport in the equilibrium situation, and the Meyer-Peter and Müller formula with Egiazaroff's theory was calibrated by means of a coefficient F_i before the effective shear stress

$$\Phi_i = 8 (F_i \mu \theta - \theta_c) \quad (4.2.1)$$

The calibration factors for both fractions appeared to be of approximately the same magnitude ($F_1 = 0.765$ and $F_2 = 0.856$). The calculation of the ripple factor is based on the diameter of the coarse fraction.

The computations are carried out with different transport layer thicknesses and both with ($\Delta x = 0.40$ m), and without ($\Delta x = 1.20$ m, $\Delta t = 2500$ s) sand elevator. In all cases there are used 3 predictor - corrector iterations, 3 iterations in the back - water calculation (with Einstein side - walls correction procedure) and $\theta = 0.7$. The calculated bed level and probability of fraction one are depicted in the figures 4.2.1 to 4.2.3.

From the figures it can be seen that there is occurring sedimentation simultaneous all over the flume, due to the increased downstream water level, and thus decreasing flow velocity in the flow direction. This almost parallel raise of the bed level is superposed by a low propagating sedimentation front caused by the change of composition. This front is not very significant because the transport capacity of the flow hardly is effected by the grain size. Further is it noticed that a very significant wave in composition is propagating in downstream direction.

The influence from the sand elevator can be seen from figure 4.2.1. As expected the sand elevator has only minor effect on the computational result. Before the sedimentation front there is a slightly lower bed level, because the sediment supply in the initial condition is decreased due to the coarser sediment in the elevator. This is only a local phenomena as the transport capacity of the flow is increasing fast when the bed level in the sand elevator raises. The steeper front in the composition wave can maybe be attributed to numerical effects, because the calculations with the sand elevator are carried out with smaller time and space step, thus less numerical diffusion.

In figure 4.2.2 and 4.2.3 the influence from the transport layer thickness on the propagation velocity of the wave are demonstrated. The general trend is that both the calculated bed level and probability of fraction one is lower than the measured values. It is difficult to recognize any front in the measured composition, but if the points in figure 4.2.2 for $X = 12$ m and $X = 15$ m are interpreted as a wave then the transport layer thickness equal 25% of the water depth seems to apply the best. In figure

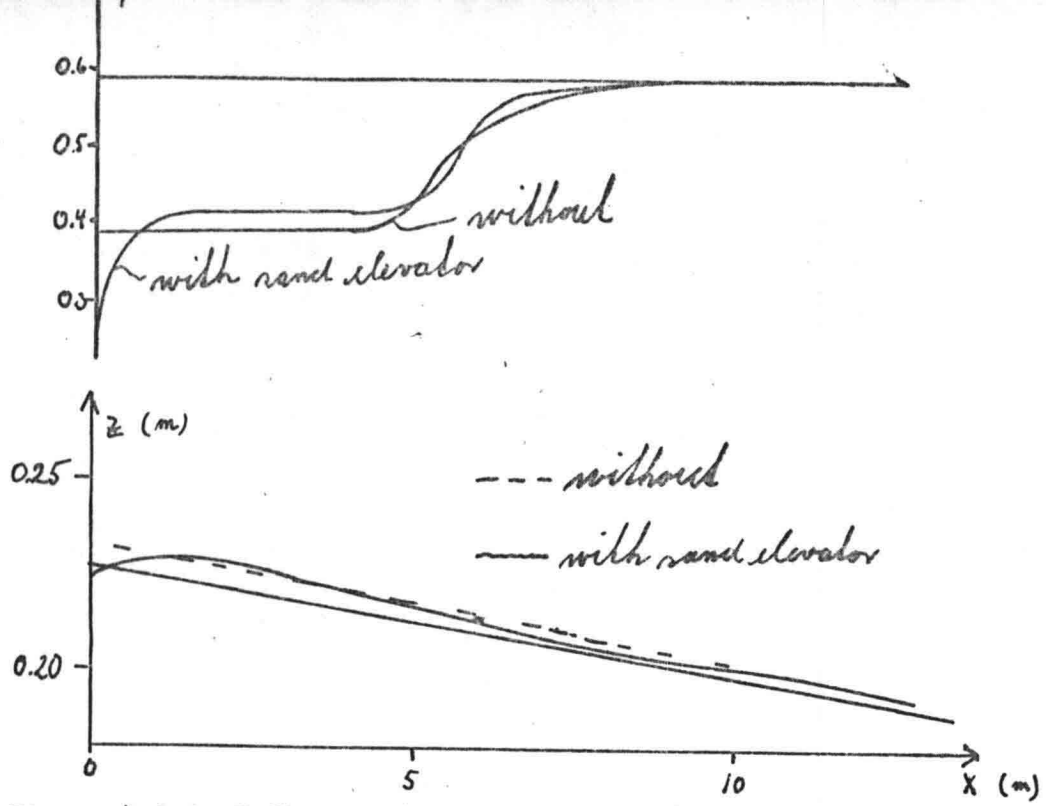


Figure 4.2.1. Influence from sand elevator, $T = 15.500$ s

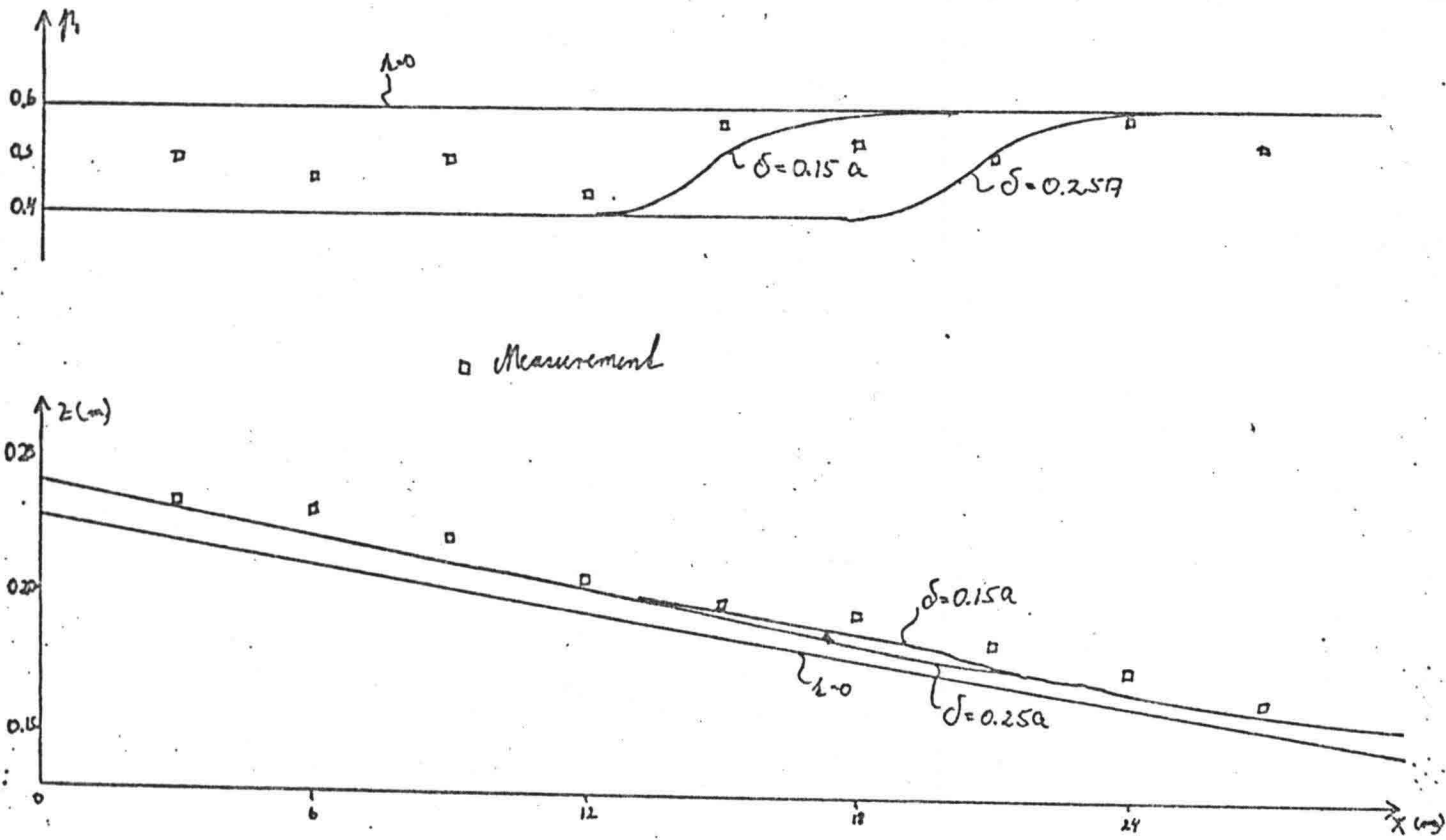


Figure 4.2.2. Bed level and composition after $T = 68.700$

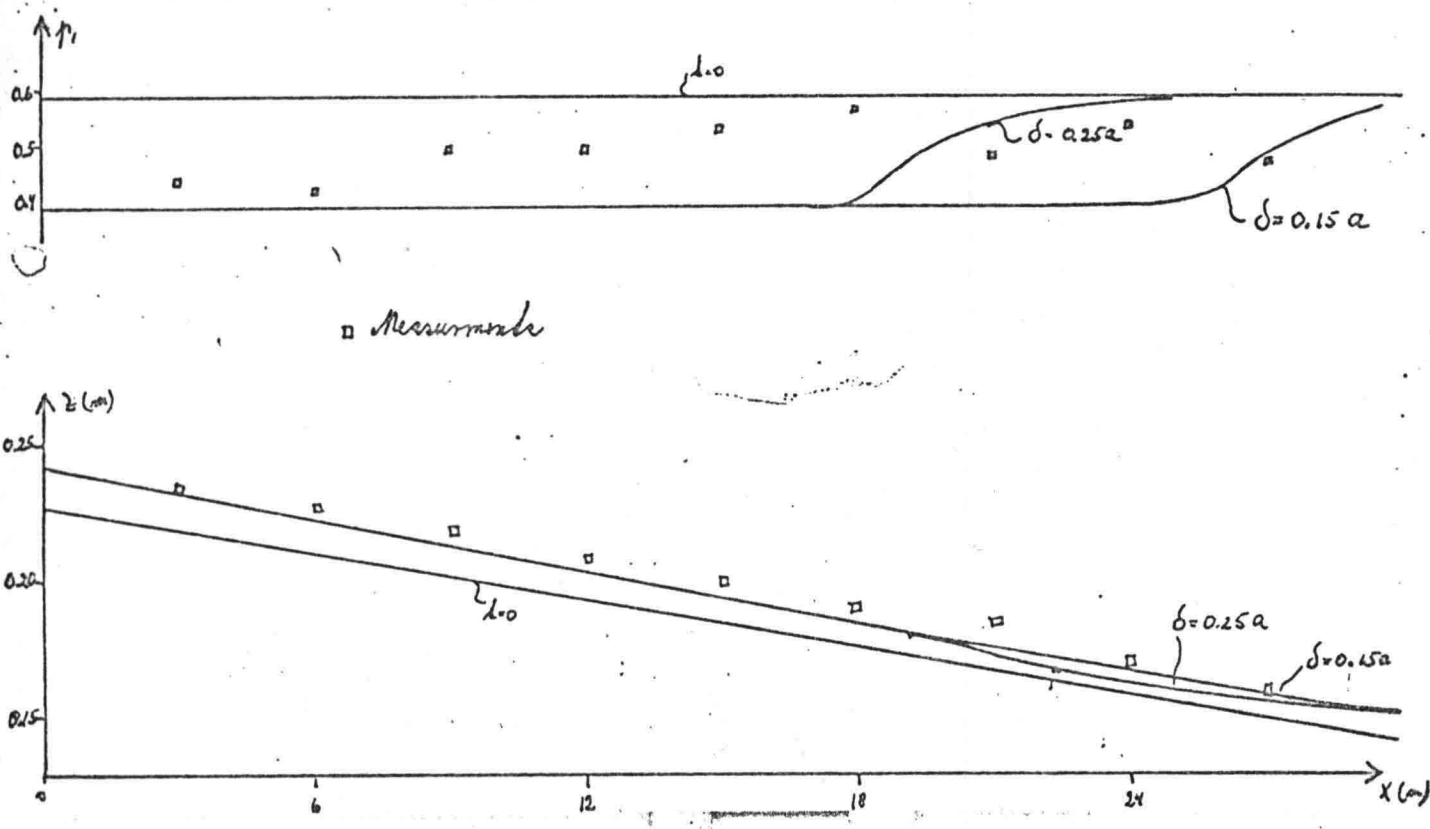


Figure 4.2.3. Bed level and composition after $T = 90.000 \text{ s}$

4.2.3 no front at all can be found in the measured values, only the trend that the composition becomes finer in down stream direction.

4.2.2. Discussion

The measurements in equilibrium indicates that the sediment in transport is only slightly finer than the sediment in the transport layer, and the same trend was expected in the upstream end of the flume after some time, but this does not seem to happen.

The explanation herefore may be that the samples of the bed are taken too deep, i.e. below the transport layer, where the coarse layer from the previous experiment is situated. The reason could also be that the model does not apply because the changes do occur too fast. If the migration velocity of a dune is estimated to the ratio between the total transport and the transport layer thickness ($0.25 \cdot a$), then one dune will approximately travel the length of the flume during the simulation period, thus the grain sorting depends on the dimensions of the individual dunes.

A cause of the disappointing result may for a deal be attributed to inflow phenomenas in the flume: the dunes need time to grow, the flow have to be tranquil etc.

With the large numbers uncertainties in the experimental conditions the model cannot be rejected on the basis of this experiment.

4.3. Sensitivity analysis

The largest applicability for a model for non-uniform sediment is for erosion processes in case of low shear stresses were selective transport takes place. No measurements from proto type or flume experiments were available, and therefore a sensitivity analysis is carried out, with the specific aim to demonstrate the influence of the transport layer thickness and the grain size characteristics on the development of the bed level.

Different transport layer thickness predictors and grain size distributions will be applied to a case where the upstream sediment supply is cut and only clear water is released into the river. In this case the upstream part of the bed level will erode gradually, until the bed forms vanish and the transport capacity of the river becomes zero. For these low shear stresses first of all the finer grains will be eroded and the coarser will remain, which results in a change of the grain size distribution in the transport layer, i.e. armoring.

The chosen examples concerns a reach of 5 km of an imaginary river, but it has been attempted to approximate a typical Dutch river regarding flow parameters. Only the grain size distribution has been changed in order to obtain different transport capacities. The characteristics of the case studied are as follows:

- Bed level gradient	$I = 6.26 \times 10^{-5}$
- Specific discharge	$q = 3.54 \text{ m}^2/\text{s}$
- Down stream water level	$h = 7.00 \text{ m}$
- Down stream bed level at $t = 0$	$z = 2.00 \text{ m}$
- Constant Chézy roughness	$C = 40 \text{ m}^{1/2}/\text{s}$
- Geometrical mean diameters	$d_{50} = 0.6 \text{ to } 1.2 \text{ mm}$
- Gradation	$\sigma_g = 1.64 \text{ to } 2.4 \text{ mm.}$

It is assumed that the grain size is logarithmic-normal distributed and no vertical gradient in the composition of the bed is present in the initial condition.

4.3.1. The computational results.

The Suzuki transport layer formula is applied with some modifications because stability problems and heavy secondary waves occurred when the formula was used in its proper form. It was estimated that the minimum transport layer thickness would be a few times the maximum grain size for (almost) zero transport, but it was in this case necessary to take

a minimum thickness equal 0.10 m in order to keep the computation time at a reasonable level. Still the celerities are very large, which was expected because the transport layer thickness appears in the denominator of the celerities, and large space steps have been applied in order to be able to use a reasonable time step.

The computational results are depicted in the figures 4.3.1 to 4.3.4. The relative diameter ('rel d') is the arithmetical mean diameter in the transport layer divided by the initial value. In table 4.3.1 the grain size diameter of the fractions characteristics as well as some of the numerical parameters in the computations are resumed. In all cases there have been applied 3 predictor - corrector iterations, 3 iterations in the back - water calculation and $\Theta = 0.70$. The number in the table refers to the tables in the figures

Figure	No.	$\Delta x(m)$	$\Delta t(months)$	No. fr.	$d_i(mm)$
4.3.1	1	200	2	1	0.6
	2	200	4	3	0.3, 0.6, 1.2
	3	200	4	3	same
	4	200	4	3	same
4.3.2	1	200	8	3	0.6, 1.2, 2.4
	2	800	1	3	same
	3	400	1	3	0.45, 0.9, 1.8
	4	400	1	3	same
4.3.3	1	800	1	1	0.9
	2	800	1	3	0.45, 0.9, 1.8

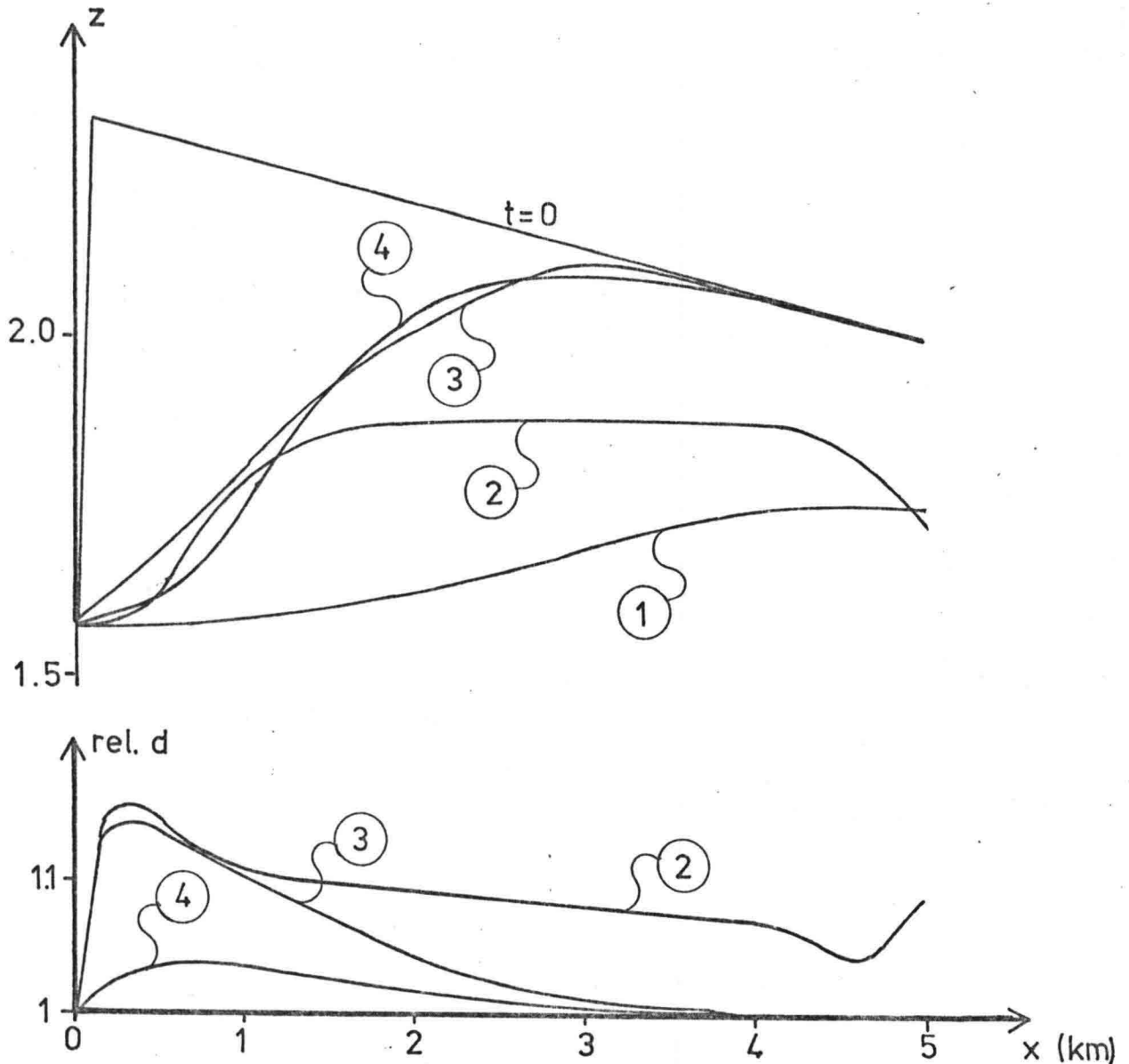
Figure	No.	Δx (m)	Δt (months)	No. fr.	d_i (mm)
	3	800	$\frac{1}{2}$	5	0.4, 0.6, 0.9, 1.35, 2.025
4.3.4	1	800	$\frac{1}{2}$	5	0.4, 0.6, 0.9, 1.35, 2.025
	2	800	1	5	same
	3	800	1	5	0.225, 0.45, 0.9, 1.8, 3.6

Table 4.3.1. Variable parameters in the computations.

In figure 4.3.1 a case where the upstream sediment supply is only reduced and the composition is kept the same as in the initial condition is depicted. In the calculations with the Engelund - Fredsoe transport formula the roughness predictor of Engelund (1967) is applied. The figure shows a considerable influence of the type of transport formula and illustrates that it is necessary to choose one transport formula in order to determine the influence of the transport layer thickness on the bed level. As Egiazaroff's theory is expected to give the right trend in the selective transport close to initiation of motion the theory will be applied and for simplicity together with the Meyer - Peter and Müller transport formula. In the figure the changes of bed composition is rather small and it is necessary to increase the mean diameter or the gradation in order to obtain significant changes.

The influence of relating the transport layer thickness to the transport rate appears clearly from figure 4.3.2. In this case no transport is released at the upstream boundary and the bed will erode until the transport capacity is zero. When the transport rate is decreasing the transport layer thickness calculated by the Suzuki method will decrease as well. The composition of the transport layer will change faster, and the transport capacity becomes zero for a remarkable higher bed levels compared with the calculation with the thick transport layer. The influence of the mean diameter is demonstrated, but the examples with $d_{50} = 1.2$ are

not so typical because already in the initial condition there is no transport of the coarsest fraction ($d = 2.4$ mm.).



- Situation after 6 years -

$\delta = 20\%$ of water depth

$d_{50} = 0.6$ mm $\sigma_g = 1.64$ mm

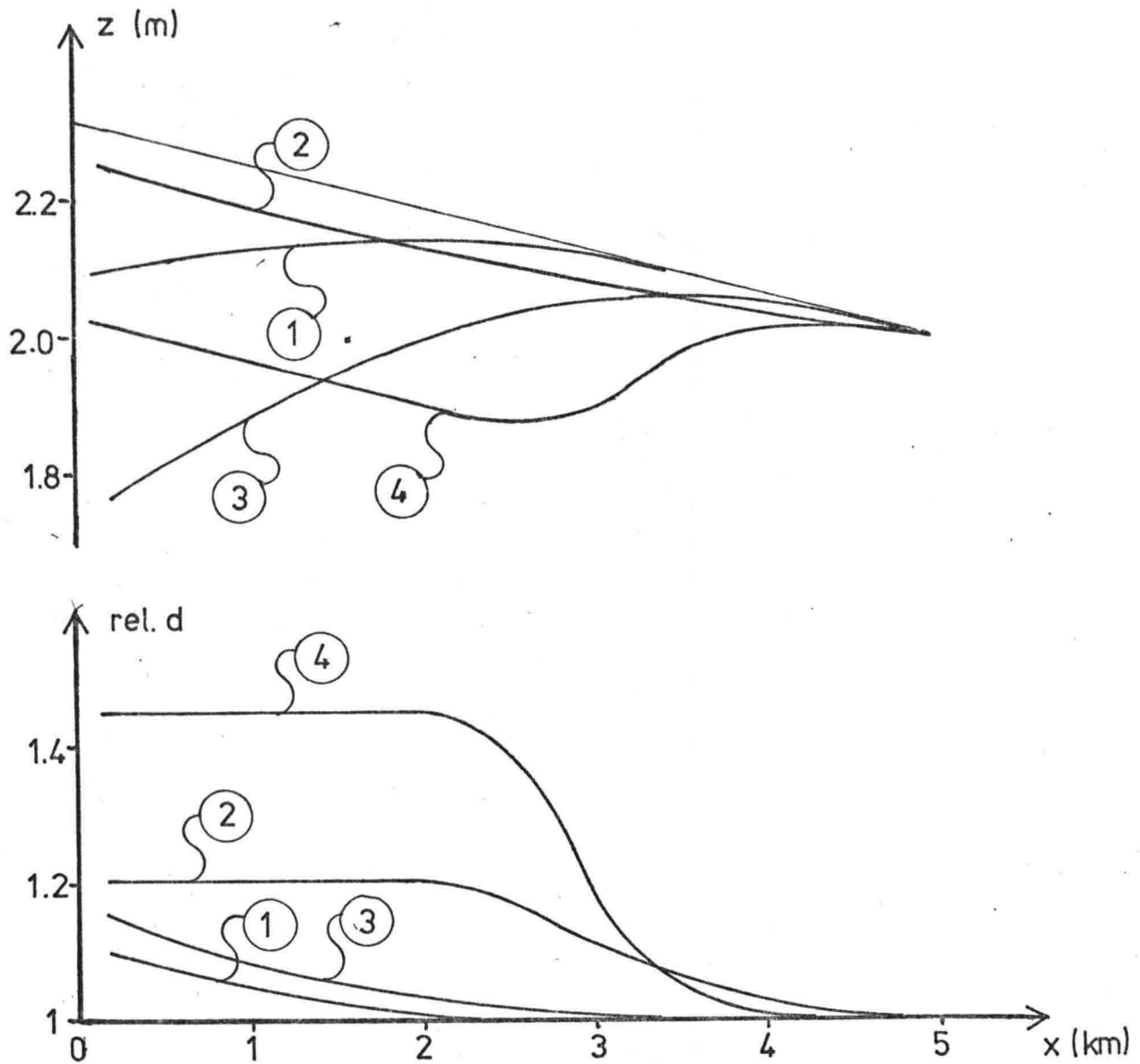
1. Engelund - Fredsoé , 1 fraction

2. Engelund - Fredsoé , 3 fractions

3. Meyer - Peter and Müller , 3 fractions

4. Meyer - Peter and Müller with Egiazaroff. th. , 3 fractions.

Figure 4.3.1. Influence from transport formula.



- Situation after 10 years -

Meyer - Peter and Müller with Egiazaroffs theory

$$\sigma_g = 1.64 \text{ mm} \quad 3 \text{ fractions}$$

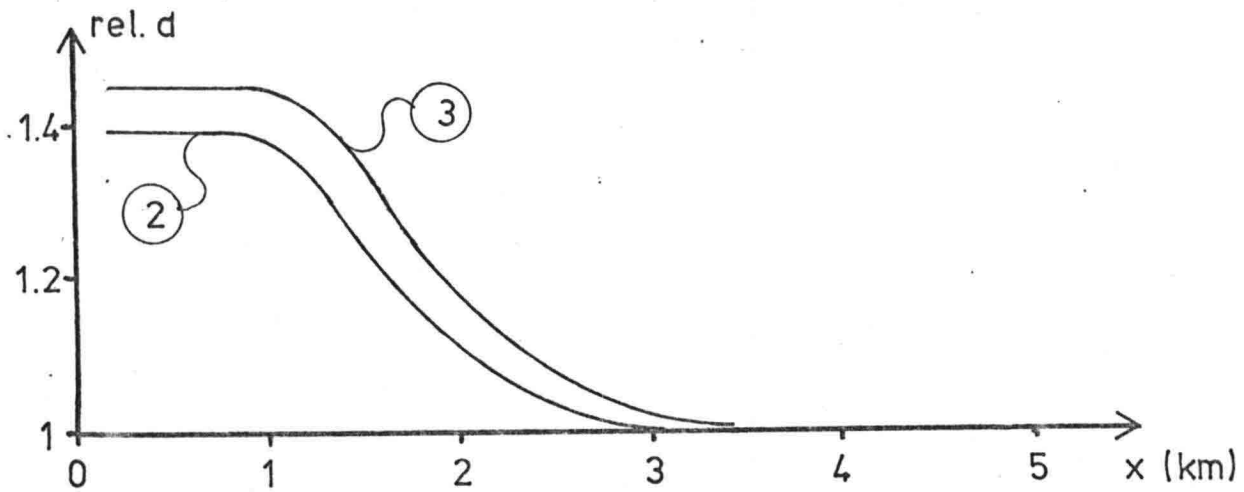
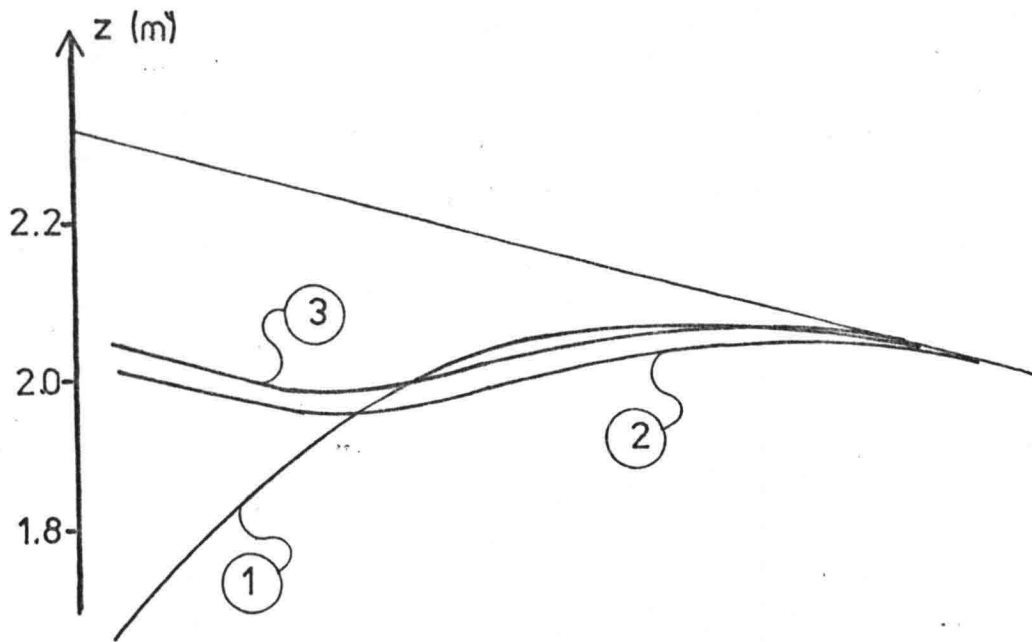
1. $\delta = 20\%$ of water depth, $d_{50} = 1.2 \text{ mm}$
2. δ by Suzuki $d_{50} = 1.2 \text{ mm}$
3. $\delta = 20\%$ of water depth, $d_{50} = 0.9 \text{ mm}$
4. δ by Suzuki, $d_{50} = 0.9 \text{ mm}$

Figure 4.3.2. Influence from transport layer thickness and mean diameter.

The trend outlined in figure 4.3.2 in the armoring of the bed does not change if the number of fractions considered in the computation are increased above the 3 fractions. In figure 4.3.3 the results from computation carried out with 1, 3 and 5 fractions are depicted. This graph demonstrates unmistakably the force of a model for non-uniform sediment as the predicted bed level from the calculations are distinctly different. Although all cases have the same gradation the computation with 5 fractions carried out with a larger maximum and smaller minimum diameter, shows a difference in calculated bed level which can probably be attributed to the following fact: the mobility of the coarsest fraction is smaller and the finest fraction is carried away faster, thus the armoring is occurring at an earlier stage. The reason that 3 fractions are sufficient to give a good qualitative picture is probably because the gradation is rather small.

The influence of the gradation on the bed level is studied in figure 4.3.4. It seems that the gradation has a considerable influence on the equilibrium situation. In the computation with $\sigma_g = 1.64$ and $\sigma_g = 1.75$ the same grain fractions are applied. The armoring occurs earlier for $\sigma_g = 1.75$ because there is more fine material available for transport and the grain size distribution changes faster. Some of the effects can be attributed to the representation of the grain size distribution in the calculations. In the example with large gradation Egiazaroff's theory provided a hiding effect as there was no transport of the finest fraction. Although the hiding effect probably is present in nature, it does not seem physically correct that there is no transport at all of the finest fraction.

It was attempted to calculate a few examples concerning erosion protection by means of supplying the coarse part of the initial transport at the upstream boundary. In the examples it was expected that the erosion would be followed by a slow propagating sedimentation front. However the model did not succeed to produce a stable solution for this case. The reason is maybe that the sedimentated material in the first grid point is not transported away because the critical shear stress increases, due to the coarser and less graded transport layer. The bed level in this point will



- Situation after 9 years -

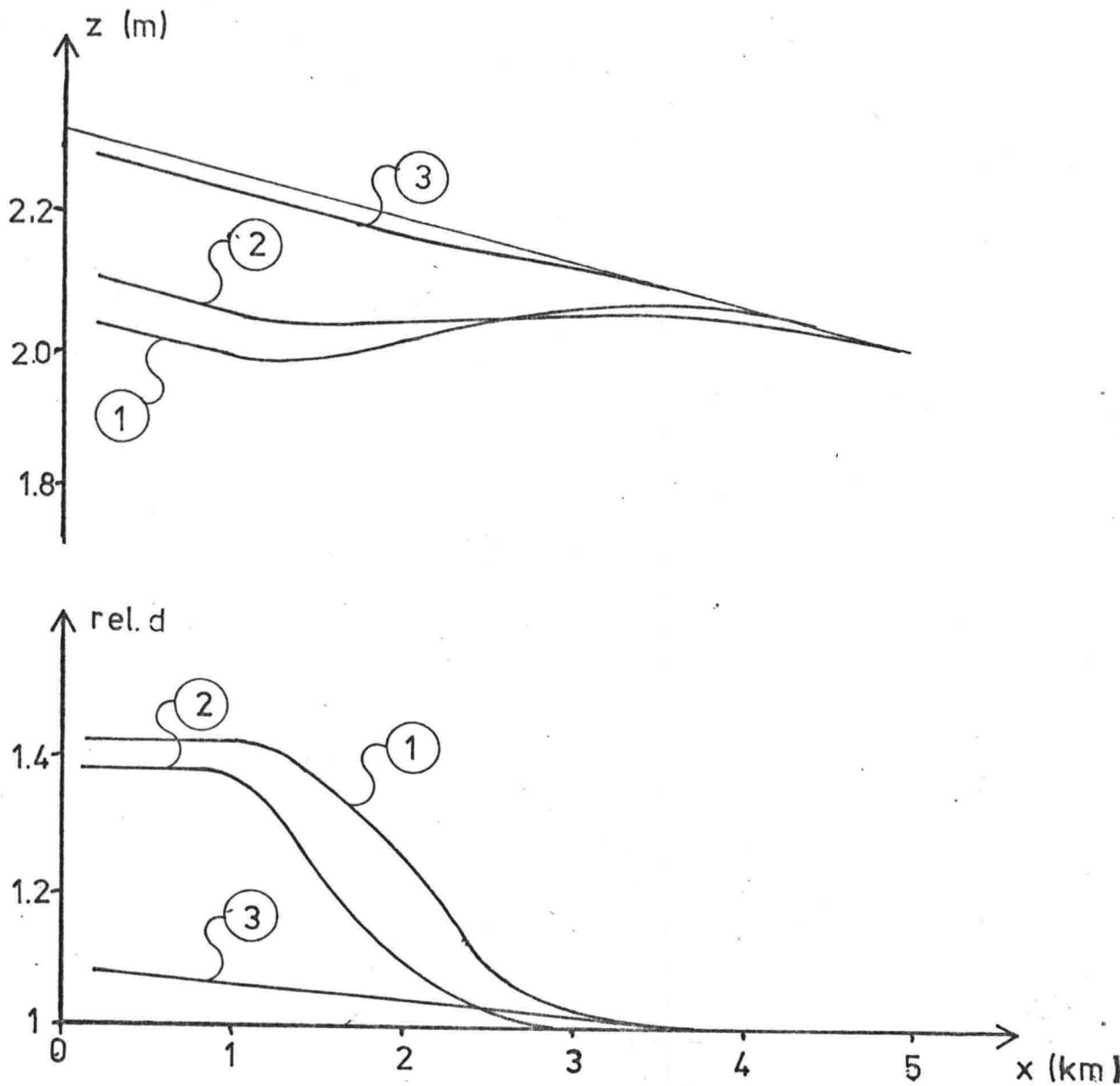
Meyer - Peter and Müller with Egiazaroff theory δ by Suzuki.

1. 1 fraction, $\sigma_g = 1$ mm

2. 3 fractions, $\sigma_g = 1.64$ mm

3. 5 fractions, $\sigma_g = 1.64$ mm

Figure 4.3.3. Influence of the number of fractions



- Situation after 9 years -

Meyer - Peter and Müller with Egazaroff's theory δ by Suzuki.

$$d_{50} = 0.9 \text{ mm}$$

5 fractions

$$1. \sigma_g = 1.64 \text{ mm}$$

$$2. \sigma_g = 1.75 \text{ mm}$$

$$3. \sigma_g = 2.40 \text{ mm}$$

Figure 4.3.4. Influence of the gradation.

therefore raise considerably until the transport finally starts which, according to figure 2.2.6, happens very sudden. This shock leads to secondary waves, which may have caused the instabilities.

4.3.2. Discussion

The calculated examples are not supposed to give a correct picture of the armoring process taking place in nature, because a lot of very important factors have been neglected. In this connection the stability of the armor layer, due to the fluctuating discharge and the variation of the roughness caused by the vanishing bed forms can be mentioned. Further more the calculations are carried out with a transport formula and a model for the critical shear stress which are not verified at all for the cases they have been applied to.

Observations from nature show that the armor layer has a thickness of a few times the maximum grain size and almost only consists of this coarsest grain. This trend is not found in the computational results which indicates that Egiazaroff's theory does not apply for cases with armoring.

However the examples demonstrated that the armoring occurs faster, and thus less erosion, if the transport layer thickness can be varied (Suzuki), for larger gradation, larger mean diameter and more fractions, a trend which seems to be physical reasonable. The examples also showed the necessity of using a model for non-uniform sediment for these cases.

Extensive measurements and experiments must be carried out and models for the sediment transport, transport layer thickness and critical shear stress must be developed for conditions very close to initiation of motion before reliable results concerning armoring can be obtained from a numerical model.

The computations have demonstrated some shortcomings of the numerical methods. The stability limit (figure 3.1.8) causes an inconvenient small time step, in these processes which are taking place over long time periods. Further more the secondary waves seem to have an unexpected large influence on the stability in the calculations.

5. Conclusions and suggestions for continuation

5.1 Conclusions

A flexible numerical model for morphological computations in rivers with graded sediment is designed. After a numerical analysis was carried out a predictor-corrector method was chosen in this model; it is providing a good accuracy for the hyperbolic problem with more celerities compared with the expected accuracy of a traditional explicit finite difference method.

However the numerical model does exhibit some shortcomings. When there is computed with relatively small courant numbers secondary waves becomes very annoying. Furthermore the computational effort that has to be contributed is inconveniently large when computations are carried out close to the threshold of motion, when the difference in magnitude of the characteristic directions is big. In this extreme case even small secondary waves seem to cause instabilities.

The mathematical model is not fully developed; especially in case of erosion of relatively fine sediment, the model cannot account for exchange of sediment between the transport layer and the passive layer. Further there is still uncertainty about the proper definition of some of the variables in the model (e.g. transport layer thickness).

The application of the model for non-uniform sediment is especially justified close to the threshold of motion. No significant difference in the predicted bed level appears, whether the calculations are carried out with one or more fractions in cases where the characteristic directions are of the same magnitude, i.e. when the shear stresses are far from the critical value.

The necessity of a model for non-uniform sediment is demonstrated in examples where the upstream sediment supply is cut and the bed level erodes until the transport capacity vanishes. The

influence of applying different transport layer thicknesses and grain size characteristics and the development of an amor layer is investigated and a physical reasonable trend is obtained when the transport layer thickness is related to the transport rate (Suzuki).

The model cannot be expected to give reliable results in cases when very fast changes takes place because the development of grain size characteristics will then depend on the dimensions of the individual dunes.

The unreliability of the component parts of the model and the shortcoming in the formulation of the model makes it necessary to carry out an extensive sensitivity analysis when the model is applied for practical problems.

5.1 Suggestions for continuation

The usefulness of the computational model can be improved by applying a solution method which has better numerical characteristics concerning stability and secondary waves. A predictor-corrector method with other finite difference methods may fulfill these demands. The alternative to apply an implicit scheme does not seem so attractive because the required computation time will be enormous.

As the computational tool for the model for non-uniform sediment is available it would be desirable to verify the model with experiments and if necessary to modify the model.

The very pronounced effect the development of an amor layer has on the bed level makes it desirable to develop reliable models for the sediment transport rate and for the transport layer-thickness close to the threshold of motion.

In order to avoid the elliptical character of the model and the belonging unstable solutions attention should be paid to the phenomenon of exchange of sediment between the transport-layer and the underlying passive layer.

- Contents:
- A 1. Linearization of model for uniform sediment.
 - A 2. Celerities in model for non-uniform sediment in case of two fractions.
 - A 3. Modified Equations for the predictor - corrector method.
 - A 4. Complex propagation factor, damping factor and relative propagation velocity for the predictor - corrector method.

A 1. Linearisation of model for uniform sediment.

The model for uniform sediment is given by the following partial differential equations

$$\frac{\partial Z}{\partial t} + f_u \frac{\partial U}{\partial X} = 0 \quad (\text{A 1.1})$$

$$U \frac{\partial U}{\partial X} + g \frac{\partial a}{\partial X} + g \frac{\partial Z}{\partial X} + g \frac{U^2}{C^2 a} = 0 \quad (\text{A 1.2})$$

$$\frac{\partial a \cdot U}{\partial X} = 0 \quad (\text{A 1.3})$$

in which $f_u = \frac{\partial f(U)}{\partial U}$, $S = f(U)$

The variables is considered to consists of a varying part (Z' , a' and U') and a constant part (Z_0 , a_0 , and U_0). Applying this princip to the partial differential equations and neglecting products term of second order ($a_0 \gg a'$, etc.) eq. A 1.3 becomes

$$U_0 a' + a_0 U' = 0 \quad \text{or} \quad a' = - \frac{a_0}{U_0} U' \quad (\text{A 1.4})$$

Applying the princip to eq. A 1.2 leads to:

$$\begin{aligned} U_0 \frac{\partial U'}{\partial X} + g \frac{\partial a'}{\partial X} + g \frac{\partial Z'}{\partial X} + g \frac{(U_0 + U')^2}{C^2 (a_0 + a')} &\approx \\ U_0 \frac{\partial U'}{\partial X} + g \frac{\partial a'}{\partial X} + g \frac{\partial Z'}{\partial X} + g \frac{U_0^2 + 2U'U_0}{C^2 a_0} \left(1 - \frac{a'}{a_0}\right) &\approx \\ U_0 \frac{\partial U'}{\partial X} + g \frac{\partial a'}{\partial X} + g \frac{\partial Z'}{\partial X} + g \frac{U_0}{C^2 a_0} (U_0 + 2U' - U_0 \frac{a'}{a_0}) &= 0 \end{aligned} \quad (\text{A 1.5})$$

By combining with eq. A 1.4, multiplying with f_{u_0} and differentiating with respect to X the following expression occurs

$$f_{u_0} \left(U_0 - g \frac{a_0}{U_0} \right) \frac{\partial^2 U'}{\partial X^2} + g \frac{\partial^2 Z'}{\partial X^2} + 3g f_{u_0} \frac{U_0}{C^2 a_0} \frac{\partial Z'}{\partial X} = 0 \quad (\text{A 1.6})$$

Eq. A 1.1 gives

$$f_{u_0} \frac{\partial U'}{\partial X} = - \frac{\partial Z'}{\partial t} \quad (\text{A 1.7})$$

and differentiated with X

$$f_{u_0} \frac{\partial^2 U'}{\partial X^2} = - \frac{\partial^2 Z'}{\partial X \partial t} \quad (\text{A 1.8})$$

Inserting eqs. A 1.7 and 8 in eq A 1.6 gives the linearised equation

$$- \left(U_0 - g \frac{a_0}{U_0} \right) \frac{\partial^2 Z'}{\partial X \partial t} + g f_{u_0} \frac{\partial^2 Z'}{\partial X^2} - 3g \frac{U_0}{C^2 a_0} \frac{\partial Z'}{\partial t} = 0 \quad (\text{A 1.9})$$

which can be written as

$$\frac{\partial Z'}{\partial t} - D \frac{\partial^2 Z'}{\partial X^2} - \frac{D}{C} \frac{\partial^2 Z'}{\partial X \partial t} = 0 \quad (\text{A 1.10})$$

where $D = \frac{U_0 f_{u_0}}{3I_0}$ (I_0 is the equilibrium bed slope)

and $C = U_0 \frac{f_{u_0}}{a_0 (1 - F^2)}$

A 2. Celerities in model for non-uniform sediment in case of two fractions

In case of two fractions and a constant specific discharge the model for non-uniform sediment can be reduced to

$$\frac{\partial S_1}{\partial x} + \delta \frac{\partial P_1}{\partial t} + \bar{p}_{1z_0} \frac{\partial Z}{\partial t} + P_1 \frac{\partial \delta}{\partial t} = 0 \quad (\text{A 2.1})$$

$$\frac{\partial S_2}{\partial x} - \delta \frac{\partial P_1}{\partial t} + \bar{p}_{2z_0} \frac{\partial Z}{\partial t} - P_1 \frac{\partial \delta}{\partial t} = 0 \quad (\text{A 2.2})$$

$$S_i = f_i (U, p_i, \dots) \quad (\text{A 2.3})$$

$$S_2 = f_2(U, p_1, \dots) \quad (\text{A 2.4})$$

$$\delta = (a, U) \quad (\text{A 2.5})$$

$$G \frac{\partial U}{\partial x} + g \frac{\partial Z}{\partial x} = R \quad (\text{A 2.6})$$

$$\frac{\partial aU}{\partial x} = \frac{\partial aU}{\partial t} = 0 \quad (\text{A 2.7})$$

S_1 can be eliminated from the model by substituting A 2.3 and 4 in respectively A 2.1 and 2, which leads to

$$f_{1u} \frac{\partial U}{\partial x} + f_{1p_1} \frac{\partial p_1}{\partial x} + \delta \frac{\partial p_1}{\partial t} + \bar{p}_{1z_0} \frac{\partial Z}{\partial t} + P_1 \frac{\partial \delta}{\partial t} = 0 \quad (\text{A 2.8})$$

$$f_{2u} \frac{\partial U}{\partial x} + f_{2p_1} \frac{\partial p_1}{\partial x} - \delta \frac{\partial p_1}{\partial t} + \bar{p}_{2z_0} \frac{\partial Z}{\partial t} - P_1 \frac{\partial \delta}{\partial t} = 0 \quad (\text{A 2.9})$$

where $f_{1u} = \frac{\partial f_1}{\partial U}$, $f_{1p_1} = \frac{\partial f_1}{\partial p_1}$ etc.

By applying eq. A 2.5 and that the specific discharge is constant, the time derivative of the transport layer thickness becomes

$$\frac{\partial \delta}{\partial t} = (\delta_u - \frac{a}{U} \delta_a) \frac{\partial U}{\partial t} \quad (\text{A 2.10})$$

where $\delta_u = \frac{\partial \delta}{\partial U}$ and $\delta_a = \frac{\partial \delta}{\partial a}$.

Equation A 2.10 inserted in eqs. A 2.8 and 9 forms, together with eq. A 2.6 and the total differential for the remaining dependent variable, a system of linear equations in the six partial derivatives. In matrix form the system yields (see eq. A 2.11)

The characteristic directions are propagation velocities for infinitesimal disturbances in the variables. Consequently the characteristic directions are the values of c for which the determinant of the matrix is vanishing.

$$\begin{vmatrix}
 \bar{p}_{1z_0} & 0 & \delta & f_{1p_1} & P_1(\delta_u - \frac{a}{u}\delta_a) & f_{1u} \\
 \bar{p}_{2z_0} & 0 & -\delta & f_{2p_1} & -P_1(\delta_u - \frac{a}{u}\delta_a) & f_{2u} \\
 0 & g & 0 & 0 & 0 & G \\
 1 & c & 0 & 0 & 0 & 0 \\
 0 & 0 & 1 & c & 0 & 0 \\
 0 & 0 & 0 & 0 & 1 & c
 \end{vmatrix}
 \begin{vmatrix}
 \partial Z / \partial t \\
 \partial Z / \partial x \\
 \partial p_1 / \partial t \\
 \partial p_1 / \partial x \\
 \partial U / \partial t \\
 \partial U / \partial x
 \end{vmatrix}
 =
 \begin{vmatrix}
 0 \\
 0 \\
 R \\
 dZ / dt \\
 dp_1 / dt \\
 dU / dt
 \end{vmatrix}
 \quad (A 2.11)$$

in which $c = \frac{dx}{dt}$

This leads to a quadratic equation in c , because the celerities belonging to the flow has a infinite speed

$$\begin{aligned}
 & -c^2 G \\
 & + c \left\{ g(\delta_u - \frac{a}{u}\delta_a) P_1 (f_{1p_1} + f_{2p_1}) - G(\bar{p}_{1z_0} f_{2p_1} - \bar{p}_{2z_0} f_{1p_1}) - \right. \\
 & \left. g(f_{1u} + f_{2u}) \right\} - \left\{ g(f_{2p_1} f_{1u} - f_{1p_1} f_{2u}) \right\} = 0 \quad (A 2.12)
 \end{aligned}$$

The quadratic equation can be written in a simplified form by introducing the following dimensionless properties

$$\phi = \frac{c}{U}$$

$$\psi_i = \frac{f_{iu}}{a}$$

$$A = \frac{\bar{p}_{2z_0} f_{1p_1} - \bar{p}_{1z_0} f_{2p_1}}{\delta U}$$

$$B = \frac{\psi_1 + \psi_2}{1 - F^2}$$

$$C = \frac{\Psi_1 f_{1p_i} - \Psi_2 f_{1p_i}}{U \delta (1 - F^2)}$$

$$D = -P_i \frac{f_{1p_i} + f_{2p_i}}{U} \frac{(\frac{u}{a} \delta u - \delta a)}{1 - F^2}$$

and recalling

$$G = U - \frac{ga}{U} = \frac{ga}{U} (F^2 - 1)$$

The quadratic equation can now be written as

$$\phi^2 - (A + B + D)\phi + C = 0 \quad (\text{A } 2.13)$$

A 3. Modified equations for the predictor - corrector methods

For the predictor - corrector method, with the Lax scheme ($\alpha = 0$) as predictor and the Crank - Nicholson scheme as corrector, the difference equations yield

$$P: \frac{z_j^* - z_j^n}{\Delta t} + C \frac{z_{j+1}^n - z_{j-1}^n}{2\Delta x} = 0 \quad (\text{A } 3.1)$$

$$C: \frac{z_j^{n+1} - z_j^n}{\Delta t} + C \left\{ \theta \frac{z_{j+1}^* - z_{j-1}^*}{2\Delta x} + (1 - \theta) \frac{z_{j+1}^n - z_{j-1}^n}{2\Delta x} \right\} = 0 \quad (\text{A } 3.2)$$

where * denotes predicted value.

The predicted value can be found from eq. A 3.1

$$z_j^* = z_j^n - C\Delta t \frac{z_{j+1}^n - z_{j-1}^n}{2\Delta x} \quad (\text{A } 3.3)$$

Applying eq. A 3.3 and a Taylor series the second term in eq. A 3.2 becomes

$$\frac{z_{j+1}^* - z_{j-1}^*}{2\Delta x} = \frac{z_{j+1}^n - z_{j-1}^n}{2\Delta x} - C\Delta t \frac{z_{j+2}^n - 2z_j^n + z_{j-2}^n}{(2\Delta x)^2}$$

$$= \frac{\partial Z}{\partial x} + \frac{1}{6} \Delta x^2 \frac{\partial^2 Z}{\partial x^2} + \dots - C \Delta t \left(\frac{\partial^2 Z}{\partial x^2} + \frac{\Delta x^2}{3} \frac{\partial^4 Z}{\partial x^4} + \dots \right) \quad (\text{A 3.4})$$

The remaining differences in eq. A 3.2 is the same as for the Crank - Nicholson scheme eqs. 3.1.6. The modified equation appears by summing the Taylor series for the differences

$$\frac{\partial Z}{\partial t} + C \frac{\partial Z}{\partial x} - \frac{1}{2} \frac{\Delta x^2}{\Delta t} \sigma^2 (2\theta - 1) \frac{\partial^2 Z}{\partial x^2} - \frac{1}{6} \frac{\Delta x^3}{\Delta t} (\sigma^3 - \sigma) \frac{\partial^3 Z}{\partial x^3} + \dots = 0 \quad (\text{A 3.5})$$

There is two possibilities for the predictor (upstream) - corrector (four points) method, because the predicted values can be applied in two ways in the four points scheme. The difference equations becomes

$$P: \frac{Z_j^* - Z_j^n}{\Delta t} + C \frac{Z_j^n - Z_{j-1}^n}{\Delta x} = 0 \quad (\text{A 3.6})$$

$$C: \frac{1}{2} \left\{ \frac{Z_{j+1}^* - Z_{j+1}^n}{\Delta t} + \frac{Z_j^{n+1} - Z_j^n}{\Delta t} \right\} + C \left\{ \theta \frac{Z_{j+1}^* - Z_j^*}{\Delta x} + (1-\theta) \right.$$

$$\left. \frac{Z_{j+1}^n - Z_j^n}{\Delta x} \right\} = 0 \quad (\text{A 3.7})$$

or

$$C: \frac{1}{2} \left\{ \frac{Z_{j+1}^{n+1} - Z_{j+1}^n}{\Delta t} + \frac{Z_j^* - Z_j^n}{\Delta t} \right\} + C \left\{ \theta \frac{Z_{j+1}^* - Z_j^*}{\Delta x} + (1-\theta) \frac{Z_{j+1}^n - Z_j^n}{\Delta x} \right\} = 0$$

$$(\text{A 3.8})$$

It seems more for the hand laying to apply eq. A 3.8 as corrector, because the calculation is then going in the direction of the characteristic, but it can be shown that they give almost the same modified equation.

The predicted value is found from eq. A 3.6 and inserted in eq. A 3.8. After multiplying with two the following differences appear

$$\frac{Z_j^{n+1} - Z_j^n}{\Delta t} = \frac{\partial Z}{\partial t} + \frac{1}{2} \Delta t \frac{\partial^2 Z}{\partial t^2} + \frac{1}{6} \Delta t^2 \frac{\partial^3 Z}{\partial t^3} + \dots$$

$$= \frac{\partial Z}{\partial t} + \frac{1}{2} \frac{\Delta x^2}{\Delta t} \sigma^2 \frac{\partial^2 Z}{\partial x^2} - \frac{1}{6} \frac{\Delta x^3}{\Delta t} \sigma^3 \frac{\partial^3 Z}{\partial x^3} + \dots \quad (\text{A 3.9})$$

$$3C \frac{Z_j^n - Z_{j-1}^n}{\Delta x} = 3C \left(\frac{\partial Z}{\partial x} - \frac{1}{2} \Delta x \frac{\partial^2 Z}{\partial x^2} + \frac{1}{6} \Delta x^2 \frac{\partial^3 Z}{\partial x^3} + \dots \right) \quad (\text{A 3.10})$$

$$-2C \frac{Z_j^n - Z_{j-2}^n}{2\Delta x} = -2C \left(\frac{\partial Z}{\partial x} - \Delta x \frac{\partial^2 Z}{\partial x^2} + \frac{2}{3} \Delta x^2 \frac{\partial^3 Z}{\partial x^3} + \dots \right) \quad (\text{A 3.11})$$

$$\begin{aligned} -2\theta\sigma C \frac{Z_j^n - 2Z_{j-1}^n + Z_{j-2}^n}{\Delta x} &= -4\theta\sigma C \left(\frac{Z_j^n - Z_{j-1}^n}{\Delta x} - \frac{Z_{j-1}^n - Z_{j-2}^n}{2\Delta x} \right) \\ &= -4\theta\sigma C \left(\frac{1}{2} \Delta x \frac{\partial^2 Z}{\partial x^2} - \frac{1}{2} \Delta x^2 \frac{\partial^3 Z}{\partial x^3} + \dots \right) \end{aligned} \quad (\text{A 3.12})$$

By summing the Taylor series for the differences the modified equation appears

$$\begin{aligned} \frac{\partial Z}{\partial t} + C \frac{\partial Z}{\partial x} - \frac{1}{2} \frac{\Delta x^2}{\Delta t} \{ (4\theta - 1)\sigma^2 - \sigma \} \frac{\partial^2 Z}{\partial x^2} \\ - \frac{1}{6} \frac{\Delta x^3}{\Delta t} \left(\sigma^3 - \frac{1}{3}\theta\sigma^2 - \sigma \right) \frac{\partial^3 Z}{\partial x^3} + \dots \end{aligned} \quad (\text{A 3.13})$$

If instead eq. A 3.7 is applied as corrector the modified equation becomes

$$\begin{aligned} \frac{\partial Z}{\partial t} + C \frac{\partial Z}{\partial x} - \frac{1}{2} \frac{\Delta x^2}{\Delta t} \{ (4\theta - 1)\sigma^2 - \sigma \} \frac{\partial^2 Z}{\partial x^2} \\ - \frac{1}{6} \frac{\Delta x^3}{\Delta t} (\sigma^3 - \sigma) \frac{\partial^3 Z}{\partial x^3} + \dots \end{aligned} \quad (\text{A 3.14})$$

i.e. only differing on the coefficient for the third derivative.

The second derivative provides numerical diffusion, and it is seen that the diffusion coefficient becomes negative for

$$0 < \sigma < \frac{1}{4\theta - 1} \quad (\text{A 3.15})$$

which means that the scheme is unstable for the $\epsilon_{3\theta}$ value of the Courant number.

A 4. Complex propagation factor for the predictor - corrector method.

The difference schemes for the predictor - corrector method is given by

$$P: \frac{Z_j^* - Z_j^n}{\Delta t} + C \frac{Z_{j+1}^n - Z_{j-1}^n}{2\Delta x} = 0 \quad (A 4.1)$$

$$C: \frac{Z_j^{n+1} - Z_j^n}{\Delta t} + C \left\{ \theta \frac{Z_{j+1}^* - Z_{j-1}^*}{2\Delta x} + (1-\theta) \frac{Z_{j+1}^n - Z_{j-1}^n}{2\Delta x} \right\} = 0 \quad (A 4.2)$$

By isolating Z_j^* in eq. A 4.1 and divide by Z_j^n the complex propagation factor for the first iteration (prediction) appears

$$\rho_1 = \frac{Z_j^*}{Z_j^n} = 1 - \sigma \frac{Z_{j+1}^n - Z_{j-1}^n}{2 Z_j^n} \quad (A 4.3)$$

Recalling the presupposed form of the numerical solution

$$Z_j^n = \rho^n \exp i j \xi \quad (A 4.4)$$

which inserted in eq. A 4.3 gives

$$\rho_1 = 1 - \sigma \frac{e^{i\xi} - e^{-i\xi}}{2} = 1 - i \sigma \sin \xi \quad (A 4.5)$$

Applying the same procedure the complex propagation factor for the second iteration (correction) can be found

$$\begin{aligned} \rho_2 &= 1 - \sigma \left\{ \theta \rho_1 i \sin \xi + (1-\theta) i \sin \xi \right\} \\ &= 1 - \theta \sigma^2 \sin^2 \xi - i \sigma \sin \xi \end{aligned} \quad (A 4.6)$$

The following expression for the complex propagation factor may apply

$$\rho_L = 1 + \sum_{k=1}^L (-i)^k \theta^{k-1} \sigma^k \sin^k \xi \quad (A 4.7)$$

where L is the number of iterations.

The applicability of eq. A 4.7 can be demonstrated. As it apply for 1 and 2 iterations the requirement is that it apply for L+1 iterations as well:

$$\begin{aligned}
 \rho_{L+1} &= 1 - \sigma \left\{ \theta \rho_L i \sin \xi + (1-\theta) i \sin \xi \right\} \\
 &= 1 - \left\{ 1 - \sum_{k=1}^L (-i)^k \theta^{L-k} \sigma^k \sin^k \xi \right\} i \sigma \theta \sin \xi + \sigma (1-\theta) i \sin \xi \\
 &= 1 + (-i) \sigma \theta \sin \xi \sum_{k=1}^L \left\{ (-i)^k \theta^{L-k} \sigma^k \sin^k \xi \right\} = \\
 &1 + \sum_{k=1}^{L+1} (-1)^k \theta^{L-k} \sigma^k \sin^k \xi \tag{A 4.8}
 \end{aligned}$$

The damping factor per wave periode can be found for $\xi \ll \frac{\pi}{2}$ by applying a Taylor series to the absolute value of the complex propagation factor

$$\begin{aligned}
 d_1 &= |\rho_1|^{nt} = (1 + \sigma^2 \sin^2 \xi)^{\frac{\pi}{\sigma \xi}} \\
 &\approx (1 + \sigma^2 \xi^2)^{\frac{\pi}{\sigma \xi}} \approx 1 + \pi \sigma \xi \tag{A 4.9}
 \end{aligned}$$

For $L \geq 2$ the damping factor becomes as for the Crank - Nicholson scheme

$$\begin{aligned}
 d_2 &= |\rho_2|^{nt} = \left[(1 - \theta \sigma^2 \sin^2 \xi)^2 + \sigma^2 \sin^2 \xi \right]^{\frac{\pi}{\sigma \xi}} \\
 &\approx \left[1 - (2\theta - 1) \sigma^2 \left(\xi - \frac{\xi^3}{6} \right)^2 \right]^{\frac{\pi}{\sigma \xi}} \approx 1 - (2\theta - 1) \pi \sigma \xi \tag{A 4.10}
 \end{aligned}$$

The relative propagation velocity for 1 iteration if for $\xi \ll \frac{\pi}{2}$:

$$\begin{aligned}
 c_{\pi_1} &= -(\sigma \xi)^{-1} \text{Arctan}(-\sigma \sin \xi) \\
 &\approx -(\sigma \xi)^{-1} \left[-\sigma \left(\xi - \frac{\xi^3}{6} + \dots \right) + \frac{\sigma^3}{3} \left(\xi - \frac{\xi^3}{6} + \dots \right)^3 \right] \\
 &1 - \frac{\xi^2}{2} (1 + 2\sigma^2) \tag{A 4.11}
 \end{aligned}$$

For two iterations the relative propagation factor yields

$$\begin{aligned}
 C_{\pi_2} &= -(\sigma \xi)^{-1} \operatorname{Arctan} \left(\frac{-\sigma \sin \xi}{1 - \theta \sigma^2 \sin^2 \xi} \right) \\
 &\approx -(\sigma \xi)^{-1} \left[\frac{-\sigma \left(\xi - \frac{\xi^3}{6} + \dots \right)}{1 - \theta \sigma^2 \left(\xi^2 + \dots \right)} + \frac{\sigma^3}{3} \left(\frac{\xi + \dots}{1 - \theta \sigma^2 \xi^2 + \dots} \right)^3 \right] \\
 &\approx 1 - \frac{1}{6} \xi^2 [1 + \sigma^2 (2\theta - 1)] \quad (\text{A 4.12})
 \end{aligned}$$

For three and more iterations the relative propagation factor becomes, as for the Crank - Nicolson scheme

$$\begin{aligned}
 C_{\pi_3} &= -(\sigma \xi)^{-1} \operatorname{Arctan} \frac{-\sigma \sin \xi (1 - \theta^2 \sigma^2 \sin^2 \xi)}{1 - \theta \sigma^2 \sin^2 \xi} \\
 &= -(\sigma \xi)^{-1} \left[\frac{-\sigma \left(\xi - \frac{\xi^3}{6} \right) (1 - \theta^2 \sigma^2 \xi^2)}{1 - \theta \sigma^2 \xi^2} \right. \\
 &\quad \left. + \frac{\sigma^3 \xi^3}{3} \left(\frac{1 - \theta^2 \sigma^2 \xi^2}{1 - \theta \sigma^2 \xi^2} \right) \right] \\
 &\approx 1 - \frac{1}{6} \xi^2 [1 + 2\sigma^2 (1 - 3\theta + 3\theta^2)] \quad (\text{A 4.13})
 \end{aligned}$$

Model for non-uniform sediment

- Users Guide -

- contents:
1. General remarks
 2. The structure of the programme
 3. The function of the programme
 4. Input
 5. Output

1. General remarks

The programme, which is in the language FORTRAN, is developed by Kim Wium Olesen at The Delft University of Technology at the department for Fluid Mechanics in 1980 - 1981.

2. The structure of the programme

The programme consists of a main programme (MAIN) and ten subroutines. MAIN is primarily reading the input data, controlling the flow in the calculation and calling subroutines.

3. The function of the programme

The programme is used to simulate the time dependent morphological changes in alluvial stream with non-uniform sediment from knowledge about the initial situation and the variation of the boundary conditions.

The calculation is based on the following input data:

- a. Model parameters
- b. Parameters describing the initial condition (bed level, depth averaged composition in transport layer and in the z_s - layer and the Chezy - roughness as a function of the space coordinate.
- c. Parameters describing the boundary conditions (down - stream water level, upstream sand input per fraction or sand lift velocity and the specific discharge) as a function of time.

The programme is integrating step - wise forward in time with the predictor - corrector method for a finitedifference scheme. For each time step the programme is calculating the

- a. Flow velocity
- b. Sediment transport for each fraction
- c. The transport layer thickness
- d. New bed level
- e. New composition of bed

The major part of the input data is written out in the head of the output and in the list of the initial condition ($T = 0$). This list must always be checked because the programme does not control the input data.

4. Input

The programme and the input data have to be supplied with suitable job control cards depending on the system the programme is ran at.

The input data have to start with a job control card followed by

- a. three cards with model parameters
- b. cards with parameters describing the initial situation
- c. cards for the boundary conditions

and at last another job control card.

Before calculation can be performed the dimension statement in MAIN (1 90 - 120) has to be corrected:

substituted * with the number of fractions (see documentation MAIN). Further the wished transport formula (SFUN), transport layer thickness (DELFUN) and the back - water calculation with or without side walls correction (BAWA) must be checked and if necessary changed into the wanted subroutine.

a. Model Parameters

Card 1: DELTAX, DELTAT, JDIM, TETA

DELTAX: (real) space step (m)

The choice of a space step depends on which wavelengths that are important for the purpose of the calculation. If the sand lift is used as boundary condition then see coments for Card 18. Attention to the fact that the calculation time is increasing proportional to $(DELTAX)^{-2}$.

DELTAT: (real) time step (s)

No stringent criterion for chosing the proper time step can be given. Experience with the model is of large use.

The following procedure can be applied for a first guess for the time step.

Estimate the maximum total transport S_{\max} and calculate $C = 5 \frac{S_{\max}}{q_{\max}}$ ('celerity' for Engeland - Hansen formula) and Courant number equal unity gives

$$\text{DELTAT} = \text{DELTAT} / C$$

Here after a small part of the total region (saving calculation time) in which large changes in bed level or composition is expected, must be tested with time steps in the neighbourhood of the first guess, until the largest time step giving sufficient accuracy is found.

JDIM: (integer) The number of grid points (-)

JDIM = L / DELTAX + 1, where L is the length of the region.

TETA: (real) Weight (-)

The weight is influencing the numerical diffusion in the model, thus also the accuracy. TETA = 0.5 gives the most accurate result, but there will be much secondary waves in the solution. TETA = 0.70 is in many cases a good choice. TETA > 0.50 for stability.

Card 2: IT 1, IT 2

IT 1: (integer) number of iterations in back-water calculation (-).

IT 1 equal an odd number gives the best accuracy. In case of relative small flow velocity gradients IT 1 = 1 gives a sufficient good accuracy. IT 1 = 3 gives an excellent result.

IT 2: (integer) number of predictor - corrector iterations (-).

IT 2 = 2 is minimum for stability, but for more than one fraction IT 2 = 3 (or more) is recommended.

Card 3: TMAX, EPS 1, EPS 2, TOP, FAC

TMAX: (real) maximum time (s).

If last output is required at a certain time T then

$TMAX = T - DELTAT.$

EPS 1: (real) stop criterion for bed level (m).

EPS 1 is the minimum change in bed level between two time steps for continuing calculation. See FAC.

EPS 2: (real) stop criterion for composition (-).

EPS 2 is the minimum change in a probability of a fraction in the transport layer. See FAC.

TOP: (real) time between output (s).

Output costs a lot in calculation time.

FAC: (real) factor for calling subroutine BIG (-).

If calculation have to be performed until equilibrium is reached, the subroutine BIG (see documentation) is called after time = $FAC \cdot TMAX$. If $FAC > 1$ BIG will not be call.

b. Initial condition

Card 4: IDIM

IDIM: (integer) number of fractions I(-).

Card 5a: D(1)

Card 5b: D(2)

Card 5x: D(I)

D(i): (real) characteristic grain diameter of fraction i (m).

Card 6: x 1, x 2

x 1, x 2: (real) break points (m).

If x 1 and x 2 are equal zero the probability of each

fraction, both in the transport layer and in the z_0 -layer and the Chezy-roughness is constant all over the region and the bed level has a constant slope. If x_1 or x_2 is not equal zero the composition, roughness and bed slope is varying over the region and more input data is required.

IF $x_1 = 0$ AND $x_2 = 0$

Card 7a: p 1

Card 7b: p 2

Card 7x: p I

p i: (real) probability of fraction i all over in the transport layer (-).

Card 8a: p1z0

Card 8x: pIz0

p1z0: (real) depth averaged probability of fraction i in the z_0 -layer (-).

Card 9: C

C: (real) the Chézy-coefficient ($m^{1/2}/s$).

Card 10: SLOPE, YO

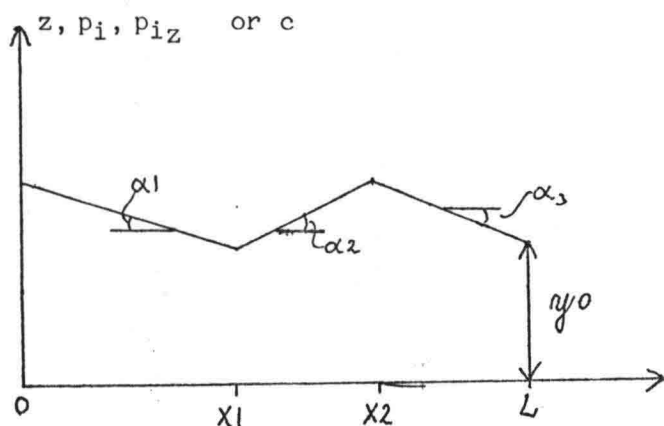
SLOPE: (real) bed slope (-).

Y0: (real) downstream bed level (m).

Note: the maximum bed level must not exceed 100m without changing in format statement 130 in subroutine WRITE.

IF x1 \neq 0 or x2 \neq 0

The variation in the initial situation is calculated in the subroutine BED. In the present version the variation is in linear steps and x1 and x2 are break points. If x1 = 0 or x2 = L respectively α_1 and α_3 can be chosen arbitrarily. See figure.



where $\alpha_1 > 0$, $\alpha_2 < 0$ and $\alpha_3 > 0$

Card 7a: $\alpha_{11}, \alpha_{21}, \alpha_{31}, \gamma_{01}$

Card 7b: $\alpha_{12}, \alpha_{22}, \alpha_{32}, \gamma_{02}$

Card 7x: $\alpha_{1x}, \alpha_{2x}, \alpha_{3x}, \gamma_{0x}$

$\alpha_{ij}, \alpha_{ji}, \gamma_{0i}$: (real) parameters for calculating the probability of fraction i in the transport layer as a function of the space coordinate.

Note: $\sum_{k=1}^I \gamma_{0k} = 1$ and $\sum_{k=1}^I \alpha_{jk} = 0$ for $j=1,2,3$

Card 8a: $\alpha_{11}, \alpha_{21}, \alpha_{31}, \gamma_{01}$

Card 8x: $\alpha_{1I}, \alpha_{2I}, \alpha_{3I}, \gamma_{0I}$

$\alpha_{1i}, \alpha_{2i}, \alpha_{3i}, \gamma_{0i}$ (real) parameters for calculating the probability of fraction i in the z_i -layer.

Card 9: $\alpha_1, \alpha_2, \alpha_3, \gamma_0$

$\alpha_1, \alpha_2, \alpha_3, \gamma_0$: (real) parameters for the Chezy coefficient.

Card 10: $\alpha_1, \alpha_2, \alpha_3, \gamma_0$

$\alpha_1, \alpha_2, \alpha_3, \gamma_0$: (real) parameters for the bed level. Note: the maximum bed level must not exceed 100m without changing in formal statement 130 in subroutine. WRITE

Card 11: DELACC

DELACC: (real) thickness of coarse layer (m).

DELACC \neq 0 only in case of erosion.

If no coarse layer DELACC = 0, and the cards 12 a - 12 x must be canceled.

IF DELACC \neq 0

Card 12a: DELTAP (1)

Card 12b: DELTAP (2)

Card 12x: DELTAP (I)

DELTAP (i): (real) probability in coarse layer (-).

The composition in the coarse layer is given by

$P_{iz} + \text{DELTAP}(i)$. Note: $\sum_{i=1}^I \text{DELTAP}(i) = 0$

c. Boundary Conditions

Card 13: IYPEH

IYPEH: (integer) parameter choosing the type of variation of the downstream water level. With present version of subroutine BOUND.

- = 1 constant
- = 2 sinusiodal
- = 3 linear steps

IF IYPEH = 1

Card 14: H

H : (real) time independent downstream water level (m).

IF IYPEH 1

Card 14: HPARM (1), HPARM (2),.....HPARM (6)

HPARM: (real array, dimension 6) parameters for calculating the time dependent value of the down stream water level. See documentation for subroutine BOUND.

Card 15: IYPEQ

I TYPE Q: (integer) Specific discharge else as for I TYPEH

IF ITYPEQ = 1

Card 16: Q

Q: (real) time independent specific discharge (m^2/s).

IF ITYPEQ = 1

Card 16: QPARAM (1), QPARAM (2),.....QPARAM (I)

QPARAM: (real array, dimension 6) see HPARAM.

Card 17: ITYPES

ITYPES: (integer) Parameters choosing the type of variation of the sand input per fraction at the upstream boundary

- = 1 constant
- = 2 sinusiodal
- = 3 linear steps
- = 4 sand lift.

IF ITYPES = 1

Card 18: SO 1 (1), SO 1 (2),.....SO 1 (I)

SO 1: (real array, dimension IDIM). Array containing the time independent sand input of each fraction including popes at upstream boundary (m^2/s).

IF ITYPES = 2 OR ITYPES = 3

Card 18a: SPARM (1,1), SPARM (1,2).....SPARM (1,6)

Card 18b: SPARM (2,1), SPARM (2,2).....SPARM (2,6)

Card 18c: SPARM (I,1), SPARM (I,2).....SPARM (I,6)

SPARM: (real - 2 - array, dimension IDIM, 6) SPARM (i,1).....
SPARM (i,6) is the parameters for calculating the time dependent variation of sand input of fraction i at upstream boundary. See subroutine BOUND.

IF ITYPE = 4

Card 18: TEMP (1), TEMP (2).....TEMP (6), XLIFT

TEMP: (real array, dimension 6) parameters for calculating the time dependent sand lift velocity. The variation is of the type 3 -linear steps (line 1820 in MAIN).

XLIFT: (real) The length of the sand lift (m). The space step must be chosen so the sand lift is ending right in between to grid points, i.e. XLIFT / DELTAX = $1\frac{1}{2}$, $2\frac{1}{2}$ etc.

5. Output

In the head of the output the name of the applied transport formula and transport layer thickness formula followed by the model parameters, the grain diameters, the thickness of the coasse layer and eventually 'DEL-TAP' are printed. Last in the head the type of and the parameters for the variation of the boundary conditions are written out. This first part of the output is performed by subroutine HEAD.

Her after a list and a plot of the calculated values at time = 0, 1 · TOP, 2 · TOP.....TMAX + DELTAT follows. These outputs start with the time and the present boundary conditions. Next a table is printed: in first column the space coordinate (x) followed by the z₀-level (z₀), the transport layer thickness (DEL), bed level (z), water depth (A), flow velocity (U) and transport per fraction included pore volume (Si). In table two the space coordinate (x), the arithmical mean grain diameter, the proba-

bility of the fractions in the transport layer (P_i) and in the z_0 - layer (p_{zoi}) is written out.

The tables are followed by two over view plots with at the left side of the plots a list of the space coordinates. The first plot shows from right to left the water level (H), the bed level (z), the z_0 - level (D) and if there is a coarse layer an indication of the bottom of the coarse layer (o). The plot is provided with a specification of the scale of the plot. The second plot outlines the composition of the transport layer ($= 1,2..$) indicates the cumulative probability of fraction \dot{c} in the transport z_0 - layer. The scale is one + equal 1% (see example on output)

The plots are only suitable for a survey because they can only solve the half of the scale, i.e. an accuracy on a half percent in the second plot.

The output at the different time levels are performed by subroutine WRITE.

 * TIME= 0.0 S *

DISCHARGE= 0.0000 M2/S
 WATERLEVEL DOWNSTREAM= 0.6940 M
 SAND LIFT VELOCITY=0.9000E-05 M/S

X (M)	Z0 (M)	QAL (M)	Z (M)	A (M)	Q (M3/S)	S1 (M2/S)	S2 (M2/S)	CHEZY
0.0	0.4632	0.0388	0.5020	0.1940	0.4124	0.2631E-06	0.5664E-06	0.3510E+02
0.40	0.4628	0.0388	0.5016	0.1940	0.4124	0.2631E-06	0.5670E-06	0.3510E+02
0.80	0.4624	0.0389	0.5012	0.1940	0.4124	0.2631E-06	0.5671E-06	0.3510E+02
1.20	0.4620	0.0388	0.5008	0.1940	0.4124	0.2647E-05	0.7452E-06	0.3510E+02
1.60	0.4616	0.0388	0.5004	0.1940	0.4124	0.2647E-05	0.7452E-06	0.3510E+02
2.00	0.4612	0.0388	0.5000	0.1940	0.4124	0.2647E-05	0.7453E-06	0.3510E+02

X (M)	P1 (MM)	P2	PZ01	PZ02
0.0	1.1880	0.2000	0.8000	0.8000
0.40	1.1880	0.2000	0.8000	0.8000
0.80	1.1880	0.2000	0.8000	0.8000
1.20	0.9075	0.7500	0.2500	0.5000
1.60	0.9075	0.7500	0.2500	0.5000
2.00	0.9075	0.7500	0.2500	0.5000

SCALE= 100 *ZM

X (M)	0	1	2	3	4	5	6	7	8	9	0
0.0	*										
0.40	*										
0.80	*										
1.20	*										
1.60	*										
2.00	*										

X (M)	0	1	2	3	4	5	6	7	8	9	0
0.0	*										
0.40	*										
0.80	*										
1.20	*										
1.60	*										
2.00	*										

Example on output

Documentation and list of programme for non-uniform sediment.

Contents: MAIN
 WRITE
 HEAD
 INTEG
 SFUN
 DELFUN
 BOUND
 BED
 BIG
 BAWA
 SUM
 PRCO
 PSTAR

M A I N

1. Purpose

Calculate morphological changes in alluvial streams.

2. Usage

See Users Guide.

3. Description of parameters

(only the most important parameters not appearing in the Users Guide will be mentioned.)

P1, P2 (real-2-array) : composition of transport layer at respectively old and new time level. First index is the number of fractions, second is the space coordinate.

PZ01, PZ02 (real-2-array) : composition of z_0 -layer at old and new time level.

S1, S2 (real-2-array) : transport per fraction.

SSUM1, SSUM2 (real array) : sum of transport per fraction.

Z1, Z2 (real array) : bed level.

DELTA 1, DELTA 2 (real array) : transport layer thickness.

U (real array) : flow velocity

Z00 (real array) : position of coarse layer.

S01, S02 (real array) : boundary condition, transport per fraction.

SOSUM1, SOSUM2 (real) : sum of transport per fraction at upstream boundary.

D (real array) : grain diameters.

C (real array) : Chézy roughness coefficients.

IN, JN (alfa-array) : name of respectively transport formula and transport layer - thickness formula.

T (real) : time.

TT (real) : print time.

TC (real) : time plus delta t.

4. Procedure required

None.

5. Method

See flow charts, Users Guide and documentation for subroutines.

6. Remark

* in DIMENSION statement 190 - 120 is the number of fractions, which must be substituted.

```
00010 C
00020 C
00030 C
00040 C
00050 C
00060 C
00070 C
00080 C
00090 C
00100 C
00110 C
00120 C
00130 C
00140 C
00150 C
00160 C
00170 C1
00180 C1
00190 C1
00200 C2
00210 C
00220 C
00230 C2
00240 C3
00250 C3
00260 C3
00270 C4
00280 C4
00290 C4
00300 C5
00310 C
00320 C
00330 100
00340 C5
00350 C7
00360 C
00370 C
00380 C71
00390 C71
00400 C71
00410 C
00420 C73
00430 C73
00440 C
00450 C
00460 C
00470 C
00480 C
00490 200
00500 300
00510 C73
00520 C74
00530 C
00540 C
00550 C
00560 C
00570 C
00580 400
00590 500
00600 C74
00610 C741
00620 C
00630 C
00640 C741
00650 C75
00660 C
00670 C
00680 C
00690 C75

*****
* MAIN PROGRAM FOR NON UNIFORM SEDIMENT *
*****

**801028.01.KWD**

DIMENSION P1(*,101),P2(*,101),PZ01(*,101),PZ02(*,101),
&
S1(*,101),S2(*,101),SSUM1(101),SSUM2(101),
&
Z1(101),Z2(101),DELTA1(101),DELTA2(101),U(101),
&
Z00(101),S01(7),S02(7),D(7),SPARM(*,6),C(101),
&
HPARM(6),QPARM(6),TEMP(6),DELTAP(7),IN(8),JN(8)

*****
READ INPUT DATA

SPACE-, TIME-STEP, LENGTH OF FLUME (JDIM) AND WEIGHT
READ (5,*) DELTAX, DELTAT, JDIM, TETA

NUMBER OF ITERATIONS IN BACK WATER (IT1)
PREDICTOR-COR. (IT2)
READ (5,*) IT1, IT2

STOP CRITERION: TMAX, EPS1, EPS2, TIME BETWEEN OUTPUT AND FAC
READ (5,*) TMAX, EPS1, EPS2, TOP, FAC

NUMBER OF FRACTION
READ (5,*) IDIM

DIAMETERS
DO 100 I1=1, IDIM
  READ (5,*) D(I1)
100 CONTINUE

INITIAL CONDITIONS

BRAEK POINTS
READ (5,*) X1, X2

IF ((X1 .EQ. 0) .AND. (X2 .EQ. 0)) GO TO 550
COMPLICATED!
TRANSPORT LAYER COMPOSITION
DO 300 I2=1, IDIM
  READ (5,*) ALFA1, ALFA2, ALFA3, Y0
  CALL BED(ALFA1, ALFA2, ALFA3, X1, X2, Z1, JDIM, DELTAX, Y0)
  DO 200 I3=1, JDIM
    P1(I2, I3)=Z1(I3)
  200 CONTINUE
300 CONTINUE

BED COMPOSITION
DO 500 I4=1, IDIM
  READ (5,*) ALFA1, ALFA2, ALFA3, Y0
  CALL BED(ALFA1, ALFA2, ALFA3, X1, X2, Z1, JDIM, DELTAX, Y0)
  DO 400 I5=1, JDIM
    PZ01(I4, I5)=Z1(I5)
  400 CONTINUE
500 CONTINUE

CHEZY-COEFFICIENT
READ (5,*) ALFA1, ALFA2, ALFA3, Y0
CALL BED(ALFA1, ALFA2, ALFA3, X1, X2, C, JDIM, DELTAX, Y0)

BED LEVEL
READ (5,*) ALFA1, ALFA2, ALFA3, Y0
CALL BED(ALFA1, ALFA2, ALFA3, X1, X2, Z1, JDIM, DELTAX, Y0)
GO TO 1050
```

```

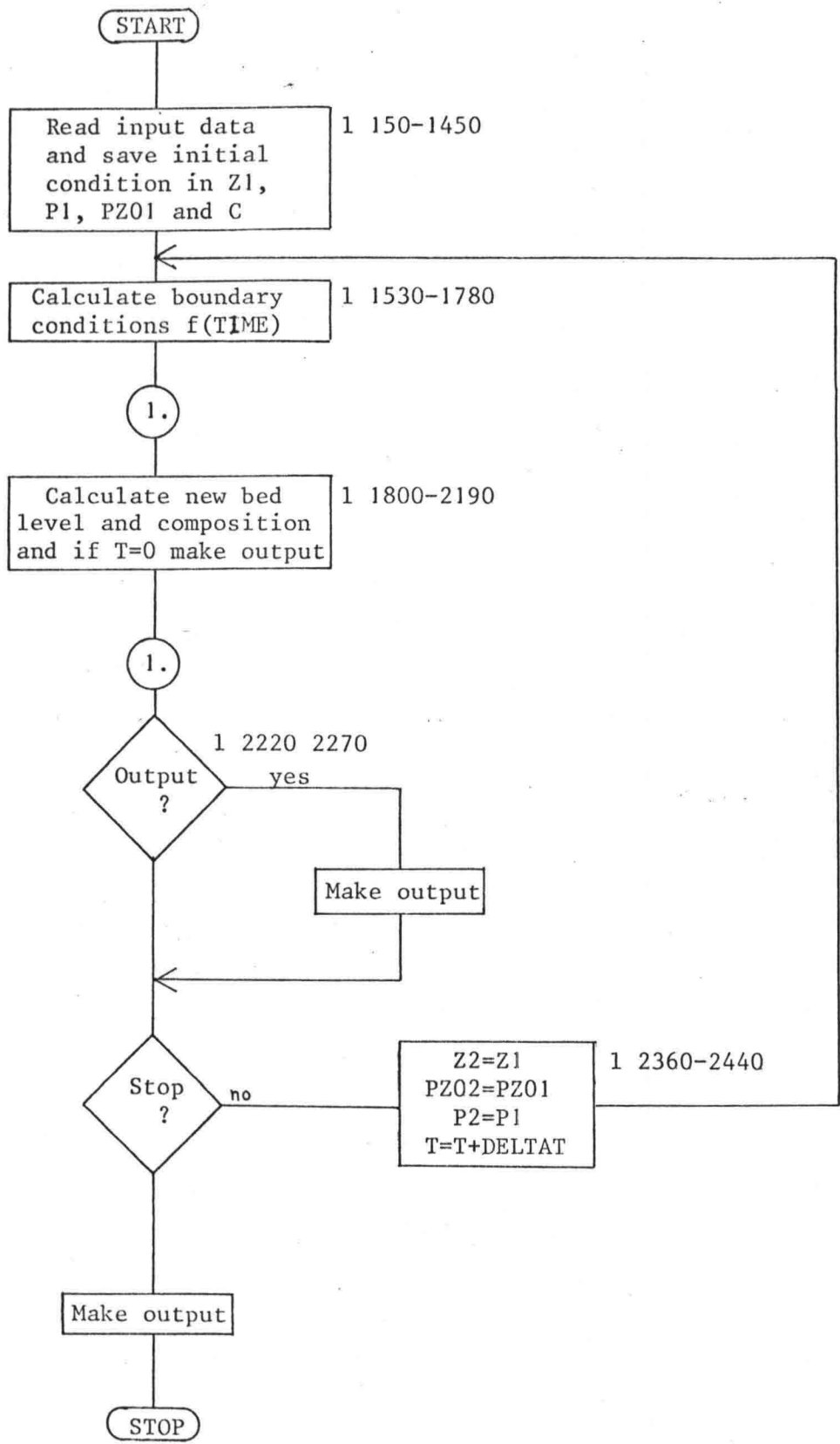
00700 C SIMPEL
00710 C76 TRANSPORTLAYER COMPOSITION CONSTANT
00720 550 DO 700 I6=1, IDIM
00730 READ (5,*) YO
00740 DO 600 I7=1, JDIM
00750 F1(I6, I7)=YO
00760 600 CONTINUE
00770 700 CONTINUE
00780 C76
00790 C77 BED COMPOSITION CONSTANT
00800 DO 900 I8=1, IDIM
00810 READ (5,*) YO
00820 DO 800 I9=1, JDIM
00830 F201(I8, I9)=YO
00840 800 CONTINUE
00850 900 CONTINUE
00860 C77
00870 C771 CHEZY-COEFFICIENT
00880 READ (5,*) YO
00890 DO 950 J=1, JDIM
00900 C(J)=YO
00910 950 CONTINUE
00920 C771
00930 C78 BED LEVEL, CONSTANT SLOPE
00940 READ (5,*) SLOPE, YO
00950 Z1(JDIM)=YO
00960 DO 1000 I10=2, JDIM
00970 Z1(JDIM+1-I10)=Z1(JDIM+2-I10)+SLOPE*DELTAX
00980 1000 CONTINUE
00990 C78
01000 C79 COARSE LAYER (DELACC=J0)
01010 1050 READ (5,*) DELACC
01020 IF (DELACC .EQ. 0) GO TO 1200
01030 DO 1100 I11=1, IDIM
01040 READ (5,*) DELTAP(I11)
01050 1100 CONTINUE
01060 C
01070 C END INITIAL CONDITIONS
01080 C8
01090 C BOUNDARY CONDITIONS
01100 C
01110 C81 TYPES
01120 C 1 CONSTANT
01130 C 2 SINUS
01140 C 3 LINEAR STEP
01150 C 4 SAND LIFT (ONLY S)
01160 C81
01170 C82 DOWNSTREAM WATERLEVEL
01180 1200 READ (5,*) IYPEH
01190 IF (IYPEH .EQ. 1) GO TO 1300
01200 READ (5,*) HPARM
01210 GO TO 1400
01220 1300 READ (5,*) H
01230 C82
01240 C83 DISCHARGE
01250 1400 READ (5,*) IYPEQ
01260 IF (IYPEQ .EQ. 1) GO TO 1500
01270 READ (5,*) QPARM
01280 GO TO 1600
01290 1500 READ (5,*) Q
01300 C83
01310 C84 SANDINPUT
01320 1600 READ (5,*) IYPES
01330 IF (IYPES .EQ. 4) GO TO 1900
01340 IF (IYPES .EQ. 1) GO TO 1800
01350 DO 1700 I12=1, IDIM
01360 READ (5,*) (SPARM(I12, J), J=1, 6)
01370 1700 CONTINUE
01380 GO TO 2000
01390 1800 READ (5,*) (S01(J), J=1, IDIM)
01400 GO TO 2000
01410 1900 READ (5,*) TEMP, XLIFT
01420 C
01430 C END BOUNDARY CONDITIONS
01440 C
01450 C END INPUT
01460 C
01470 C *****
01480 C1 INITIALISE
01490 2000 T=0
01500 IT=TOP
01510 STOP=1.0
01520 C1
01530 C2 CALCULATA BOUNDARY CONDITIONS
01540 2050 IF (IYPEH .NE. 1) CALL BOUND(IYPEH, HPARM, T, H)
01550 IF (IYPEQ .NE. 1) CALL BOUND(IYPEQ, QPARM, T, Q)
01560 C21 SANDINPUT
01570 IF (IYPES .EQ. 1) GO TO 2300
01580 IF (IYPES .EQ. 4) GO TO 2500
01590 DO 2200 I1=1, IDIM
01600 DO 2100 I2=1, 6
01610 TEMP(I2)=SPARM(I1, I2)
01620 2100 CONTINUE
01630 CALL BOUND(IYPES, TEMP, T, YO)
01640 S01(I1)=YO
01650 TX=T+DELTAT
01660 CALL BOUND(IYPES, TEMP, TX, YO)
01670 S02(I1)=YO
01680 2200 CONTINUE
01690 GO TO 2575
01700 2300 DO 2400 I3=1, IDIM
01710 S02(I3)=S01(I3)
01720 2400 CONTINUE
01730 GO TO 2575
01740 2500 ITYPE=3
01750 CALL BOUND(ITYPE, TEMP, T, V1)
01760 TX=T+DELTAT
01770 CALL BOUND(ITYPE, TEMP, TX, V2)
01780 C21
01790 C2

```

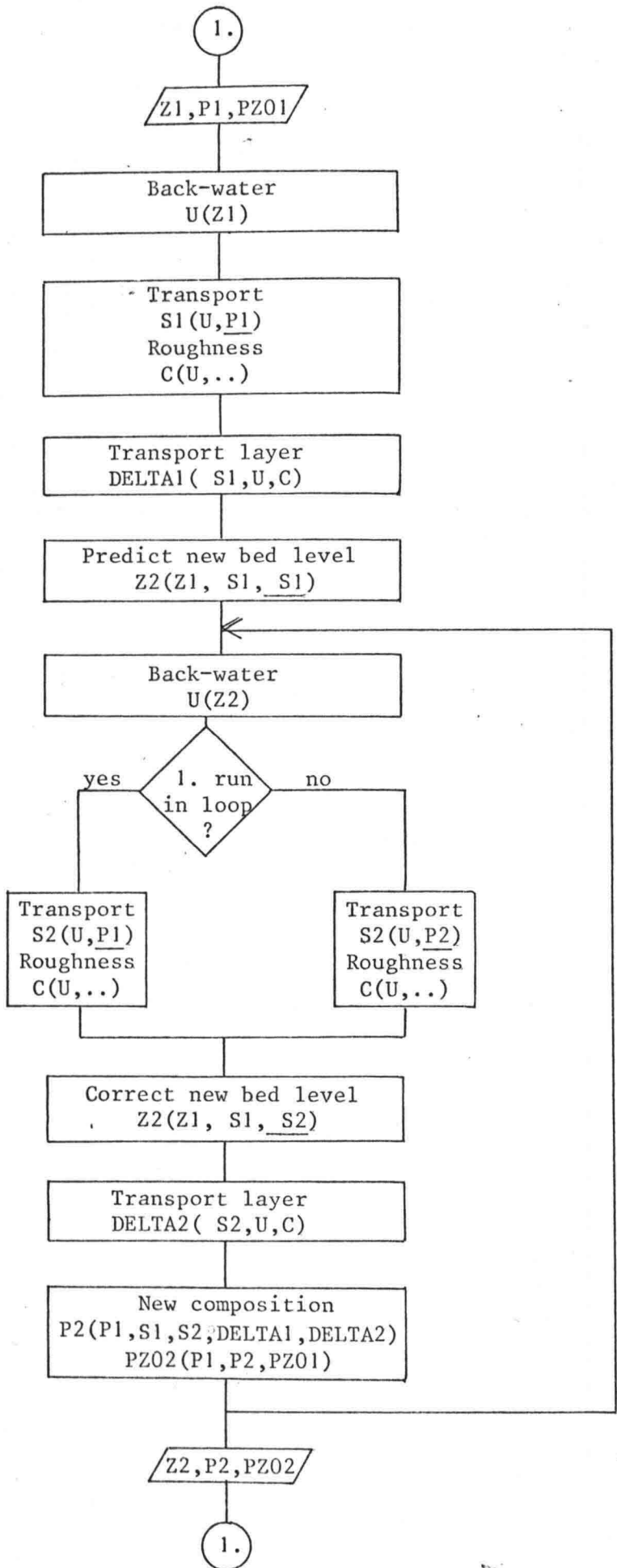
```

01800 C3 'PREPARATION'
01810 2575 CALL RAWA(Z1,U,JDIM,Q,C,H,DELTA1,IT1)
01820 CALL SFUN(S1,U,D,P1,IN,JDIM,IDIM,Q,C)
01830 CALL SUM(S1,SSUM1,JDIM,IDIM)
01840 CALL DELFUN(SSUM1,U,DELTA1,JN,Q,JDIM,C)
01850 IF (T.NE.0) GO TO 2800
01860 IF (DELACC.EQ. 0) GO TO 2700
01870 C31 POSITION OF COARSE LAYER
01880 DO 2600 I5=1,JDIM
01890 Z00(I5)=Z1(I5)-DELTA1(I5)-DELACC
01900 2600 CONTINUE
01910 C31
01920 2700 CALL HEAD(IN,JN,DELTA1,DELTA1,JDIM,IDIM,TETA,IT1,IT2,
01930 & TMAX,EPS1,EPS2,TOP,ITYPEH,H,HPARM,ITYPER,Q,QPARM,
01940 & ITYPE,S,S01,SPARM,TEMP,XLIFT,DELACC,DELTA1,FAC,D)
01950 CALL WRITE(S1,P1,PZ01,Z1,DELTA1,Z00,U,D,S01,JDIM,IDIM,C,
01960 & DELACC,T,DELTA1,Q,H,V1,XLIFT)
01970 C5
01980 C5
01990 C5
02000 2800 SOSUM1=0
02010 SOSUM2=0
02020 DO 2950 J1=1,IDIM
02030 SOSUM1=SOSUM1+S01(J1)
02040 SOSUM2=SOSUM2+S02(J1)
02050 2950 CONTINUE
02060 CALL PRCO(SSUM1,SSUM1,Z1,Z2,JDIM,DELTA1,DELTA1,TETA,
02070 & SOSUM1,SOSUM2,V1,V2,XLIFT)
02080 DO 3100 I02=1,IT2
02090 CALL RAWA(Z2,U,JDIM,Q,C,H,DELTA1,IT1)
02100 IF (I02.EQ. 1) CALL SFUN(S2,U,D,P1,IN,JDIM,IDIM,Q,C)
02110 IF (I02.NE. 1) CALL SFUN(S2,U,D,P2,IN,JDIM,IDIM,Q,C)
02120 CALL SUM(S2,SSUM2,JDIM,IDIM)
02130 CALL DELFUN(SSUM2,U,DELTA2,JN,Q,JDIM,C)
02140 & CALL PRCO(SSUM1,SSUM2,Z1,Z2,JDIM,DELTA1,DELTA1,TETA,
02150 & SOSUM1,SOSUM2,V1,V2,XLIFT)
02160 CALL DELFUN(SSUM2,U,DELTA2,JN,Q,JDIM,C)
02170 CALL PSTAR(S1,S2,P1,P2,PZ01,PZ02,Z1,Z2,DELTA1,
02180 & DELTA2,S01,S02,Z00,DELACC,JDIM,IDIM,
02190 & TETA,DELTA1,DELTA1,DELTA1,V1,V2,XLIFT)
02200 3100 CONTINUE
02210 C5
02220 C5
02230 C6 OUTPUT?
02240 TC=T+DELTA1
02250 IF (TC.LT. TT) GO TO 3200
02260 CALL WRITE(S2,P2,PZ02,Z2,DELTA2,Z00,U,D,S02,JDIM,IDIM,C,
02270 & DELACC,TC,DELTA1,Q,H,V2,XLIFT)
02280 C6 TT=TT+TOP
02290 C7
02300 C7 MORE TIMESTEP
02310 3200 IF (T.GE. TMAX) GO TO 3300
02320 TTT=TMAX*FAC
02330 IF (T.GE. TTT) CALL BIG(P1,P2,Z1,Z2,JDIM,IDIM,EPS1,
02340 & EPS2,STOP)
02350 C7 IF (STOP.EQ. 0.0) GO TO 3300
02360 C8
02370 C8 NEW TIMESTEP
02380 T=T+DELTA1
02390 DO 3225 I=1,JDIM
02400 Z1(I)=Z2(I)
02410 DO 3225 J=1,IDIM
02420 P1(J,I)=P2(J,I)
02430 PZ01(J,I)=PZ02(J,I)
02440 3225 CONTINUE
02450 3250 CONTINUE
02460 C8 GO TO 2050
02470 C9
02480 C9 STOP
02490 3300 T=T+DELTA1
02500 CALL WRITE(S2,P2,PZ02,Z2,DELTA2,Z00,U,D,S02,JDIM,IDIM,C,
02510 & DELACC,T,DELTA1,Q,H,V2,XLIFT)
02520 C9 END

```



Flow chart MAIN programme



Flow chart: calculation of new bed level and composition

W R I T E (810225.03)

1. Purpose

Making output of the time dependent variables.

2. Usage

Call WRITE (S2, P2, PZ02, Z2, DELTA 2, Z00, U, D, SO2, JDIM, IDIM,
C,DELACC , T, DELTAX, Q, H, V2, XLIFT).

3. Description of parameter

'all parameters unchanged on exit'.

4. Procedures required

Subrouline INTEG

5. Method

See subroutine and output description.


```

00010 SUBROUTINE WRITE (S,P,PZO,Z,DELTA,ZOO,U,D,SO,JDIM,IDIM,C,
00020 & DELACC,T,DELTA,X,G,H,V,XLIFT)
00030 C
00040 C SUBROUTINE MAKING OUTPUT
00050 C
00060 C **801110.01.KWD**
00070 C
00080 DIMENSION S(IDIM,JDIM),P(IDIM,JDIM),Z(JDIM),DELTA(JDIM),
00090 & ZOO(JDIM),U(JDIM),SO(IDIM),D(IDIM),LINE(120),
00100 & PZO(IDIM,JDIM),OUT(14),C(JDIM)
00110 C
00120 DATA LINE /120 * 1H /,IST/1H-/
00130 DATA LSEV/1H7/
00140 DATA LBLANC,LDDD,LHHH,LZZZ,LOOO,LONE,LTWO,LTH,LFOUR,LFIVE
00150 & ,LSIX / 1H ,1HD,1HH,1HZ,1HO,1H1,1H2,1H3,1H4,1H5,1H6/
00160 C1 MAKE HEAD
00170 WRITE (6,5)
00180 WRITE (6,20) T
00190 WRITE (6,10)
00200 WRITE (6,30) Q
00210 WRITE (6,40) H
00220 C11 LIFT OR SANDINPUT?
00230 IF (XLIFT .EQ. 0) GO TO 1000
00240 WRITE (6,50) V
00250 GO TO 1200
00260 1000 WRITE (6,60)
00270 DO 1100 I1=1,IDIM
00280 WRITE (6,70) I1,SO(I1)
00290 1100 CONTINUE
00300 C11
00310 C1
00320 C2 HEAD OF LIST
00330 1200 WRITE (6,80)
00340 J2=55+11*IDIM
00350 DO 1300 I2=1,J2
00360 LINE(I2)=IST
00370 1300 CONTINUE
00380 WRITE (6,90) LINE
00390 IF (IDIM .EQ. 1) WRITE (6,111)
00400 IF (IDIM .EQ. 2) WRITE (6,112)
00410 IF (IDIM .EQ. 3) WRITE (6,113)
00420 IF (IDIM .EQ. 4) WRITE (6,114)
00430 IF (IDIM .EQ. 5) WRITE (6,115)
00440 IF (IDIM .EQ. 6) WRITE (6,116)
00450 IF (IDIM .EQ. 7) WRITE (6,117)
00460 WRITE (6,90) LINE
00470 C2
00480 C3 LIST 1
00490 J3=6+IDIM
00500 DO 1700 I5=1,JDIM
00510 OUT(1)=(I5-1)*DELTA X
00520 OUT(5)=Q/U(I5)
00530 OUT(3)=DELTA(I5)
00540 OUT(4)=Z(I5)
00550 OUT(6)=U(I5)
00560 OUT(2)=Z(I5)-DELTA(I5)
00570 DO 1600 I6=7,J3
00580 OUT(I6)=S(I6-6,I5)
00590 1600 CONTINUE
00600 J4=J3+1
00610 OUT(J4)=C(I5)
00620 WRITE (6,130) (OUT(J),J=1,J4)
00630 1700 CONTINUE
00640 C3
00650 C31 BOTTOM OF LIST 1
00660 WRITE (6,90) LINE
00670 C31
00680 C4 HEAD OF LIST 2
00690 C41 MAKE BLANC IN LINE
00700 DO 1800 I7=1,120
00710 LINE(I7)=LBLANC
00720 1800 CONTINUE
00730 C41
00740 C42 MAKE ----- IN LINE
00750 J=(2*IDIM+2)*7+2
00760 DO 1900 I7=1,J
00770 LINE(I7)=IST
00780 1900 CONTINUE
00790 WRITE (6,90) LINE
00800 IF (IDIM .EQ. 1) WRITE (6,171)
00810 IF (IDIM .EQ. 2) WRITE (6,172)
00820 IF (IDIM .EQ. 3) WRITE (6,173)
00830 IF (IDIM .EQ. 4) WRITE (6,174)
00840 IF (IDIM .EQ. 5) WRITE (6,175)
00850 IF (IDIM .EQ. 6) WRITE (6,176)
00860 IF (IDIM .EQ. 7) WRITE (6,177)
00870 WRITE (6,90) LINE
00880 C4
00890 C5 LIST 2
00900 J1=IDIM+2
00910 J2=IDIM+3
00920 J3=2*IDIM+2
00930 DO 2100 I11=1,14
00940 OUT(I11)=0
00950 2100 CONTINUE
00960 DO 2400 I12=1,JDIM
00970 DM=0
00980 OUT(1)=(I12-1)*DELTA X
00990 DO 2200 I13=3,J1
01000 OUT(I13)=P(I13-2,I12)
01010 DM=P(I13-2,I12)*D(I13-2)+DM
01020 2200 CONTINUE
01030 DO 2300 I14=J2,J3
01040 OUT(I14)=PZO(I14-J1,I12)
01050 2300 CONTINUE
01060 OUT(2)=DM*1000
01070 WRITE(6,210) (OUT(J),J=1,J3)
01080 2400 CONTINUE
01090 C5
01100 C6 BOTTOM OF LIST 2
01110 WRITE (6,90) LINE
01120 C6
01130 C
01140 C PLOT
01150 C
01160 C7 SCALE
01170 IF (T .NE. 0) GO TO 2600
01180 HX=Z(1)+Q/U(1)
01190 IF (HX .GT. 1) GO TO 2550
01200 I=1.0/HX
01210 ISCALE=I*100
01220 GO TO 2600
01230 2550 IF (HX .GT. 10) GO TO 2575
01240 I=10/HX

```

```

01250      ISCALE=I*10
01260      GO TO 2600
01270      2575 ISCALE=100/HX
01280      C7
01290      C8 INITIALISE LINE
01300      2600 DO 2700 I14=1,120
01310          LINE(I14)=LBLANC
01320      2700 CONTINUE
01330      C8
01340      C9 MAKE Z-PLOT
01350          WRITE (6,240) ISCALE
01360          WRITE (6,250)
01370          DO 2900 I15=1,JDIM
01380              X=(I15-1)*DELTA
01390              Z=Z(I15)-DELTA(I15)
01400              IF (DELACC.EQ. 0) GO TO 2800
01410              A=Z00(I15)*ISCALE
01420              CALL INTEG(A,L1)
01430              IF (Z00(I15).LT. Z0) LINE(L1)=L000
01440      2800      A=Z0*ISCALE
01450          CALL INTEG(A,L2)
01460          LINE(L2)=L000
01470          A=Z(I15)*ISCALE
01480          CALL INTEG(A,L3)
01490          LINE(L3)=LZZZ
01500          A=A+Q/U(I15)*ISCALE
01510          CALL INTEG(A,L4)
01520          LINE(L4)=LHHH
01530          WRITE (6,260) X,LINE
01540          IF (DELACC.NE. 0) LINE(L1)=LBLANC
01550          LINE(L2)=LBLANC
01560          LINE(L3)=LBLANC
01570          LINE(L4)=LBLANC
01580      2900 CONTINUE
01590          WRITE (6,250)
01600          WRITE (6,80)
01610      C9
01620      C10 MAKE P-PLOT
01630          WRITE (6,270)
01640          WRITE (6,280)
01650          DO 3200 I16=1,JDIM
01660              X=(I16-1)*DELTA
01670              PS=0
01680              DO 3000 I17=1,JDIM
01690                  PS=P(I17,I16)*100+PS
01700                  CALL INTEG(PS,L)
01710                  IF (I17.EQ. 1) LINE(L)=LONE
01720                  IF (I17.EQ. 2) LINE(L)=LTWO
01730                  IF (I17.EQ. 3) LINE(L)=LTH
01740                  IF (I17.EQ. 4) LINE(L)=LFIVE
01750                  IF (I17.EQ. 5) LINE(L)=LSIX
01760                  IF (I17.EQ. 6) LINE(L)=LSIX
01770                  IF (I17.EQ. 7) LINE(L)=LSEV
01780      3000 CONTINUE
01790          WRITE (6,260) X,LINE
01800          DO 3100 I18=1,122
01810              LINE(I18)=LBLANC
01820      3100 CONTINUE
01830      3200 CONTINUE
01840          WRITE (6,280)
01850          5 FORMAT (1H1,25(' '))
01860          10 FORMAT (1H ,25(' '))
01870          20 FORMAT (1H , * TIME=' ,F14.1, ' S *')
01880          30 FORMAT (1H0, ' DISCHARGE=' ,F10.4, ' M2/S')
01890          40 FORMAT (1H0, ' WATERLEVEL DOWNSTREAM=' ,F10.4, ' M')
01900          50 FORMAT (1H0, ' SAND LIFT VELOCITY=' ,E10.4, ' M/S')
01910          60 FORMAT (1H0, ' SAND INPUT')
01920          70 FORMAT (1H , ' FRACTION' ,I1,E14.4, ' M2/S')
01930          80 FORMAT (1H0)
01940          90 FORMAT (1H ,122A1)
01950          117 FORMAT (1H , ' X(M) Z0(M) DEL(M) Z(M) A(M) U(M/S)',
01960              & ' S1 (M2/S) S2 (M2/S) S3 (M2/S) S4 (M2/S) S5 (M2/S)',
01970              & ' S6 (M2/S) S7 (M2/S) CHEZY')
01980          116 FORMAT (1H , ' X(M) Z0(M) DEL(M) Z(M) A(M) U(M/S)',
01990              & ' S1 (M2/S) S2 (M2/S) S3 (M2/S) S4 (M2/S) S5 (M2/S)',
02000              & ' S6 (M2/S) CHEZY')
02010          115 FORMAT (1H , ' X(M) Z0(M) DEL(M) Z(M) A(M) U(M/S)',
02020              & ' S1 (M2/S) S2 (M2/S) S3 (M2/S) S4 (M2/S) S5 (M2/S)',
02030              & ' CHEZY')
02040          114 FORMAT (1H , ' X(M) Z0(M) DEL(M) Z(M) A(M) U(M/S)',
02050              & ' S1 (M2/S) S2 (M2/S) S3 (M2/S) S4 (M2/S) CHEZY')
02060          113 FORMAT (1H , ' X(M) Z0(M) DEL(M) Z(M) A(M) U(M/S)',
02070              & ' S1 (M2/S) S2 (M2/S) S3 (M2/S) CHEZY')
02080          112 FORMAT (1H , ' X(M) Z0(M) DEL(M) Z(M) A(M) U(M/S)',
02090              & ' S1 (M2/S) S2 (M2/S) CHEZY')
02100          111 FORMAT (1H , ' X(M) Z0(M) DEL(M) Z(M) A(M) U(M/S)',
02110              & ' S1 (M2/S) CHEZY')
02120          130 FORMAT (1H ,F9.2,5F7.4,8E11.4)
02130          171 FORMAT (1H , ' X(M) DM(MM)',
02140              & ' F1',
02150              & ' PZ01')
02160          172 FORMAT (1H , ' X(M) DM(MM)',
02170              & ' F1',
02180              & ' PZ01 PZ02')
02190          173 FORMAT (1H , ' X(M) DM(MM)',
02200              & ' F1',
02210              & ' PZ01 PZ02 PZ03')
02220          174 FORMAT (1H , ' X(M) DM(MM)',
02230              & ' F1',
02240              & ' PZ01 PZ02 PZ03 PZ04')
02250          175 FORMAT (1H , ' X(M) DM(MM)',
02260              & ' F1',
02270              & ' PZ01 PZ02 PZ03 PZ04 PZ05')
02280          176 FORMAT (1H , ' X(M) DM(MM)',
02290              & ' F1',
02300              & ' PZ01 PZ02 PZ03 PZ04 PZ05 PZ06')
02310          177 FORMAT (1H , ' X(M) DM(MM)',
02320              & ' F1',
02330              & ' PZ01 PZ02 PZ03 PZ04 PZ05 PZ06 PZ07')
02340          210 FORMAT (1H ,F9.2,F7.4,13F7.4)
02350          240 FORMAT (1H0, ' X(M) SCALE=' ,I4, ' +/M')
02360          250 FORMAT (1H ,9(' -'), ' 0',120(' +'))
02370          260 FORMAT (1H ,F9.2, ' *',120A1)
02380          270 FORMAT (1H , ' X(M)')
02390          280 FORMAT (1H ,9(' -'), ' 0',9(' +'), '1',9(' +'), '2',9(' +'), '3',
02400              & ' 9(' +'), '4',9(' +'), '5',9(' +'), '6',9(' +'), '7',
02410              & ' 9(' +'), '8',9(' +'), '9',9(' +'), '0')
02420          RETURN
02430          END

```

H E A D (801030.01)-

1. Purpose

Making the head of the output.

2. Usage

Call HEAD (IN, JN, DELTAT, DELTAX, JDIM, IDIM, TETA, IT1, IT2,
TMAX, EPS1, EPS2, TOP, IYPEH, H, HPARM, IYPEQ, Q,
QPARM, IYPE S, SO1, SPARM, TEMP, XLIFT, DELACC,
DELTAP, FAC, D).

3. Description of parameters

'all parameters unchanged on exit'.

4. Procedure required

none

5. Method

See subroutine and output description.

```

00010 SUBROUTINE HEAD(IN,JN,DELTAT,DELTAX,JDIM,IDIM,TETA,IT1,
00020 IT2,TMAX,EPS1,EPS2,TOF,ITYPEH,H,
00030 HPARM,ITYPEQ,Q,QPARM,ITYPES,S01,SPARM,
00040 TEMP,XLIFT,DELACC,DELTAP,FAC,D)
00050 C
00060 C
00070 C
00080 C
00090 C
00100 SUBROUTINE MAKING THE HEAD OF OUTPUT
00110 **B01030.01.KW0**
00120 C
00130 DIMENSION IN(8),JN(8),D(IDIM),HPARM(6),QPARM(6),TEMP(6),
00140 S01(IDIM),SPARM(IDIM,6),DELTAP(IDIM)
00150
00160 WRITE (6,10)
00170 WRITE (6,20)
00180 WRITE (6,30)
00190 WRITE (6,20)
00200 WRITE (6,20)
00210 WRITE (6,20)
00220 WRITE (6,40)
00230 WRITE (6,20)
00240 WRITE (6,10)
00250 WRITE (6,50) IN
00260 WRITE (6,60) JN
00270 WRITE (6,70) DELTAT
00280 WRITE (6,80) DELTAX
00290 X=(JDIM-1)*DELTAX
00300 WRITE (6,90) X
00310 WRITE (6,100) X
00320 DO 1000 I1=1,IDIM
00330 WRITE (6,110) I1,D(I1)
00340 1000 CONTINUE
00350 WRITE (6,120) TETA
00360 WRITE (6,130)
00370 WRITE (6,140) IT1
00380 WRITE (6,150) IT2
00390 WRITE (6,180)
00400 WRITE (6,190) TMAX
00410 XX=TMAX*FAC
00420 WRITE (6,195) XX
00430 WRITE (6,200) EPS1
00440 WRITE (6,210) EPS2
00450 WRITE (6,220) TOP
00460 WRITE (6,225) DELACC
00470 IF (DELACC .EQ. 0) GO TO 1010
00480 DO 1005 I6=1,IDIM
00490 WRITE (6,228) I6,DELTAP(I6)
00500 1005 CONTINUE
00510 1010 WRITE (6,230)
00520 WRITE (6,235)
00530 WRITE (6,240)
00540 IF (ITYPEH .EQ. 1) WRITE (6,270) H
00550 IF (ITYPEH .EQ. 2) WRITE (6,280) HPARM
00560 IF (ITYPEH .EQ. 3) WRITE (6,290) HPARM
00570 WRITE (6,250)
00580 IF (ITYPEQ .EQ. 1) WRITE (6,270) Q
00590 IF (ITYPEQ .EQ. 2) WRITE (6,280) QPARM
00600 IF (ITYPEQ .EQ. 3) WRITE (6,290) QPARM
00610 WRITE (6,260)
00620 IF (ITYPES .EQ. 1) GO TO 1100
00630 IF (ITYPES .EQ. 2) GO TO 1200
00640 IF (ITYPES .EQ. 3) GO TO 1300
00650 IF (ITYPES .EQ. 4) GO TO 1400
00660 1100 DO 2000 I2=1,IDIM
00670 WRITE (6,270) S01(I2)
00680 2000 CONTINUE
00690 GO TO 1500
00700 1200 DO 3000 I3=1,IDIM
00710 WRITE (6,280) SPARM(I3,1),SPARM(I3,2),SPARM(I3,3)
00720 ,SPARM(I3,4),SPARM(I3,5),SPARM(I3,6)
00730 3000 CONTINUE
00740 GO TO 1500
00750 1300 DO 4000 I4=1,IDIM
00760 WRITE (6,290) SPARM(I4,1),SPARM(I4,2),SPARM(I4,3)
00770 ,SPARM(I4,4),SPARM(I4,5),SPARM(I4,6)
00780 4000 CONTINUE
00790 GO TO 1500
00800 1400 WRITE (6,300) TEMP
00810 1500 WRITE (6,100)
00820 WRITE (6,10)
00830 10 FORMAT (1H,43(' '))
00840 20 FORMAT (1H,'*',41(' '), '*')
00850 30 FORMAT (1H,'* TRANSPORTMODEL FOR NON-UNIFORM SEDIMENT *')
00860 40 FORMAT (1H,'*',9(' '), 'KIM WIUM OLESEN 1980',10(' '),
00870 '*')
00880 50 FORMAT (1HO,'TRANSPORTFORMULA: ',8A4)
00890 60 FORMAT (1HO,'TRANSPORTLAYER-FORM: ',8A4)
00900 70 FORMAT (1HO,'TIMESTEP=',F10.1,' S')
00910 80 FORMAT (1HO,'SPACESTEP=',F9.2,' M')
00920 90 FORMAT (1HO,'LENGTH OF FLUME=',F7.2,' M')
00930 100 FORMAT (1H)
00940 110 FORMAT (1H,'DIAMETER D',I1,'=',3PF10.4,' MM')
00950 120 FORMAT (1HO,'WEIGHT TETA=',F7.3)
00960 130 FORMAT (1HO,'ITERATIONS:')
00970 140 FORMAT (1H,I1,' IN BACK WATER')
00980 150 FORMAT (1H,I1,' IN PREDIC.-COR.')
00990 180 FORMAT (1HO,'STOPCRITERION')
01000 190 FORMAT (1H,'TMAX=',F12.1,' S')
01010 195 FORMAT (1H,'CALL BIG AFTER ',F12.1,' S')
01020 200 FORMAT (1H,'EPS1=',E14.4,' M')
01030 210 FORMAT (1H,'EPS2=',E14.4)
01040 220 FORMAT (1HO,'TIME BETWEEN OUTPUT=',F12.1,' S')
01050 225 FORMAT (1HO,'COARSE LAYER-DELACC=',F12.5,' M')
01060 228 FORMAT (1H,'DELTAP',I2,F7.4)
01070 230 FORMAT (1HO,'BOUNDARY CONDITIONS:')
01080 235 FORMAT (1H,20(' '))
01090 240 FORMAT (1HO,'DOWNSTREAM WATERLEVEL H (M)')
01100 250 FORMAT (1HO,'DISCHARGE Q (M2/S)')
01110 260 FORMAT (1HO,'SANDINPUT (M2/S)')
01120 270 FORMAT (1H,'CONSTANT',E14.4)
01130 280 FORMAT (1H,'SINUS',6E14.4)
01140 290 FORMAT (1H,'STEP',6E14.4)
01150 300 FORMAT (1H,'SAND LIFT',6E14.4)
01160 RETURN
01170 END

```

I N T E G (801111.01)

1. Purpose

Rounding a real number up or down and put it equal one if the value is larger than 120 and smaller than one.

2. Usage

Call INTEG (A,L).

3. Description of parameters

A (real) 'unchanged on exit'

L (integer) rounded value of A 'changed on exit'.

4. Procedure required

none

5. Method

See comments.

```
00010           SUBROUTINE INTEG(A,L)
00020           C
00030           C           SUBROUTINE CUTTING OFF AND ROUNDING UP OR DOWN, AND
00040           C           CHECKING FOR OVER AND UNDERFLOW IN LINE
00050           C
00060           C           **801111.01.KWD**
00070           C
00080           C1          CUT OFF
00090           C           L=A
00100           C1
00110           C2          RESIDUAL > 0.5
00120           C           C=A-L
00130           C           IF (C .GE. 0.5) L=L+1
00140           C2
00150           C3          STILL ROOM IN LINE
00160           C           IF ((L .GT. 120) .OR. (L .LT. 1)) L=1
00170           C3
00180           C           RETURN
00190           C           END
```

S F U N (810225.06)

1. Purpose

Calculating the transport and correcting the roughness

2. Usage

Call SFUN (S1, U, D, P1, IN, JDIM, IDIM, Q, C)

Call SFUN (S2, U, D, P2, IN, JDIM, IDIM, Q, C)

3. Description of parameters

S (real-2-array)	: transport per fraction 'changed on exit'
U (real-array)	: flow velocity 'unchanged on exit'
D (real-array)	: grain diameters 'unchanged on exit'
P (real-2-array)	: composition of transport layer 'unchanged on exit'
IN (alfa-array)	: name of transport formula 'changed on exit'
JDIM (integer)	: number of space-step. Dimension of S, P, U, and C 'unchanged on exit'
IDIM (integer)	: number of fractions. Dimension of S, P and D 'unchanged on exit'
Q (real)	: specific discharge 'unchanged on exit'
C (real-array)	: Chézy coefficient 'changed on exit'

4. Procedures required

none

5. Method

Roughness calculated with the Engeland - Hansen method. Transport calculated with the Meyer - Peter and Müller formula.

```

00010 SUBROUTINE SFUN(S,U,D,P,IN,JDIM,IDIM,Q,C)
00020 C
00030 C SUBROUTINE CALCULATING THE SEDIMENTTRANSPORT
00040 C
00050 C **B10225.06.KWD**
00060 C
00070 DIMENSION S(IDIM,JDIM),P(IDIM,JDIM),U(JDIM),D(IDIM),IN(8),
00080 & C(JDIM)
00090 C
00100 C1 HERE THE NAME OF THE TRANSPORTFORMULA
00110 DATA IN1,IN2,IN3,IN4,IN5,IN6,IN7,IN8/
00120 &4HMEYE,4HR-FE,4HTER ,4HAND ,4HMULL,4HER ,4H ,4H /
00130 C1
00140 IN(1)=IN1
00150 IN(2)=IN2
00160 IN(3)=IN3
00170 IN(4)=IN4
00180 IN(5)=IN5
00190 IN(6)=IN6
00200 IN(7)=IN7
00210 IN(8)=IN8
00220 C2 TRANSPORT AND ROUGHNESS -CALCULATION
00230 DO 200 I1=1,JDIM
00240 C21 MEAN DIAMETER
00250 DM=0
00260 DO 10 J1=1,IDIM
00270 DM=DM+P(J1,I1)*D(J1)
00280 10 CONTINUE
00290 C21
00300 C22 CALCULATION OF THE CHEZY-ROUGHNESS (ENGELUND-HANSEN)
00310 FU=U(I1)**9/(Q*DM**3)
00320 IF ((FU .GT. 2.2632E7) .AND. (FU .LT. 2.5568E12)) GO TO 30
00330 C SHEAR STRESS TECO<0.06 OR TECO>1.1
00340 TECO=FU**0.25*8.699E-4
00350 TESK=TECO
00360 GO TO 60
00370 C30 IF (FU .GT. 4.7464E7) GO TO 40
00380 C 0.06<TECO<0.3
00390 TECO=FU**2.174*6.1553E-18
00400 TESK=0.13645*TECO**0.292
00410 GO TO 60
00420 C40 IF (FU .GE. 1.6201E10) GO TO 50
00430 C 0.3<TECO<0.9
00440 FX=(FU*5.726E-13)**0.2
00450 TEPR=U(I1)**2/(C(I1)**2*1.65*DM)
00460 C45 TECO=SQRT((FX*TEPR**0.2-0.06)/0.4)
00470 EPS=ABS(TECO-TEPR)
00480 TEPR=TECO
00490 IF (EPS .GT. 1E-4) GO TO 45
00500 TESK=0.06+0.4*TECO**2
00510 GO TO 60
00520 C 0.9<TECO<1.1
00530 C50 TECO=FU**0.03965*0.3544
00540 TESK=TECO**5.245*0.6673
00550 C60 C(I1)=U(I1)/((TECO*1.65*DM)**0.5)
00560 C22
00570 RIB=(TESK/TECO)**0.75
00580 DO 100 I2=1,IDIM
00590 VX=RIB*TECO*DM-0.047*D(I2)
00600 IF (VX .LT. 0) VX=0
00610 S(I2,I1)=VX**1.5*P(I2,I1)*53.64
00620 100 CONTINUE
00630 200 CONTINUE
00640 C2
00650 RETURN
00660 END

```

D E L F U N (801111.01)

1. Purpose

Calculating the transport layer thickness as a function of the total transport, roughness coefficient, flow velocity and depth.

2. Usage

Call DELFUN (SSUM1, DELTA1, JN, Q, JDIM, C) or

Call DELFUN (SSUM2, DELTA2, JN, Q, JDIM, C)

3. Description of parameters

S (real array)	: total transport 'unchanged on exit'
U (real array)	: flow velocity 'unchanged on exit'
DELTA (real array)	: transport layer thickness 'changed on exit'
C (real array)	: Chézy roughness coefficient 'unchanged on exit'
JN (alfa array)	: name of transport layer thickness formula 'changed on exit'
Q (real)	: specific discharge 'unchanged on exit'
JDIM (real)	: number of space step, dimension of S, U, DELTA, and C 'unchanged on exit'

4. Procedure required

none

5. Method

Here transport layer thickness equal 25% of water depth.


```

00010 SUBROUTINE DELFUN(S,U,DELTA,JN,Q,JDIM,C)
00020 C
00030 C SUBROUTINE CALC. THE TRANSPORTLAYERTHICKNESS
00040 C
00050 C **B01111.01.KWD**
00060 C
00070 DIMENSION S(JDIM),U(JDIM),C(JDIM),JN(8),DELTA(JDIM)
00080 C
00090 C1 HERE THE NAME!
00100 DATA JN1,JN2,JN3,JN4,JN5,JN6,JN7,JN8/
00110 &4HDELTA,4HA = ,4H0.25,4H*A ,4H ,4H ,4H /
00120 JN(1)=JN1
00130 JN(2)=JN2
00140 JN(3)=JN3
00150 JN(4)=JN4
00160 JN(5)=JN5
00170 JN(6)=JN6
00180 JN(7)=JN7
00190 JN(8)=JN8
00200 C1
00210 C2 DELTA-FORMULA
00220 DO 100 I1=1,JDIM
00230 DELTA(I1)=0.25*Q/U(I1)
00240 100 CONTINUE
00250 C2
00260 RETURN
00270 END

```

```

00010 SUBROUTINE BOUND(ITYPE,PARM,T,Y)
00020 C
00030 C SUBROUTINE CALCULATING THE BOUNDARY CONDITIONS (Q,H,SI)
00040 C
00050 C **B01027.01.KWD**
00060 C
00070 C DIMENSION PARM(6)
00080 C
00090 C WHICH TYPE?
00100 IF (ITYPE .EQ. 3) GO TO 100
00110 C1 SINUS
00120 C Y=Y1+Y2*SIN(Y3*T+Y4)+Y5*T (Y6=0)
00130 Y=PARM(1)+PARM(2)*SIN(PARM(3)*T+PARM(4))+PARM(5)*T
00140 GO TO 200
00150 C1
00160 C2 LINEAR-STEP
00170 C T<Y1 Y=Y3+Y4*T
00180 C Y1<T<Y2 Y=Y3+Y4*Y1+Y5*(T-Y1)
00190 C T>Y2 Y=Y3+Y4*Y1+Y5*(Y2-Y1)+Y6*(T-Y2)
00200 100 A=PARM(1)*PARM(4)+PARM(3)
00210 B=A+PARM(5)*(PARM(2)-PARM(1))
00220 IF (T .LE. PARM(1)) Y=PARM(3)+PARM(4)*T
00230 IF ((T .GT. PARM(1)) .AND. (T .LE. PARM(2))) Y=A+PARM(5)*
00240 & (T-PARM(1))
00250 IF (T .GT. PARM(2)) Y=B+PARM(6)*(T-PARM(2))
00260 C2
00270 200 RETURN
00280 END

```

```

00010 SUBROUTINE BED(ALFA1,ALFA2,ALFA3,X1,X2,Z1,JDIM,DELTA,X,Y0)
00020 C
00030 C SUBROUTINE CALCULATING INITIAL BEDLEVEL AND -COMPOSITION
00040 C
00050 C **B01028.01.KWD**
00060 C
00070 C DIMENSION Z1(JDIM)
00080 C
00090 C1 INITIALISE
00100 Z1(JDIM)=Y0
00110 C1
00120 C2 GO ON
00130 DO 100 I1=2,JDIM
00140 X=(JDIM+1-I1)*DELTA
00150 IF (X .GT. X2) ALFA=ALFA3
00160 IF ((X .GT. X1) .AND. (X .LE. X2)) ALFA=ALFA2
00170 IF (X .LE. X1) ALFA=ALFA1
00180 Z1(JDIM+1-I1)=Z1(JDIM+2-I1)+ALFA*DELTA
00190 100 CONTINUE
00200 C2
00210 RETURN
00220 END

```

B O U N D (801029.01)

1. Purpose

Calculating the boundary conditions (S_i , H, Q, V) as a function of time. Here linear step and sinusoidal.

2. Usage

Only use if ITYPEy \neq 1

Call BOUND (ITYPEy, yPARM, T, y)

where y is S_i , H, Q or V.

3. Description of parameters

ITYPE (integer)	: Choice of type of variation 'unchanged exist'
PARM (real array)	: 6 parameters to describe the time dependent variation 'unchanged on exist'
T (real)	: time 'unchanged on exist'
y (real)	: Calculated value for the boundary condition 'changed on exist'

4. Procedure required

none

5. Method

See comments in subroutine.

6. Remark

Generally six variables to describe the time dependent variation of the boundary condition. Subroutine head is prepared for these two types of variation.

B E D (801028.01)

1. Purpose

Calculating the initial conditions: bed level, Chézy-coefficients and composition. Here version 1 - linear steps.

2. Usage

Only use if $x1 \neq 0$ and $x2 \neq 0$

Call BED (ALFA1, ALFA2, ALFA3, X1, X2, Z1, JDIM, DELTAX, YO)

3. Description of parameters

ALFA1, ALFA2, ALFA3 (real) : Slopes ALFA1 for $X \leq X1$

ALFA2 for $X1 < X \leq X2$

ALFA3 for $X > X2$

'unchanged on exist'

X1, X2 (real)

: Break points

'unchanged on exist'

Z (real array)

: Bed level, Chézy coefficients or probability of a fraction in the transport layer or in the z_0 -layer.

'changed on exist'

JDIM (integer)

: Dimension of Z-array

'unchanged on exist'

YO (real)

: Value for Z (JDIM)

'unchanged on exist'

4. Procedure required

none

5. Method

See coments in subroutine.

6. Remark

Generaly four parameters (ALFA1, ALFA2, ALFA3, yo) to calculate the initial conditions.

BIG (801028.01) -

1. Purpose

Stop calculation if equilibrium is reached

2. Usage

Called after a fraction of the maximum time TMAX·FAC

Call BIG (P1, P2, Z1, Z2, JDIM, IDIM, EPS1, EPS2, STOP)

3. Description of parameters

P1, P2 (real-2-array) : Composition of transport layer at respectively old and new time level
'unchanged on exit'
Z1, Z2 (real-2-array) : bed level at old and new time level
'unchanged on exit'
JDIM (integer) : dimension of Z1, Z2, P1 and P2
'unchanged on exit'
IDIM (integer) : dimension of P1 and P2
'unchanged on exit'
EPS1, EPS2 (real) : stop criterions. Maximum change in respectively bed level and bed composition
'unchanged on exit'
STOP (real) : is taking the value one if equilibrium is reached.
'changed on exit'

4. Procedure required

none

5. Method

If the largest change in bedlevel is less than EPS1 the largest change in the bed composition is found and if that is less than EPS2 then STOP = 0. Otherwise STOP = 1.

6. Remark

If there is little damping the routine has to be used with caution because of the secondary waves.

```

00010 SUBROUTINE BIG(P1,P2,Z1,Z2,JDIM,IDIM,EPS1,EPS2,STOP)
00020 C
00030 C
00040 C
00050 C
00060 C
00070 C
00080 C
00090 C
00100 C1 BED LEVEL NOT CHANGING
00110 GROT=0.0
00120 DO 100 I1=1,JDIM
00130 A=ABS(Z2(I1)-Z1(I1))
00140 IF (A .GT. GROT) GROT=A
00150 100 CONTINUE
00160 IF (GROT .GT. EPS1) GO TO 400
00170 C1
00180 C2 BED COMPOSITION NOT CHANGING
00190 GROT=0.0
00200 DO 300 I2=1,JDIM
00210 DO 200 I3=1,IDIM
00220 A=ABS(P2(I3,I2)-P1(I3,I2))
00230 IF (A .GT. GROT) GROT=A
00240 200 CONTINUE
00250 300 CONTINUE
00260 IF (GROT .GT. EPS2) GO TO 400
00270 GO TO 500
00280 C2
00290 C3 DON'T STOP
00300 400 STOP=1.0
00310 GO TO 600
00320 C3
00330 C4 DO STOP
00340 500 STOP=0.0
00350 C4
00360 600 RETURN
00370 END

```

B A W A (801028.03) back water calculation.

1. Purpose

Calculating the depth averaged flow velocity for given bed level, Chézy roughness, discharge and down stream water level.

2. Usage

Call BAWA (Z1, U, JDIM, Q, C, H, DELTAX, IT1)

Call BAWA (Z2, U, JDIM, Q, C, H, DELTAX, IT2)

3. Description of parameters

Z (real array)	: bed level 'unchanged on exist'
U (real array)	: flow velocity 'unchanged on exist'
JDIM (integer)	: dimension of Z, U and C 'unchanged on exist'
Q (real)	: specific discharge 'unchanged on exist'
C (real array)	: Chézy roughness coefficient for the bed 'changed on exist'
H (integer)	: Down stream water level 'unchanged on exist'
DELTAX (real)	: Space step 'unchanged on exist'
IT1 (integer)	: number of iterations 'unchanged on exist'

4. Procedure required

none

5. Method

The flow velocity is calculated with an iterative finite difference method. In the first iteration the flow velocity is treated explicit and implicit in the following iterations. Side wall correction is performed with

the Einstein method.

6. Remark

The width (B), the Nekusudses sand roughness (AKW) and the cinematic viscosity (VISC) must be changed into the present values.

```
00010 SUBROUTINE BAWA(Z,U,JDIM,Q,C,H,DELTA,X,IT1)
00020 C
00030 C SUBROUTINE MAKING THE BACKWATER-CALCULATION
00040 C WITH SIDE-WALL CORRECTION
00050 C
00060 C **801028.03.KWO**
00070 C
00080 DIMENSION Z(JDIM),U(JDIM),C(JDIM)
00090 C
00100 C1 INITIALISE
00110 U(JDIM)=Q/(H-Z(JDIM))
00120 C WIDTH OF FLUME
00130 K=0.50
00140 C FIRST GUESS FOR CHEZY COEFFICIENT FOR WALL
00150 CWP=63
00160 C NIKURADSES GRAIN ROUGHNESS FOR WALL
00170 AKW=1E-5
00180 C CINEMATIC VISCOSITY
00190 VISC=1.0000E-6
00200 C1
00210 C2 CALCULATA U
00220 I3=JDIM-1
00230 DO 400 I2=1,IT1
00240 DO 300 I1=1,I3
00250 C21 CALCULATA MEAN U AND C
00260 IF (I2.NE.1) GO TO 100
00270 UAV=U(JDIM+1-I1)
00280 CAV=0.5*(C(JDIM+1-I1)+C(JDIM-I1))
00290 GO TO 200
00300 100 UAV=0.5*(U(JDIM+1-I1)+U(JDIM-I1))
00310 CAV=0.5*(C(JDIM+1-I1)+C(JDIM-I1))
00320 C21
00330 C3 CALCULATE HYDRAULIC RADIUS FOR WALL (RW) AND
00340 C3 CHEZY COEFFICIENT FOR WALL CWC
00350 200 A=Q/UAV
00360 DO 250 J=1,25
00370 RW=A*(CAV/CW)**2/(1+2*A/B*(CAV/CW)**2)
00380 CWC=18*ALOG10(12*RW/(AKW+1.11*VISC*CWP/UAV))
00390 EPS=ABS(CWC-CWP)
00400 CWP=CWC
00410 IF (EPS.LE.0.010) GO TO 275
00420 250 CONTINUE
00430 C3
00440 C22 CALCULATA FRICTION TERM
00450 275 R=9.81*UAV**2/(CWC**2*RW)
00460 C22
00470 C23 CALCULATE "G"-TERM
00480 G=UAV-9.81*Q/UAV**2
00490 C23
00500 C24
00510 U(JDIM-I1)=U(JDIM+1-I1)+((Z(JDIM+1-I1)-Z(JDIM-I1))*
00520 & 9.81+R*DELTA)/G
00530 C24
00540 300 CONTINUE
00550 400 CONTINUE
00560 RETURN
00570 END
```

S U M (801028.01)

1. Purpose

Summating the transport per fraction to get the total transport for prediction of new bed level.

2. Usage

Call SUM (S1, SSUM, JDIM, IDIM)

Call SUM (S2, SSUM, JDIM, IDIM)

3. Description of parameters

S (real-2-array)	: transport per fraction 'unchanged on exist'
SSUM (real - array)	: total transport 'changed on exist'
JDIM (integer)	: dimension of S and SSUM 'unchanged on exist'
IDIM (integer)	: dimension of S 'unchanged on exist'

4. Procedure required

none

5. Method

Simple summation

```
00010 SUBROUTINE SUM(S,SSUM,JDIM,IDIM)
00020 C
00030 C SUBROUTINE CALCULATING THE TOTAL TRANSPORT
00040 C
00050 C **801028.01.KWD**
00060 C
00070 C DIMENSION S(IDIM,JDIM), SSUM(JDIM)
00080 C
00090 DO 200 I1=1,JDIM
00100 SSUM(I1)=0.0
00110 DO 100 I2=1,IDIM
00120 SSUM(I1)=S(I2,I1)+SSUM(I1)
00130 100 CONTINUE
00140 200 CONTINUE
00150 RETURN
00160 END
```

P R C O (801028.02), Predictor - Corrector - iteration.

1. Purpose

Calculating the bed level at new time level for given transport and bed level at old time level and predicted transport at new time level.

2. Usage

Predictor:

Call PRCO (SSUM1, SSUM1, Z1, Z2, JDIM, DELTAX, DELTAT, TETA, SOSUM1, SOSUM1, V1, V1, XLIFT)

Corrector:

Call PRCO (SSUM1, SSUM2, Z1, Z2, JDIM, DELTAX, DELTAT, TETA, SOSUM1, SOSUM2, V1, V2, XLIFT)

3. Description of parameters

SSUM1 (real array)	: total transport at old time level 'unchanged on exict'
SSUM2 (real array)	: predicted total transport at new time level 'unchanged on exict'
Z1 (real array)	: bed level at old time level 'unchanged on exict'
Z2 (real array)	: corrected bed level at new time level 'changed on exict'
JDIM (integer)	: dimension of SSUM1, SSUM2, Z1 and Z2 'unchanged on exict'
DELTAX (real)	: space step 'unchanged on exict'
DELTAT (real)	: time step 'unchanged on exict'
TETA (real)	: weight, TETA at new time level, (1 - TETA) at old 'unchanged on exict'
SOSUM1, SOSUM2 (real)	: total transport at upstream boundary at respectitily old and new time level

'unchanged on exist'

V1, V2 (real) : source / sink term in continuity equation
(sand lift velocity)
'unchanged on exist'

XLIFT (real) : length of sand lift
'unchanged on exist'

4. Procedure required

none

5. Method

The new bed level is calculated with predictor - corrector method 'inside' for the Crank - Nicholson scheme and at the down stream boundary with the four point scheme.

6. Remark

If the bed level and composition is fixed at the upstream boundary (boundary condition) lines 120-140 have to be changed into $Z2(1) = Z1(1)$.

```

00010 SUBROUTINE PRCD(SSUM1,SSUM2,Z1,Z2,JDIM,DELTA,DELTAT,TETA,
00020 S,SOSUM1,SOSUM2,V1,V2,XLIFT)
00030 C
00040 C SUBROUTINE MAKING THE PREDICTOR CORRECTOR ITERATION
00050 C
00060 C **B01028.02.KWD**
00070 C
00080 C DIMENSION SSUM1(JDIM), SSUM2(JDIM), Z1(JDIM), Z2(JDIM)
00090 C
00100 C W=(XLIFT-2*DELTA)/(2*DELTA)
00110 C1 AT THE UPSTREAMBOUNDARY CRANK-NICHOLSON SKEME
00120 Z2(1)=Z1(1)-DELTAT/(2*DELTA)*((1-TETA)*(SSUM1(2)-SOSUM1)
00130 +TETA*(SSUM2(2)-SOSUM2))+((1-TETA)*V1+TETA*V2)
00140 *DELTAT*W
00150 W=1
00160 C1
00170 C2 'INSIDE' CRANK-NICHOLSON SKEME
00180 I2=JDIM-1
00190 DO 100 I1=2,I2
00200 C0 SAND LIFT
00210 IF ((V1 .EQ. 0) .AND. (V2 .EQ. 0)) GO TO 50.
00220 Y=(I1-1)*DELTA
00230 IF (Y .LE. XLIFT) GO TO 10
00240 W=0
00250 10 IF (Y .NE. XLIFT) GO TO 50
00260 W=0.5
00270 C0
00280 50 Z2(I1)=Z1(I1)-DELTAT/(2*DELTA)*
00290 ((1-TETA)*(SSUM1(I1+1)-SSUM1(I1-1))
00300 +TETA*(SSUM2(I1+1)-SSUM2(I1-1)))
00310 +((1-TETA)*V1+TETA*V2)*DELTAT*W
00320 100 CONTINUE
00330 C2
00340 C3 AT THE DOWNSTREAM BOUNDARY 4-POINTS SKEME
00350 Z2(JDIM)=Z1(JDIM)-Z2(JDIM-1)+Z1(JDIM-1)-DELTAT*2/DELTA*
00360 ((1-TETA)*(SSUM1(JDIM)-SSUM1(JDIM-1))
00370 +TETA*(SSUM2(JDIM)-SSUM2(JDIM-1)))
00380 C3
00390 RETURN
00400 end

```

P S T A R (801026.01)

1. Purpose

Calculating the new composition of the transport layer and the Z_0 -layer for given old and new: transport per fraction, bed level and transport layer thickness and for given old composition of the transport layer and the Z_0 -layer.

2. Usage

Call PSTAR (S1, S2, P1, P2, PZ01, PZ02, Z1, Z2, DELTA1, DELTA2, S01, S02, Z00, DELACC, JDIM, IDIM, TETA, DELTAX, DELTAT, DELTAP, V1, V2, XLIFT)

3. Description of parameters

S1, S2 (real-2-array) : transport per fraction at respectively old and new level
'unchanged on exist'

P1 (real-2-array) : Composition of transport layer at old time level
'unchanged on exist'

P2 (real-2-array) : Composition of transport layer at new time level
'changed on exist'

PZ01 (real-2-array) : Composition of Z_0 -layer at old time level
'unchanged on exist'

PZ02 (real-2-array) : Composition of Z_0 -layer at new time level
'changed on exist'

Z1, Z2 (real array) : Bed level at respectively old and new time level
'unchanged on exist'

DELTA1, DELTA2 (real array): Transport layer thickness at old and new time level
'unchanged on exist'

S01, S02 (real array) : Sand input per fraction at upstream boundary

	'unchanged on exict'
ZOO (real array)	: Position of coarse layer 'unchanged on exict'
DELACC (real)	: Initial thickness of coarse layer 'unchanged on exict'
JDIM (integer)	: Dimension of Z1, Z2, DELTA1, DELTA2, ZOO, S1, S2, P1, P2, PZ01 and PZ02 'unchanged on exict'
IDIM (integer)	: Dimension of S01, S02, DELTAP, S1, S2, P1, P2, PZ01 and PZ02. 'unchanged on exict'
TETA (real)	: Weight 'unchanged on exict'
DELTA X (real)	: Space step 'unchanged on exict'
DELTA T (real)	: Time step 'unchanged on exict'
DELTA P (real array)	: Composition in coarse layer $P_{cor} = DELTAP (*) + PZ01 (*)$ 'unchanged on exict'
V1, V2 (real)	: Sand lift velocity at respectively old and new time level 'unchanged on exict'
XLIFT (real)	: Length of sand lift 'unchanged on exict'

4. Procedure

none

5. Method

The new composition is calculated with the predictor-corrector (Crank-Nicholson) method applied on the continuity equation per fraction. See flow chart.

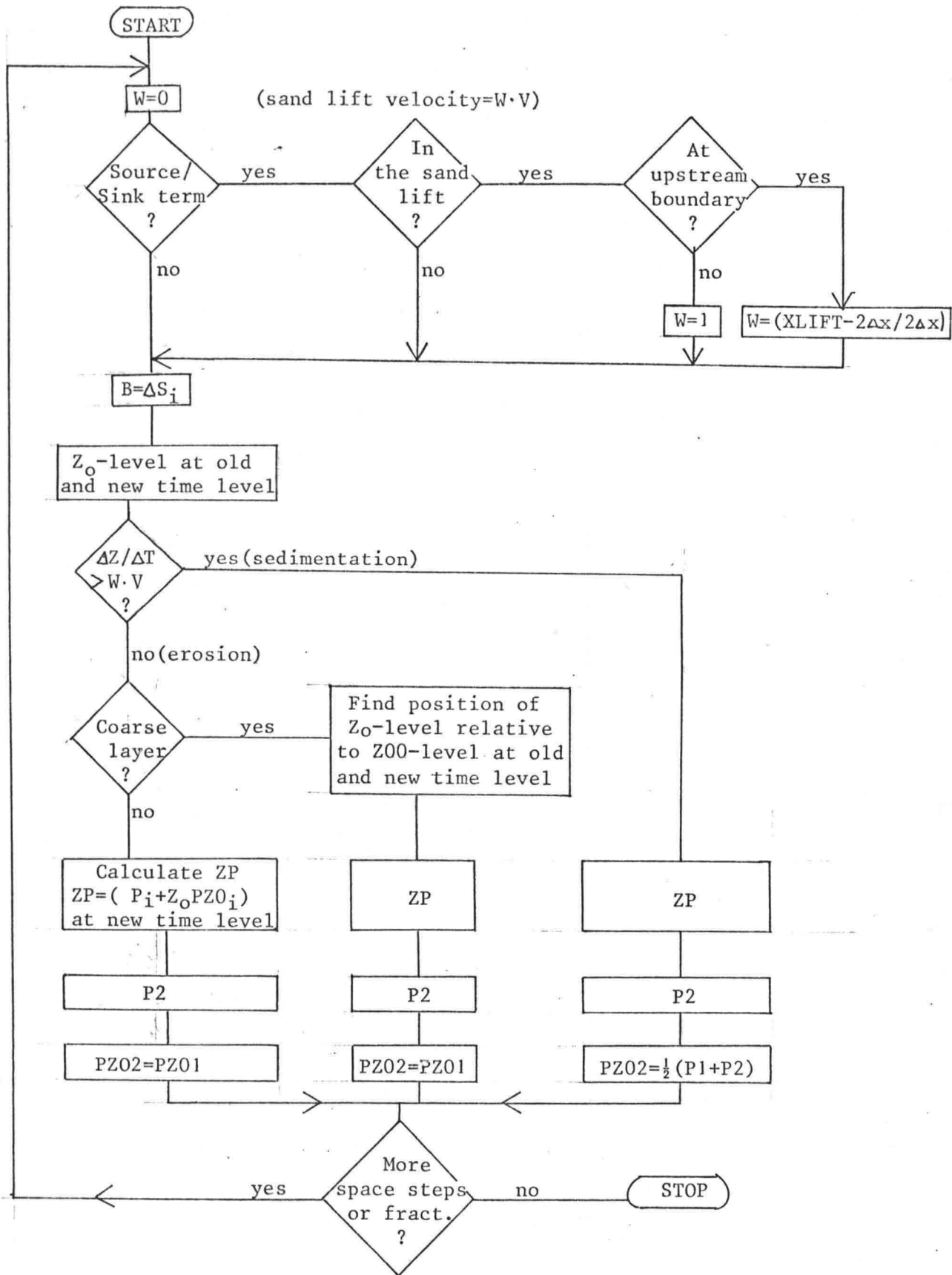
6. Remark

If the bed level and composition is fixed at the opstream boundary (boundary condition) lines 180-190 have to be changed into $B = 0$.

```

00010 SUBROUTINE PSTAR(S1,S2,P1,P2,PZ01,PZ02,Z1,Z2,DELTA1,DELTA2
00020 & ,S01,S02,Z00,DELACC,JDIM,JDIM,JDIM,TETA,DELTA,
00030 & DELTAT,DELTAF,V1,V2,XLIFT)
00040 C
00050 C SUBROUTINE CORRECTING P AND PZO
00060 C
00070 C **801026.01.KWO**
00080 C
00090 DIMENSION S1(IDIM,JDIM),S2(IDIM,JDIM),P1(IDIM,JDIM),
00100 & P2(IDIM,JDIM),PZ01(IDIM,JDIM),PZ02(IDIM,JDIM),
00110 & Z1(JDIM),Z2(JDIM),DELTA1(JDIM),DELTA2(JDIM),
00120 & Z00(JDIM),S01(IDIM),S02(IDIM),DELTAF(IDIM)
00130 C
00140 C DO
00150 DO 1500 I1=1, IDIM
00160 DO 1400 I2=1, JDIM
00170 CO SAND LIFT
00180 W=0
00190 IF ((V1 .EQ. 0) .AND. (V2 .EQ. 0)) GO TO 50
00200 W=1
00210 Y=(I2-1)*DELTA
00220 IF (Y .LE. XLIFT) GO TO 10
00230 W=0
00240 10 IF ((Y .NE. XLIFT) .AND. (Y .NE. 0)) GO TO 50
00250 W=(XLIFT-2*DELTA)/(2*DELTA)
00260 CO
00270 50 IF (I2 .NE. 1) GO TO 100
00280 C1 AT UPSTREAM BOUNDARY
00290 B=(TETA*(S2(I1,2)-S02(I1))+ (1-TETA)*(S1(I1,2)-
00300 & S01(I1)))*0.5
00310 GO TO 300
00320 C1
00330 100 IF (I2 .EQ. JDIM) GO TO 200
00340 C2 'INSIDE'
00350 B=(TETA*(S2(I1,I2+1)-S2(I1,I2-1))+ (1-TETA)*
00360 & (S1(I1,I2+1)-S1(I1,I2-1)))*0.5
00370 GO TO 300
00380 C2
00390 C3 AT DOWNSTREAM BOUNDARY
00400 B=TETA*(S2(I1,JDIM)-S2(I1,JDIM-1))+ (1-TETA)*
00410 & (S1(I1,JDIM)-S1(I1,JDIM-1))+DELTA/(2*DELTA)
00420 & *(Z02*PZ02(I1,JDIM-1)+DELTA2(JDIM-1)*P2(I1,JDIM-1)
00430 & -Z01*PZ01(I1,JDIM-1)-DELTA1(JDIM-1)*P1(I1,JDIM-1))
00440 B=2*B
00450 C3
00460 C4 ZO LEVEL
00470 300 Z01=Z1(I2)-DELTA1(I2)
00480 Z02=Z2(I2)-DELTA2(I2)
00490 C4
00500 C5 SEDIMENTATION/EROSION ?
00510 A=Z2(I2)-Z1(I2)
00520 AA=A-W*DELTA*( (1-TETA)*V1+TETA*V2)
00530 IF (AA .GE. 0) GO TO 1300
00540 C5
00550 C6 EROSION:
00560 IF (DELACC .EQ. 0) GO TO 1200
00570 A=Z00(I2)+DELACC
00580 IF (Z01 .LE. Z00(I2)) GO TO 400
00590 IF (Z01 .GE. A) GO TO 500
00600 GO TO 600
00610 400 X1=0
00620 Y1=0
00630 GO TO 700
00640 500 X1=DELACC
00650 Y1=0
00660 GO TO 700
00670 600 X1=Z01-Z00(I2)
00680 Y1=X1
00690 700 IF (Z02 .LE. Z00(I2)) GO TO 800
00700 IF (Z02 .GE. A) GO TO 900
00710 GO TO 1000
00720 800 X2=0
00730 Y2=0
00740 GO TO 1100
00750 900 X2=DELACC
00760 Y2=0
00770 GO TO 1100
00780 1000 X2=Z02-Z00(I2)
00790 Y2=X2
00800 C61 STAR ZP
00810 1100 ZP=Z01*PZ01(I1,I2)+DELTA1(I2)*P1(I1,I2)+X1*DELTAF(I1)
00820 & -DELTAT/DELTA*(V1*(1-TETA)*(PZ01(I1,I2)+Y1*
00830 & DELTAF(I1))+V2*TETA*(PZ01(I1,I2)+Y2*DELTAF(I1)))
00840 & *DELTA*W
00850 C61
00860 P2(I1,I2)=(ZP-PZ01(I1,I2)*Z02-X2*DELTAF(I1))/
00870 & DELTA2(I2)
00880 PZ02(I1,I2)=PZ01(I1,I2)
00890 GO TO 1400
00900 C62 NO COARSE LAYER
00910 1200 ZP=Z01*PZ01(I1,I2)+DELTA1(I2)*P1(I1,I2)-
00920 & DELTA/DELTA*(V1*(1-TETA)+V2*TETA)
00930 & *PZ01(I1,I2)*DELTA*W
00940 P2(I1,I2)=(ZP-PZ01(I1,I2)*Z02)/DELTA2(I2)
00950 PZ02(I1,I2)=PZ01(I1,I2)
00960 GO TO 1400
00970 C62
00980 C6
00990 C7 SEDIMENTATION
01000 1300 ZP=Z01*PZ01(I1,I2)+DELTA1(I2)*P1(I1,I2)-
01010 & DELTA/DELTA*(V1*(1-TETA)+V2*TETA)
01020 & *PZ01(I1,I2)*DELTA*W
01030 A=(Z02-Z01)/2
01040 P2(I1,I2)=(ZP-PZ01(I1,I2)*Z01-A*P1(I1,I2))
01050 & / (A+DELTA2(I2))
01060 PZ02(I1,I2)=(Z01*PZ01(I1,I2)+A*(P1(I1,I2)+
01070 & P2(I1,I2)))/Z02
01080 C7
01090 1400 CONTINUE
01100 1500 CONTINUE
01110 RETURN
01120 END

```



Flow chart: PSTAR

List and description of numerical model for uniform sediment.

The numerical model is designed with the following simplifications:

- The roughness is constant in space and time
- The boundary conditions are not varying in time.

The programme consists of a MAIN programme and four subroutines. In MAIN the input parameters are read, the transport is calculated with the Engelund - Hansen formula, the subroutines are called and the flow in the calculation is controlled.

In the subroutine STBAWA the back - water calculation is carried out and the predictor - corrector iterations in STPRCO. In STHEAD the head of the output is made and in STWRITE the outputs at the different time level are produced.

The output starts with a head where the numerical parameters, the grain diameter, Chézy - coefficient and the initial and boundary conditions are listed. The output at the different time levels starts with the time in seconds followed by a list with from left to right: space coordinate (X), bed level (Z), water depth (A), flow velocity (U), the Courant number (COU) and the sediment transport included pore volume (S). In a overview plot an indication of the bed level "Z" and the water level "H" are plotted.

The flow velocity is not recalculated after last corrections of the bed level, so the flow velocity, water depth and water level in the output belongs to the previous iteration step.

```

00060 C
00070 C **B01008.02.KWD**
00080 C *****
00090 C
00100 DIMENSION Z(2,401), S(2,401), U(401)
00110 C
00120 C1 INPUT
00130 C1.1 SPACE AND TIMESTEP, AND LENGTH OF FLUME (JDIM)
00140 READ (5,*) DELTAX, DELTAT, JDIM
00150 C1.1
00160 C1.2 WEIGTH, NUMBER OF ITERATIONS IN BACKWATER CALCULATION
00170 C1.2 AND PREDICTOR - CORRECTOR ITERATION (MIN 2, STABIBITY 3)
00180 READ (5,*) TETA, NITE, IO
00190 C1.2
00200 C1.3 STOP CRITERION AND TIME BETWEEN OUTPUT
00210 READ (5,*) TMAX, TOP
00220 C1.3
00230 C1.4 SED. INPUT AT UPSTREAM BOUNDARY AND GRAIN DIAMETER
00240 READ (5,*) SXEQO, D
00250 C1.4
00260 C1.5
00270 C1.5 HYDRAULICS PARAMETER
00280 READ (5,*) SLOPE, Q, H, C
00290 C1.5
00300 C1
00310 C MAKE HEAD
00320 CALL STHEAD(DELTAX, DELTAT, JDIM, TETA, NITE, IO, TMAX,
00330 & TOP, SXEQO, D, SLOPE, Q, H, C)
00340 C
00350 C2 COMPUTE BEDLEVEL FROM SLOPE
00360 DO 100 I1=1, JDIM
00370 Z(1, I1)=(JDIM-I1)*SLOPE*DELTAX+0.010
00380 CONTINUE
00390 C2 100
00400 C3 START AT TIME = 0
00410 T=0.0
00420 TT= 0.0
00430 C3
00440 C4 FIRST ITERATION
00450 ITERNR=0
00460 ITERNR=ITERNR+1
00470 C4
00480 C5 COMPUTE BACKWATERCURVE
00490 CALL STBWA(Z, U, JDIM, Q, C, H, DELTAX, NITE, ITERNR)
00500 C5
00510 C6 COMPUTE SEDIMENT TRANSPORT
00520 C6.1 PREDICTOR OR CORRECTOR?
00530 I2=2
00540 IF (ITERNR .EQ. 1) I2=1
00550 C6.1
00560 C6.3 S=F(U) WITH THE ENGELUND-HANSEN EQ.
00570 DO 400 I3=1, JDIM
00580 S(I2, I3)= 0.009851*U(I3)**5/(D*C**3)
00590 CONTINUE
00600 C6
00610 C7 PREPARE S FOR SUBROUTINE STPRCD
00620 C7.1 PREDICTOR OR CORRECTOR?
00630 IF (ITERNR .NE. 1) GO TO 600
00640 DO 500 I4=1, JDIM
00650 S(2, I4)=S(1, I4)
00660 CONTINUE
00670 C7
00680 C7 500
00690 C8 CALL STPRCD(S, Z, JDIM, DELTAX, DELTAT, TETA, SXEQO)
00700 MORE ITERATIONS?
00710 IF (ITERNR .LT. IO) GO TO 300
00720 C8
00730 C9 OUTPUT?
00740 IF ((T .LT. TT) .AND. (T .NE. 0.0)) GO TO 700
00750 CALL STWRIT(U, Z, S, DELTAX, T, JDIM, Q, DELTAT)
00760 TT=TT+TOP
00770 C9
00780 C9 700
00790 C10 IF (T .GE. TMAX) GO TO 1000
00800 C11 MAKE READY FOR NEXT TIMESTEP
00810 T=T+DELTAT
00820 DO 900 I6=1, JDIM
00830 Z(1, I6)=Z(2, I6)
00840 CONTINUE
00850 C11
00860 C12 COMPUTE FOR NEW TIMESTEP
00870 GO TO 200
00880 C12
00890 C12 1000
00900 CALL STWRIT(U, Z, S, DELTAX, T, JDIM, Q, DELTAT)
00910 END

```



```

00900 SUBROUTINE STHEAD(DELTA, DELTAT, JDIM, TETA, NITE, IO,
00910 & TMAX, TOP, SXEQO, D, SLOPE, Q, H, C)
00920 C
00930 C
00940 C
00950 C
00960 C
00970 WRITE (6,10)
00980 WRITE (6,20)
00990 WRITE (6,10)
01000 WRITE (6,50)
01010 WRITE (6,50)
01020 10 FORMAT (1H,37('*'))
01030 20 FORMAT (1H,'*TRANSPORTMODEL FOR UNIFORM SEDIMENT*')
01040 WRITE (6,40)
01050 40 FORMAT (1H,'PARAMETERLIST:')
01060 WRITE (6,50)
01070 50 FORMAT (1H)
01080 WRITE (6,60) DELTAT
01090 60 FORMAT (1H,'TIMESTEP = ',F10.1,' SEC.')
01100 WRITE (6,70) DELTAX
01110 70 FORMAT (1H,'SPACESTEP = ',F10.3,' M.')
01120 X1=DELTA*(JDIM-1)
01130 WRITE (6,80) X1
01140 80 FORMAT (1H,'LENGTH OF FLUME = ',F10.2,' M.')
01150 WRITE (6,90) SLOPE
01160 90 FORMAT (1H,'INITIAL BED SLOPE = ',E12.4)
01170 WRITE (6,110) Q
01180 110 FORMAT (1H,'DISCHARGE = ',F10.4,' M2/S')
01190 WRITE (6,120) H
01200 120 FORMAT (1H,'WATERLEVEL DOWNSTREAM = ',F10.4,' M')
01210 WRITE (6,130) C
01220 130 FORMAT (1H,'CHEZY-COEFFICIENT = ',F10.2,' M1/2/S')
01230 WRITE (6,140) D
01240 140 FORMAT (1H,'GRAIN DIAMETER = ',3PF10.2,' MM')
01250 WRITE(6,150) SXEQO
01260 150 FORMAT (1H,'SANDINPUT = ',E12.4,' M2/S')
01270 WRITE (6,160) TETA
01280 160 FORMAT (1H,'WEIGHT TETA = ',F10.5)
01290 WRITE (6,170) NITE, IO
01300 170 FORMAT (1H,'I2, ITERATIONS IN BACKWATER CURVE AND ',I2,
01310 & 'IN PRE.-COR.')
01320 WRITE (6,180) TMAX, EPS
01330 180 FORMAT (1H,'STOP CRITERION TMAX = ',E14.4,' S')
01340 WRITE (6,190) TOP
01350 190 FORMAT (1H,'TIME BETWEEN OUTPUT = ',E14.4,' S')
01360 C
01370 C
01380 RETURN
01390 END

```

```

01400 SUBROUTINE STWRIT(U,Z,S,DELTA,T,JDIM,Q,DELTAT)
01410 C
01420 C
01430 C
01440 DIMENSION Z(2,JDIM), S(2,JDIM), U(JDIM)
01450 DIMENSION LINE(82)
01460 DATA LBLANK, LASTER, LZZ, LHH/ 1H, 1H*,1HZ,1HH/
01470 C
01480 C2 CALCULATE SCALEFACTOR
01490 IF (T.NE. 0.0) GO TO 200
01500 SCALE= 70/(Z(1,1)+Q/U(1))
01510 C2
01520 C3 HEADLINE 1
01530 200 Y=T+DELTAT
01540 WRITE (6,300) Y
01550 WRITE (6,400)
01560 C3 HEADLINE 2
01570 WRITE (6,500) SCALE
01580 WRITE (6,700)
01590 C3
01600 C4 OUTPUT
01610 DO 1000 I3=1,JDIM
01620 C4.1 MAKE BLANK IN LINE
01630 DO 800 I4=1,82
01640 LINE(I4)=LBLANK
01650 CONTINUE
01660 800 C4.1
01670 C1 CALCULATE WATER DEPTH AND C-NUMBER
01680 A=Q/U(I3)
01690 COU= (5*S(2,I3)/Q)/(1-U(I3)**2/(9.81*A))
01700 & *(DELTAT/DELTA)*U(I3)
01710 C1
01720 X=DELTA*(I3-1)
01730 C4.2 MAKE * IN LINE
01740 A1=Z(2,I3)*SCALE
01750 A2=(Z(2,I3)+A)*SCALE
01760 C4.21 CUT OFF AND ROUND UP OR DOWN
01770 L1=A1
01780 C1=A1-L1
01790 IF (C1.GE. 0.5) L1=L1+1
01800 L2=A2
01810 C2=A2-L2
01820 IF (C2.GE. 0.5) L2=L2+1
01830 C4.21
01840 C4.22 STILL ROOM AT THE PAPER?
01850 IF ((L2.GT. 82).OR. (L2.LT. 1)) L2=1
01860 IF ((L1.GT. 82).OR. (L1.LT. 1)) L1=1
01870 C4.22
01880 C4.23 MAKE *
01890 LINE(1)=LASTER
01900 LINE(L1)=LZZ
01910 LINE(L2)=LHH
01920 C4.23
01930 WRITE (6,900) X, Z(2,I3), A, U(I3), COU,S(2,I3),
01940 & LINE
01950 1000 CONTINUE
01960 WRITE (6,700)
01970 300 FORMAT (1H1,' TIME = ',F14.1,' SECONDS')
01980 400 FORMAT (1H,45('-',))
01990 500 FORMAT (1H,' X(M) Z(M) A(M) U(M/S) COU-N S(M2/S)
02000 & SCALE = ',F10.3,' (+/M)')
02010 700 FORMAT (1H,45('-',),3X,82(+))
02020 900 FORMAT (1H,F7.2,4F7.4,E10.3,3X,82A1)
02030 RETURN
02040 END

```

```

02050 SUBROUTINE STBAWA(Z,U,JDIM,Q,C,H,DELTA,NITE,ITERNR)
02060 C
02070 C **801008.02.KWD**
02080 C
02090 DIMENSION Z(2,JDIM), U(JDIM)
02100 C
02110 CO PREDICTOR OR CORRECTOR?
02120 IO=2
02130 IF (ITERNR .EQ. 1) IO=1
02140 CO
02150 C
02160 C1 INITIALISE
02170 U(JDIM)=Q/(H-Z(IO,JDIM))
02180 C1
02190 C2 CALCULATE U
02200 I3=JDIM-1
02210 DO 500 I2=1,NITE
02220 DO 1000 I1=1,I3
02230 C2.1 CALCULATA U-AVERAGE (UAV)
02240 IF (I2 .NE. 1) GO TO 20
02250 UAV =U(JDIM+1-I1)
02260 GO TO 30
02270 UAV=0.5*(U(JDIM+1-I1)+U(JDIM-I1))
02280 C2.1
02290 C2.2 CALCULATA FRICTION-TERM R
02300 R=9.81*UAV**3/(C**2*Q)
02310 C2.2
02320 C2.3 CALCULATA G-TERM
02330 G=UAV-9.81*Q/UAV**2
02340 C2.3
02350 C2.4
02360 U(JDIM-I1)=U(JDIM+1-I1)+((Z(IO,JDIM+1-I1)-
02370 Z(IO,JDIM-I1))*9.81+R*DELTA)/G
02380 C2.4
02390 C2
02400 1000 CONTINUE
02410 500 CONTINUE
02420 RETURN
02430 END

```

```

02440 SUBROUTINE STPRCO(S,Z,JDIM,DELTA,DELTA,TETA,SXEQO)
02450 C
02460 C **801006.01.KWD**
02470 C
02480 DIMENSION S(2,JDIM), Z(2,JDIM)
02490 C
02500 C3 AT THE UPSTREAM BOUNDARY
02510 Z(2,1)=Z(1,1)-DELTA/(2*DELTA)*(TETA*(S(2,2)-SXEQO)+
02520 (1-TETA)*(S(1,2)-SXEQO))
02530 C3
02540 IO=JDIM-1
02550 DO 1000 I1=2, IO
02560 C1 'INSIDE' CRANK-NICHOLSON SKEME
02570 Z(2,I1)=Z(1,I1)-DELTA/(2*DELTA)*((1-TETA)*(S(1,I1+1)-
02580 S(1,I1-1))+TETA*(S(2,I1+1)-S(2,I1-1)))
02590 C1
02600 1000 CONTINUE
02610 C2 AT THE DOWNSTREAM BOUNDARY 4-POINTS SKEME
02620 Z(2,JDIM)=Z(1,JDIM)-Z(2,JDIM-1)+Z(1,JDIM-1)-2*DELTA/
02630 DELTA*((1-TETA)*(S(1,JDIM)-S(1,JDIM-1))+
02640 TETA*(S(2,JDIM)-S(2,JDIM-1)))
02650 C2
02660 RETURN
02670 END

```

Literature Survey

A literature survey is carried out in order to get some insight into the already performed numerical modelling for morphological processes in rivers, and maybe obtain some inspiration for a choice of a numerical method. A model for uniform and some for non-uniform sediment will be treated.

E 1. Chollet and Cunge (1980)

Chollet and Cunge developed a one dimensional numerical model for uniform sediment with a variable roughness. Roughness predictors in morphological models are often of the simple Manning - Strickler type (Manning's n a function of d_{50}), but here the Engelund and Einstein roughness predictors are applied after a few modifications are carried out. Also the sediment transport is calculated by the formulas of Engelund and Einstein.

The computation involves in this case not only solution of the back-water curve, continuity equation for sediment and the transport calculation, but also a calculation of the roughness

$$F(R, U, a) = 0 \quad (\text{E 1.1})$$

There is, opposite to most other numerical models for river morphology, applied an implicit finite difference method: the four point scheme. The derivatives in the differential equations are approximated as outlined in chapter 3 and the functions (for instance E 1.1) are discretized like

$$F(x, t) = \theta \frac{F_{j+1}^{n+1} + F_j^{n+1}}{2} + (1 - \theta) \frac{F_{j+1}^n + F_j^n}{2} \quad (\text{E 1.2})$$

in which the notation from chapter 3 is applied.

The transport formulas and roughness predictors are linearized with respect to the bed level (ΔZ) and the water level (Δh). For each reach Δx (each

time the four points scheme is applied) a system of two linear algebraic equations occurs

$$A_1 \Delta h_j + B_1 \Delta Z_j + C_1 \Delta h_{j+1} + D_1 \Delta Z_{j+1} + H_1 = 0$$

(E 1.3)

$$A_2 \Delta h_j + B_2 \Delta Z_j + C_2 \Delta h_{j+1} + D_2 \Delta Z_{j+1} + H_2 = 0$$

where $\Delta Z_j = Z_j^{n+1} - Z_j^n$, etc.

In case of N calculations points there are $2(N-1)$ equations and $2N$ unknown, which is sufficient as there are two boundary conditions.

The four points scheme has very good numerical characteristics: dissipate, stable for $\theta > \frac{1}{2}$ and it is rather accurate; but the linearization must be justified by applying a small time step. The linearization is in fact the same as only make one Newton - iteration.

The linearization of the transport formula and roughness predictor can be very elaborate, which makes this solution method very little flexible. Further more if the method were applied to the model for non - uniform sediment, the number of algebraic equations (eq. E 1.3) would increase considerable and so the calculation time.

E2. Deigaard (1980)

Deigaard developed a one dimensional numerical model for non - uniform sediment in order to study the longitudinal grain sorting in alluvial rivers due to different transport rates of grains with different sizes. The initial profile of the rivers are described by a decreasing exponential function, which causes two time scales in the model: one for the change in grain size and one for the longitudinal bed profile, the last one much the largest. This implies that the bed composition is in some sort of temporarily equilibrium. The aim of the study has been to obtain this quasi-steady grain size distribution.

The set of equation Deigaard uses is

$$\delta \frac{\partial p_i}{\partial t} + p_i \frac{\partial Z}{\partial t} + \frac{\partial S_i}{\partial x} = 0 \quad (\text{E 2.1})$$

$$S_i = p_i \cdot f(a, I, d_i, \dots) \quad (\text{E 2.2})$$

where a is constant over the reach - equal downstream water depth. The transport layer thickness is equal 15% of the water depth and the transport is calculated with the Engelund - Fredsoe (1976) transport model.

The continuity equation per fraction only applies in case of sedimentation because $\bar{p}_{iZ_0} = p_i$ (chap 2.4. As the model only is used to obtain an equilibrium in composition the choice of a transport layer thickness only influences the time scale and not the equilibrium situation ($\frac{\partial p_i}{\partial t} \approx 0$).

The computations are carried out with the upstream scheme, which, according to the numerical analysis in chapter 3, is very inaccurate for Courant number not close to unity, and only stable for Courant numbers less than one. The damping factor per wave length for the upstream scheme is

$$d = 1 - \pi \xi (1 - \sigma) \quad (\text{E 2.3})$$

The numerical model is only applied to problems where the wave lengths are very large, i.e. there is many points per wave length and $\xi \rightarrow 0$, so the accuracy is not a problem - also because the celerities have the same magnitude. Due to the long wave lengths is it not critical that the continuity equation per fraction (eq. E 2.1) is in a non - conservative form.

The scheme has the advantage that it is providing very little secondary waves, so it seems very suitable for the cases it is applied to, but for a general numerical model, where also short waves can have interest, the scheme is not applicable.

E 3. Schen [17]

The model has been developed in order to study the influence of hydraulic

sorting on the longitudinal grain size distribution in aggrading and degrading alluvial streams. The more specific aim has been to explain the fact, that the cumulative distribution curve for the sediment in the bed exhibit three straight lines divided by two discontinuity points, by means of Einstein hiding factor.

The flow velocity is calculated by the Manning formula

$$U = \frac{1.486}{n} a^{2/3} I^{1/2} \quad (\text{E 3.1})$$

where Manning's n is calculated using Strickler's formula

$$n = 0.0342 d_{50}^{1/6} \quad (\text{E 3.2})$$

The continuity equation per sediment fraction is the one derived in chapter 1.2 and the transport layer is chosen constant equal 2 inch, so a reliable time scale cannot be expected.

Schen applies the following explicit finite difference scheme

$$\Delta Z_j = -\Delta Z_{j+1} + 2C (Z_j^n - Z_{j+1}^n) \frac{t}{x} \quad (\text{E 3.3})$$

in which $Z_j = Z_j^{n+1} - Z_j^n$.

The scheme is in fact a four point scheme with $\theta = 0$. The complex propagation factor is

$$\rho = 1 - i 2\sigma \tan \frac{\xi}{2} \quad (\text{E 3.4})$$

and

$$|\rho| = \sqrt{1 + 4\sigma^2 \tan^2 \frac{\xi}{2}} > 1 \quad (\text{E 3.5})$$

Although the bed friction has a positive influence on the stability is it incomprehensible how Schen can compute with such a unstable scheme, especially because he is carrying out calculations in which there are relative short wave lengths. Never the less he is obtaining computational results from which he suggests a modification of Einstein hiding factor.

EH. HEC - 6, US Army Corps of Engineering (1977)

The HEC - 6 is a commercial programme for non - uniform sediment developed by W.A. Thomas. In the model Einstein's bed load formula is applied, but also silt and clay transport are considered. The model has a lot of sophistry: consolidation of clay and silt, Carnot formula for expansion loss etc. It is a one dimensional quasi steady flow model, where the flow cross section is divided into a part which has a moveable bed and one which does not. The model does not simulate the roughness but it does allow variation of Manning's n with the discharge.

The bottom of the transport layer is defined as the equilibrium depth, i.e. the level for which there would be zero transport of the finest grain there is stable in the top (armor) layer. The trend in this definition is in agreement with the models described in chapter 2.3, as the transport layer thickness decreases for increasing grain diameter, but, in cases where there is no armor layer, it seems to be an unreasonable approach.

The stability of the armor layer is tested at each step, and if it is found unstable the grains are considered to be completely mixed over the new transport layer.

The applied numerical method is

$$\frac{z_j^{n+1} - z_j^n}{\Delta t} + \frac{S_{j+1}^{n+\frac{1}{2}} - S_{j-1}^{n+\frac{1}{2}}}{2 \Delta x} = 0 \quad (E 4.1)$$

where $S_j^{n+\frac{1}{2}}$ is a weighted average of the transport between the two time levels, i.e. the Crank - Nicholson scheme. It does not appear very clearly in [19] whether eq. E 4.1 is solved with a predictor - corrector method or with a fully implicit scheme.

The computation of the morphological changes are based on a lot of assumptions there hardly have been verified. In this respect can be mentioned:

- Einstein's transport formula involves a hiding factor which has been the subject of modification for several scientists.

- It seems more reasonable to define the transport layer thickness as half a significant dune height, when there is no armor layer.
- The complete mixing of the destructed armour layer is not always taking place, as experiments show that a part of the unstable armour layer remains intact at the river bottom.

Emmett and Thomas (1978) has applied the model to a reservoir, and found that extensive data collection had to be carried out in order to calibrate the model to obtain reliable results.

References

1. Abbot, M.B., Computational Hydraulics, Pitmann, London 1979.
2. Challet, J.P. and Cunge, J.A., Simulation of unsteady flow in alluvial streams, Int. Symp. on river sedimentation March 24 - 29 1980, Chin. Soc. of Hydr. Eng., Beijing, China 1980.
3. Day, T.J., A study of the transport of gradet sediments, Report No. IT190, Hydraulic Research Station, Wallingford, England, April 1980.
4. Deigaard, R., Longitudinal and transverse sorting of grain sizes in alluvial rivers, Technical University of Denmark, Lyngby 1980.
5. Delft Hydraulic Laboratory, Report number R657 - VIII / M 1314 del V, Proeven met vlakke bodem zonder transport, December 1978.
6. Egiazaroff, P.I., L'équation du transport des alluvions non cohesives par un courant fluide, Proc. IAHR Paris 1957.
7. Egiazaroff, P.I., Calculation of non - uniform sediment concentration, Proc. ASCE HY 4, July 1965.
8. Engelund, F. and Hansen, E., A monograph on sediment transport in alluvial streams, ^FT_{eknisk} ^LFor_{lag}, Copenhagen 1967.
9. Engelund, F. and Fredsoe, J., A sediment transport model for straight alluvial channels, Nordic Hydrology 7, 1976, pp 293 - 306.
10. Fredsoe, J., Dimensions of stationary dunes. Part 1. Low sediment transport rate, Progress Report no. 49, Technical University of Denmark, Institute of hydrodynamics and hydraulics engineering.
11. Guy, H.P., Simons, D.B. and Richardson, E.V., Summary of alluvial channel data from flume experiments, 1956 - 1961, U.S. Geological Survey Professional Paper 462 - I, 1966.

12. Jansen, P.Ph. (Ed), Principles of river engineering, Pitman, London 1979.
13. Klaassen, G.J., Lecture notes for b74 Vloeistofmechanica b.o., Alluviale ruwheid, April 1981.
14. Prins, A., Sedimenttransport, Lecture notes, Delft University of Technology, Dept. of Civil Engineering, Delft 1978.
15. Ribberink, J.S., Bed load formulae for non-uniform sediment, Delft University of Technology, Dept. of Civil Engineering, Fluid Mechanics Group, Internal Report no. 4-78, 1978.
16. Ribberink, J.S., Morphological modelling for révers with non-uniform sediment, Delft University of Technology, Dept. of Civil Engineering, Fluid Mechanics Group, Internal Report no. 1-80, 1980.
17. Shen, H.W., Sediment sorting processes in certain aggrading and degrading streams, Department of Civil Engineering, Colorado State University, Fort Collins.
18. Suzuki, K., On the propagation of a disturbance in the bed composition of an open channel, Report R 1976 / 09 / L, Delft University of Technology, Dept. of Civil Engineering, 1976.
19. U.S. Army Corps of Engineering - HEC, HEC - 6 Scour and deposition in rivers and reservoirs, Users Manual, March 1977.
20. Vanoni, V.A., Sedimentation engineering, ASCE - manuals and reports on engineering practice - No. 54, New York.
21. Vreugdenhil, C.B., Waterloopkundige berekenigen I, Delft University of Technology, Dept. of Civil Engineering, Lecturenotes b84, August 1979.
22. Vreugdenhil, C.B., Waterloopkundige berekeningen II, Delft University of Technology, Dept. of Civil Engineering, Lecturenotes b85, December 1980.

23. Vreugdenhil, C.B., Numerical effects in models for river morphology, to be published in a book in homage to A. Preissmann, Pitman, London, 1981.
24. de Vries, M., Morphological computations, Delft University of Technology, Dept. of Civil Engineering, Lecture notes f 10 a, 1981.
25. White, W.R., Paris, E. and Bethers, R., The frictional characteristics of alluvial streams: a new approach, Proc. Instn. Engrs., Vol. 69, 1980.
26. Yassin, A.M., Mean roughness coefficient in open channels with different roughnesses of bed and side walls, Zürich 1953.
27. Havinga, H., Transportmetingen (incl. Deventer baggerproef). Lecture notes for b74 Vloeistof mechanica Arnhem , The Netherlands 1981.

List of main symbols.

a	water depth	(m)
c	celerity, propagation velocity	(m/s)
c_r	relative propagation velocity	(-)
d	numerical damping factor	(-)
d_i	characteristic diameter of fraction i	(m)
f	Darcy - Weisbach roughness coefficient	(-)
h	water level	(m)
j	$j\Delta x$: space coordinate	(-)
k	wave number	(m^{-1})
n	$n\Delta t$: time coordinate	(-)
P_i	probability of fraction i in transport layer	(-)
$P_{i_{z_0}}$	probability of fraction i in z_0 - layer	(-)
q	specific discharge	(m^2/s)
u	flow velocity	(m/s)
z	bed level	(m)
z_0	$z - \delta$, z_0 -level	(m)
C	Chezy roughness coefficient	($m^{1/2}/s$)
D_{num}	numerical diffusion coefficient	(m^2/s)
D_{ph}	physical diffusion coefficient	(m^2/s)
F	Froude number	(-)
H	dune height	(m)
$P_{\Delta x}$	cell Peclet number	(-)
R	friction term in back-water curve	(m/s^2)
S	total sediment transport include pore volume	(m^3/s)
S_i	sediment transport of fraction i include pore volume	(m^3/s)
ξ	dimensionless space step	(-)
σ	Courant number	(-)
ρ	complex propagation factor	(-)
θ	weight in implicit finite difference schemes	(-)
θ	dimensionless shear stress	(-)
θ'	effective dimensionless shear stress	(-)
μ	$= \frac{\theta'}{\theta}$ ripple factor	(-)
Δx	space step	(m)
Δt	time step	(s)

ϕ	dimensionless celerity	(-)
$\bar{\phi}$	dimensionless transport rate	(-)
γ	dimensionless transport concentration	(-)
δ	transport layer thickness	(m)

